Norwegian University of Life Sciences • Universitetet for miljø- og biovitenskap
Department of Ecology and Natural Resource Management
Philosophiae Doctor (PhD) Thesis 2011:22

Improving Forest Inventory and Monitoring by Combining Remotely Sensed Three-Dimensional and Spectral Information

Bedre skogtaksering og overvåkning ved kombinasjon av fjernmålt tredimensjonal- og spektralinformasjon

Hans Ole Ørka

Improving Forest Inventory and Monitoring by Combining Remotely Sensed Three-Dimensional and Spectral Information

Bedre skogtaksering og overvåkning ved kombinasjon av fjernmålt tredimensjonal- og spektralinformasjon

Philosophiae Doctor (PhD) Thesis

Hans Ole Ørka

Dept. of Ecology and Natural Resource Management
Norwegian University of Life Sciences

Ås 2011

Thesis number 2011:22
ISSN 1503-1667
ISBN 978-82-575-0986-6

PhD supervisors
Professor Erik Næsset
Department of Ecology and Natural Resource Management
Norwegian University of Life Sciences
P.O. Box 5003, NO – 1432 Ås, Norway

Dr. Terje Gobakken
Department of Ecology and Natural Resource Management
Norwegian University of Life Sciences
P.O. Box 5003, NO – 1432 Ås, Norway

Dr. Ole Martin Bollandsås
Department of Ecology and Natural Resource Management
Norwegian University of Life Sciences
P.O. Box 5003, NO – 1432 Ås, Norway

Evaluation committee
Dr. Ross A. Hill
School of Conservation Sciences
Bournemouth University, UK
Talbot Campus, Fern Barrow, Poole, Dorset, BH12 5BB, United Kingdom

Dr. Sorin C. Popescu
Department of Ecosystem Science and Management
Texas A&M University, Texas, USA
TAMU 2120 1500 Research Parkway, Suite B223, College Station, TX 77843, USA

Professor Svein Solberg
Department of Ecology and Natural Resource Management
Norwegian University of Life Sciences
&
Norwegian Forest and Landscape Institute
P.O. Box 115, N – 1431 Ås, Norway

PREFACE

This thesis has been submitted as part of my doctoral studies. The thesis, together with an academic training component, a trial lecture and a public defense, completes the Doctor of Philosophy degree. My doctoral studies were funded by the Norwegian University of Life Sciences and a travel grant from the Research Council of Norway.

I would like to thank my supervisor, Professor Erik Næsset, for giving me the opportunity to write this thesis by initially obtaining the funding for the scholarship and then for hiring me. Thanks for giving me the freedom to follow my own ideas, as well as for all the good suggestions, ideas and comments on my work. Thanks to my co-supervisors, Dr. Terje Gobakken and Dr. Ole Martin Bollandsås, for all their supervision. The two of you were always around and ready for my thoughts and discussions.

A special thanks to Dr. Michael A. Wulder for hosting me at the Pacific Forestry Center (PFC) in 2009. I learned a lot from you in organizing the scientific work, Mike - it was encouraging. In addition, thanks to all the people in and around the Forest Geomatics group at PFC for making the stay an experience for life. A special thanks to Maja Kaffanke, our Canadian grandmother, who made the stay in Victoria pleasant and memorable for the entire family. I would also like to thank Dr. Ilkka Korpela for cooperation and for involving me in your research. Your enthusiasm and speed was inspiring! You also taught me the "lean forward strategy", which I will need when my time as a PhD student is history.

Thanks to my fellow colleagues at INA, especially Dr. Even Bergseng for being around during my entire PhD period. Erik's unique ability in finding funding has made the research group grow quickly; it will take too much space to thank all of you, so I will just thank you all together. THANKS for the coffee, discussions, inspiration, ideas, chocolate, encouragement and being nice colleagues. Hopefully, we will get some more time together!

I would also like to thank my family, especially the grandmothers of my children, for helping us out when long days at work were needed. And most importantly, thanks to my loving wife, Janne, and to our children Halvor, Johanne and Torbjørn for their help and support in making the PhD period something more than just reading scientific ("salami") literature, kilometers of software codes and manuscripts full of red ink.

Ås, March 22, 2011

Hans Ole Ørka

CONTENTS

ABSTRACT

Forest inventory has benefited from remote sensing for more than 80 years. Spectral information from aerial cameras has been the dominant data source during this period. However, over the past decade the use of three-dimensional data from airborne laser scanning (ALS) has substantially improved the accuracy of forest inventory, although there currently seems to be certain limitations for ALS in terms of providing tree species information, wall-to-wall maps in large area inventory and multi-temporal acquisitions in forest monitoring. In all of these cases, spectral information may be complementary to three-dimensional information, and the combination of the two data sources may improve both forest inventory and monitoring. In this thesis, the potential for combining three-dimensional data from ALS and spectral information recorded by ALS (intensity), as well as multispectral aerial cameras and satellite sensors, was investigated. This thesis focuses on tree species identification, delineation of the subalpine zone and the quantifying effects of sensors and seasons in multi-temporal acquisitions. Improvement in the accuracy of tree species identification was obtained in relation to both intensity and spectral information from aerial imagery. Aerial imagery seems to be a more stable spectral data source for tree species identification compared to intensity. A correct species identification for 85 – 90% of the dominant trees seems within reach. Moreover, it was revealed that both the three-dimensional and spectral information from ALS were affected by the sensor used and the season of data acquisition. At the moment, calibration with contemporary field measurements is needed for individual acquisitions. Estimates of individual tree height and stem diameter can be accurately derived for all multi-temporal acquisitions when calibrated with field data. Tree species identification was significantly better under leaf-off than leaf-on canopy conditions, but did not differ between sensors. Furthermore, a sample of three-dimensional data covering 8.4% of Hedmark County, Norway, was combined with full coverage Landsat imagery to help delineate the subalpine zone. The delineation of the subalpine zone boundaries was found to be accurate. Combining three-dimensional and spectral information may improve forest inventory and monitoring in many circumstances, although challenges and costs are increased by using multiple data sources and must be compared against the advantage of the higher information level obtained.

SAMMENDRAG

I skogtaksering har man hatt nytte av fjernmålte data i over 80 år. Spektralinformasjon fra flybilder har vært den dominerende datakilden gjennom disse årene. De siste 10 årene har imidlertid tredimensjonale data fra flybåren laserscanning (FLS) vesentlig forbedret skogtakseringen. Sammenligning av FLS med andre metoder for fjernmåling har vist at FLS er den mest nøyaktige metoden for prediksjon av skoglig informasjon. FLS har likevel noen begrensinger, blant annet i forhold til å fremskaffe informasjon om treslag, gi heldekkende kart i regionale og nasjonale takseringer og i forhold til skogovervåkning som involverer multitemporale data. Der FLS har begrensinger kan spektral informasjon være komplementær til den tredimensjonale informasjonen. I denne avhandlingen undersøkes mulighetene for å kombinere tredimensjonal informasjon fra FLS med spektral informasjon fra FLS (intensitet), digitale flybårne kamera og satellitter. Avhandlingen fokuserer på treslagsidentifikasjon av enkelttrær, kartlegging av den subalpine sonen og på kvantifikasjon av effektene som følge av flygninger med ulike sensorer og til ulike årstider ved skogtakstasjon. Identifikasjonen av treslag basert på tredimensjonal data fra FLS ble forbedret med både spektrale data fra intensitet og fra flykamera. Flybilder ser ut til å være en mer stabil spektral datakilde enn intensitet. Korrekt identifikasjon av treslag for 85 – 90 % av de dominante trærne er innen rekkevidde. Videre ble det påvist forskjeller i både den tredimensjonale og spektrale informasjonen fra FLS mellom ulike flygninger med ulike sensorer og til ulike årstider. På det nåværende tidspunkt er både feltdata og FLS-data fra det samme tidsrommet nødvendig. Dette fordi predikert høyde og diameter på enkelttrær har god nøyaktighet når modellene er kalibrert mot feltdata uavhengig av sensor og årstid for flygning. Bruk av data fra flygninger som ble gjort da det ikke var lauv på trærne ga signifikant nøyaktigere treslagsklassifikasjon. I Hedmark ble tredimensjonal data som dekket 8.4 % av arealet, kombinert med fulldekkende spektral informasjon fra Landsat for å kartlegge den subalpine sonen. Grensene til den subalpine sonen ble med denne metoden nøyaktig estimert. Kombinering av tredimensjonal og spektral informasjon kan forbedre skogtaksering og skogovervåkningen under de fleste omstendigheter, men det er utfordringer og økte kostnader knyttet til å bruke kombinerte datakilder. Ulempene må vurderes opp mot fordelene ved økt tilgang på nøyaktig informasjon.

LIST OF PAPERS

I. Ørka, H.O., Næsset, E., & Bollandsås, O.M. (2009). Classifying species of individual trees by intensity and structure features derived from airborne laser scanner data. *Remote Sensing of Environment, 113*, 1163-1174

II. Ørka, H.O., Næsset, E., & Bollandsås, O.M. (2010). Effects of different sensors and leaf-on and leaf-off canopy conditions on echo distributions and individual tree properties derived from airborne laser scanning. *Remote Sensing of Environment, 114*, 1445-1461

III. Ørka, H.O., Gobakken, T., Næsset, E., Ene, L., & Lien, V. (submitted). Improving airborne laser scanning tree species identification utilizing intensity normalization and multispectral imagery.

IV. Ørka, H.O., Wulder, M.A., Gobakken, T., & Næsset, E. (submitted). Subalpine zone delineation using LiDAR and Landsat imagery.

Synopsis

1. INTRODUCTION

Knowledge about the state and development of forests is crucial for sustainable forest management and decision making at different spatial scales. Forest managers require information about individual trees, forest stands and the forest property. Information on forest biophysical properties such as volume, stem density, mean height and basal area distributed on tree species provide the basis for forest management planning. Public administration and policy makers need information about the forest resources on an administrative scale for the implementation, evaluation and development of forest policies. Administrative units could be the entire nation or regions within the nation. Today, reporting according to international conventions and agreements, particularly in relation to climate change, has increased the need for forest information on a national level.

To obtain the required forest resource information a forest inventory is carried out, with the spatial scale of interest either being an individual tree, a stand, a region or an entire nation. Terrestrial surveys have and continue to be important in forest inventories. The first surveys utilized visual estimation of forest resources. During the 19th and beginning of the 20th centuries objective measurements, the use of sampling techniques and developments in mathematical statistics increased the accuracy of forest inventories (Loetsch & Haller, 1964). In addition, progress in the field of forest inventory has benefited from the development in remote sensing, which started in Germany in the 1920s (Loetsch & Haller, 1964). The dominant remotely sensed data source over the ensuing 80 to 90 years has been aerial imagery, which provides both spectral information and information about the horizontal structure of the forests (Figure 1). Photo interpretation of aerial imagery has been utilized for stand delineation and derivation of certain forest attributes (Magnusson et al., 2007). As opposed to non-stereo aerial imagery, laser remote sensing has the capability to provide direct three-dimensional measurements of the forest canopy, including information about both the horizontal and vertical structure of forests. Over the past decade, the use of three-dimensional data from airborne laser scanning (ALS) in forest inventory has become operational (Næsset, 2004). The three-dimensional measurements taken by ALS appear as a number of dense xyz coordinates (0.1 - < 10 m^{-2}) referred to as a point cloud (Figure 1). Such three-dimensional information has significantly improved the efficiency of forest stand inventories (Eid et al., 2004). Forest inventories supported by ALS is now the dominant method for obtaining forest resource information at the stand level within the Nordic countries, and is also becoming more and more used elsewhere. Furthermore, ALS is under development to support forest

inventories on the individual tree (Persson et al., 2002) and regional levels as well (Næsset et al., 2009).

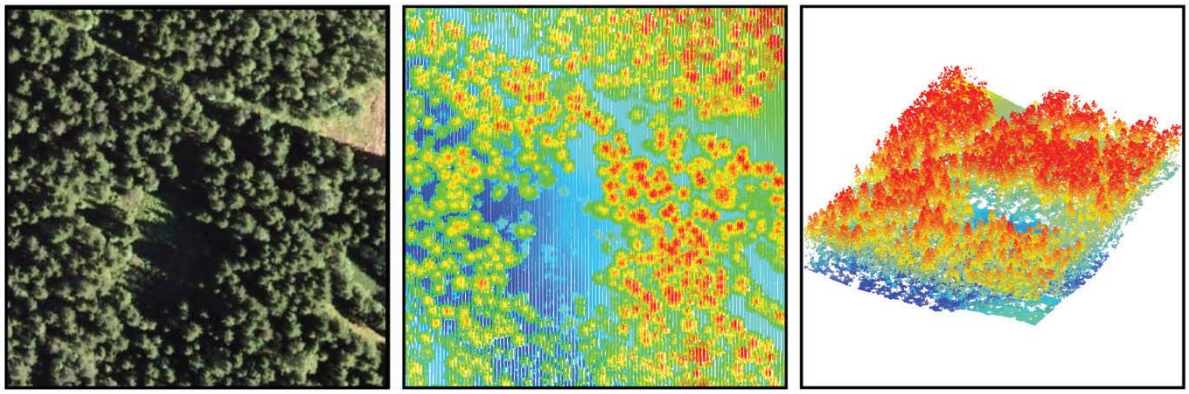

Figure 1 - Illustration of spectral information in natural colors acquired by an aerial digital camera (left) and three-dimensional information acquired using ALS (middle) from the same forested area. The right illustration shows the three-dimensional information from the same area in a side view. In the ALS illustrations, height (*z*) values are increasing from blue to red through green and yellow.

Comparisons of ALS with other remote sensing methods such as RaDAR (RAdio Detection And Ranging) (Huang et al., 2009; Hyde et al., 2006; Hyde et al., 2007; Nelson et al., 2007) and optical sensors (Hyde et al., 2006; Hyyppä & Hyyppä, 1999; Lefsky et al., 2001) have revealed that airborne laser is among the most capable remote sensing techniques in terms of accuracy for essential forest properties such as height, volume and biomass. RaDAR is also capable of capturing three-dimensional information, but faces the problem of saturation at certain biomass levels (20 - 250 Mg ha^{-1}), which does not seem to be a problem when utilizing lasers (Balzter, 2001; Drake et al., 2002; Patenaude et al., 2005). Photo interpretation of stereo imagery also provides three-dimensional measurements, though the accuracy of important inventory properties is lower than when using ALS (Eid & Næsset, 1998; Magnusson et al., 2007). As a result, when considering the accuracy of forest biophysical properties, ALS is the first choice in forest inventory and monitoring. Although ALS-based forest inventories provide high accuracies of forest biophysical properties, we face a few challenges when using ALS in relation to: 1) providing information about tree species, 2) providing wall-to-wall map products in large area forest inventories, and 3) in forest monitoring due to challenges with multi-temporal datasets.

Information about tree species is an important parameter for forest inventories, although it is still not easily obtained from three-dimensional ALS data (McRoberts et al., 2010). Since crown allometry, branches, leaf structure, etc. differ among species, the three-dimensional point cloud obtained from ALS may have different characteristics for different tree species. One obvious example is the differences between spruce and birch. Spruce

crowns tend to be more conical while birch is more elliptical, whereas the branches and leaves of spruce and birch exhibit differences as well. Additionally, spectral information is known to offer species information (Brandtberg, 2002; Carleer & Wolff, 2004; Key et al., 2001), especially the differences between coniferous and deciduous trees in near infrared wavelengths is well known. These two sources of information may be seen as complementary because three-dimensional data provide the structural characteristics and spectral data reflectance characteristics of tree species. Thus, combining three-dimensional and spectral information may improve tree species identification in comparison to only using three-dimensional data.

The use of airborne sensors for large area inventory is limited by the high acquisition costs. Hence, a strategy for using ALS in large area forest inventories is to sample the area using ALS and then utilize sampling theory to provide estimates for the biophysical properties of interests, e.g. utilize ALS as a strip sampling tool (Næsset et al., 2009). Therefore, no wall-to-wall map products can be presented which cover the entire area. In terms of medium spatial resolution satellite imagery, spectral information provides large area cover with appropriate spatial resolution at limited cost, which has relevance for many forestry applications (c.f. Cohen & Goward, 2004; Wulder, 1998). Utilizing such spectral information, together with ALS as a strip sampling tool, could provide additional information to large area inventories. The subalpine zone – the area between the forest and alpine vegetation communities – is an example of an area in which the demand for information is increasing. Substantial changes in the position and extent of the subalpine zone are expected as a result of a warmer climate. Today, low productivity or non-merchantable forests, such as those forests found in the subalpine zone, are not routinely subject to inventory programs in many countries. Combining remotely sensed three-dimensional and spectral information to map the subalpine zone is highly relevant because of the high field inventory costs in remote mountainous areas.

So far, the utilization of ALS in forest monitoring is not very common. The primary reason for this is that monitoring is conducted at time intervals of 5 to 10 years, which corresponds to the period that ALS has thus far been used in forest inventory (Næsset, 2004). Consequently, ALS has yet to be developed for such tasks, though a few examples of forest monitoring using ALS over short time intervals does exist (e.g. Næsset & Gobakken, 2005; Solberg et al., 2006b; Yu et al., 2004; Yu et al., 2006). However, the analyses carried out in these studies might better be referred to as change detection, or change estimation, than monitoring. Forest monitoring, change detection or change estimation using multi-temporal

ALS data will without doubt be more common in the future. Even so, using multi-temporal ALS datasets remains a challenge, as the lifespan of ALS sensors is often less than four years. Monitoring programs often revisit areas after 5 to 10 years if no special events have occurred. In most cases, ALS data available for monitoring will therefore originate from different sensors. Technological developments in ALS sensors have advanced quite quickly, and sensor specifications and functionality are also rapidly changing. Over time, changes in sensors' specifications and functionality may result in point clouds with highly different properties compared to previous campaigns. Moreover, seasonal differences, for example in relation to the phenology of trees, may also impact the properties of the point cloud. Such seasonal differences are well-known for influencing remotely sensed imagery (Jensen, 2000). The most extreme seasonal changes are those in the canopy conditions of deciduous trees between winter and summer (leaf-on/leaf-off). Systematical shifts in estimated properties caused by changing sensor properties or seasonal differences could exert an influence on conclusions inferred from multi-temporal observations by either under or overestimating the true changes, thereby alternatively making the changes undetectable. When both the three-dimensional and spectral information are utilized multi-temporally, both sources of information must be evaluated based on differences between sensors and seasons. This area has been little covered in scientific literature, and it is necessary to quantify the differences in the point clouds between multi-temporal datasets, and how such differences influence forest inventory estimates, before ALS can be implemented in forest monitoring applications.

In the three specific cases discussed above, in which three-dimensional data from ALS have limitations in forest inventory, the combination of ALS with spectral information may improve the capabilities, but also challenges, of such inventories. A combination of using different remote sensing sources is also referred to as data fusion, and is well-known in image remote sensing (Pohl & van Genderen, 1998). Expectations for the potential of combining ALS and spectral information were high 10 years ago, and were characterized as bringing airborne data acquisition to a new "revolutionary" level (Ackermann, 1999). In this thesis, I have investigated the potential for combining three-dimensional and spectral information in forest inventory and the resultant challenges from the use of such multi-temporal information. The three-dimensional data used in the current thesis is the point cloud obtained from ALS. The spectral information tested comes from various sources, including the spectral information recorded by ALS for each three-dimensional coordinate. The monospectral signal recorded by ALS is referred to as the intensity, which is a measure of the energy recorded by the sensor from the backscattered signal. Aerial and satellite imagery are

two other sources of spectral information investigated. Such imagery is multispectral, meaning that reflectance is recorded for multiple electromagnetic wavelengths. Typically, reflectance values are recorded for the visible portion of light, e.g. red, green and blue, in addition to infrared reflectance in such multispectral sensors.

The main objective of this thesis was to investigate the potential of combining remotely sensed three-dimensional and spectral information for forest inventory and monitoring purposes. In order to achieve this, the specific objectives of the thesis concentrate on: 1) individual tree species identification using three-dimensional and intensity information from ALS (Papers I, II & III), 2) combining three-dimensional measurements from ALS with digital multispectral aerial images for tree species identification (Paper III), 3) combining three-dimensional measurements from ALS and medium spatial resolution multispectral satellite images for providing a wall-to-wall map of the subalpine zone (Paper IV), and 4) studying the effects of different sensors and seasons on the ALS measurements, which is highly relevant for an assessment of how ALS data can best be used for forest monitoring purposes (Paper II and part of Paper III). Figure 2 illustrates the relationship between the specific objectives and individual papers of this thesis.

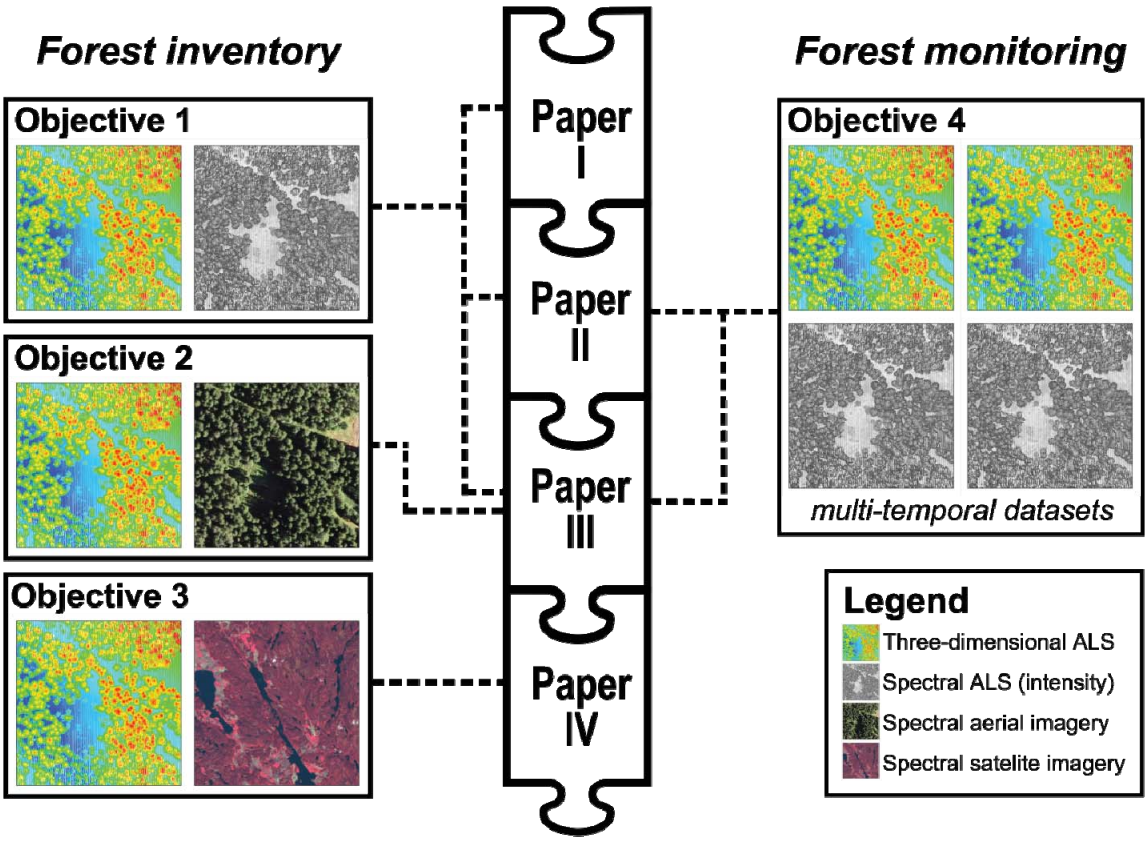

Figure 2 – The relationship between the specific objectives, papers and data sources brought together in the current thesis

2. BACKGROUND

2.1. Approaches for combining three-dimensional and spectral information

The combining of various data sources is a strategy to improve the accuracy of remote sensing products. Different approaches for data fusion are described in the literature. Hutchinson (1982) presented approaches for combining map-based ancillary data (e.g. maps of geology, soils, vegetation or topography) and spectral satellite information. In addition, Pohl and van Genderen (1998) review various approaches for combining the imagery of different spatial, temporal and spectral resolutions. Many of the approaches described by Hutchinson (1982) and Pohl and van Genderen (1998) may be directly used when combining the three-dimensional information obtained from ALS with spectral information. Table 1 summarizes these approaches in relation to the combining of three-dimensional and spectral information, and examples of the different approaches utilized in forest inventory are presented.

Table 1 - Overview of approaches utilized for combining three-dimensional and spectral information in forest inventory

Approach	Description	Example reference
Information level	Process data source individually for information extraction.	Koukoulas & Blackburn (2005)
Model inclusion	Three-dimensional and spectral data are both included in models, e.g. used for the prediction or classification of forest or tree properties.	Hyde et al. (2006) Schreier et al. (1985)
Extrapolation	Relationships between three-dimensional estimates of forest properties and spectral derived variables are established and used to create predictions over an area larger than the extent of the ALS data.	Hudak et al. (2002) Wulder & Seemann (2003)
Stratification	One data source is used to produce strata, e.g. for laser model development or area estimation in sample-based approaches.	Næsset (2004) Nelson et al. (2004)
Post-classification	Biophysical forest properties are predicted using one data source. They are further distributed with the estimates from another data source, e.g. ALS estimated volume is distributed for tree species based on the species' proportions obtained from spectral information.	Packalén & Maltamo (2006)

2.2. Three-dimensional information for forest inventory

ALS is a remote sensing method operated from an aircraft based on LIght Detection And Ranging (LiDAR) technology. LiDAR is also known as laser altimetry and is operated from

multiple platforms, including aircrafts such as airplanes and helicopters. In addition, LiDAR systems operated on the ground are referred to as terrestrial LiDAR and those carried by satellites are known as spaceborne LiDAR. Moreover, various technical implementations using LiDAR exist and are used in forestry applications.

LiDAR technology is an active method which means that it emits light. The light emitted by airborne LiDAR sensors is usually a short, 10 ns (3 m), infrared pulse (Baltsavias, 1999). The main principle of LiDAR is ranging, with pulse ranging being the most common method used, although other methods also exist (Wehr & Lohr, 1999). In pulse ranging, the distance between the sensor and the target is determined by converting the elapsed time between emission and detection of a pulse by the sensor to a range by multiplying half the travel time with the speed of light (3×10^8 m s^{-1}). Furthermore, the emitted pulse is georeferenced such that the position of the target can be determined. One such measurement will appear as an xyz coordinate in the laser point cloud (Figure 1). A single point represented by the x, y, z coordinates is referred to as an echo. With airborne sensors, the georeferencing of the emitted pulse is achieved by global navigation satellite systems (GNSS) and inertial navigation systems (INS).

When the emitted pulse hits a surface it will cover a specific area, which is called the laser "footprint." Based on a specific footprint size obtained with a system, the system can be classified as small footprint (< 1 m) and large footprint (> 5 m) LiDAR. The large footprint systems are research systems primarily developed to support satellite missions (Blair et al., 1994; Blair et al., 1999). Small footprint sensors were originally developed for topographic mapping, which is still the most important application of small footprint LiDARs. LiDAR systems can be grouped into discrete return (DR) or full-waveform recording (FW) sensors. The information recorded by LiDARs differs between DR and FW sensors. DR sensors typically record one to four echoes or height measurements per emitted pulse based on the backscattered light. In contrast, FW sensors record the entire backscattered energy in narrow bins. FW systems typically record backscattered energy at a rate of 0.5–2 ns, which is equivalent to 15–60 cm vertical bins. The majority of large footprint systems are FW systems. Additionally, the first small footprint systems used in forestry were FW sensors (Aldred & Bonnor, 1985; Nilsson, 1996). Today, the majority of commercial ALS sensors available are small footprint DR sensors. Small footprint FW systems were not commercially available until 2004 (Mallet & Bretar, 2009).

Moreover, LiDARs may be grouped into profiling systems and scanning systems. A scanning system has a scanning device which distributes the emitted pulses in different

directions so that a corridor beneath the aircraft is covered. Overlapping parallel flight lines enable wall-to-wall mapping of an area. A profiling LiDAR only provides xyz data from a narrow strip directly underneath the aircraft, creating height profiles across the landscape. The first LiDARs developed were profiling systems. Nowadays, scanning systems dominate forest inventory. In the current thesis, the LiDAR technology and system used are small footprint discrete return airborne scanning sensors.

To the best of my knowledge, the first published attempts to use airborne lasers to measure forests was conducted three decades ago by the Leningrad Scientific Research Institute of Forestry in the Soviet Union (Solodukhin et al., 1977). In the beginning of the 1980s similar studies were conducted in North America (Aldred & Bonnor, 1985; Nelson et al., 1984). Forest properties such as tree height, biomass and stem volume were estimated highly accurately by airborne lasers (Aldred & Bonnor, 1985; Maclean & Krabill, 1986; Nelson et al., 1984; Nelson et al., 1988).

Forest inventory using ALS has been operational since 2002 (Næsset, 2004). The ALS-based forest inventory first implemented in Norway is referred to as the area-based method. The target for this method is to provide accurate estimates of biophysical properties on the stand level. The method uses a two stage approach in which stand delineation and pre-stratification are obtained from photo interpretation of aerial images. Field measurements of forest properties from accurately georeferenced sample plots are related to three-dimensional measurements taken from exactly the same area, and prediction models are developed. The entire area of interest is gridded into gird cells that are the same size as the sample plots. The three-dimensional measurements inside each of these grid cells and prediction models developed are exploited to estimate the biophysical property of interest. The predicted values for all grid cells within a stand are then summarized to obtain stand values.

Another concept is to base the inventory on the identification and characterization of individual trees in the inventory area of interest The potential of such individual tree methods has been demonstrated in a number of studies in which properties such as tree position, tree height and tree volume have been accurately predicted, at least as far as dominant trees are concerned (Maltamo et al., 2004; Persson et al., 2002; Solberg et al., 2006a). Individual tree methods are used operationally and have been commercially available from at least 2006 (Johansson, 2007). However, a major problem for individual tree methods is that only dominant trees (or co-dominant) can be identified. Studies have shown that approximately 50% of trees are indentified in heterogeneous forests and about 75% in more homogeneous forests (Persson et al., 2002; Solberg et al., 2006a). Another drawback is that this method

requires high pulse density ALS data, which thereby increases costs compared to the area-based method. The advantages of individual tree methods is that less field data for calibration is required and that additional information about the forests can be gained, which otherwise may be hard to obtain in an economically feasible way (Hyyppä et al., 2008).

Hybrid methods concerning a combination of area-based and individual tree-based methods also exist. The most frequently used hybrid inventory methods are based on measurements of individual tree properties using ALS and then aggregating this individual tree information over plots or stands (Breidenbach et al., 2010; Hyyppä et al., 2001; Popescu et al., 2002). More information-driven approaches, e.g. utilizing both methods to provide supplementary information or utilizing individual tree methods in specific stands of high economical value, are yet not common according to my understanding.

For large area inventories covering counties, states or provinces, LiDAR may be used as a sampling tool. The first regional forest inventory with LiDAR was conducted in Delaware in the US (Nelson et al., 2003a). In the Delaware study, a profiling LiDAR was operated. Airborne profiling lasers have proven their capability in establishing regional estimates of biomass and carbon at both the state and provincial levels (Boudreau et al., 2008; Nelson et al., 2004). Such sampling-based applications utilizing data from ALS have recently been demonstrated along with the development of statistical estimators required to yield statistically sound estimates for the area in question (Andersen et al., 2009; Gregoire et al., 2011; Ståhl et al., 2011).

2.3. Monospectral information from ALS: intensity

In addition to the three-dimensional information, most ALS systems record spectral information based on the backscattered laser signal (Wehr & Lohr, 1999). This spectral information is frequently referred to as intensity. For discrete return lasers, intensity often represents the peak amplitude of the returned pulse. However, sensor algorithms for both echo triggering and intensity recordings are proprietary to the sensor vendors, and accurate descriptions of the intensity recordings are normally not available. The intensity captured by current commercial LiDAR systems offers a radiometric resolution of 8-bit, 12-bit or 16-bit (Höfle & Pfeifer, 2007). The wavelength of the emitted pulse and the subsequent recorded wavelength is 1064 nm in most commercial LiDAR systems used for forestry applications. The main focus of LiDAR sensor vendors has been to provide accurate three-dimensional measurements for topographic mapping. Hence, the intensity recorded has been of little interest, although a decade ago researchers began to explore the possibilities of utilizing this

information for forest inventory purposes (Brandtberg et al., 2003; Holmgren & Persson, 2004).

The main reason for the limited use of intensity is that the intensity provided by ALS is noisy. The recorded intensity value is dependent on many factors, such as the range from sensor to target, incidence angle, atmospheric transmittance and transmitted power (Ahokas et al., 2006; Wagner et al., 2006). Calibration or normalization of the intensity to remove noise associated with some of these factors is suggested as being necessary to fully employ the potential of intensity data (Ahokas et al., 2006). Calibration methods based on both physical and more data-driven approaches are suggested (Ahokas et al., 2006; Coren & Sterzai, 2006; Höfle & Pfeifer, 2007). Of all the previously mentioned factors, normalization based on the range from the sensor to the target, known as range normalization, is the most mature. Methods to normalize intensity caused by sensors specific properties have been developed, e.g. normalization based on the Automatic Gain Control of Leica sensors (Korpela, 2008) and for the differences in intensity between scan directions in Optech Airborne Laser Terrain Mappers (ALTM) sensors, which is referred to as banding (Paper III).

The use of intensity was demonstrated for discrimination between coniferous and deciduous trees as far back as 1985 (Schreier et al., 1985). Since the pioneering study by Schreier et al. (1985), the use of intensity has been little explored up until a few years ago (Hyyppä et al., 2008). Intensity has shown potential in forest inventory for improving biophysical properties following the area-based method (Hudak et al., 2006; Lim et al., 2003) and individual tree methods (Vauhkonen et al., 2010), both with raw and normalized intensities (Kim et al., 2009a; Korpela et al., 2010). The use of range normalized intensity provided more accurate predictions of biomass fractions (total aboveground, branches and foliage) than models utilizing three-dimensional information following the area-based method (Garcia et al., 2010). In addition, intensity was utilized to estimate live and dead biomass in mixed coniferous forests in the US, with the intensity being of vital importance for the estimation of dead biomass (Kim et al., 2009b). In a study by Hudak et al. (2006), the combination of three-dimensional and intensity variables had a higher accuracy than those methods only using three-dimensional variables when modeling basal area following the area-based method. Hudak et al. (2006) also reported that tree density was better estimated by only utilizing intensity, rather than three-dimensional variables. A large number of studies include both three-dimensional and intensity variables in tree species identification of individual trees (See Table 1, Paper III). Morsdorf et al. (2010) expanded the individual tree species identification approach and demonstrated the use of intensity and three-dimensional

information to discriminate between different vegetation strata in a multilayered forest. Plot level species proportions have been reported to be more accurate when estimated with intensity as opposed to three-dimensional data (Donoghue et al., 2007). Furthermore, intensity has be utilized for discerning age classes (Farid et al., 2006a; Farid et al., 2006b), in land-cover classification (Antonarakis et al., 2008; Brennan & Webster, 2006), in lichen classification (Korpela, 2008), in mire-type classification (Korpela et al., 2009) and in forest fractional cover models (Hopkinson & Chasmer, 2009).

2.4. Spectral information from aerial imagery

Aerial imagery was the first remote sensing technology utilized in forest inventory. Based on photo interpretation, various forest properties could be estimated. For a long time analog photographs were used in forest inventory. At the end of the last century aerial imagery became digital, thereby increasing the possibilities for the automated processing of such imagery without first digitizing them by scanning them. Operational forest inventory following the area-based method still benefits from stand delineation and pre-stratification obtained by means of photo interpretation. It has been suggested to obtain stand delineation from ALS or multispectral images by automated methods. However, the combination of laser derived canopy height models and aerial images does not seem to improve forest stand delineation in comparison to only using ALS data or aerial imagery (Mustonen et al., 2008). Although Mustonen et al. (2008) reported that three-dimensional information was highly usable for stand delineation, photo interpretation is still the dominant technique for stand delineation in area-based ALS inventories.

Furthermore, aerial imagery has been a powerful tool in terms of obtaining species information. In Finland, the demand for species-specific information at the stand level has resulted in a large focus on developing the area-based method to provide such information. The inclusion of aerial imagery has been important since imagery is already needed for photo interpretation. Species-specific stand attributes such as volume, stem number, basal area, basal area median diameter, tree height and diameter distributions were predicted using variables derived from ALS and aerial imagery (Packalén & Maltamo, 2006, 2007, 2008). Direct inclusion of spectral variables was utilized in these studies. In an improved procedure for combining ALS and aerial imagery, the accuracy obtained was higher when compared to only using three-dimensional information from ALS (Packalén et al., 2009).

Moreover, integration of airborne hyperspectral imagery and airborne LiDAR improved estimation of the basal area, above-ground biomass and quadratic stem diameter in

a northern temperate forest in US (Anderson et al., 2008). The increase in variation explained was 8-9% and errors were 5-8% lower than when using individual sensors.

Utilizing multispectral imagery as stratification information in an ALS-based tree identification approach improved tree height, volume and biomass estimates for pine trees, though not for deciduous trees (Popescu & Wynne, 2004; Popescu et al., 2004). In another hybrid inventory system, multispectral image variables were directly used in the prediction of species-specific timber volume (Breidenbach et al., 2010). However, this study did not provide any comparisons with the use of three-dimensional data as the sole remote sensing data.

Moreover, the accuracy of identification for Scots pine, Norway spruce and deciduous trees was improved by a combination of laser (both three-dimensional and intensity) and multispectral images acquired in summer and autumn. The improvements compared to only using laser were 5 and 8 percentage points for the summer and autumn acquisition, respectively (Holmgren et al., 2008). Other studies have reported improvements by combining three-dimensional and multispectral data in the identification of individual tree species without presenting direct comparisons (Heinzel et al., 2008; Persson et al., 2004).

2.5. Spectral information from satellite imagery

Spectral information from satellites has been available ever since the launch of the first Landsat satellite in 1972. The Landsat program has developed since then, and a total of six satellites have been delivering spectral information of the earth's surface on a routinely and systematic basis. In addition to the Landsat program, a number of satellites have been launched and delivered information in a variety of spatial, spectral, radiometric and temporal resolutions. Satellite images are often classified after the spatial resolution of images by the Ground Sampling Distance (GSD). Satellite imagery with a GSD of less than 10 m is referred to as high spatial resolution (HSR) imagery. Medium spatial resolution satellite (MSR) imagery has a GSD of 10 – 100 m, whereas coarse spatial resolution (CSR) imagery has a GSD of 100s to 1000s of meters (Franklin & Wulder, 2002).

HSR satellites are now able to deliver centimeter scale imagery, thus making such imagery more and more equal to imagery acquired from digital airborne sensors. As a result, HSR satellite imagery has nearly the same range of application as airborne imagery in forest inventory. For example, HSR satellite imagery can be utilized in individual tree inventory (Gougeon & Leckie, 2006; Wulder et al., 2004) to help support forest stand delineation (Wulder et al., 2008b) and facilitate estimation of biophysical forest properties (Mora et al.,

2010a; Mora et al., 2010b). Although the availability of HSR satellite imagery has increased over the last few years, there are few examples of the combination of such information and laser data. The combination of three-dimensional ALS and spectral information from the QuickBird satellite was used to delineate stand boundaries and classify tree species within these stands. Both stand delineation and tree species identification were improved by combining the two data sources as compared to using either of them separately (Ke et al., 2010). Additionally, the combination of spectral information from QuickBird and ALS improved the accuracy of canopy height estimates by 5.4 – 6.8% compared to only using laser variables (Hyde et al., 2006). Still, biomass prediction was not improved using additional variables derived from the QuickBird sensor (Hyde et al., 2006). Another suggested application is to update forest inventory data using a laser operated as a sampling tool and HSR imagery (Hilker et al., 2008).

MSR satellite images have been important through the provision of data with sufficient spatial detail over large areas at low cost in order to meet a range of information needs (Cohen & Goward, 2004; Falkowski et al., 2009). The opening of the United States Geological Survey (USGS) Landsat archive to provide free data (Woodcock et al., 2008) has further accentuated the use of this data. Although MSR imagery is suggested to be inappropriate for supporting forest planning (Holmgren & Thuresson, 1998), a range of forestry applications is presented in the literature. To provide wall-to-wall maps of forest resources and obtaining forest statistics of small areas in national forest inventories, is among its more important applications (Tomppo et al., 2008). Furthermore, MSR imagery is the far most common satellite data used in combination with laser data for forest inventory. The combination of variables from Landsat and LiDAR yielded the most accurate estimates of canopy height and biomass in a North American study investigating multi-sensor synergy (Hyde et al., 2006). The improvements in canopy height estimation were 12.3 - 14.0% when compared to only using LiDAR, and the corresponding improvement for biomass was 1.4%. This accuracy was better than combining ALS data with either HSR QuickBird imagery, InSAR data or both (Hyde et al., 2006). By using the Advanced Land Imager (ALI) on board the Earth Observation 1 (EO-1) satellite, estimates of basal area and tree density were improved compared to only using LiDAR at 11.7% and 4.1%, respectively (Hudak et al., 2006).

Furthermore, various methods for predicting canopy height from laser and Landsat using extrapolation (c.f. Table 1) were presented by Hudak et al. (2002). Both aspatial (regression) and spatial (kriging, co-kriging) methods for prediction were tested, and an

integrated technique of ordinary co-kriging and ordinary least squares regression proved to be the best method for estimating and mapping canopy height. Hudak et al. (2002) also tested different sampling approaches which could be used, and concluded that a 250 m spacing of point samples was the best approach for the tested methods. Extrapolation using a LiDAR sample covering a small area and full coverage MSR spectral data are common. Wulder and Seemann (2003) extended laser estimates of height from a sample using a profiling large footprint LiDAR to a larger area using segmented Landsat imagery. The segmented Landsat imagery was created based on spatial and spectral variables. Based on empirical relationships between laser estimated canopy height and spectral values of segments, the canopy height was estimated for an entire landscape based on a laser sample covering 0.48% of the area. The accuracy of the final model as expressed by the coefficient of variation (R^2) and standard error (SE), was 0.67 and 3.3 m, respectively. Similarly, segmented Landsat imagery and a 600 km transect of profiling laser from 1997 and 2002 were used to characterize various changes in a boreal forest at the image segment level, and both growth- and disturbance-related changes were identified (Wulder et al., 2007b). Imagery from the Indian remote sensing satellite and the k-NN technique were used to extend canopy height predictions from laser to cover a larger area in Scotland, obtaining accuracies of 2 – 31% (RMSE) (McInerney et al., 2010). Moreover, MSR satellite imagery plays an important role in stratification in large area inventories in which lasers are used as sampling tools (Næsset et al., 2009; Nelson et al., 2003b; Nelson et al., 2004).

Also, spectral information from CSR imagery and three-dimensional LiDAR data have been combined to provide global forest resource maps. Lefsky (2010) provided the first global map of canopy height using the Moderate Resolution Imaging Spectroradiometer (MODIS) and the Geoscience Laser Altimeter System (GLAS). In the study by Lefsky (2010), MODIS represented the full coverage of spectral information and GLAS provided three-dimensional data from worldwide samples, with a footprint of approximately 65 meters.

3. MATERIALS

3.1. Study areas

Three study areas were used in the current thesis: 1) Østmarka forest reserve (18 km^2), 2) the municipality of Aurskog-Høland (890 km^2), and 3) the county of Hedmark (27,400 km^2). All study areas were located in southeastern Norway (Figure 1), which is the main forestry area in Norway, with most of the forest under management. The dominant vegetation zone is the boreal forest (Olson et al., 2001). However, Østmarka forest reserve and Aurskog-Høland are

located at the northern border of a "temperate broadleaf and mixed forest" (Olson et al., 2001). Hence, hardwood trees are found scattered throughout the landscape, particularly on southern facing slopes. In Hedmark, the boreal forest is diminishing at higher altitudes where alpine and tundra vegetation zones occupy the area. The annual precipitation in the area is between 400 – 700 mm year,[1] with the highest levels on the coast as they start to decrease towards the interior (Moen, 1999). The average annual temperature is between -2 º and 5º C (Moen, 1999).

Figure 2 - Map of the three study areas;
Østmarka forest reserve, municipality of *Aurskog-Høland* and the county of *Hedmark*

3.2. Field data

Field data were collected at 28, 40 and 26 locations in Østmarka, Aurskog-Høland and Hedmark, respectively. In Østmarka and Aurskog-Høland, field data were collected to support analyses on the individual tree level. Therefore, tree positions and individual tree

properties were recorded. The field work in Østmarka was carried out during the summer of 2003, while the field measurements in Aurskog-Høland were carried out during the autumn of 2007 and the winter of 2008. The sample plots were positioned with differential Global Navigation Satellite Systems (dGNSS), and the mean positional accuracy was approximately 12 cm. The plot size was 1000 m^2 for all plots except for four plots in Aurskog-Høland, which were 500 m^2 in size. Tree positions were measured as polar coordinates from the plot center with a tape measure and compass in Østmarka, and with a total station in Aurskog-Høland. Tree properties were recorded for 435 sample trees in Østmarka and 4,299 trees in Aurskog-Høland. The stem diameter and tree species were registered for all trees. In Østmarka, crown radii and tree heights were also measured.

In Hedmark, the overall goal was to provide a wall-to-wall map of the subalpine zone. The boundaries of the subalpine zone (the forest and tree lines) were mapped at 26 subjectively selected locations during the summer of 2008. At all locations, both the forest and tree lines were digitized using handheld GPS attached to a PDA, and ALS data were also acquired for all locations. For additional information and a description of the field data collection, see the individual papers.

3.3. Remote sensing data

Three-dimensional data were collected at all sites with ALS, using different Optech Airborne Laser Terrain Mappers (ALTM). The Optech ALTM sensors recorded spectral information by means of laser intensity in addition to the three-dimensional coordinates. Furthermore, spectral information was available by multispectral digital aerial images acquired in Aurskog-Høland with Vexcel Ultracam D and Applanix Digital Sensor System sensors. Finally, spectral information by means of Landsat satellite imagery covering Hedmark was utilized for mapping of the subalpine zone. A list of the sensors and acquisition settings for the remote sensing data used in the current thesis appear in Table 2.

4. METHODS

The analysis and statistical methods used on individual tree crown segments and grid cells included exploratory data analysis, linear models and various parametric and non-parametric classification methods. Explorative data analysis was comprised of data visualization by means of probability density and box-and-whisker plots, while linear models included analysis of covariance models (ANCOVA), linear mixed effects models and general linear models. Classification methods were utilized in all papers and consisted of heuristic

Table 2 - Sensor and acquisition settings for remote sensing data

	Study area	Østmarka			Aurskog-Høland			Hedmark	
	Paper	I, II	II	II	III		III	IV	IV
Acquisition settings	Date of acquisition	06.18.2005	04.17.2005	10.09.2003	06.12.2006		06.29.2005	Summer 2006	06.03.2007 06.10.2007
	Platform	Piper Navajo fixed-wing	Piper Navajo fixed-wing	Hughes 500 helicopter	Piper Navajo fixed-wing		Piper Navajo fixed-wing	Piper Navajo fixed-wing	Landsat 5 satellite
	Canopy conditions	leaf-on	leaf-off	leaf-on	leaf-on		leaf-on	leaf-on	leaf-on
	Flying altitude (m)	750	750	600	800		3,100	800	705,000
	Flying speed (ms^{-1})	75	75	35	75		80	75	-
Sensor settings	Sensor	Optech ALTM 3100	Optech ALTM 3100	Optech ALTM 1233	Optech ALTM 3100	Applanix DSS	Vexcel UltraCam D	Optech ALTM 3100	TM
	Range capture (no. of echoes)	1-4	1-4	2	1-4	-	-	1-4	-
	Pulse repletion frequency (kHz)	100	100	33	100	-	-	100	-
	Scan frequency	70	70	50	70	-	-	55	-
	Mean pulse density (m^{-2})	5.1	5.1	5.0	7.2	-	-	2.7	-
	Resolution (m)[a]	0.21	0.21	0.18	0.25	0.12	0.275/0.84	0.21	28.5
	Wavelength(s) (nm)	1064	1064	1064	1064	500-600 600-700 800-960	390-690 390-530 470-660 570-690 670-940	1064	450-520 520-600 630-690 760-900 1550-1750 2080-2350
	Lens (mm)	-	-	-	-	60	101.4	-	-

[a] Resolution refers to the footprint size of ALS data and the ground sampling distance (GSD) for image data.

classification, linear discriminant analysis (LDA), binomial logistic regression, support vector machines (SVM) and classification and regression trees (CART).

In Papers I, II and III, information from intensity and aerial multispectral imagery was directly included in models for identifying species at an individual tree level. In Østmarka, raw intensity values were used because sufficient information to normalize the intensity values was lacking. In Aurskog-Høland, the intensities were normalized for two effects (range and banding). Furthermore, multispectral information was tied to the xyz coordinates from the first returns in Aurskog-Høland, utilizing the method described by Packalén et al. (2009). In the method by Packalén et al. (2009) multispectral information is transferred to xyz coordinates as attributes using the interior and exterior orientation parameters of the image sensor. In Østmarka and Aurskog-Høland, the laser echoes and spectral attributes were tied to individual trees. In Østmarka, field measurements of tree positions, crown radii and the assumption of circular crowns were used to tie echoes to individual trees. In Aurskog-Høland, an individual tree crown segmentation algorithm was used to tie the echoes to trees (Ene et al., in review), and from the echoes tied to individual trees, features were derived from three-dimensional and spectral information (cf. Papers I, II, and III for details). In Paper I, we carried out an analysis of covariance (ANCOVA) to investigate the potential of different features within the classification. Furthermore, the classification accuracy of single features was tested using LDA. Based on the ANCOVA and LDA, we selected features from various groups and combined them into a final classification. In Paper III, classification accuracies of groups of features were tested using cross-validation in which feature selection and classification were combined. The classification methods used were LDA, SVM, as well as a special implementation of CART referred to as random forest (Breiman, 2001). In Paper II, three-dimensional and spectral features were combined to support tree species identification without subsequent feature selection. The classification method random forest producer utilized has a built-in feature selection procedure that makes other feature selection processes prior to classification unnecessary (Breiman, 2001). The classification accuracy was assessed using an error matrix and the proportion of correctly classified trees for single species (producer's accuracy), in total (overall accuracy) and the kappa coefficient in all papers (Cohen, 1960; Story & Congalton, 1986).

Paper II focused on the challenges using multi-temporal datasets. The differences in both intensity and three-dimensional information among three different ALS acquisitions were investigated. Comparisons between all three acquisitions in Østmarka (Table 2) were carried out using explorative data analysis and two-tailed *t*-tests. In addition, relationships

between the maximum height of laser echoes inside the crown delineations and field measured tree heights were modeled with a linear mixed model. The sample plot was used as a random effect in the model due to the hierarchical data structure. Relationships both with and without a fixed tree species effect were tested. For modeling the stem diameter, a model formulation consisting of the maximum laser height inside crown delineations and the crown width, as proposed by Hyyppä et al. (2001), was utilized. Also, a mixed modeling approach was used for the stem diameter, with the sample plot as a random effect. The stem diameter model was developed with and without tree species as a fixed effect. Differences in tree species identification obtained with the random forest algorithm were evaluated using Cohen's kappa coefficient and its variance (Cohen, 1960).

In Paper IV, three-dimensional and spectral information were combined by means of extrapolation. This approach utilized proxies for the canopy cover of trees and shrubs derived from three-dimensional ALS data. The proxies were further used in a heuristic classification to classify areas based on international definitions of forest, other wooded land and other land by the United Nations Food and Agricultural Organizations (FAO, 2006) into three cover types: 1) forest, 2) subalpine zone and 3) alpine, using tree height and canopy coverage thresholds. A sensitivity analysis was conducted to test the impact of using thresholds other than the one implicitly given by the definitions in the heuristic classification. Moreover, a binomial logistic regression was established to model the relationship between the ALS derived cover types, Landsat imagery and spatial data. A binomial response variable, in which cover type forest was set equal to 1 and cover type alpine was set equal to 0, was established. The explanatory variables in the model comprise spectral variables derived from Landsat imagery and variables derived from a digital terrain model. This approach supported the extrapolation of ALS derived cover types to the entire area in the form of a probability surface. The density estimation of all cover types supported the development of alpha-cuts to separate the probability surface into hard classes, which is necessary for area estimation. The validation of the cover type classes in the ALS data was conducted with a image gradient approach (Pitas, 2000; Wulder et al., 2007a). The binomial logistic regression classification was validated with a test dataset, resulting in an error matrix (Cohen, 1960; Story & Congalton, 1986).

5. MAJOR FINDINGS

5.1. Combining three-dimensional ALS data and intensity (Objective 1)

Both the three-dimensional and intensity information from ALS were related to tree species. The accuracies obtained with three-dimensional, intensity and combined information appear in Table 3. Used for tree species identification, the three-dimensional information derived from ALS yielded overall accuracies (percentage of trees correctly classified) of 74 – 77% for dominant trees, depending on study area and classification method. The ALS intensity alone yielded slightly lower accuracies of 63 – 73%. The accuracy increased when combining intensity and three-dimensional data with 12 percentage points in Østmarka, but a slight decrease in accuracy was observed in Aurskog-Høland. The identification of species of "Small trees" (Table 3) was most successful when only using three-dimensional data, although a fairly low accuracy was obtained (65%). In Østmarka, classification accuracies between 87 to 93% were obtained for different acquisitions when combining three-dimensional and spectral information from ALS. In specific cases such as under leaf-off canopy conditions, even higher accuracies could be obtained.

Table 3 - Overall accuracies (percentage of trees correctly classified) obtained for tree species identification in Papers I, II and III using three-dimensional ALS data (Three-dimensional) and ALS intensity (Spectral), separate and combined (Combined).

Paper	Dataset[a]	Three-dimensional	Spectral	Combined
I	Large trees	77	73	88.6
I	Small trees	65	55	63.6
II	ALTM 3100 leaf-off	-	-	97.1 - 98.1
II	ALTM 3100 leaf-on	-	-	86.9 - 90.1
II	ALTM 1233 leaf-on	-	-	90.0 - 93.4
III	ALTM 3100 leaf-on	73.9 – 76.5	63.2 – 70.8	72.0 – 75.8

[a] See respective paper for details.

5.2. Combining three-dimensional ALS data and digital aerial imagery (Objective 2)

Adding spectral information from digital aerial images improved the overall classification accuracy by 8.4 – 14.7 percentage points compared to only using three-dimensional information (Table 4). The improvements using combined data instead of image data alone was 8.6 – 14.3 percentage points. This improvement was dependent on the image sensor and classification method used. The Applanix DSS camera flown together with the ALS sensor gave a classification accuracy of 88.6%, while using the Vexcel Ultracam resulted in a slightly lower accuracy of 87.0% when combined with three-dimensional ALS data. Utilizing both intensity and image data in combination with three-dimensional ALS data did not improve tree species identification further.

Table 4 - Overall accuracies (percentage of trees correctly classified) obtained for tree species identification in Paper III using three-dimensional ALS data (Three-dimensional) and digital aerial imagery (Spectral), both separate and combined (Combined)

Paper	Dataset[a]	Three-dimensional	Spectral	Combined
III	Applanix	73.9 - 76.5	72.9 - 79.1	87.2 - 88.6
III	Vexcel	73.9 - 76.5	70.9 - 75.7	84.3 - 87.0
III	ALS[b]	-	-	72.0 - 75.8
III	Applanix + ALS[b]	-	-	84.7 - 88.3
III	Vexcel + ALS[b]	-	-	82.3 - 85.6

[a] See respective paper for details.
[b] Both three-dimensional and spectral data from ALS. See Table 3 above for details.

5.3. Combining three-dimensional ALS data and MSR satellite images (Objective 3)

The subalpine zone delineation derived from ALS proxies by a heuristic classification was found to be accurate using an image gradient technique for validation and a sensitivity analysis of the selected thresholds. An underestimation of tree height of approximately 0.5 m and a species effect on canopy coverage were identified. In the binomial logistic regression developed, the variables included in the final model were elevation, slope, latitude, normalized difference vegetation index (NDVI) and brightness from the tassel-cap transformation. The use of estimated probability density functions provided alpha-cuts to separate the probability surface into a hard classification of cover types. The overall accuracy of the hard classification was 69%. The total area covered by the subalpine zone in Hedmark was estimated to be 3660 $km^{2,}$ which represents 14% of the total area.

5.4. Effects on the multi-temporal ALS acquisitions (Objective 4)

The distributions of intensity and three-dimensional information provided by ALS differed between sensors and canopy conditions. More specifically, the laser height distributions for deciduous trees shifted towards the ground for the leaf-off acquisition of single and last (last echoes of many) echoes compared to the leaf-on acquisition. However, the first echoes (first echoes of many) was slightly higher for deciduous trees under the leaf-off canopy conditions. The three-dimensional measurements of evergreen coniferous trees (spruce) did not differ between the two acquisitions with the same sensor. However, different sensors produced significantly different height distributions and metrics in almost all cases.

The differences in raw intensity between canopy conditions were most pronounced in the first echoes, in which the intensity distribution was extremely skewed towards lower values under leaf-off compared to leaf-on canopy conditions. Even the intensity distributions of single and last echoes were affected by canopy conditions. Nonetheless, the intensity obtained using the same sensor under leaf-off and leaf-on conditions did not differ for spruce

trees. The intensity distributions acquired with different sensors diverged significantly. We observed a difference in the shape of the intensity distribution between the two sensors, particularly for deciduous trees. For deciduous trees, lower intensities were obtained with the ALTM 1233 sensor in comparison to the ALTM 3100 sensor.

Differences in the accuracy of estimated individual tree properties were minor among all three acquisitions when the models were calibrated with field measurements. However, the intercept of tree height models varied between all acquisitions, thereby suggesting that individual tree height models must be calibrated with field data to maintain accuracy. The parameters of stem diameter models did not differ significantly among the three acquisitions. Furthermore, the accuracy of tree species classification differ between sensors. Yet, a leaf-off acquisition of ALS data improved the identification of coniferous and deciduous trees by 8 percentage points.

The intensity is noisy and should be calibrated. In Aurskog-Høland, range normalization and banding normalization were both carried out. It was revealed that intensity normalization improved tree species identification by 5 – 11 percentage points compared to only using raw intensities. By comparison, range normalization was better than banding normalization, when used in the identification of tree species.

6. DISCUSSION

6.1. Tree species identification (Objective 1 and 2)

Three-dimensional information is better in terms of classification accuracy than intensity in the current thesis, and similar results have been reported in other studies under leaf-on canopy conditions (Brandtberg et al., 2003; Holmgren & Persson, 2004; Reitberger et al., 2008). Nevertheless, there are also several studies in which contradictory results have been reported. Under leaf-off conditions, intensity has been reported to contribute more than three-dimensional information in helping to identify coniferous and deciduous trees (Reitberger et al., 2008). Moreover, Korpela et al. (2010) reported that only intensity features were important for identifying boreal tree species in Finland. Consequently, a clear suggestion if either intensity or three-dimensional information is better is difficult to give. Today, the majority of ALS sensors provide intensity recordings. Thus, if intensity is delivered the opportunity to utilize both intensity and three-dimensional measurements is present. Furthermore, if intensity is to be utilized in tree species identification, the results from the current thesis, and other studies (Gatziolis, 2009; Korpela et al., 2010), indicates that the intensity should be normalized.

The current research revealed that combining intensity and three-dimensional information improved classification accuracy under certain circumstances. When considering the dominant trees in Østmarka and Aurskog-Høland, the increase in overall accuracy compared to only using three-dimensional data was 12 percentage points in Østmarka, whereas in Aurskog-Høland the overall accuracy decreased by 1 percentage point. In other studies, increases in overall accuracies up to approximately 10% have been reported (Brandtberg et al., 2003; Holmgren & Persson, 2004). Reitberger et al. (2008) obtained a large increase in accuracy by combining three-dimensional information and intensity under leaf-off, but not leaf-on conditions, though studies in which the intensity did not improve classification accuracy have also been reported (e.g. Moffiet et al., 2005). The classification accuracy obtained in tree species identification with normalized intensity from two different sensors differed by 10 percentage points in a Finnish study (Korpela et al., 2010). Hence, there are problems in providing stable improvements by intensity in classification accuracies across study areas and acquisition. Future research in the area of tree species identification using intensity should focus on the differences in accuracy obtained in different study areas and with different acquisitions to obtain more knowledge of factors affecting intensity and their normalization. The stability of classification accuracy under otherwise similar conditions is a key requirement for the operational use of intensity in forest inventory.

Spectral information from aerial imagery improved tree species classification accuracy in the current study by 9 – 13 and 11 – 15 percentage points, respectively, using the Vexcel Ultracam and the Applanix DSS the camera. Similar improvements of 5 and 8 percentage points were obtained using summer and autumn imagery from a Zeiss/Intergraph Digital Mapping Camera in a Swedish study (Holmgren et al., 2008). The study by Holmgren et al. (2008) is the only other study in addition to this thesis which has reported separate accuracies for ALS, aerial imagery, and both combined, on the individual tree level. Studies reporting improvement in species identification based on the inclusion of spectral information other than on the individual tree level have been made (e.g Jones et al., 2010; Packalén et al., 2009). The results from the current thesis indicate that aerial imagery is a more stable spectral information source than intensity for improving tree species identification. Aerial imagery is often available in most practical inventories because imagery is also used for stand delineation in most cases.

Extending the use of hyperspectral data is a highly interesting option as well. Hyperspectral data consist of many narrow and contiguous spectral bands (Shippert, 2004). The increased detail of the electromagnetic spectrum may provide information beyond what

is possible to obtain with multispectral imagery (Shippert, 2004). Additionally, refinement might also be possible using multispectral images. One possibility for refinement using multispectral images could be to only select the 10% brightest pixels inside each crown segment for use in species identification (Persson et al., 2004). Moreover, the viewing geometry of aerial imagery sensors should be better incorporated. Depending on the overlaps between images in the acquisition, a tree may be viewed from a number of various angles. Thus, the spectral response will differ depending on the viewing geometry. In extending the work of this thesis, these effects should be better accounted for.

One of the objectives in Paper I was to test different features and their suitability for species identification. It was revealed that a majority of the features derived comprised relevant information for species identification. In Paper II, we used the non-parametric random forest algorithm, which has an internal feature selection process. A comparison of the two strategies demonstrated that non-parametric techniques with no feature selection strategy yielded similar accuracies compared to using linear discrimination analysis with feature selection as in Paper I (Ørka et al., 2009). For this reason, a modified version of the feature selection strategy in Paper I was implemented in Paper III. There is the potential to further test different classification strategies (c.f. Ørka et al., 2009). Such studies must incorporate a range of different ALS acquisitions and study areas to provide general results.

Practical implementation of the approach used in Papers I, II and III is straightforward in relation to individual tree inventory. A number of sample trees with known species are necessary for model calibration. To gather detailed information on individual trees in the field is expensive, and there are some studies testing the effect on the accuracy of reducing the sample sizes (Korpela et al., 2010). However, the number of samples trees needed in an individual tree inventory is not yet clear. One option for obtaining inexpensive samples for calibration of species classification models is to use photo interpretation. Independent on how the sample data are gathered they would result in a calibrated classification model being used to assign a class to each segment. An alternative to extensive field measurement could be to utilize unsupervised classification methods which would not need field data for calibration (Ørka et al., 2009; Reitberger et al., 2008). The problem with this, however, is that unsupervised methods may not achieve the same classification accuracies (Ørka et al., 2009). Furthermore, the use of prior information from an area-based inventory might aid in the identification of individual tree species.

The possibility of more than one tree from different species in a segment is not accounted for using the method presented in the current thesis. One alternative to account for

more than one tree species per segment is to use a soft classifier, which instead of assigning a specific tree species to a specific segment assigns the probability that a specific segment belongs to a specific tree species. Another possibility is to use methods which assign "doubt" to segments for which there is a high degree of uncertainty with regard to which tree species it belongs to (Ripley, 1996). Improvements in the crown delineation algorithms, to reduce the number of segments with more than one tree, will also facilitate individual tree species identification.

Further practical issues in implementing the approach include the time of ALS acquisition and handling of trees not identified by the segmentation process. First, trees not identified by a segmentation algorithm must be classified by other means than individual tree classification. This is also relevant for suppressed or short trees (e.g. Table 3, "Small trees") which are difficult to classify by means of individual tree species classification. To identify the species of such trees the area-based method should be used supplementary to individual tree methods to provide e.g. the number of trees within different species. Second, in the current study the highest overall accuracy was achieved under leaf-off conditions, which was 8 percentage points higher than under leaf-on conditions. Other studies comparing leaf-on and leaf-off acquisitions for identification of coniferous and deciduous trees have reported 11 – 16 percentage points higher accuracies under leaf-off canopy conditions (Heurich, 2006; Reitberger et al., 2008). Consequently, the leaf-off period seems attractive for ALS acquisition when identification of coniferous and deciduous tree species is needed.

The current research has documented that the direct inclusion of three-dimensional and spectral information in tree-species identification of dominant trees provides overall accuracies along the order of 87 - 98%. Similarly, applying three-dimensional data alone provides overall accuracies for dominant trees of between 75 to 80%. Hence, spectral data provides a complementary source of information, and in combination with three-dimensional data, it seems to improve tree species identification. In any case, the use of intensity seems to be both promising and problematic, while at the moment aerial imagery seems to be a more stable spectral information source for tree species identification. The aerial imagery that was acquired simultaneously with the ALS data provided the highest accuracy in the current thesis. Consequently, multiple sensors carried on the same airborne platform should be considered in order to achieve a high accuracy for the lowest possible cost.

6.2. Large area inventory extrapolation (Objective 3)

In the current thesis, ALS and MSR satellite imagery were combined to support delineation of the subalpine zone. Extrapolation is an increasingly attractive method when used to combine high resolution and coarser resolution remotely sensed data sources. In Paper IV, extrapolation is utilized in remote mountainous areas with low biomass and little available information. The proposed method of combining ALS and MSR satellite imagery succeeded in mapping the subalpine zone in Hedmark, and provided new information for the area and extent of the subalpine zone. This example demonstrates that a combination of ALS operated as a strip sampling tool and spectral information can be utilized to derive additional spatial information in large area forest inventories without increasing field measurement costs. Similar approaches using LiDAR and extrapolation with a range of different satellite sources have been presented in other studies (see Section 2.5).

The interest for information about the subalpine zone is increasing. In a global meta-analysis by Harsch et al. (2009), half of the studied tree lines had advanced over the course of the last century. The approach presented here offers an improved capacity to map and monitor the entire area covered by forests and trees. The subalpine zone represents a part of the forest-tundra ecotone that covers large areas of the northern hemisphere. The projected change in the climate with global warming will exert a considerable impact on the extent and location of the ecotone (ACIA, 2004). Thus, approaches to support monitoring like the current is needed. Furthermore, studies of climate change may be aided by the ability to map and monitor the subalpine zone over large areas and not only at specific sites. This is desirable since the impact of climate change will likely be different among regions (Dalen & Hofgaard, 2005). In addition, changes found over time will be important for describing the change processes and the rates of transition among cover types.

The proposed approach for delineating the subalpine zone was implemented without field calibration. A heuristic classification of ALS data based on derived proxies of tree height and canopy cover was used to delineate the cover types: forest, subalpine zone and alpine areas. However, not using field calibration increases the risk of systematic errors. Validation of the approach, together with a sensitivity analysis, indicated a small systematic shift in laser height measurements, though not in canopy coverage. The systematic underestimation of tree height with lasers is well-known in the research community. Næsset (2009a) reported individual tree height underestimations in the subalpine zone in the range of 0.35 – 1.47 m in another subalpine zone area in Norway. In the study by Næsset (2009a), both sensors and tree species influenced individual tree height measurements. In the current

thesis, species composition was also found to be a source of systematic errors in the subalpine zone delineation using ALS. Canopy coverage at a spruce site was systematically underestimated. Hopkinson and Chasmer (2009) have suggested that some calibration of canopy cover proxies might be necessary. Despite the aforementioned problems, the proposed approach seems to be an attractive alternative for providing information about the subalpine zone when also taking into consideration the low implementation costs. The calibration of ALS cover type classification with field measurements could increase the accuracy of ALS delineation, but will also significantly increase costs.

In the current thesis, the accuracy obtained for classification with the binomial logistic regression model and alpha-cuts was within the range of expected accuracies in satellite image classification (Wilkinson, 2005). This study attempted to map the transition zone. Transitions are challenging in remote sensing because they are a mix of the two adjacent vegetation communities (Foody, 1996; Hill et al., 2007). In light of the high mixing that was present, the obtained accuracy was considered to be acceptable (Wilkinson, 2005). The ability of the presented method to calibrate the alpha-cuts with the ALS-derived cover type classes is attractive and extends previous alpha-cut methods used to characterize the subalpine zone (Hill et al., 2007; Ranson et al., 2004). The alpha-cut calibration was made possible by means of the heuristic classification of three-dimensional data. The possibility to use the proposed approach to produce both a probability map and hard classes increases its applicability. Hard classes derived using alpha-cuts are needed to estimate the area and extent of the subalpine zone. Furthermore, the presented probability map is more suitable for monitoring future changes in the subalpine zone than a map with hard classes (Foody, 2001).

The Landsat satellite is highly suitable for the presented approach in terms of both accessibility and spatial resolution. However, a major challenge for utilizing optical satellite imagery is the limited temporal resolution. A low temporal resolution will reduce the availability of cloud free imagery, which is a problem in many forest areas. For example, the Landsat satellite only provided five images at a specific scene location in Hedmark with less than 10% cloud coverage in the growing seasons from 1987 to 2010. Hence, when extending the proposed approach to monitoring, the availability of imagery will be a critical factor. About five other existing satellite programs will provide spectral information similar to that of Landsat does today (Wulder et al., 2008a). These optical satellites will increase the chances of cloud free images in a monitoring context due to increased temporal resolution. Future, optical space missions are planned, and alternatives to Landsat include Landsat Data Continuity Mission (LDCM), Advanced Visible and Near-Infrared Radiometer (AVINIR-2)

and the Sentinels (Wulder et al., 2008a). The possibility of RaDAR sensors to increase the availability of full-coverage data by acquiring imagery of areas with 100% cloud cover makes such information interesting as a full coverage source for use in the presented approach.

In the current thesis, only airborne lasers were utilized. In large area inventories the use of spaceborne LiDAR is attractive, particularly in combination with spectral information similar to the approach presented. Unfortunately, the availability of spaceborne LiDAR sensors is limited. The National Aeronautics and Space Administration's (NASA) ICESat-1 satellite that was operational from 2003 to 2009 provided samples (footprints) from all over the world that were suitable for forest inventory (Boudreau et al., 2008), also in combination with spectral information (Duncanson et al., 2010). NASA has planed another spaceborne LiDAR mission called ICESat-2. The benefits from ICESat-2 in forest inventory and monitoring will be limited due to the sensor properties (Nelson et al., 2010). Moreover, NASA's proposed satellite mission DESDynI was planned to include a spaceborne LiDAR sensor operated in sampling mode and a full coverage RaDAR sensor, though the mission was cancelled in February 2011. The LiDAR onboard the DESDynI would have been superior in the assessment of vegetation for large areas (Nelson et al., 2010).

In the near future, no spaceborne LiDARs suitable for forest inventory and monitoring applications are planned to be launched. Because of this, methods such as the one presented here that combine ALS from sample locations and full coverage satellite data will be useful in future large area inventories for providing wall-to-wall map products.

6.3. Issues related to utilization of ALS in forest monitoring (Objective 4)

In the current thesis, no monitoring applications were implemented or tested. However, some essential aspects of using multi-temporal datasets were addressed by empirical analyses. The effects of sensors and seasons (canopy conditions) on the three-dimensional measurements of ALS were reported in earlier studies (Hopkinson, 2007; Næsset, 2005; Næsset, 2009b). This thesis complements previous work on sensors and seasonal effects by investigating the effects on individual trees, as well as the intensity.

Seasonal effects, e.g. leaf-on and leaf-off canopy conditions, are important for forest monitoring (Yu et al., 2006), but also for operational forest inventory (Næsset, 2005). In monitoring, changing canopy conditions might interfere with change estimates (Yu et al., 2006). In operational inventory, leaf-off acquisition of ALS data has been tested to improve the estimates of biophysical properties in mixed forests, and the accuracy was unaffected or

slightly improved using leaf-off data (Næsset, 2005). In the current thesis, the effects of canopy conditions on the last (last echoes of many) and single echoes were most pronounced. The large influence on last echoes was also reported on plot level by Næsset (2005). The minor impact on the height distributions of first echoes (first echoes of many) identified in Paper II is related to the shift in proportions between first and single echoes. The number of single echoes was 20% lower under leaf-off compared to leaf-on canopy conditions. Thus, more first than single echoes were recorded under leaf-on conditions, when the amount of biological matter is higher in the tree crowns. This shift in echo proportions led to higher height values of first echoes under leaf-off conditions. Furthermore, the effect of canopy conditions on intensity was notable. All echo categories were affected, especially the first echoes, which had lower values under leaf-off conditions. The lower intensity values of first echoes also contributed to the high accuracies obtained for tree species identification under leaf-off conditions. The effects on the intensity may be attributed to phenomena which result from the shift in proportions between first and single echoes. The intensities of first echoes are higher under leaf-on conditions when the amount of biomass in the crown is high and most of the emitted energy is reflected immediately, which results in a "strong return" with high intensity. Under leaf-off conditions, the amount of biomass in the tree crowns is lower, thereby allowing more energy to penetrate further into the crown, resulting in a "weak return" with low intensity. In addition, the reflectance and structure of branches and other tree parts will influence the intensity. Both the current thesis and the study by Næsset (2005) analyzed the effects in the change from leaf-off to leaf-on canopy conditions. However, both studies only considered the extreme seasonal effects in canopy conditions (leaf-off vs. leaf-on). In this thesis, the October 2003 flight may have been affected by changes in canopy conditions due to senescence. Such within seasonal effects on the intensity and three-dimensional information of ALS are not yet quantified, and remain a topic for future research.

The use of different sensors impacts the three-dimensional recordings of ALS (Chasmer et al., 2006; Hopkinson, 2007; Næsset, 2005, 2009a). In the current thesis, the effects of using different sensors on the obtained point cloud were quantified on individual trees. For that reason, it was possible to study the effects of different sensors on the point clouds of various tree species. It was revealed that there were species-specific effects from the sensors. One combination of echo categories (first of many and single echoes) did produce nearly equal metrics for spruce trees with different sensors, but not for deciduous trees. Moreover, the current thesis also points out that there are challenges related to using different ALS sensors for individual tree change estimation, e.g. in growth analysis. Still, it

should be mentioned that the point clouds were stable between acquisitions for spruce trees when identical sensors were used. It has been reported in other studies that the effects of different study areas are small when sensors and acquisition settings are identical (Næsset et al., 2005; Næsset, 2007). Therefore, if the same sensor and acquisition settings are used in forest monitoring, change estimation using ALS might be possible without field calibration.

The effects of sensors and seasons did not considerably affect the accuracies of tree height and stem diameter when using models calibrated with field data in the current study. However, one exception was the high accuracies for tree species identification under leaf-off conditions. Similarly, it has been reported that field data calibration provided similar results independent of canopy conditions and sensors in area-based inventory (Næsset, 2005; Næsset & Gobakken, 2008; Næsset, 2009b). Approaches using laser proxies are attractive in order to reduce field measurement costs (e.g. Paper IV). Alternatively, field measurement costs may be reduced by the reuse of models developed in previous projects (Næsset, 2007; Næsset, 2009b). The rapid technological development of laser sensors seen over the past few decades is likely to continue in the future. Thus, it seems to be unrealistic at the present time that monitoring can achieve the same accuracies when not calibrated with field data. Future research should focus on quantifying the loss in accuracy when reducing the amount of field data for model calibration. The sampling design should be further addressed in terms of plot sizes, plot numbers and location of plots (pre-stratification) (e.g. Gobakken & Næsset, 2008; Hawbaker et al., 2009).

The intensity is noisy and often undocumented. Despite these problems, identification of tree species was improved by 10% in Østmarka using raw intensities. Additionally, normalization of the intensity by the sensor-to-target range improved tree species identification by 8 percentage points, while sensor-specific intensity normalization improved tree species identification slightly. Even so, stability for the results in tree species identification seems to be a problem (cf. Section 6.1). These problems will also be a challenge in forest monitoring or change estimation. Different sensors may produce different intensity values. Furthermore, it is likely that some sensors have the possibility to adjust sensor settings, which in turn will affect the intensities recorded. In Østmarka, the intensity values recorded on the sample plots ranged from 1 – 170 (numerical values in Paper I represented by 1/10). Similarly, the range in intensity values for sample plots in Aurskog-Høland was 1 to 95. In both studies, the ALTM 3100 was flown with approximate the same settings. Weather conditions and the wetness of the surface will influence the intensity recordings. Hence, in terms of calibrated intensity values and accuracies of forest biophysical

properties, stable deliverables obtained from intensity should be achieved before a widespread utilization of intensity can be expected.

Paper IV was motivated by the anticipated changes in the tree line due to climate change and the need for information on the rate of these changes. However, only an approach to support monitoring was developed. Forest monitoring studies combining three-dimensional and spectral data are rare. Nevertheless, one example utilizing profiling LiDAR and segmented Landsat satellite imagery exists (Wulder et al., 2007b), and inventory updates have been conducted with a combination of three-dimensional and spectral information (Hilker et al., 2008; Wulder & Seemann, 2003). The majority of studies utilizing ALS for estimating changes over short time spans have only utilized three-dimensional information (Næsset & Gobakken, 2005; Solberg et al., 2006b; Yu et al., 2004; Yu et al., 2006). A combination of three-dimensional and spectral information in forest monitoring and change estimation studies should be investigated based on the promising results of combining such information in forest inventory. Future research should also include testing of the proposed procedure for delineating the subalpine zone based on multi-temporal remote sensing datasets and field observations.

7. CONCLUSIONS

This thesis points at the potential for improvements in forest inventory and monitoring on two different spatial scales by combining remotely sensed three-dimensional and spectral information. First, combining three-dimensional and spectral information improved the accuracy of individual tree species identification in the thesis. Nonetheless, stable classification accuracies were not obtained using intensity and more research is needed to fully understand the potential and limitations of the intensity. Until that time comes, the use of aerial imagery seems to be the best spectral information source available which is suitable for tree species identification in combination with three-dimensional information. Second, the presented method for combining three-dimensional information and medium resolution satellite images seems suitable for mapping the current state and monitoring future changes in the extent and location of the subalpine zone on a regional scale. In forest monitoring, contemporary field and ALS campaigns seem to be needed to keep the accuracies at acceptable levels. Large differences between measurements conducted by various ALS sensors and under different canopy conditions necessitate field calibration. To summarize, combining three-dimensional and spectral information may improve forest inventory and monitoring, although the challenges and costs will be increased by using multiple data

sources and must therefore be compared against the advantage of the higher information level obtained. Furthermore, the use of combined three-dimensional and spectral information in forest inventory and monitoring will probably increase in the future due to the increasing availability of aircraft carrying multiple sensors, as well as improvements in using a combination of more than one remote sensing source, as reported in the current thesis and other studies.

REFERENCES

ACIA (2004). *Impacts of a warming arctic: Arctic climate impact assesment*: Cambridge University Press.

Ackermann, F. (1999). Airborne laser scanning - present status and future expectations. *ISPRS Journal of Photogrammetry and Remote Sensing, 54*, 64-67.

Ahokas, E., Kaasalainen, S., Hyyppä, J., & Suomalainen, J. (2006). Calibration of the Optech ALTM 3100 laser scanner intensity data using brightness targets. *International Archives of Photogrammetry, Remote Sensing and Spatial Information Sciences, XXXVI, Part 1/A*

Aldred, A.H., & Bonnor, G.H. (1985). Application of airborne laser to forest surveys. *Canadian Forestry Service, Petawawa National Forestry Institute, Information Report PI-X-51*, 62 p.

Andersen, H.-E., Barrett, T., Winterberger, K., Strunk, J., & Temesgen, H. (2009). Estimating forest biomass on the western lowlands of the Kenai Peninsula of Alaska using airborne lidar and field plot data in a model-assisted sampling design. In, *IUFRO Div. 4 Symposium, Extending Forest Inventory and Monitoring* (p. 5). Québec City, Quebec, Canada

Anderson, J.E., Plourde, L.C., Martin, M.E., Braswell, B.H., Smith, M.L., Dubayah, R.O., Hofton, M.A., & Blair, J.B. (2008). Integrating waveform lidar with hyperspectral imagery for inventory of a northern temperate forest. *Remote Sensing of Environment, 112*, 1856-1870.

Antonarakis, A.S., Richards, K.S., & Brasington, J. (2008). Object-based land cover classification using airborne LiDAR. *Remote Sensing of Environment, 112*, 2988-2998.

Baltsavias, E.P. (1999). Airborne laser scanning: basic relations and formulas. *ISPRS Journal of Photogrammetry and Remote Sensing, 54*, 199-214.

Balzter, H. (2001). Forest mapping and monitoring with interferometric synthetic aperture radar (InSAR). *Progress in Physical Geography, 25*, 159.

Blair, J.B., Coyle, B.D., Bufton, J.L., & Harding, D.J. (1994). Optimization of an airborne laser altimeter for remote sensing of vegetation and tree canopies. In, *Proceedings of Geoscience and Remote Sensing Symposium, 1994. IGARSS '94. Surface and Atmospheric Remote Sensing: Technologies, Data Analysis and Interpretation* (pp. 939-941): Institute of Electrical and Electronics Engineers.

Blair, J.B., Rabine, D.L., & Hofton, M.A. (1999). The laser vegetation imaging sensor: a medium-altitude, digitisation-only, airborne laser altimeter for mapping vegetation and topography. *ISPRS Journal of Photogrammetry & Remote Sensing, 54*, 115-122.

Boudreau, J., Nelson, R.F., Margolis, H.A., Beaudoin, A., Guindon, L., & Kimes, D.S. (2008). Regional aboveground forest biomass using airborne and spaceborne LiDAR in Quebec. *Remote Sensing of Environment, 112*, 3876-3890.

Brandtberg, T. (2002). Individual tree-based species classification in high spatial resolution aerial images of forests using fuzzy sets. *Fuzzy Sets and Systems, 132*, 371-387.

Brandtberg, T., Warner, T.A., Landenberger, R.E., & McGraw, J.B. (2003). Detection and analysis of individual leaf-off tree crowns in small footprint, high sampling density LIDAR data from the eastern deciduous forest in North America. *Remote Sensing of Environment, 85*, 290-303.

Breidenbach, J., Næsset, E., Lien, V., Gobakken, T., & Solberg, S. (2010). Prediction of species specific forest inventory attributes using a nonparametric semi-individual tree crown approach based on fused airborne laser scanning and multispectral data. *Remote Sensing of Environment, 114*, 911-924.

Breiman, L. (2001). Random forests. *Machine Learning, 45*, 5-32.

Brennan, R., & Webster, T.L. (2006). Object-oriented land cover classification of LiDAR-derived surfaces. *Canadian Journal of Remote Sensing, 32*, 162-172.

Carleer, A., & Wolff, E. (2004). Exploitation of very high resolution satellite data for tree species identification. *Photogrammetric Engineering and Remote Sensing, 70*, 135-140.

Chasmer, L., Hopkinson, C., Smith, B., & Treitz, P. (2006). Examining the influence of changing laser pulse repetition frequencies on conifer forest canopy returns. *Photogrammetric Engineering and Remote Sensing, 72*, 1359-1367.

Cohen, J. (1960). A coefficient of agreement for nominal scales. *Educational and Psychological Measurement, 20*, 37-46.

Cohen, W.B., & Goward, S.N. (2004). Landsat's role in ecological applications of remote sensing. *Bioscience, 54*, 535-545.

Coren, F., & Sterzai, P. (2006). Radiometric correction in laser scanning. *International Journal of Remote Sensing, 27*, 3097-3104.

Dalen, L., & Hofgaard, A. (2005). Differential regional treeline dynamics in the Scandes Mountains. *Arctic Antarctic and Alpine Research, 37*, 284-296.

Donoghue, D.N.M., Watt, P.J., Cox, N.J., & Wilson, J. (2007). Remote sensing of species mixtures in conifer plantations using LiDAR height and intensity data. *Remote Sensing of Environment, 110*, 509-522.

Drake, J.B., Dubayah, R.O., Clark, D.B., Knox, R.G., Blair, J.B., Hofton, M.A., Chazdon, R.L., Weishampel, J.F., & Prince, S.D. (2002). Estimation of tropical forest structural characteristics using large-footprint lidar. *Remote Sensing of Environment, 79*, 305-319.

Duncanson, L.I., Niemann, K.O., & Wulder, M.A. (2010). Integration of GLAS and Landsat TM data for aboveground biomass estimation. *Canadian Journal of Remote Sensing, 36*, 129-141.

Eid, T., & Næsset, E. (1998). Determination of stand volume in practical forest inventories based on field measurements and photo-interpretation: The Norwegian experience. *Scandinavian Journal of Forest Research, 13*, 246-254.

Eid, T., Gobakken, T., & Næsset, E. (2004). Comparing stand inventories for large areas based on photo-interpretation and laser scanning by means of cost-plus-loss analyses. *Scandinavian Journal of Forest Research, 19*, 512-523.

Ene, L., Næsset, E., & Gobakken, T. (in review). Single tree detection in heterogeneous boreal forests using airborne laser scanning and area based stem number estimates

Falkowski, M.J., Wulder, M.A., White, J.C., & Gillis, M.D. (2009). Supporting large-area, sample-based forest inventories with very high spatial resolution satellite imagery. *Progress in Physical Geography, 33*, 403-423.

FAO (2006). Global Forest Resources Assessment 2005 - Progress towards sustainable forest management. In, *FAO Forestry Paper 147*. Rome: Food and Agriculture Organization of the United Nations.

Farid, A., Goodrich, D.C., & Sorooshian, S. (2006a). Using airborne lidar to discern age classes of cottonwood trees in a riparian area. *Western Journal of Applied Forestry, 21*, 149-158.

Farid, A., Rautenkranz, D., Goodrich, D.C., Marsh, S.E., & Sorooshian, S. (2006b). Riparian vegetation classification from airborne laser scanning data with an emphasis on cottonwood trees. *Canadian Journal of Remote Sensing, 32*, 15-18.

Foody, G.M. (1996). Fuzzy modelling of vegetation from remotely sensed imagery. *Ecological Modelling, 85*, 3-12.

Foody, G.M. (2001). Monitoring the magnitude of land-cover change around the southern limits of the Sahara. *Photogrammetric Engineering and Remote Sensing, 67*, 841-848.

Franklin, S.E., & Wulder, M.A. (2002). Remote sensing methods in medium spatial resolution satellite data land cover classification of large areas. *Progress in Physical Geography, 26*, 173-205.

Garcia, M., Riano, D., Chuvieco, E., & Danson, F.M. (2010). Estimating biomass carbon stocks for a Mediterranean forest in central Spain using LiDAR height and intensity data. *Remote Sensing of Environment, 114*, 816-830.

Gatziolis, D. (2009). LiDAR intensity normalization in rugged forested terrain. In S.C. Popescu, R. Nelson, K. Zhao & A. Neuenschwander (Eds.), *Proceedings of Silvilaser 2009 - The 9th international conference on lidar applications for assessing forest ecosystems*. Texas A&M University, College Station, Texas, USA

Gobakken, T., & Næsset, E. (2008). Assessing effects of laser point density, ground sampling intensity, and field sample plot size on biophysical stand properties derived from airborne

laser scanner data. *Canadian Journal of Forest Research-Revue Canadienne De Recherche Forestiere, 38*, 1095-1109.

Gougeon, F.A., & Leckie, D.G. (2006). The individual tree crown approach applied to Ikonos images of a coniferous plantation area. *Photogrammetric Engineering and Remote Sensing, 72*, 1287-1297.

Gregoire, T., Ståhl, G., Næsset, E., Gobakken, T., Nelson, R., & Holm, S. (2011). Model-assisted estimation of biomass in a LiDAR sample survey in Hedmark county, Norway. *Canadian journal of forest research-Revue canadienne de recherche forestier, 41*, 83-95.

Harsch, M., A., Hulme, P., E., McGlone, M., S., & Duncan, R., P. (2009). Are treelines advancing? A global meta-analysis of treeline response to climate warming. *Ecology Letters, 12*, 1040-1049.

Hawbaker, T.J., Keuler, N.S., Lesak, A.A., Gobakken, T., Contrucci, K., & Radeloff, V.C. (2009). Improved estimates of forest vegetation structure and biomass with a LiDAR-optimized sampling design. *Journal of Geophysical Research-Biogeosciences, 114*

Heinzel, J., Weinacker, H., & Kock, B. (2008). Full automatic detection of tree species based on delineated single tree crowns - a data fusion approach for airborne laser scanning data and aerial photographs. *Silvilaser 2008, Edinburgh, UK*

Heurich, M. (2006). Evaluierung und entwicklung von automatiserten erfassung von waldstructuren aus daten flugzuggetragener fernerkundungssenoren. *Forstkuche Forshungsberichte München, 2002*, p329.

Hilker, T., Wulder, M.A., & Coops, N.C. (2008). Update of forest inventory data with lidar and high spatial resolution satellite imagery. *Canadian Journal of Remote Sensing, 34*, 5-12.

Hill, R.A., Granica, K., Smith, G.M., & Schardt, M. (2007). Representation of an alpine treeline ecotone in SPOT 5 HRG data. *Remote Sensing of Environment, 110*, 458-467.

Höfle, B., & Pfeifer, N. (2007). Correction of laser scanning intensity data: Data and model-driven approaches. *ISPRS Journal of Photogrammetry and Remote Sensing, 62*, 415-433.

Holmgren, J., & Persson, Å. (2004). Identifying species of individual trees using airborne laser scanner. *Remote Sensing of Environment, 90*, 415-423.

Holmgren, J., Persson, Å., & Söderman, U. (2008). Species identification of individual trees by combining high resolution LIDAR data with multi-spectral images. *International Journal of Remote Sensing, 29*, 1537-1552.

Holmgren, P., & Thuresson, T. (1998). Satellite remote sensing for forestry planning - A review. *Scandinavian Journal of Forest Research, 13*, 90-110.

Hopkinson, C. (2007). The influence of flying altitude, beam divergence, and pulse repetition frequency on laser pulse return intensity and canopy frequency distribution. *Canadian Journal of Remote Sensing, 33*, 312-324.

Hopkinson, C., & Chasmer, L. (2009). Testing LiDAR models of fractional cover across multiple forest ecozones. *Remote Sensing of Environment, 113*, 275-288.

Huang, S.L., Hager, S.A., Halligan, K.Q., Fairweather, I.S., Swanson, A.K., & Crabtree, R.L. (2009). A comparison of individual tree and forest plot height derived from lidar and InSAR. *Photogrammetric Engineering and Remote Sensing, 75*, 159-167.

Hudak, A.T., Lefsky, M.A., Cohen, W.B., & Berterretche, M. (2002). Integration of lidar and Landsat ETM+ data for estimating and mapping forest canopy height. *Remote Sensing of Environment, 82*, 397-416.

Hudak, A.T., Crookston, N.L., Evans, J.S., Falkowski, M.J., Smith, A.M.S., Gessler, P.E., & Morgan, P. (2006). Regression modeling and mapping of coniferous forest basal area and tree density from discrete-return lidar and multispectral satellite data. *Canadian Journal of Remote Sensing, 32*, 126-138.

Hutchinson, C. (1982). Techniques for combining Landsat and ancillary data for digital classification improvement. *Photogrammetric Engineering & Remote Sensing, 48*, 123-130.

Hyde, P., Dubayah, R., Walker, W., Blair, J.B., Hofton, M., & Hunsaker, C. (2006). Mapping forest structure for wildlife habitat analysis using multi-sensor (LiDAR, SAR/InSAR, ETM plus , Quickbird) synergy. *Remote Sensing of Environment, 102*, 63-73.

Hyde, P., Nelson, R., Kimes, D., & Levine, E. (2007). Exploring LiDAR-RaDAR synergy - predicting aboveground biomass in a southwestern ponderosa pine forest using LiDAR, SAR and InSAR. *Remote Sensing of Environment, 106*, 28-38.

Hyyppä, H., & Hyyppä, J. (1999). Comparing the accuracy of laser scanner with other optical remote sensing data sources for stand attributes retrieval. *The Photogrammetric Journal of Finland, 16*, 5 -15.

Hyyppä, J., Kelle, O., Lehikoinen, M., & Inkinen, M. (2001). A segmentation-based method to retrieve stem volume estimates from 3-D tree height models produced by laser scanners. *IEEE Transactions on Geoscience and Remote Sensing, 39*, 969-975.

Hyyppä, J., Hyyppä, H., Leckie, D., Gougeon, F., Yu, X., & Maltamo, M. (2008). Review of methods of small-footprint airborne laser scanning for extracting forest inventory data in boreal forests. *International Journal of Remote Sensing, 29*, 1339-1366.

Jensen, J.R. (2000). *Remote sensing of the environment, An earth resource perspective*. Upper Saddle river, New Jersey: Prentice Hall.

Johansson, K. (2007). Enkelttretakst med laser - det største siden fotosyntesen (in norwegian). *Glommen*, 14 - 15.

Jones, T.G., Coops, N.C., & Sharma, T. (2010). Assessing the utility of airborne hyperspectral and LiDAR data for species distribution mapping in the coastal Pacific Northwest, Canada. *Remote Sensing of Environment, 114*, 2841-2852.

Ke, Y.H., Quackenbush, L.J., & Im, J. (2010). Synergistic use of QuickBird multispectral imagery and LIDAR data for object-based forest species classification. *Remote Sensing of Environment, 114*, 1141-1154.

Key, T., Warner, T.A., McGraw, J.B., & Fajvan, M.A. (2001). A comparison of multispectral and multitemporal information in high spatial resolution imagery for classification of

individual tree species in a temperate hardwood forest. *Remote Sensing of Environment, 75*, 100-112.

Kim, S., McGaughey, R.J., Andersen, H.E., & Schreuder, G. (2009a). Tree species differentiation using intensity data derived from leaf-on and leaf-off airborne laser scanner data. *Remote Sensing of Environment, 113*, 1575-1586.

Kim, Y., Yang, Z.Q., Cohen, W.B., Pflugmacher, D., Lauver, C.L., & Vankat, J.L. (2009b). Distinguishing between live and dead standing tree biomass on the North Rim of Grand Canyon National Park, USA using small-footprint lidar data. *Remote Sensing of Environment, 113*, 2499-2510.

Korpela, I., Koskinen, M., Vasander, H., Holopainen, M., & Minkkinen, K. (2009). Airborne small-footprint discrete-return LiDAR data in the assessment of boreal mire surface patterns, vegetation, and habitats. *Forest Ecology and Management, 258*, 1549-1566.

Korpela, I., Ørka, H.O., Maltamo, M., Tokola, T., & Hyyppä, J. (2010). Tree species classification using airborne LiDAR - Effects of stand and tree parameters, downsizing of training set, intensity normalization, and sensor type. *Silva Fennica, 44*, 319-339.

Korpela, I.S. (2008). Mapping of understory lichens with airborne discrete-return LiDAR data. *Remote Sensing of Environment, 112*, 3891-3897.

Koukoulas, S., & Blackburn, G.A. (2005). Mapping individual tree location, height and species in broadleaved deciduous forest using airborne LIDAR and multi-spectral remotely sensed data. *International Journal of Remote Sensing, 26*, 431-455.

Lefsky, M.A., Cohen, W.B., & Spies, T.A. (2001). An evaluation of alternate remote sensing products for forest inventory, monitoring, and mapping of Douglas-fir forests in western Oregon. *Canadian Journal of Forest Research-Revue Canadienne De Recherche Forestiere, 31*, 78-87.

Lefsky, M.A. (2010). A global forest canopy height map from the Moderate Resolution Imaging Spectroradiometer and the Geoscience Laser Altimeter System. *Geophysical Research Letters, 37*, L15401.

Lim, K., Treitz, P., Baldwin, K., Morrison, I., & Green, J. (2003). Lidar remote sensing of biophysical properties of tolerant northern hardwood forests. *Canadian Journal of Remote Sensing, 29*, 658-678.

Loetsch, F., & Haller, K. (1964). *Forest inventory: Statistics of forest inventory and information from aerial photographs*. München, Germany: BLV Verlagsgesellschaft.

Maclean, G.A., & Krabill, W.B. (1986). Gross-merchantable timber volume estimation using an airborne lidar system. *Canadian Journal of Remote Sensing, 12*, 7-18.

Magnusson, M., Fransson, J.E.S., & Olsson, H. (2007). Aerial photo-interpretation using Z/I DMC images for estimation of forest variables. *Scandinavian Journal of Forest Research, 22*, 254-266.

Mallet, C., & Bretar, F. (2009). Full-waveform topographic lidar: State-of-the-art. *ISPRS Journal of Photogrammetry and Remote Sensing, 64*, 1-16.

Maltamo, M., Mustonen, K., Hyyppä, J., Pitkanen, J., & Yu, X. (2004). The accuracy of estimating individual tree variables with airborne laser scanning in a boreal nature reserve. *Canadian Journal of Forest Research-Revue Canadienne De Recherche Forestiere, 34*, 1791-1801.

McInerney, D.O., Suarez-Minguez, J., Valbuena, R., & Nieuwenhuis, M. (2010). Forest canopy height retrieval using LiDAR data, medium-resolution satellite imagery and kNN estimation in Aberfoyle, Scotland. *Forestry, 83*, 195-206.

McRoberts, R.E., Tomppo, E.O., & Næsset, E. (2010). Advances and emerging issues in national forest inventories. *Scandinavian Journal of Forest Research, 25*, 368-381.

Moen, A. (1999). *National atlas of Norway: Vegetation*. Hønefoss: Norwegian Mapping Authority, Hønefoss.

Moffiet, T., Mengersen, K., Witte, C., King, R., & Denham, R. (2005). Airborne laser scanning: Exploratory data analysis indicates potential variables for classification of individual trees or forest stands according to species. *ISPRS Journal of Photogrammetry and Remote Sensing, 59*, 289-309.

Mora, B., Wulder, M.A., & White, J.C. (2010a). Segment-constrained regression tree estimation of forest stand height from very high spatial resolution panchromatic imagery over a boreal environment. *Remote Sensing of Environment, 114*, 2474-2484.

Mora, B., Wulder, M.A., & White, J.C. (2010b). Identifying leading species using tree crown metrics derived from very high spatial resolution imagery in a boreal forest environment. *Canadian Journal of Remote Sensing, 36*, 332–344.

Morsdorf, F., Marell, A., Koetz, B., Cassagne, N., Pimont, F., Rigolot, E., & Allgower, B. (2010). Discrimination of vegetation strata in a multi-layered Mediterranean forest ecosystem using height and intensity information derived from airborne laser scanning. *Remote Sensing of Environment, 114*, 1403-1415.

Mustonen, J., Packalén, P., & Kangas, A. (2008). Automatic segmentation of forest stands using a canopy height model and aerial photography. *Scandinavian Journal of Forest Research, 23*, 534-545.

Næsset, E. (2004). Accuracy of forest inventory using airborne laser scanning: Evaluating the first Nordic full-scale operational project. *Scandinavian Journal of Forest Research, 19*, 554-557.

Næsset, E. (2005). Assessing sensor effects and effects of leaf-off and leaf-on canopy conditions on biophysical stand properties derived from small-footprint airborne laser data. *Remote Sensing of Environment, 98*, 356-370.

Næsset, E., Bollandsås, O.M., & Gobakken, T. (2005). Comparing regression methods in estimation of biophysical properties of forest stands from two different inventories using laser scanner data. *Remote Sensing of Environment, 94*, 541-553.

Næsset, E., & Gobakken, T. (2005). Estimating forest growth using canopy metrics derived from airborne laser scanner data. *Remote Sensing of Environment, 96*, 453-465.

Næsset, E. (2007). Airborne laser scanning as a method in operational forest inventory: Status of accuracy assessments accomplished in Scandinavia. *Scandinavian Journal of Forest Research, 22*, 433-442.

Næsset, E., & Gobakken, T. (2008). Estimation of above- and below-ground biomass across regions of the boreal forest zone using airborne laser. *Remote Sensing of Environment, 112*, 3079-3090.

Næsset, E. (2009a). Influence of terrain model smoothing and flight and sensor configurations on detection of small pioneer trees in the boreal-alpine transition zone utilizing height metrics derived from airborne scanning lasers. *Remote Sensing of Environment, 113*, 2210-2223.

Næsset, E. (2009b). Effects of different sensors, flying altitudes, and pulse repetition frequencies on forest canopy metrics and biophysical stand properties derived from small-footprint airborne laser data. *Remote Sensing of Environment, 113*, 148-159.

Næsset, E., Gobakken, T., & Nelson, R. (2009). Sampling and mapping forest volume and biomass using airborne LIDARs. *Proceedings of the Eight Annual Forest Inventory and Analysis Symposium, Monterey, CA, USA*, 297-301.

Nelson, R., Krabill, W., & Maclean, G. (1984). Determining Forest Canopy Characteristics Using Airborne Laser Data. *Remote Sensing of Environment, 15*, 201-212.

Nelson, R., Krabill, W., & Tonelli, J. (1988). Estimating Forest Biomass and Volume Using Airborne Laser Data. *Remote Sensing of Environment, 24*, 247-267.

Nelson, R., Parker, G., & Hom, M. (2003a). A portable airborne laser system for forest inventory. *Photogrammetric Engineering and Remote Sensing, 69*, 267-273.

Nelson, R., Valenti, M.A., Short, A., & Keller, C. (2003b). A multiple resource inventory of Delaware using airborne laser data. *Bioscience, 53*, 981-992.

Nelson, R., Short, A., & Valenti, M. (2004). Measuring biomass and carbon in Delaware using an airborne profiling LIDAR. *Scandinavian Journal of Forest Research, 19*, 500-511.

Nelson, R., Neuenschwander, A.L., Ranson, K.J., & Cook, B. (2010). Current characteristics of two space Lidars: ICESat-2 and DESDynL-Lidar. In, *Proceedings of SilviLaser 2010*. Freiburg, Germany

Nelson, R.F., Hyde, P., Johnson, P., Emessiene, B., Imhoff, M.L., Campbell, R., & Edwards, W. (2007). Investigating RaDAR-LiDAR synergy in a North Carolina pine forest. *Remote Sensing of Environment, 110*, 98-108.

Nilsson, M. (1996). Estimation of tree weights and stand volume using an airborne LIDAR system. *Remote Sensing of Environment, 56*, 1-7.

Olson, D.M., Dinerstein, E., Wikramanayake, E.D., Burgess, N.D., Powell, G.V.N., Underwood, E.C., D'Amico, J.A., Itoua, I., Strand, H.E., Morrison, J.C., Colby, J.L., Allnutt, T.F., Ricketts, T.H., Kura, Y., Lamoreux, J.F., Wettengel, W.W., Hedao, P., & Kassem, K.R. (2001). Terrestrial Ecoregions of the World: A New Map of Life on Earth. *Bioscience, 51*, 933-938.

Ørka, H.O., Næsset, E., & Bollandsås, O.M. (2009). Comparing classification strategies for ALS tree species recognition. In S.C. Popescu, R. Nelson, K. Zhao & A. Neuenschwander (Eds.), *Proceedings of Silvilaser 2009 - The 9th international conference on lidar applications for assessing forest ecosystems* (pp. 46 - 53). Texas A&M University, College Station, Texas, USA

Packalén, P., & Maltamo, M. (2006). Predicting the plot volume by tree species using airborne laser scanning and aerial photographs. *Forest Science, 52*, 611-622.

Packalén, P., & Maltamo, M. (2007). The k-MSN method for the prediction of species-specific stand attributes using airborne laser scanning and aerial photographs. *Remote Sensing of Environment, 109*, 328-341.

Packalén, P., & Maltamo, M. (2008). Estimation of species-specific diameter distributions using airborne laser scanning and aerial photographs. *Canadian Journal of Forest Research-Revue Canadienne De Recherche Forestiere, 38*, 1750-1760.

Packalén, P., Suvanto, A., & Maltamo, M. (2009). A two stage method to estimate species-specific growing stock. *Photogrammetric Engineering and Remote Sensing, 75*, 1451-1460.

Patenaude, G., Milne, R., & Dawson, T.P. (2005). Synthesis of remote sensing approaches for forest carbon estimation: reporting to the Kyoto Protocol. *Environmental Science & Policy, 8*, 161-178.

Persson, Å., Holmgren, J., & Söderman, U. (2002). Detecting and measuring individual trees using an airborne laser scanner. *Photogrammetric Engineering and Remote Sensing, 68*, 925-932.

Persson, Å., Holmgren, J., Söderman, U., & Olsson, H. (2004). Tree species classification of individual trees in Sweden by combining high resolution laser data with high resolution near-infrared digitalt images. *International Archives of Photogrammetry, Remote Sensing and Spatial Information Sciences, Vol. XXXVI, Part 8/W2*, 204-207.

Pitas, I. (2000). *Digital image processing algorithms and applications*. New York: Wiley.

Pohl, C., & van Genderen, J.L. (1998). Multisensor image fusion in remote sensing: concepts, methods and applications. *International Journal of Remote Sensing, 19*, 823-854.

Popescu, S.C., Wynne, R.H., & Nelson, R.F. (2002). Estimating plot-level tree heights with lidar: local filtering with a canopy-height based variable window size. *Computers and Electronics in Agriculture, 37*, 71-95.

Popescu, S.C., & Wynne, R.H. (2004). Seeing the trees in the forest: Using lidar and multispectral data fusion with local filtering and variable window size for estimating tree height. *Photogrammetric Engineering and Remote Sensing, 70*, 589-604.

Popescu, S.C., Wynne, R.H., & Scrivani, J.A. (2004). Fusion of small-footprint lidar and multispectral data to estimate plot-level volume and biomass in deciduous and pine forests in Virginia, USA. *Forest Science, 50*, 551-565.

Ranson, K.J., Sun, G., Kharuk, V.I., & Kovacs, K. (2004). Assessing tundra-taiga boundary with multi-sensor satellite data. *Remote Sensing of Environment, 93*, 283-295.

Reitberger, J., Krzystek, P., & Stilla, U. (2008). Analysis of full waveform LIDAR data for the classification of deciduous and coniferous trees. *International Journal of Remote Sensing, 29*, 1407-1431.

Ripley, B.D. (1996). *Pattern recognition and neural networks*. Cambridge: Cambridge University Press.

Schreier, H., Lougheed, J., Tucker, C., & Leckie, D. (1985). Automated measurements of terrain reflection and height variations using an airborne infrared laser system. *International Journal of Remote Sensing, 6*, 101-113.

Shippert, P. (2004). Why use hyperspectral imagery? *Photogrammetric Engineering & Remote Sensing, 70*, 377 - 380.

Solberg, S., Næsset, E., & Bollandsås, O.M. (2006a). Single tree segmentation using airborne laser scanner data in a structurally heterogeneous spruce forest. *Photogrammetric Engineering and Remote Sensing, 72*, 1369-1378.

Solberg, S., Næsset, E., Hanssen, K.H., & Christiansen, E. (2006b). Mapping defoliation during a severe insect attack on Scots pine using airborne laser scanning. *Remote Sensing of Environment, 102*, 364-376.

Solodukhin, V.I., Zukov, A.Y., Mazugin, I.N., Bokova, T.K., & Polezhai, V.M. (1977). Vozmozhnosti lazernoi aeros emki profilei lesa (Possibilities of laser aerial photography for forest profiling). *Lesnoe Khozyaistvo (Forest Management), 10*, 53-58.

Ståhl, G., Holm, S., Gregoire, T., Gobakken, T., Næsset, E., & Nelson, R. (2011). Model-based inference for biomass estimation in a LiDAR sample survey in the county of Hedmark County, Norway. *Canadian journal of forest research-Revue canadienne de recherche forestier, 41*, 96-107.

Story, M., & Congalton, R.G. (1986). Accuracy assessment - a users perspective. *Photogrammetric Engineering and Remote Sensing, 52*, 397-399.

Tomppo, E., Olsson, H., Stahl, G., Nilsson, M., Hagner, O., & Katila, M. (2008). Combining national forest inventory field plots and remote sensing data for forest databases. *Remote Sensing of Environment, 112*, 1982-1999.

Vauhkonen, J., Korpela, I., Maltamo, M., & Tokola, T. (2010). Imputation of single-tree attributes using airborne laser scanning-based height, intensity, and alpha shape metrics. *Remote Sensing of Environment, 114*, 1263-1276.

Wagner, W., Ullrich, A., Ducic, V., Melzer, T., & Studnicka, N. (2006). Gaussian decomposition and calibration of a novel small-footprint full-waveform digitising airborne laser scanner. *ISPRS Journal of Photogrammetry and Remote Sensing, 60*, 100-112.

Wehr, A., & Lohr, U. (1999). Airborne laser scanning - an introduction and overview. *ISPRS Journal of Photogrammetry and Remote Sensing, 54*, 68-82.

Wilkinson, G.G. (2005). Results and implications of a study of fifteen years of satellite image classification experiments. *IEEE Transactions on Geoscience and Remote Sensing, 43*, 433-440.

Woodcock, C.E., Allen, R., Anderson, M., Belward, A., Bindschadler, R., Cohen, W., Gao, F., Goward, S.N., Helder, D., Helmer, E., Nemani, R., Oreopoulos, L., Schott, J., Thenkabail, P.S., Vermote, E.F., Vogelmann, J., Wulder, M.A., & Wynne, R.H. (2008). Free access to Landsat imagery. *Science, 320*, 1011.

Wulder, M. (1998). Optical remote-sensing techniques for the assessment of forest inventory and biophysical parameters. *Progress in Physical Geography, 22*, 449-476.

Wulder, M.A., & Seemann, D. (2003). Forest inventory height update through the integration of lidar data with segmented Landsat imagery. *Canadian Journal of Remote Sensing, 29*, 536-543.

Wulder, M.A., White, J.C., Niemann, K.O., & Nelson, T. (2004). Comparison of airborne and satellite high spatial resolution data for the identification of individual trees with local maxima filtering. *International Journal of Remote Sensing, 25*, 2225-2232.

Wulder, M.A., Han, T., White, J.C., Butson, C.R., & Hall, R.J. (2007a). An approach for edge matching large-area satellite image classifications. *Canadian Journal of Remote Sensing, 33*, 266-277.

Wulder, M.A., Han, T., White, J.C., Sweda, T., & Tsuzuki, H. (2007b). Integrating profiling LIDAR with Landsat data for regional boreal forest canopy attribute estimation and change characterization. *Remote Sensing of Environment, 110*, 123-137.

Wulder, M.A., White, J.C., Goward, S.N., Masek, J.G., Irons, J.R., Herold, M., Cohen, W.B., Loveland, T.R., & Woodcock, C.E. (2008a). Landsat continuity: Issues and opportunities for land cover monitoring. *Remote Sensing of Environment, 112*, 955-969.

Wulder, M.A., White, J.C., Hay, G.J., & Castilla, G. (2008b). Towards automated segmentation of forest inventory polygons on high spatial resolution satellite imagery. *Forestry Chronicle, 84*, 221-230.

Yu, X.W., Hyyppä, J., Kaartinen, H., & Maltamo, M. (2004). Automatic detection of harvested trees and determination of forest growth using airborne laser scanning. *Remote Sensing of Environment, 90*, 451-462.

Yu, X.W., Hyyppä, J., Kukko, A., Maltamo, M., & Kaartinen, H. (2006). Change detection techniques for canopy height growth measurements using airborne laser scanner data. *Photogrammetric Engineering and Remote Sensing, 72*, 1339-1348.

Paper I

Remote Sensing of Environment 113 (2009) 1163–1174

Contents lists available at ScienceDirect

Remote Sensing of Environment

journal homepage: www.elsevier.com/locate/rse

Classifying species of individual trees by intensity and structure features derived from airborne laser scanner data

Hans Ole Ørka *, Erik Næsset, Ole Martin Bollandsås

Department of Ecology and Natural Resource Management, Norwegian University of Life Sciences, P.O. Box 5003, NO-1432 Ås, Norway

ARTICLE INFO

Article history:
Received 12 October 2007
Received in revised form 7 January 2009
Accepted 7 February 2009

Keywords:
Airborne laser scanning
Intensity
Species classification
Spruce
Birch

ABSTRACT

The objective of this study was to identify candidate features derived from airborne laser scanner (ALS) data suitable to discriminate between coniferous and deciduous tree species. Both features related to structure and intensity were considered. The study was conducted on 197 Norway spruce and 180 birch trees (leaves on conditions) in a boreal forest reserve in Norway. The ALS sensor used was capable of recording multiple echoes. The point density was 6.6 m^{-2}. Laser echoes located within the vertical projection of the tree crowns, which were assumed to be circular and defined according to field measurements, were attributed to three categories: "first echoes of many", "single echoes", or "last echoes of many echoes". They were denoted FIRST, SINGLE, and LAST, respectively. In tree species classification using ALS data features should be independent of tree heights. We found that many features were dependent on tree height and that this dependency influenced selection of candidate features. When we accounted for this dependency, it was revealed that FIRST and SINGLE echoes were located higher and LAST echoes lower in the birch crowns than in spruce crowns. The intensity features of the FIRST echoes differed more between species than corresponding features of the other echo categories. For the FIRST echoes the intensity values tended to be higher for birch than spruce. When using the various features for species classification, maximum overall classification accuracies of 77% and 73% were obtained for structural and intensity features, respectively. Combining candidate features related to structure and intensity resulted in an overall classification accuracy of 88%.

1. Introduction

In recent years, high resolution sampling density airborne laser scanning (ALS) has become readily available, providing *x*, *y*, *z* point datasets with 5–20 height measurements per square meter. Such data are useful for terrain, vegetation, and forest mapping. From these dense point clouds, individual trees can be identified by means of various segmentation procedures. These procedures extract the outline of the tree crowns. Individual tree segmentation is often done by using an ALS-derived canopy height model (e.g. Hyyppä et al., 2001; Persson et al., 2002; Solberg et al., 2006), but also other methods are used, like for example clustering (Morsdorf et al., 2004). When the outline of a tree crown is defined, laser echoes inside the segment can be tied to the tree and information about the tree such as stem position, height, and stem diameter can be derived (e.g. Persson et al., 2002; Solberg et al., 2006). This high resolution tree information can form a basis for forest planning by aggregating information to management units (Hyyppä et al., 2001).

Tree species is another parameter that may be derived from laser echoes inside individual tree segments. Species classification on a individual tree level using ALS-derived features has been accomplished in boreal forest in Scandinavia (Holmgren et al., 2008; Holmgren & Persson, 2004; Liang et al., 2007), in mixed coniferous and deciduous forest in central Europe (Heurich, 2006; Reitberger et al., 2008), in deciduous forest in western Virginia (Brandtberg, 2007; Brandtberg et al., 2003), and in sub-tropical forest in Queensland, Australia (Moffiet et al., 2005). Individual tree species information could also be found using high spatial resolution images (e.g. Brandtberg, 2002; Carleer & Wolff, 2004; Key et al., 2001; Olofsson et al., 2006). However, acquisition of both ALS data and imagery will increase inventory costs. Furthermore, because ALS provides more accurate estimates of biomass and height compared to image remote sensing methods (Hyde et al., 2006; Hyyppä & Hyyppä, 1999), the possibilities of utilize ALS data also to discriminate between tree species are of interest in order to control data acquisition cost.

Structural features of the tree crowns can be derived from ALS height measurements and such features might be considered for tree species classification. The basic idea behind using structural features for tree species classification is that different species have different crown properties such as crown shape, reflectivity, and location of biomass. For example, crown shapes for spruce trees tend to be conical, whereas more spherical or rounded shapes are found for deciduous trees. Deciduous trees also tend to allocate more biomass higher in the crown. The structural differences of tree crowns will

* Corresponding author. Tel.: +47 64965799; fax: +47 64965802.
E-mail address: hans-ole.orka@umb.no (H.O. Ørka).

0034-4257/$ – see front matter © 2009 Elsevier Inc. All rights reserved.
doi:10.1016/j.rse.2009.02.002

influence on the recorded laser echoes. When a laser echo is recorded, the elapsed time between emission and receipt of a significant amount of returned energy is converted to range. Since the position and orientation of the platform are known by Global Navigation Satellite Systems (GNSS) and Inertial Navigation System (INS), the position of the target can be calculated. To trigger a laser echo from a tree crown or any other surface, the properties of the surface hit by the laser pulse is of importance. One example is the high rate of success in detecting power lines. A power line covers just a small portion of a laser footprint, but is still detectable in an ALS dataset because of the high reflectivity of power lines. On the other hand, a tree crown surface represented by branches and leaves often covering the entire laser footprint has lower reflectivity and a different structure. The laser pulse will therefore tend to penetrate into the canopy before a significant echo is recorded by the sensor (Gaveau & Hill, 2003). Thus, different crown properties affect the distribution of laser echoes within and on the surface of the tree crowns. This may lead to distinct echo height distributions for separate species. Therefore, it might be useful for automated species classification based on ALS data to identify which structural features derived from the echo height distribution that are most suited to distinguish species.

In addition to the spatial coordinates of laser echoes, most ALS systems measure the intensity of the backscattered laser signal (Wehr & Lohr, 1999). For pulse lasers, intensity often represents the peak amplitude of the returned pulse. It is expected that this value could assist species classification. Already in 1985, Schreier et al. (1985) demonstrated classification of individual trees into conifers and broadleaves partly based on airborne laser intensity. Since then the use of laser intensity has been little explored. This is mainly because of lack of methods for radiometric calibration of intensity values (Kaasalainen et al., 2005). However, recently some authors have tested intensity features for tree species classification (Brandtberg, 2007; Brandtberg et al., 2003; Holmgren et al., 2008; Holmgren & Persson, 2004; Moffiet et al., 2005; Reitberger et al., 2008) and for discerning age classes (Farid et al., 2006a,b) as well as land-cover classes (Brennan & Webster, 2006) where deciduous and coniferous forest were treated as separate classes. Despite the lack of calibration methods, intensity features derived from ALS data may improve classification (e.g. Brandtberg et al., 2003; Holmgren et al., 2008). As methods for calibration of the intensity mature, the usefulness of intensity used for individual tree species classification may increase.

In species classification, features derived from the laser height distribution, such as the mean height of the laser echoes, could be used directly in the classification algorithm (e.g. Brennan & Webster, 2006) or as a scaled feature, for example normalized with tree height (Holmgren & Persson, 2004). In individual tree classification, independence of tree height is important, especially in forests where tree height distributions differ between species. To ensure this independence features should be scaled. Brandtberg (2007) normalized the 3D point cloud using estimated tree height to ensure independence. Holmgren and Persson (2004) used relative height features, i.e., laser height features divided by the laser estimated height, to separate Norway spruce and Scots pine. It should be noted, however, that it has so far not been tested if scaling methods really produce independence of tree height. Robust scaling may be important for practical applications covering large areas. In large forested landscapes, species-specific height distributions will vary in the landscape according to soil properties, management history, and a number of other factors. Hence, selection of robust and unbiased classification features is important.

The aim of this study was to identify candidate ALS-derived features suitable for classification of spruce and birch. In order to reach our aim, we (1) conducted an analysis of differences in (1a) structural- and (1b) intensity features between spruce and birch trees, and (2) tested the classification performance of candidate features.

2. Materials and methods

2.1. Study area

The study area is located in the southwestern corner of Østmarka forest reserve. The forest reserve is located a few kilometers outside Oslo in southeastern Norway (59°50′N, 11°02′E, 190–370 masl). The size of the forest reserve is about 1800 ha. No logging or other silvicultural treatments has been carried out since the 1940s. Today the forest appears with large within stand variation in ages and sizes of trees. The forest is dominated by Norway spruce (*Picea abies* (L.) Karst.) and is partly multilayered. Deciduous trees are found scattered in the landscape. Birch (*Betula* spp.) and aspen (*Poplus tremula* L.) are the most commonly occurring deciduous species. An adjacent area outside the reserve was also included to cover managed forest in younger and intermediate age classes in the study.

2.2. Field data

During summer 2003, 20 circular field plots (0.1 ha) in the reserve and eight plots just outside the reserve were established. The plots were subjectively selected. The plots inside the reserve were selected according to three criteria, i.e., (1) they should be spruce-dominated, (2) have multiple canopy layers, and (3) be located on gentle terrain slopes. These field data were also used in studies by Solberg et al. (2006) and Bollandsås and Næsset (2007). The plots outside the reserve were selected to cover productive forest in young and intermediate age classes.

On each sample plot, we callipered diameter at breast height (DBH) of all trees with DBH $\geq$3 cm and recorded polar coordinates of each tree from the plot center. The polar coordinates of the trees were determined using tape measure and a compass. The compass had a foresight and was attached to a tripod to reduce pointing errors. In addition a local correction of the deviation between magnetic and true north were applied. Plot center coordinates were determined using differential Global Navigation Satellite Systems (GNSS) by means of Global Positioning System (GPS) and Global Navigation Satellite System (GLONASS). Random errors reported from the post-processing combined with empirical experience reported by Næsset (2001) indicated an average error of 10 cm for the planimetric coordinates of the plot centers. For further details about the GNSS setup and post-processing, see Solberg et al. (2006) and Bollandsås and Næsset (2007).

Selection of sample trees on each plot was performed in three steps, i.e., (1) four sample trees where systematically selected being the first non-suppressed coniferous trees found going clockwise around the plot after passing each cardinal direction. (2) The second step was to select four coniferous trees among all social status classes, being the next tree to each of the first sample trees according to increasing azimuth from plot center, and (3) the last step was to sample all deciduous trees on the plot. In addition, we subjectively selected some deciduous trees outside, but close to the plot. The last step was accomplished to get a better balance between number of selected coniferous and deciduous trees. The tree with the longest distance to plot center was located 26.8 m from the center.

Tree height, height to crown base, and crown radius were measured on the sample trees. Crown radius was calculated as the average of radii measured in the four cardinal directions. Tree height was measured using a Vertex III hypsometer. A summary of characteristics of field measured spruce and birch trees appear in Table 1.

2.3. Airborne laser scanner data

ALS data used in this study were acquired 18 June 2005 under leaf-on conditions with the Optech ALTM 3100 sensor. The sensor operated

Table 1
Summary of field measurements of trees.

Tree species	Characteristic	*n*	Mean	Std	Min	Max
Norway spruce	Tree height (m)	209	17.6	8.6	1.8	33.8
	Stem diameter (cm)	209	23.7	12.9	1.7	51.0
	Crown radius (m)	209	1.5	0.6	0.5	2.9
	Crown base height (m)	209	4.2	3.7	0.0	16.1
Birch	Tree height (m)	203	12.1	6.4	1.6	29.1
	Stem diameter (cm)	203	14.1	9.2	2.1	39.5
	Crown radius (m)	203	1.4	0.7	0.3	4.2
	Crown base height (m)	194	5.8	4.4	0.0	18.9

with a laser pulse repetition rate of 100 kHz and a scanning frequency of 70 Hz. In total, eleven individual flight lines were flown to cover the field plots. Individual strips overlapped with about 15%. Average flight speed was 75 ms^{-1} at a mean altitude of 750 m a.g.l. The maximum scan angle of 20° yielded a swath width of about 260 m. Pulses transmitted at half scan angles that exceed 8° were excluded from the final dataset in order to eliminate erroneous edge points as ALS sensors with oscillating mirrors have less accurate determination of *z* and across track coordinates at the scan edge. These errors occur because of the difficulty of modeling the rapid deceleration and acceleration that occur when the mirror is turning. Hence, the total scan angle used was 16°. The beam divergence was 0.28 mrad which yielded an average footprint size of about 21 cm. The average point spacing was 0.37 m by 0.54 m which gave an average point density of 5.09 m^{-2}. The recorded mean point density inside the tree segments of the studied trees was 6.6 m^{-2} and the standard deviation was 3.2 m^{-2}. Point density variation is partly caused by overlapping flight lines. Using ALS data from overlapping flight lines are frequently used in operational forest inventory and is probably the only way to obtain species information over large areas in a "wall-to-wall"context. However, since the ALS is a sample device, the higher point density will only lead to a more precise determination of laser-derived features.

Initial processing of the data was accomplished by the contractor (Blom Geomatics, Norway). Planimetric coordinates (*x* and *y*) and ellipsoidal height values were computed for all echoes. One of the flight lines was flown perpendicular to the other flight lines and used in matching and correction for systematic errors between swaths. Ground points were found and classified using the progressive Triangular Irregular Network (TIN) densification algorithm (Axelsson, 1999) of the Terrascan software (Terrasolid Ltd., 2004). A TIN was created from the planimetric coordinates and corresponding heights of the laser echoes classified as ground points. The ellipsoidal height accuracy of the TIN model was expected to be around 20–30 cm (e.g. Hodgson & Bresnahan, 2004; Kraus & Pfeifer, 1998; Reutebuch et al., 2003). The heights above the ground surface were calculated for all echoes by subtracting the respective TIN heights from all echoes recorded.

Older ALS systems (e.g. Optech ALTM 1210) typically record two echoes for each pulse, i.e., first and last echoes. The ALTM 3100 sensor used in this study is capable of recording up to four echoes per pulse. To separate different echoes acquired by such a system there has to be a certain time interval between the echoes. This time interval is known as the vertical resolution (Baltsavias, 1999). The vertical resolution for the sensor used in this study varies between 2.1 m for the two first echoes to 3.8 m for the other echoes. If four echoes are detected by the ALTM 3100 sensor, they are labeled as "first echo of many", "second echo", "third echo", and "last echo of many". If there are three echoes, they are labeled "first echo of many", "second echo", and "last echo of many". Furthermore, if two echoes are recorded they are labeled "first echo of many" and "last echo of many". Finally, if only one echo is recorded it is labeled as a "single echo". "Single echoes" are registered if the distance between the first echo and the last echo is less than 2.1 m or if it is not enough energy to trigger a second echo.

In this study, ALS data were delivered by the contractor as two datasets to be as close to the structure of the data provided by the ALTM 1210 sensor as possible, i.e., with "first echoes of many" plus "single echoes" as one dataset and "last echoes of many" plus "single echoes" as a second dataset. The use of two echoes, i.e., first and last, is common in operational ALS-assisted forest inventories in Norway (Næsset, 2004a). However, in this particular study, we split the two datasets based on spatial coordinates of the echoes into three different datasets containing the individual echo categories, i.e., (1) "first echoes of many", (2) "single echoes", and (3) "last echoes of many". The echo categories were denoted as "FIRST", "SINGLE", and "LAST", respectively. These three echo categories were used in the analysis. The relations between echoes of the same pulse have been outlined as important information to separate tree species (Brandtberg, 2007) and have been tested in tree species classification (Holmgren & Persson, 2004). However, given the structure of the data delivery in the present study, it was not possible to reconstruct the original data structure and tie the different echoes of each pulse to each other. Each echo category was therefore treated separately.

The intensity values used in this study were the uncalibrated intensity as recorded by the sensor. The intensity data recorded by ALS are noisy and will vary with target and sensor properties. Several studies have explained this noise by varying reflectivity with different directions of different target surfaces (Song et al., 2002; Wotruba et al., 2005). Hence, intensity of a target as measured by ALS will change with the scan angle of the emitted pulse (Kaasalainen et al., 2005). This could be adjusted for, but we did not have sufficient information to apply such a radiometric correction of the raw intensity values.

2.4. Computation of features of individual tree segments

In the present study, we did not use any crown delineation algorithm to identify the individual tree segments. Instead, we computed the crown radius for each tree as the mean of the field

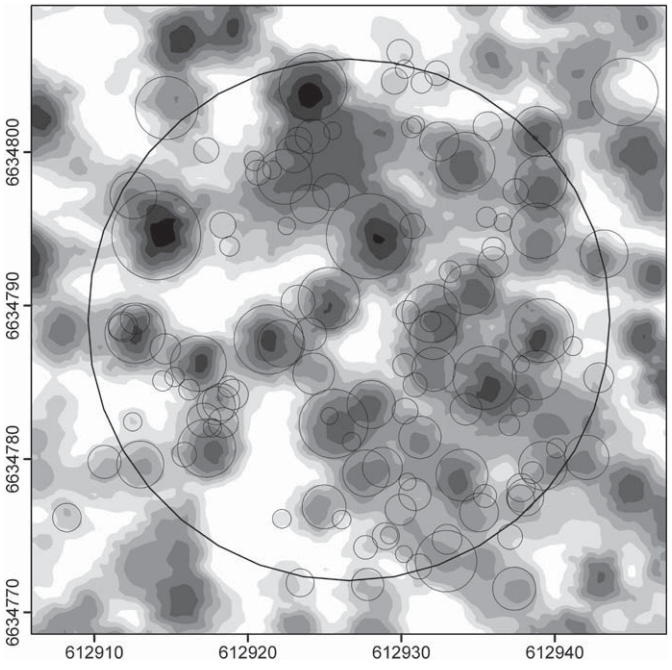

Fig. 1. Example of crown map (plot #14) showing the heterogeneous structure of the forest which lead to a number of overlapping crowns. The crown shapes are draped above a canopy surface model interpolated from laser echoes.

measured radii in the four cardinal directions and this quantity was used to buffer the field-measured stem position producing circular crown outlines (Fig. 1).

After having generated the circular tree segments, each laser echo was assigned to its corresponding tree crown. For trees with overlapping crowns, echoes in the overlapping zone were assigned to the tallest tree. Since laser measurements always will underestimate true tree height (Gaveau & Hill, 2003), echoes with higher *z*-value than the actual field-measured tree height were deleted. This correct for errors caused by erroneous positions and the assumption of circular crowns.

In area-based forest inventory where the ALS-related metrics are derived from the laser height distribution of a plot or certain target area (cf. Næsset, 2002), laser echoes between the ground surface (the TIN surface) and a threshold of, say, 2 m, are often considered as echoes from stones or under-vegetation and thus not included in analyses of the canopy (Næsset, 2002; Næsset & Bjerknes, 2001). A Ground Threshold Value (GTV) of 2 m is in accordance with the work by Nilsson (1996). In forestry, parameters like diameter, age, and basal area are most commonly registered at breast height, i.e., the point of the stem located 1.3 m above ground. We argue that breast height should be used as the GTV in individual tree assessment based on ALS data for consistency, unless there are specific reasons not to, for example when *a priori* knowledge of the height of the under-vegetation exist (Holmgren, 2004). In the multi-layered forest in our study area we also wanted to keep as much information as possible about the small trees. Hence, in the present work we used breast height (1.3 m) as the GTV.

For each tree segment, we used the point cloud to calculate four groups of structural features, i.e., (1) Normalized Height Features (NHF), (2) Canopy Penetration Depth (CPD), (3) Other Height Features (OHF), and (4) Crown Density Features (CDF). We also used one group of intensity features, i.e., Laser Intensity Features (LIF). From the echo height distribution we computed maximum (HMAX), mean (HMEAN), and height percentiles at 10% intervals (H10, H20, …., H80, H90) for each segment. These features were scaled to produce NHF and CPD (Eqs. (1)–(2)) described in Section 2.5. We selected the H10, H50, and H90 percentiles for further analysis. In addition we computed Other Height Features (OHF) including kurtosis (HKURT) and skewness (HSKEW) of the laser height distributions. Furthermore, standard deviation (HSTD), scaled according to Eq. (1), and coefficient of variation (HCV) for the laser height values were calculated in the OHF group. The features were calculated from all echoes above the GTV and for separate echo categories, i.e., FIRST, SINGLE and LAST.

Crown density features (CDF) were calculated in accordance with canopy density calculation in area-based forest inventory (Næsset, 2004c). The crown was divided into vertical crown layers by dividing field-measured tree height minus the GTV value (1.3 m) into 10 layers of equal height. Crown density was calculated for each echo category as the proportion of echoes above layer number 0 (>GTV), 1, …, 9, to total number of echoes in that category for each tree, and these densities were denoted as D0, D1, …, D9. D1, D5, and D9 were selected for further analysis.

Laser intensity features (LIF) derived for each individual tree were maximum intensity (IMAX), mean intensity (IMEAN), median intensity (IMEDIAN), kurtosis (IKURT), skewness (ISKEW), standard deviation (ISTD), and coefficient of variation (ICV) for echoes above GTV for the separate echo categories.

2.5. Scaling of laser height features

As stated above, two different scaling methods were applied in order to ensure independence of tree height and to utilize laser height features (i.e., HMAX, HMEAN, H10, H20, …., H90, HSTD) in species classification. In our study, two scaling approaches were used, i.e., (1) normalized with tree height to produce NHF (Eq. (1)) and (2) transformed to CPD using tree height (Eq. (2)):

$$\mathrm{NHF} = \frac{\mathrm{LHF}}{h} \tag{1}$$

where

NHF laser-derived height feature normalized with field-measured tree height,
h field-measured tree height,
LHF laser-derived height feature, i.e., HMAX, HMEAN, H10, H20, …., H90, HSTD.

$$\mathrm{CPD} = h - \mathrm{LHF} \tag{2}$$

where

CPD laser-derived height feature scaled to crown penetration depth,
h field-measured tree height,
LHF laser-derived height feature, i.e. HMAX, HMEAN, H10, H20, …., H90.

2.6. Tree height and laser echo categories

The forest in the Østmarka forest reserve is heterogeneous with complicated structure and a number of overlapping tree crowns (Fig. 1). The spatial distribution and size of the trees will influence on the number of echoes returned from inside a tree segment. In addition, not all the field-measured trees will have echoes of all categories. For short trees, FIRST and LAST echoes in particular will be limited in number because of the limited vertical resolution of the ALS sensor. In order to calculate all the defined variables for a tree, at least three echoes above GTV in each echo category are needed. This requirement reduced the number of trees subject to analysis significantly. We therefore analyzed two separate datasets, i.e., (1) one containing trees hit by at least three echoes of each category above GTV and (2) one with those trees not satisfying the criteria of the first dataset, but with at least three SINGLE echoes above GTV for each tree. The first dataset comprised 201 trees and was labeled Large Trees because it on average contained higher trees (Table 2) than the Small Trees dataset of 176 trees. The field-measured tree height distributions of each species for the two tree categories are displayed in Fig. 2. For the two datasets, we computed and reported the proportions of echoes in the different echo categories (FIRST, SINGLE, LAST) as observed in the sample trees above and below GTV (Table 3). The proportions of echoes were computed relative to the sum of FIRST and SINGLE echoes. This information is interesting in evaluating the split into tree categories and to assist evaluation of crown density features.

Table 2
Summary of number of trees and heights in the two tree categories used in the analysis.

Tree categories	Tree species	*n*	Tree height (m)			
			Mean	Std	Min	Max
Small Trees	Spruce	78	9.6	5.5	2.6	27.8
	Birch	98	8.5	4.5	2.4	24.0
Large Trees	Spruce	119	23.8	4.2	12.0	33.8
	Birch	82	17.6	4.3	9.2	29.1

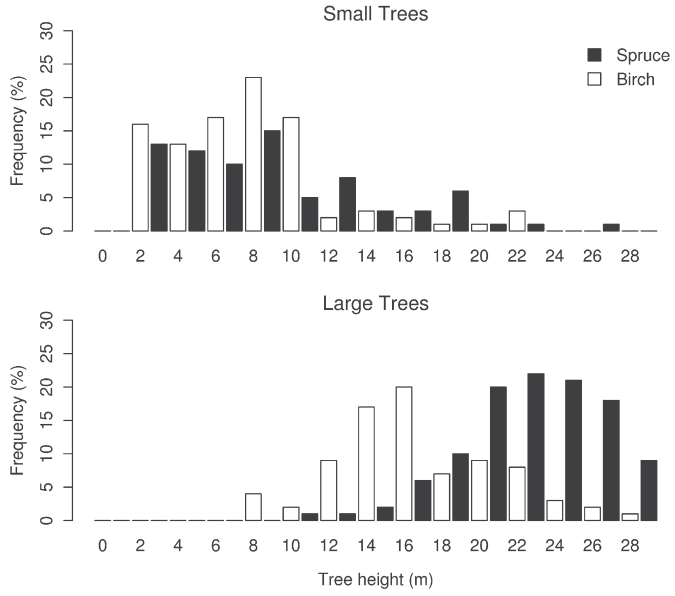

Fig. 2. Histogram of tree height distribution in the two datasets labeled Small Trees and Large Trees. The dataset Large Trees contains trees hit by at least tree pulses with all echo categories and the dataset Small Trees contains the remaining trees with at least tree pulses with echoes of the SINGLE category.

2.7. Analysis of differences between tree species

Generally, a laser feature can be used for species classification if it differs significantly between species (e.g. Brandtberg et al., 2003; Holmgren & Persson, 2004). Instead of only analyzing differences in mean values using *t*-tests or analysis of variance we incorporated tree heights into our analysis. Hence, we computed a linear regression model including tree species and field-measured tree height as covariates and the specific laser features as the response variable. Tree species was included as a dummy variable. Such analyses are often refereed to as analysis of covariance (ANCOVA). The full model (Eq. (5)) was estimated with ordinary least square regression using the R stats package (R Development Core Team, 2007). In addition, simpler models were estimated by removing one (Eq. (4)) or two (Eq. (3)) of the latter terms of the full model (Eq. (5)). All together three different models were estimated:

$$\mathrm{LF} = \beta_0 + \beta_1 SP \tag{3}$$

$$\mathrm{LF} = \beta_0 + \beta_1 SP + \beta_2 h \tag{4}$$

$$\mathrm{LF} = \beta_0 + \beta_1 SP + \beta_2 h + \beta_3 h{*}SP \tag{5}$$

where

LF	laser-derived feature, i.e., all features in the five feature groups (NHF, CPD, OHF, CDF, LIF),
h	field-measured tree height,
SP	dummy variable for tree species. $SP=1$ if spruce and $SP=-1$ if birch.

The "best" model of the three estimated, was selected using *F* statistics, also known as the partial *F*-test. Simpler models, i.e., fewer parameters estimated, were selected if they did not have significantly ($p \leq 0.05$) lower explanatory power than more complex models. The *F* statistics was computed with the *anova*-function of the R stat package (R Development Core Team, 2007) and it was computed by dividing the difference in model residual sum of squares by the ratio of model residual sum of squares by degrees of freedom for the more complex model (Eq. (6)). In the complex model, one parameter more than in the simple model is estimated.

$$F = \frac{\mathrm{RSS}_1 - \mathrm{RSS}_2}{\mathrm{RSS}_2 / \mathrm{DF}_2} \tag{6}$$

where

RSS_1	residual sum of squares of simpler model, e.g. Eq. (4),
RSS_2	residual sum of squares of complex model, e.g. Eq. (5),
DF_2	degrees of freedom of complex model, e.g. Eq. (5).

If the best model selected based on Eq. (6) was the full model (Eq. (5)) the estimated β_0 is the intercept, β_1 is the change in intercept for species (plus for spruce and minus for birch), β_2 is the estimated slope for tree height, and β_3 is the change in slope for tree species (plus for spruce and minus for birch). The significance of the model terms (SP, h, $h{*}SP$) was tested using an *F*-test. The null hypothesis tested was that the betas ($\beta_1, \beta_2, \beta_3$) were equal to zero when all other terms were included in model, i.e., using adjusted sum of squares — also called Type III-test. In order to compare variance explained for different features, we compute single term coefficients of variation using adjusted sum of square for the single term divided by the sum of single term sum of squares plus residual sum of squares, i.e.,

$$\eta^2_{\mathrm{effect}} = \frac{\mathrm{SS}_{\mathrm{effect}}}{\mathrm{SS}_{\mathrm{total}}} \times 100 \tag{7}$$

where

η^2_{effect}	eta-squared for effect, i.e. tree species (SP), tree height (h) or interaction ($h{*}SP$),
$\mathrm{SS}_{\mathrm{effect}}$	adjusted sum of squares for single model terms, i.e. tree species (SP), tree height (h) or interaction ($h{*}SP$),
$\mathrm{SS}_{\mathrm{total}}$	adjusted sum of squares for all model terms i.e. tree species (SP), tree height (h) or interaction ($h{*}SP$), and the error term.

In variance analysis such measures are often referred to as the correlation ratio or eta-squared (η^2_{effect}) (Kline, 2004). Eta-squared will sum to 100 for all model terms. However, the sum of eta-squared (η^2_{effect}) for all terms is different from the coefficient of determination (R^2) although both are measures of explained variability. The reason for this difference is that in computation of η^2 adjusted sum of square is used and in computation of R^2 sequential sum of square is used. We used eta-squared for the tree species term (η^2_{SP}), or as referred to in this study, the proportion of variability explained by tree species, to identify candidate features. Candidate features should have a high proportion of variability explained by tree species (η^2_{SP}) and explained variability should be higher for tree species than by other model terms.

In order to test classification performance of candidate features (objective 2), classification was carried out using Linear Discriminant

Table 3
Proportion (%) of echoes relative to the sum of FIRST and SINGLE echoes for the two tree categories (Large Trees and Small Trees) split on tree species and above and below ground threshold value (GTV = 1.3 m).

Tree species	Echo category	Large Trees		Small Trees	
		H>=GTV	H<GTV	H>=GTV	H<GTV
Norway spruce	FIRST	35	0	12	0
	SINGLE	62	3	81	7
	LAST	21	20	5	10
Birch	FIRST	41	0	25	0
	SINGLE	52	7	65	10
	LAST	18	26	2	26

Analysis (LDA). The estimation was conducted using the *lda*-function of the R package MASS (Venables & Ripley, 2002) using equal prior probabilities and full cross validation. From the resulting error matrix, accuracy was computed for each tree species and for the overall classification. Classification was carried out for single candidate features. Features with low overall accuracy were removed from the set of candidate features. Finally, classification was carried out for the combination of the "best" candidate feature in each feature group and for separate echo categories.

In addition to the analysis described above, we also visualized the distribution of normalized laser heights and the raw intensity values by density plots. The plots will identify differences in the height and intensity distributions between species. Density estimation is a method used to estimate probability density functions from sample data. Density estimates are very useful in exploration and presentation of data (Silverman, 1986). In this study, we used the kernel estimator to estimate the density function. The density function was computed with the R stats package (R Development Core Team, 2007) using a Gaussian kernel and bandwidth selection using the Silverman's "rule-of-thumb" (Venables & Ripley, 2002). The kernel density plots will produce a better visualization of the height- and intensity distributions than histograms, but interpretation will be the same.

3. Results

The results of the analysis of covariance (ANCOVA) (Eqs. (3)–(5)) and model selection procedure (Eq. (6)) are summarized in Table 4. The analysis revealed that many of the computed laser features differed significantly between tree species. In 52 of 72 estimated models, tree species was a significant ($p<0.05$) explanatory variable of the specific laser feature analyzed. However, selected models also demonstrated that analyzed laser features were influenced by tree height. For the 72 laser features tested, 41 models included the covariate (tree height). Among these 41 models, 13 also included the interaction term. Comparing proportion of variability explained by tree species (η^2_{SP}) in the selected model and the simple one-way ANOVA model (Eq. (3)) illustrates that tree height would influence selection of candidate variables if we did not considered tree height as a covariate (Fig. 3).

3.1. Differences in structural features between tree species (Objective 1a)

The height distributions of laser echoes for different species, echo categories, and tree height categories (Large Trees and Small Trees) are visualized in Fig. 4. The normalized laser height features (NHF) computed from FIRST and SINGLE echoes for birch trees were larger than for spruce trees (Table 4). Conversely, NHF computed from LAST echoes were smaller for birch trees than for spruce trees. The highest proportion of variability explained (η^2_{SP}) obtained for tree species from NHF was 11% for Large Trees and 17% for Small Trees. However, a similar or higher proportion of the variation was explained by tree height. Moreover, we also carried out the ANCOVA with height features scaled as crown penetration depth (CPD) (Eq. (2)). CPD from FIRST and SINGLE echoes were significantly deeper for spruce compared to birch (Table 4). In the CPD group, only features not influence by tree height, i.e., CPD computed from SINGLE echoes and

Table 4
Summary of analysis of covariance (ANCOVA)[a].

Laser feature[b]	Large Trees																Small Trees					
	FIRST						SINGLE						LAST				SINGLE					
	SP		*h*		*h*SP		*SP*		*h*		*h*SP		*SP*		*h*		*h*SP		*SP*		*h*		*h*SP	
HMAX (NHF)	−4	**	+3	*			−3	*	+3	*			+0	ns	**+13**	***			−6	**	+8	***		
HMEAN (NHF)	−6	***	+6	***	+3	**	**−11**	***	**+11**	***			+7	***	**+15**	***			**−17**	***	**+15**	***		
H10 (NHF)	−7	***	+3	*	+4	**	−5	***	+8	***			+5	***	+7	***			**−12**	***	**+11**	***		
H50 (NHF)	−5	***	+5	**	+3	**	−9	***	+7	***			+6	***	**+13**	***			**−17**	***	**+17**	***		
H90 (NHF)	−2	*	+4	**			−9	***	+6	***			+1	ns	**+10**	***			−9	***	+9	***	+2	*
HMAX (CPD)	**+11**	***					+4	**					+1	ns					+3	*	+2	*		
HMEAN (CPD)	+6	***	+9	***	−3	**	**+26**	***					+1	ns	**+25**	***	−2	**	+9	***	**+31**	***		
H10 (CPD)	+5	***	**+11**	***	−3	**	**+16**	***					+2	*	**+31**	***	−3	**	+5	***	**+37**	***		
H50 (CPD)	+5	***	+5	***	−3	**	**+19**	***					+1	ns	**+17**	***	−3	**	**+11**	***	**+25**	***		
H90 (CPD)	+2	*	+3	*			**+18**	***					−1	ns	+4	**			+6	***	+8	***		
HSD (NHF)	**+10**	***	−1	ns	−7	***	+0	ns	−9	***			+2	ns	−0	ns	−2	*	+7	***	−5	**		
HCV	**+11**	***	−2	*	−8	***	+1	ns	−9	***			−6	***	−3	**			**+11**	***	−7	***		
HKURT	**−13**	***	+2	*			**−14**	***					−0	ns	+3	*			−1	ns				
HSKEW	+7	***	−2	*			**+18**	***					−4	**	−3	*			+2	ns	−7	***		
D1	+1	ns					**+12**	***					**+11**	***					+1	ns	**+16**	***		
D5	**−10**	***	+7	***	+6	***	+0	ns	+5	**			**+13**	***	+5	***			−2	*	**+27**	***		
D9	+1	ns					−20	***	+6	***			**+17**	***					−7	***	**+19**	***		
IMAX	**−19**	***					−3	*					+1	ns					+2	ns	+2	ns	−4	*
IMEAN	**−18**	***					−1	ns					**+19**	***	−6	***			+2	ns	+0	ns	−5	**
IMEDIAN	**−14**	***					−1	ns					**+18**	***	−6	***			+2	ns	+0	ns	−5	**
ISD	−8	***					−3	*					+3	*					−0	ns	+6	**		
ICV	+2	ns					−2	ns					+2	ns					+0	ns	+5	**		
IKURT	−4	**					+1	ns					−5	***	+3	*			+4	**	+1	ns	−5	**
ISKEW	+2	*					−2	*					−11	***	+5	***			+0	ns				

The sign of the regression coefficients[c] variability explained by (η^2_{effect}) model terms, and the significant level[d] of the term for selected models are displayed for different tree height categories, echo categories, and model terms, i.e., tree species (*SP*), tree height (*h*), and the interaction term (*h*SP*). Model terms with higher variability explained (η^2_{effect}) than 10 appear in bold.

[a] The displayed models are the best ones (i.e. Eq. (3), Eq. (4), or Eq. (5)) selected according to Eq. (6).

[b] HMAX = maximum height of laser height distribution; HMEAN = mean height of laser height distribution; H10, H50, and H90 = 10, 50, and 90 percentiles of laser height distribution; HSD = standard deviation of laser height distribution; HCV = coefficient of variation of laser height distribution; HKURT = kurtosis of laser height distribution; HSKEW = skewness of laser height distribution. Abbreviations in parenthesis refer to scaling method, i.e. normalized height features (NHF) (Eq. (1)) or canopy penetration depth (CPD) (Eq. (2)). D1, D5, and D9 = crown densities corresponding to proportions of laser echoes above layer # 1, 5, and 9, see text for further details; IMAX = maximum value of laser intensity distribution.; IMEAN = mean value of laser intensity distribution.; IMEDIAN = median value of laser intensity distribution.; ISD = standard deviation of laser intensity distribution.; ICV = coefficient of variation of laser intensity distribution.; IKURT = kurtosis of laser intensity distribution.; ISKEW = skewness of laser intensity distribution.

[c] Plus (+)for species (*SP*) and interaction (*h*SP*) represent higher values for spruce compared to birch. Plus (+) for tree height (*h*) represent increasing values with increasing tree height.

[d] Level of significance: ns = not significant (>0.05); *<0.05; **<0.01; ***<0.001.

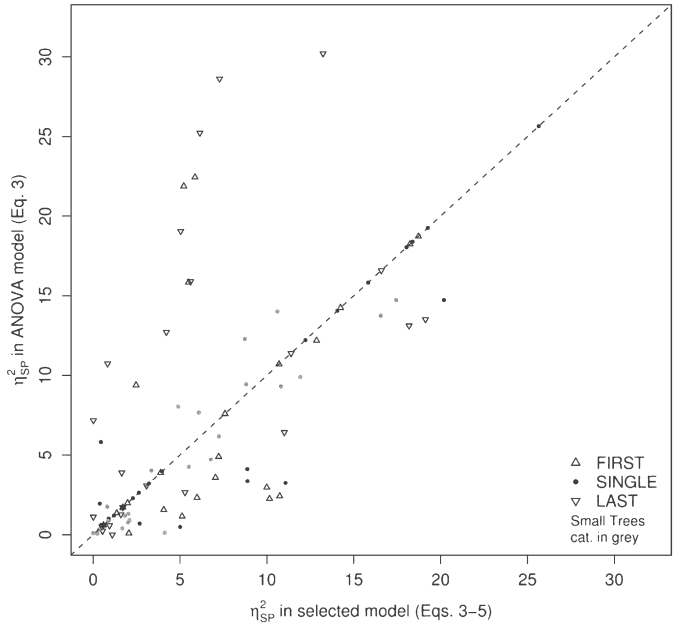

Fig. 3. Proportion of variability explained by tree species (η^2_{SP}) for different laser features in ANOVA model (Eq. (3)) compared to in selected ANCOVA model (Eqs. (3)–(5)). Laser features in the upper left of the plot have lower explained variability of tree species when tree height is introduced as covariate. Laser features in the lower right of the plot will explain more of the difference between tree species when the covariate is introduced. Laser features at the 1:1 line are features where the ANOVA model (Eq. (3)) is selected as the one with the significantly highest variability explained.

HMAX from FIRST echoes, had potential for tree species classification. The Small Trees category was highly influenced by tree height both within NHF and CPD.

The effect of the two different scaling methods is illustrated with proportion of variability explained by the tree species term (η^2_{SP}) in

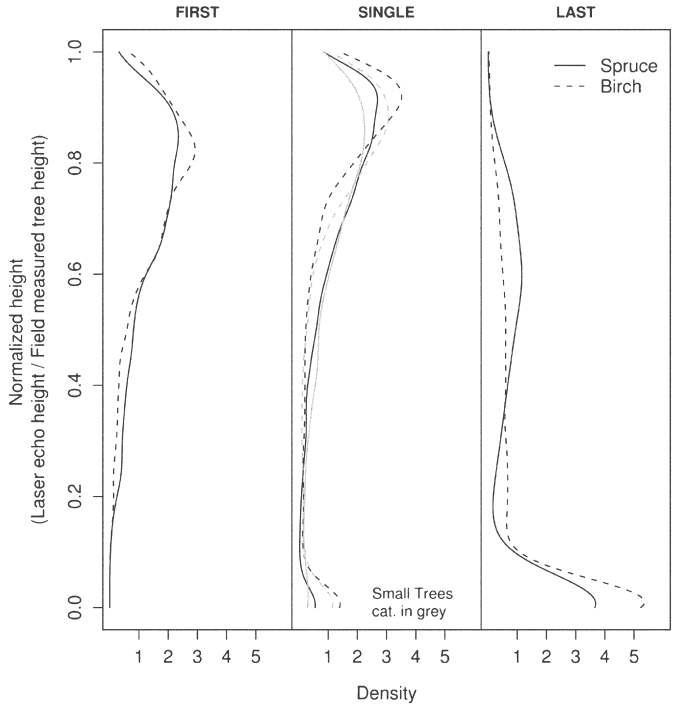

Fig. 4. Normalized laser height distributions, estimated as kernel density, for different tree species and echo categories for both tree categories. The Small Trees dataset is only represented by SINGLE echoes.

percentile (H10–H90) models (Fig. 5). The proportion of variability explained for percentiles derived from SINGLE echoes scaled to crown penetration depth (CPD) were on average 11% higher than the corresponding relative heights (NHF).

The normalized standard deviation (HSTD) and coefficient of variation (HCV) differed between the two species for FIRST echoes and FIRST and LAST echoes, respectively, in the Large Trees category (Table 4). For Small Trees, both HSTD and HCV differed between species. However, both features were always dependent on tree height in the Small Tree category. HCV was found to be as good as HSTD or better in terms of proportion of variability explained by the models. The analysis also revealed that HSTD and HCV in general were lower for birch trees for all echo categories.

Skewness (HSKEW) and kurtosis (HKURT) were found to have potential for tree species classification for the Large Trees category when computed from FIRST and SINGLE echoes (Table 4). Skewness and kurtosis for the FIRST and SINGLE echoes indicated that the distribution was more skewed, sharp, and a bit more shifted upwards for birch than for spruce (Table 4 and Fig. 4).

The differences in crown density between tree species were most pronounced for features computed from LAST echoes (Table 4, Fig. 6). For FIRST echoes, the largest differences were found in the intermediate parts and for SINGLE echoes the largest differences were found in the lower and upper part of the crown. Small Trees crown density features were highly influenced by tree height and were only statistically significant in the upper parts of the tree crown. Furthermore, it was also found that tree heights significantly influenced the values of most crown density features also for the Large Trees category.

3.2. Differences in intensity features between species (Objective 1b)

The estimated distributions of uncalibrated intensity for the two species for each echo category and for the two tree categories are plotted in Fig. 7. The main difference in the intensity distributions was between the echo categories. SINGLE echoes had higher intensities compared to FIRST and LAST echoes. Both FIRST and LAST echoes had approximately half the mean intensity values compared to SINGLE echoes, i.e., 56 and 41%, respectively. There was no clear difference

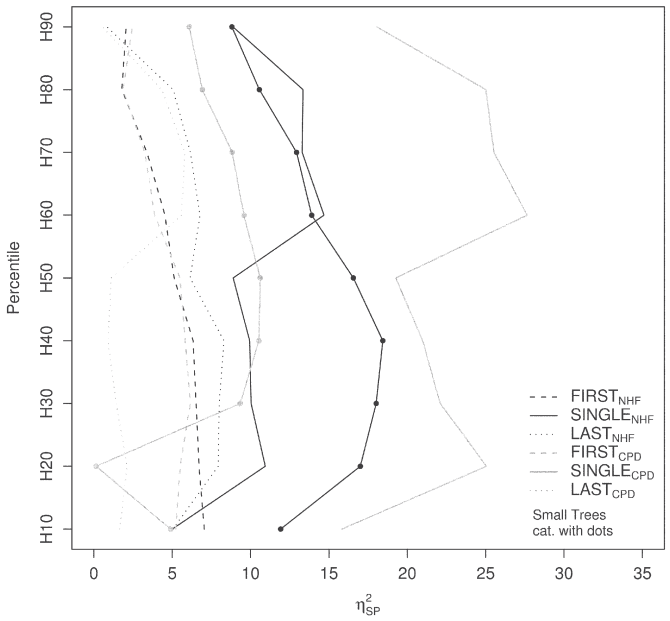

Fig. 5. Proportion of variability explained by tree species (η^2_{SP}) for different percentiles (H10–H90) and scaling methods, i.e., normalized height features (NHF) (Eq. (1)) and crown penetration depth features (CPD) (Eq. (2)), displayed for echo- and tree categories.

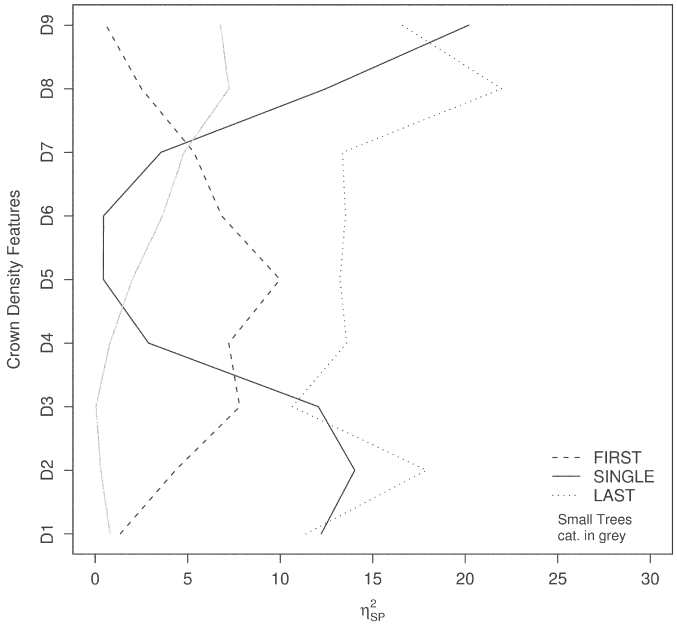

Fig. 6. Proportion of variability explained by tree species (η^2_{SP}) for different crown density features (D1–D9), echo- and tree categories. Crown densities are computed as the number of echoes of an echo category above a given vertical layer as a proportion of total number of echoes of that specific category, see text for further details.

between tree species in the density plots (Fig. 7). The ANCOVA (Table 4) revealed that laser intensity features were higher for birch trees than for spruce with exception of the LAST echoes where the opposite effect was observed. The largest proportions of variability explained were in intensity features from FIRST echoes (IMAX, IMEAN, IMEDIAN) and LAST echoes (IMEAN, IMEDIAN). Furthermore, features derived from the LAST echoes were significantly related to tree height. For Small Trees, none of the computed intensity features, except from IKURT, differed between the two species (Table 4).

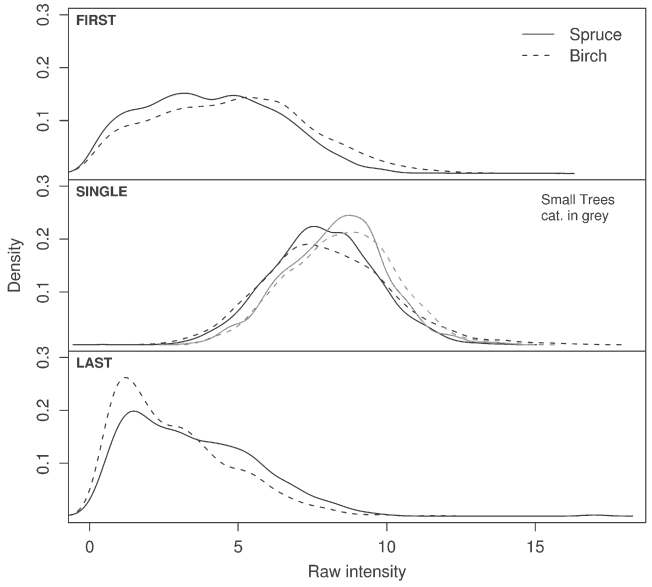

Fig. 7. Laser intensity distributions, estimated as kernel density, for different tree species and echo categories for both tree categories. The Small Trees dataset is only represented by SINGLE echoes.

Table 5
The three features[a] within tree categories, echo categories, and feature groups[a] with the highest proportion of explained variability (η^2_{SP}) for tree species in ANCOVA model.

Feature groups[b]	Large Trees			Small Trees
	FIRST	SINGLE	LAST	SINGLE
NHF	H10(59)	*HMEAN(60)*	HMEAN (74)	***HMEAN(64)***
	HMEAN(58)	H50(61)	H50(74)	***H50(64)***
	H50(55)	H90(61)	H10(70)	*H10(62)*
CPD	*HMAX (61)*	***HMEAN(75)***	H10(58)	H50(66)
	HMEAN(71)	***H50(74)***	H50(28)	HMEAN(65)
	H50(72)	***H90(69)***	HMEAN(52)	H90(64)
OHF	***HKURT(70)***	***HSKEW(70)***	**HCV(69)**	***HCV(65)***
	HCV(57)	***HKURT(72)***	HSKEW(66)	HSD(63)
	HSD(55)	HCV(55)	HSD(53)	HSKEW(56)
CDF	*D5 (58)*	***D9(67)***	***D9(67)***	D9(58)
	D1(61)	***D1(70)***	***D5(77)***	D5(52)
	D9(54)	D5(60)	*D1(65)*	D1(55)
LIF	***IMAX(73)***	ISD(55)	***IMEAN(67)***	IKURT(51)
	IMEAN(70)	IMAX(58)	*IMEDIAN(66)*	IMEDIAN(55)
	IMEDIAN(66)	ISKEW(59)	*ISKEW(65)*	IMEAN(53)

Overall accuracy of classification for single features is shown in parenthesis. Italic letters indicate that variability explained by tree species (η^2_{SP}) is greater than 10 and no other model term has higher explained variability (η^2_h,η^2_{h*SP}). Bold letters indicate candidate features having both high η^2_{SP} for tree species and high overall accuracy.
[a] Symbols explained in Table 4.
[b] NHF = normalized height features, CPD = crown penetration depth, OHF = other height features, CDF = crown density features, and LIF = laser intensity features.

3.3. Classification performance of candidate features (Objective 2)

The overall classification accuracies of the three features with highest proportion of variability explained by tree species (η^2_{SP}) in the five feature groups (NHF, CPD, OHM, CDF, and LIF) are presented in Table 5. Laser features with proportions of variability explained by tree species (η^2_{SP}) higher than 10 and where a greater proportion of variability was explained by tree species than by other model terms are presented in italics. Features presented in bold were considered as candidate features. In addition to meeting the criteria for proportion of variability explained by tree species (η^2_{SP}), the candidate features had high (>67%) overall classification accuracies.

Combining the candidate features with highest proportions of variability explained by tree species (η^2_{SP}) in each feature group and echo category increased the overall accuracy obtained for the Large Trees category. The combination of candidate features yielded an overall accuracy of 88% for Large Trees and 64% for Small Trees (Table 6).

4. Discussion and conclusions

4.1. Materials and methods

In this study, the main focus was on identifying candidate laser-derived features suitable for discriminating between coniferous

Table 6
Classification performance for a combination of features selected.

Tree categories	Features selected[a]			Classification accuracy (%)		
	FIRST	SINGLE	LAST	Spruce	Birch	Overall
Large Trees	HKURT	HMEAN(CPD)	HCV	93.3	81.7	88.6
	IMAX	HSKEW	D9			
		D9	IMEAN			
Small Trees		HMEAN(NHF)		57.7	68.4	63.6
		HCV				

The features are selected from the candidate features (Table 5) having the highest (η^2_{SP}) in each feature group[b], echo category, and tree category.
[a]Symbols explained in Table 4.
[b]NHF = normalized height features, CPD = crown penetration depth, OHF = other height features, CDF = crown density features, and LIF = laser intensity features.

(spruce) and deciduous (birch) species. The study area is located in a forest reserve, and the tree height distributions observed in such a forest are likely to be different from those found in a managed forest. However, we found the data suitable for this study because datasets with large variation in tree size and spatial distribution of trees may provide a better basis for selecting robust laser features for species classification compared to less complex forests.

A possible source of error in the analyses are related the matching of field and laser data. The quality of this matching is dependent on the accuracy of the field measured tree coordinates and the assumption of circular crowns. However, the assumption of circular crown outlines as measured and reconstructed from field data will probably be more accurate than an outline produced by a segmentation algorithm in a relatively complex forest like the current. Moreover, tilting stems will offset the tree top positions relative to the measured positions registered in breast height using compass and measure tape. All these positional errors and errors in determining the true crown outline may cause commission of echoes from neighboring trees and omission of echoes from the tree in question. If there are between species commission and omission errors, they will tend to even out the differences in echo distributions between species. Since spruce is the most frequently occurring species in the study area, it is likely that echo distributions of birch trees will be more similar to echo distributions of spruce trees. Hence, computed features will be more similar between species. Therefore, identified candidate features probably are robust features not affected by these commission and omission errors.

4.2. General remarks on laser features and tree height scaling

This study has demonstrated that there are significant differences in many laser-derived features between spruce and birch. Therefore, many laser features may contribute to an improved tree species classification of individual trees based on ALS data. From the different types of features considered, i.e., normalized height features, canopy penetration features, crown density features, and uncalibrated laser intensity features, we identified laser features suitable to discriminate between the two species (Table 5). In the identification of features both echo category and tree size category were important. A specific type of feature may work well for species discrimination when it is computed for a certain echo category, but provide little or no useful information when computed from other echo categories. The identified candidate features varied also highly between tree categories (Large Trees and Small Trees).

We also found that many laser-derived features are affected by tree height. The relationship between laser derived features and tree height may also be linked to other properties which are related to tree height, e.g. size and shape (i.e. allometry) and the interior structure of the tree crown. Thus, changes in laser features with increasing tree heights will occur for both laser height features and laser crown density features, but to a smaller degree for laser intensity features. Therefore, discriminating between species based on structural properties derived from ALS data may be challenging in a forest where different species have different height distributions. *A priori* knowledge of forest structure and variation in species may therefore be important. Laser height features used must be scaled, trees stratified into height classes, or tree heights must be included in a classification algorithm. The two simple scaling methods applied in this study, i.e., normalization with tree heights and canopy penetration depth, failed to provide independence of tree height in most cases. Selected candidate features for Large Trees were only selected from crown penetration depth scaling. From the normalized height features often used in individual tree species classification no features was selected for the Large Tree category. However, if we had based our selection on the ANOVA model, such features might have been selected (Fig. 3). The overall accuracy of normalized HMEAN computed from LAST echoes was 74% (Table 5) and were among the highest in this study. However, the proportion of variability explained was 7% for tree species (η^2_{SP}) and 15% for tree height (η^2_h) (Table 4).

4.3. Structural features

The main differences between spruce and birch in general are the rounder (spherical) crowns of birch compared to the more conical crowns of spruce. In addition, the higher crown base height and allocation of biomass higher up in the crowns are typical for many deciduous tree species. These two differences were also expressed in the laser-derived features, see illustration in Fig. 8. First, the values of laser features computed from FIRST and SINGLE echoes revealed that echoes from these categories were reflected higher in birch trees than in spruce trees. The plausible explanation for this is the differences in crown shape between the species. It is also likely that other crown structural characteristic influenced on the echo distributions, such as crown density, leaf area, and leaf orientation (Gaveau & Hill, 2003). Secondly, the higher proportion of LAST echoes in the crown of spruce trees may be explained by the relatively lower crown base of spruce. In addition to having lower crown base, spruce trees also have a larger proportion of the crown located at a lower level in the tree. Both the differences in crown base height and crown biomass distribution will tend to allow more LAST echoes to penetrate below GTV for birch trees instead of being recorded in the canopy.

The 1–2 cm long needles of spruce in comparison to the ca 5–6 × 5 cm plane birch leaves is another obvious difference that influences the crown structure. ALS data are influenced by the vertical distribution of biomass/leaf area (Coops et al., 2007; Magnussen & Boudewyn, 1998). Hence, the higher number of echoes in the upper crown of birch trees may also be attributed to denser and more compact tree crowns of this species. This effect is also expressed by the smaller variation in height of laser echoes in birch trees described by standard deviation and coefficient of variation. Especially SINGLE echoes were located at a point relatively higher up in birch crowns compared to spruce trees (Fig. 4). However, spruce had a higher portion of SINGLE echoes than birch (Table 3). This may be attributed

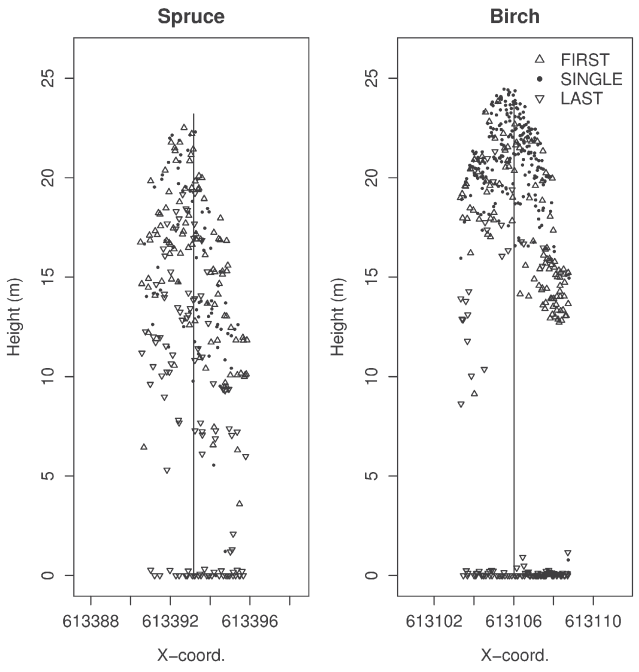

Fig. 8. Echoes of different categories plotted for two individual trees of spruce and birch.

to the fact that for spruce trees more echoes are located at a point where no additional echoes will be recorded, i.e., near the stem where no further penetration can be expected. In addition, the reflectivity properties of canopy elements, i.e., foliage, bark, and stem, will influence the distribution of laser echoes. In the wavelengths typically used by ALS sensors birch has higher reflectivity than spruce (Kuusk, A. pers comm.). Hence, FIRST and SINGLE echoes will tend to be recorded higher in the crown for birch trees.

In the Small Trees category only SINGLE echoes were observed. The main reason for this is probably the limited vertical resolution (2.1 m) of the laser sensor used. Another factor which will influence on the probability of reflecting three echoes or more of each category from an individual tree, which is the criteria for Large Trees, is the tree crown diameter. Hence, number of echoes will be low in the Small Trees category as a result of the limited vertical resolution and small crown diameters. Our analysis showed that SINGLE echoes were found higher in birch trees than spruce trees. This pattern coincides with what we found for the Large Trees category. In addition, it is important to notice the higher impact of tree height on laser height features computed from the Small Trees category. The large impact of tree height in this tree category resulted in quite few selected candidate features and made the selection of candidate features less convincing.

4.4. Intensity features

Among the intensity features, we found that the uncalibrated intensities from the FIRST echoes were the only ones that carried information useful for species discrimination. It seems that the uncalibrated intensities of FIRST echoes mostly are functions of the canopy reflectance of trees. Reflection from birch tends to be higher than for spruce for all canopy elements, i.e., stem, branches and leaf/needles, in the wavelength used by the current sensor (1064 nm) (Kuusk, A. pers comm.). The FIRST echoes are also likely to be less influenced by the biomass than subsequent echoes. The intensity of the LAST echo will be influenced by reflection and absorption higher up in the crown, and thus a higher intensity of e.g. the FIRST echo will tend to result in a lower intensity of LAST echoes, as we observed in this study. However, Reitberger et al. (2008) found that the mean intensity of laser echoes inside a tree produced higher classification accuracies than mean intensity of the upper 10% of the crown, but they did not distinguish between echo categories. A high proportion of reflections from the top of a tree will most likely be SINGLE echoes and hence the intensity will be higher and less different between species.

The advantage of intensity features computed from FIRST echoes is that they are independent of tree heights, at least for Large Trees, which we found not to be the case for the majority of the other derived features. We expected that intensity of SINGLE echoes of the Small Trees would be quite similar to FIRST echoes of the Large Trees, i.e., that the intensity primarily would be a function of species reflectivity. However, we found that intensity features were of little value for classification of spruce and birch when tree heights were <5–10 m. The difficulties of distinguishing between young conifers and young broadleaves were also reported by Schreier et al. (1985).

A large variability was inherent in the uncalibrated intensity values we used, and just a small portion of this variability seemed to be attributed to differences between species. Radiometric calibration of ALS intensities is not yet common practices in classification studies because of lack of appropriate methods (Boyd & Hill, 2007; Kaasalainen et al., 2005). Factors such as variable scan angle and flying altitude, atmospheric attenuation, and lack of stability of emitted pulse energy introduce noise to the recorded intensities. Using radiometric calibrated intensities instead of the raw intensities may yield less noise in the computed intensity features. Hence, radiometric calibrated intensities features may be more suited to distinguish between tree species.

4.5. Selected candidate features

We found that normalized height features were of little value in classification of larger trees, opposed to other studies. For example, Brandtberg et al. (2003) found that the normalized maximum height from first echoes had the highest overall tree species classification accuracy in a deciduous forest in eastern USA. In a Swedish study (Holmgren & Persson, 2004), the 90 percentile calculated for all echoes within the crown produced the lowest overall accuracy of features selected. Normalized percentiles tended to produce a very low accuracy using waveform data under leaf-on conditions in Germany (Reitberger et al., 2008), but was the group with second highest overall accuracy in another study conducted in the same area (Heurich, 2006). The new scaling method proposed in the present study, i.e., the canopy penetration depth scaling, is promising as a method to scale laser height features.

The other height features included variability features such as standard deviation (HSTD) and coefficient of variation (HCV) and features describing the shape of the distribution, i.e., kurtosis (HKURT) and skewness (HSKEW). HCV was selected as a candidate feature from the LAST echoes for Large Trees and from the Small Trees category. It should also be noted that HCV always was higher ranked than HSTD. Holmgren and Persson (2004) selected normalized standard deviation from all laser echoes within the tree crown as a candidate feature and overall accuracy was in the lower end compared to other features in the study. Also in a German study the standard deviations produce the lowest overall accuracies of features considered (Heurich, 2006). Our results indicate that the coefficient of variation should be used rater than the normalized standard deviation. In the study by Brandtberg et al. (2003), both standard deviation and kurtosis were selected as candidate features from the first echoes. In our study, kurtosis from FIRST and SINGLE echoes are recommended as features in addition to skewness for SINGLE echoes. The descriptions which kurtosis and skewness provide of the laser height distribution seem to be important in tree species classification.

Crown density features from the intermediate and upper part of the crown for LAST echoes and in the upper and lower part of the crown for SINGLE echoes are suggested as candidate variables in the present study. In a study from Germany, CDFs computed from a dual recording sensor provided the highest overall tree species classification accuracy under leaf-on conditions (Heurich, 2006). However, CDFs derived from waveform data in the same study area did not perform as well (Reitberger et al., 2008). In other studies, measures of crown density have been defined as proportion of echoes traveling below GTV (Moffiet et al., 2005) or as the proportion of echoes found above crown base to the total number of echoes (Holmgren & Persson, 2004). In both these latter studies, such features were shown to be of great importance in species classification. Also in our study density features contributed significantly to the separation of spruce and birch when computed from appropriate echo categories.

The three laser intensity features expressing the largest difference between species were suggested as candidate features in our study. These were the maximum intensity (IMAX), mean intensity (IMEAN) of FIRST echoes, and the mean intensity (IMEAN) of LAST echoes. Mean intensity and standard deviation of intensity computed for all echoes were among the three best features in a Swedish study (Holmgren & Persson, 2004). In another Swedish study, mean intensity was incorporated as the third classification feature (Holmgren et al., 2008). However, Moffiet et al. (2005) found that raw intensity features did not contribute to species classification in their study. In a study in North America, three of the six best features were derived from the intensity distribution of first echoes (Brandtberg et al., 2003). Reitberger et al. (2008) found mean intensity of the tree

useful in classification of coniferous and deciduous trees — both as a single feature and in combination with one or two other features.

4.6. Classification performance

In spite of the complex forest in the current study, the obtained classification accuracy of 88% for Large Trees is promising. In the current study, the sample trees were not segmented, but delineated on the basis of field measurements. Segmentation will most likely reduce the number of detected sub-dominant trees (Solberg et al., 2006) compared to the number of trees of these categories that were included in the current study. Thus, an increased classification accuracy would be expected if the trees were detected by a segmentation algorithm since less trees are detected and since these trees on average will have more laser echoes than the sub-dominant trees of this study. In other studies dealing with discrimination between coniferous and deciduous trees overall accuracies are at the same level as found in our study. Reitberger et al. (2008) obtain an overall accuracy of 85% classifying deciduous and coniferous trees whereas Holmgren et al. (2008) obtained an overall accuracy of 88% when classifying spruce, pine, and birch. Under leaf-off conditions Liang et al. (2007) achieve an overall accuracy of 90% when separating coniferous (spruce and pine) and deciduous (birch) trees. In another study conducted in the Østmarka forest reserve in which only intensity features were considered, an accuracy of 74% was achieved when classifying into three different categories, i.e., spruce, birch, and aspen trees (Ørka et al., 2007).

The overall classification accuracy for Small Trees was low (65%). Hence, classification of small individual trees may be a challenging task. The number of trees in the Small Trees category found by an segmentation algorithm will be low, since these trees likely are sub-dominant or suppressed (Solberg et al., 2006). In forest inventory tree species distribution for Small Trees may be classified using an area-based approach as an alternative to the individual tree classification. An area-based approach will have a higher number of echoes available to compute features from the echo distributions. Therefore, features will be more stable and may be more suitable for separating coniferous and deciduous tree species.

In addition to being influenced by crown characteristics, echo distributions are also affected by the laser acquisition parameter settings or sensor specific settings like e.g. pulse repetition frequency, beam divergence, and flying altitude (Chasmer et al., 2006; Goodwin et al., 2006; Hopkinson, 2007; Næsset, 2004b; Næsset, 2009). Thus, the selection of suitable features for tree species classification may be influenced by the ALS sensors and acquisition parameters used.

To conclude, promising classification results for spruce and birch were obtained using identified candidate ALS-derived structural- and intensity features. These candidate features included intensity features and different structural features derived from different echo categories. The echo category (FIRST, SINGLE, or LAST) is important in whether the feature is selected as a candidate feature or not. Further research should include validation of the suggested candidate variables on independent datasets, testing features from subsequent echoes of the same pulse, and assessment of radiometrically calibrated intensities.

References

Axelsson, P. (1999). Processing of laser scanner data—Algorithms and applications. *ISPRS Journal of Photogrammetry and Remote Sensing*, *54*, 138–147.

Baltsavias, E. P. (1999). Airborne laser scanning: Basic relations and formulas. *ISPRS Journal of Photogrammetry and Remote Sensing*, *54*, 199–214.

Bollandsås, O. M., & Næsset, E. (2007). Estimating percentile-based diameter distributions in uneven-sized Norway spruce stands using airborne laser scanner data. *Scandinavian Journal of Forest Research*, *22*, 33–48.

Boyd, D. S., & Hill, R. A. (2007). Validation of airborne LIDAR intensity values from a forested landscape using HYMAP data: Preliminary analysis. *International Archives of Photogrammetry, Remote Sensing and Spatial Information Sciences*, *XXXVI* Part 3/W52.

Brandtberg, T. (2002). Individual tree-based species classification in high spatial resolution aerial images of forests using fuzzy sets. *Fuzzy Sets and Systems*, *132*, 371–387.

Brandtberg, T. (2007). Classifying individual tree species under leaf-off and leaf-on conditions using airborne LIDAR. *ISPRS Journal of Photogrammetry and Remote Sensing*, *61*, 325–340.

Brandtberg, T., Warner, T. A., Landenberger, R. E., & McGraw, J. B. (2003). Detection and analysis of individual leaf-off tree crowns in small footprint, high sampling density LIDAR data from the eastern deciduous forest in North America. *Remote Sensing of Environment*, *85*, 290–303.

Brennan, R., & Webster, T. L. (2006). Object-oriented land cover classification of LIDAR-derived surfaces. *Canadian Journal of Remote Sensing*, *32*, 162–172.

Carleer, A., & Wolff, E. (2004). Exploitation of very high resolution satellite data for tree species identification. *Photogrammetric Engineering and Remote Sensing*, *70*, 135–140.

Chasmer, L., Hopkinson, C., Smith, B., & Treitz, P. (2006). Examining the influence of changing laser pulse repetition frequencies on conifer forest canopy returns. *Photogrammetric Engineering and Remote Sensing*, *72*, 1359–1367.

Coops, N. C., Hilker, T., Wulder, M. A., St-Onge, B., Newnham, G., Siggins, A., et al. (2007). Estimating canopy structure of Douglas-fir forest stands from discrete-return LIDAR. *Trees-Structure and Function*, *21*, 295–310.

Farid, A., Goodrich, D. C., & Sorooshian, S. (2006a). Using airborne LIDAR to discern age classes of cottonwood trees in a riparian area. *Western Journal of Applied Forestry*, *21*, 149–158.

Farid, A., Rautenkranz, D., Goodrich, D. C., Marsh, S. E., & Sorooshian, S. (2006b). Riparian vegetation classification from airborne laser scanning data with an emphasis on cottonwood trees. *Canadian Journal of Remote Sensing*, *32*, 15–18.

Gaveau, D. L. A., & Hill, R. A. (2003). Quantifying canopy height underestimation by laser pulse penetration in small-footprint airborne laser scanning data. *Canadian Journal of Remote Sensing*, *29*, 650–657.

Goodwin, N. R., Coops, N. C., & Culvenor, D. S. (2006). Assessment of forest structure with airborne LIDAR and the effects of platform altitude. *Remote Sensing of Environment*, *103*, 140–152.

Heurich, M. (2006). Evaluierung und entwicklung von automatiserten erfassung von waldstructuren aus daten flugzuggetragener fernerkundungssenoren. *Forstkuche Forshungsberichte München*, *2002*, 329.

Hodgson, M. E., & Bresnahan, P. (2004). Accuracy of airborne LIDAR-derived elevation: Empirical assessment and error budget. *Photogrammetric Engineering and Remote Sensing*, *70*, 331–339.

Holmgren, J. (2004). Prediction of tree height, basal area and stem volume in forest stands using airborne laser scanning. *Scandinavian Journal of Forest Research*, *19*, 543–553.

Holmgren, J., & Persson, Å. (2004). Identifying species of individual trees using airborne laser scanner. *Remote Sensing of Environment*, *90*, 415–423.

Holmgren, J., Persson, A., & Soderman, U. (2008). Species identification of individual trees by combining high resolution LIDAR data with multi-spectral images. *International Journal of Remote Sensing*, *29*, 1537–1552.

Hopkinson, C. (2007). The influence of flying altitude, beam divergence, and pulse repetition frequency on laser pulse return intensity and canopy frequency distribution. *Canadian Journal of Remote Sensing*, *33*, 312–324.

Hyde, P., Dubayah, R., Walker, W., Blair, J. B., Hofton, M., & Hunsaker, C. (2006). Mapping forest structure for wildlife habitat analysis using multi-sensor (LIDAR, SAR/InSAR, ETM plus, Quickbird) synergy. *Remote Sensing of Environment*, *102*, 63–73.

Hyyppä, H., & Hyyppä, J. (1999). Comparing the accuracy of laser scanner with other optical remote sensing data sources for stand attributes retrieval. *Photogrammetric Journal of Finland*, *16*, 5–15.

Hyyppä, J., Kelle, O., Lehikoinen, M., & Inkinen, M. (2001). A segmentation-based method to retrieve stem volume estimates from 3-D tree height models produced by laser scanners. *IEEE Transactions on Geoscience and Remote Sensing*, *39*, 969–975.

Key, T., Warner, T. A., McGraw, J. B., & Fajvan, M. A. (2001). A comparison of multispectral and multitemporal information in high spatial resolution imagery for classification of individual tree species in a temperate hardwood forest. *Remote Sensing of Environment*, *75*, 100–112.

Kline, R. B. (2004). *Beyond significance testing: Reforming data analysis methods in behavioral research.* Washington, D.C.: American Psychological Association.

Kaasalainen, S., Ahokas, E., Hyyppa, J., & Suomalainen, J. (2005). Study of surface brightness from backscattered laser intensity: Calibration of laser data. *IEEE Geoscience and Remote Sensing Letters*, *2*, 255–259.

Kraus, K., & Pfeifer, N. (1998). Determination of terrain models in wooded areas with airborne laser scanner data. *ISPRS Journal of Photogrammetry and Remote Sensing*, *53*, 193–203.

Liang, X., Hyyppä, J., & Matikainen, L. (2007). Deciduous–coniferous tree classification using difference between first and last pulse laser signatures. *International Archives of Photogrammetry, Remote Sensing and Spatial Information Sciences*, *XXXVI*, 253–257 PART 3/W52.

Magnussen, S., & Boudewyn, P. (1998). Derivations of stand heights from airborne laser scanner data with canopy-based quantile estimators. *Canadian Journal of Forest Research-Revue Canadienne De Recherche Forestiere*, *28*, 1016–1031.

Moffiet, T., Mengersen, K., Witte, C., King, R., & Denham, R. (2005). Airborne laser scanning: Exploratory data analysis indicates potential variables for classification of individual trees or forest stands according to species. *ISPRS Journal of Photogrammetry and Remote Sensing*, *59*, 289–309.

Morsdorf, F., Meier, E., Kotz, B., Itten, K. I., Dobbertin, M., & Allgower, B. (2004). LIDAR-based geometric reconstruction of boreal type forest stands at single tree level for forest and wildland fire management. *Remote Sensing of Environment*, *92*, 353–362.

Næsset, E. (2001). Effects of differential single- and dual-frequency GPS and GLONASS observations on point accuracy under forest canopies. *Photogrammetric Engineering and Remote Sensing*, *67*, 1021–1026.

Næsset, E. (2002). Predicting forest stand characteristics with airborne scanning laser using a practical two-stage procedure and field data. *Remote Sensing of Environment*, *80*, 88–99.

Næsset, E. (2004a). Accuracy of forest inventory using airborne laser scanning: Evaluating the first Nordic full-scale operational project. *Scandinavian Journal of Forest Research*, *19*, 554–557.

Næsset, E. (2004b). Effects of different flying altitudes on biophysical stand properties estimated from canopy height and density measured with a small-footprint airborne scanning laser. *Remote Sensing of Environment*, *91*, 243–255.

Næsset, E. (2004c). Practical large-scale forest stand inventory using a small-footprint airborne scanning laser. *Scandinavian Journal of Forest Research*, *19*, 164–179.

Næsset, E. (2009). Effects of different sensors, flying altitudes, and pulse repetition frequencies on forest canopy metrics and biophysical stand properties derived from small-footprint airborne laser data. *Remote Sensing of Environment*, *113*, 148–159.

Næsset, E., & Bjerknes, K. O. (2001). Estimating tree heights and number of stems in young forest stands using airborne laser scanner data. *Remote Sensing of Environment*, *78*, 328–340.

Nilsson, M. (1996). Estimation of tree weights and stand volume using an airborne LIDAR system. *Remote Sensing of Environment*, *56*, 1–7.

Olofsson, K., Wallerman, J., Holmgren, J., & Olsson, H. (2006). Tree species discrimination using Z/I DMC imagery and template matching of single trees. *Scandinavian Journal of Forest Research*, *21*, 106–110.

Ørka, H. O., Næsset, E., & Bollandsås, O. M. (2007). Utilizing airborne laser intensity for tree species classification. *International Archives of Photogrammetry, Remote Sensing and Spatial Information Sciences*, *XXXVI*, 300–304 Part 3/W52.

Persson, Å., Holmgren, J., & Söderman, U. (2002). Detecting and measuring individual trees using an airborne laser scanner. *Photogrammetric Engineering and Remote Sensing*, *68*, 925–932.

R Development Core Team (2007). *R: A language and environment for statistical computing.* Vienna: R Foundation for Statistical Computing.

Reitberger, J., Krzystek, P., & Stilla, U. (2008). Analysis of full waveform LIDAR data for the classification of deciduous and coniferous trees. *International Journal of Remote Sensing*, *29*, 1407–1431.

Reutebuch, S. E., McGaughey, R. J., Andersen, H. E., & Carson, W. W. (2003). Accuracy of a high-resolution LIDAR terrain model under a conifer forest canopy. *Canadian Journal of Remote Sensing*, *29*, 527–535.

Schreier, H., Lougheed, J., Tucker, C., & Leckie, D. (1985). Automated measurements of terrain reflection and height variations using an airborne infrared laser system. *International Journal of Remote Sensing*, *6*, 101–113.

Silverman, B. W. (1986). *Density estimation.* London: Chapman and Hall.

Solberg, S., Næsset, E., & Bollandsås, O. M. (2006). Single tree segmentation using airborne laser scanner data in a structurally heterogeneous spruce forest. *Photogrammetric Engineering and Remote Sensing*, *72*, 1369–1378.

Song, J., Han, S., Yu, K., & Kim, Y. (2002). Assessing the possibility of land-cover classification using LIDAR intensity data.*International Archives of Photogrammetry, Remote Sensing and Spatial Information Sciences*, *XXXIV*, 256–259 Part 3B.

Terrasolid Ltd. (2004). *TerraScan user's guide.* Helsinki: Terrasolid Ltd.

Venables, W. N., & Ripley, B. D. (2002). *Modern applied statistics with S.* New York: Springer.

Wehr, A., & Lohr, U. (1999). Airborne laser scanning — An introduction and overview. *ISPRS Journal of Photogrammetry and Remote Sensing*, *54*, 68–82.

Wotruba, L., Morsdorf, F., Meier, E., & Nüesch, D. (2005). Assessment of sensor characteristics of an airborne laser scanner using geometric reference targets. *International Archives of Photogrammetry, Remote Sensing and Spatial Information Sciences*, *XXXVI*, 1–7 Part 3/W19.

Paper II

Remote Sensing of Environment 114 (2010) 1445–1461

Contents lists available at ScienceDirect

Remote Sensing of Environment

journal homepage: www.elsevier.com/locate/rse

Effects of different sensors and leaf-on and leaf-off canopy conditions on echo distributions and individual tree properties derived from airborne laser scanning

Hans Ole Ørka *, Erik Næsset, Ole Martin Bollandsås

Department of Ecology and Natural Resource Management, Norwegian University of Life Sciences, P.O. Box 5003, NO-1432 Ås, Norway

ARTICLE INFO

Article history:
Received 5 October 2009
Received in revised form 15 January 2010
Accepted 30 January 2010

Keywords:
Airborne laser scanning
Leaf-on canopy conditions
Leaf-off canopy conditions, Sensors
Individual trees
Intensity
Tree height
Stem diameter
Species classification

ABSTRACT

The objectives of this study were to quantify and analyze differences in laser height and laser intensity distributions of individual trees obtained from airborne laser scanner (ALS) data for different canopy conditions (leaf-on vs. leaf-off) and sensors. It was also assessed how estimated tree height, stem diameter, and tree species were influenced by these differences. The study was based on 412 trees from a boreal forest reserve in Norway. Three different ALS acquisitions were carried out. Leaf-on and leaf-off data were acquired with the Optech ALTM 3100 sensor, and an additional leaf-on dataset was acquired using the Optech ALTM 1233 sensor. Laser echoes located within the vertical projection of the tree crowns were attributed to different echo categories ("first echoes of many", "single echoes", "last echoes of many") and analyzed. The most pronounced changes in laser height distribution from leaf-on to leaf-off were found for the echo categories denoted as "single" and "last echoes of many" where the distributions were shifted towards the ground under leaf-off conditions. The most pronounced change in the intensity distribution was found for "first echoes of many" where the distribution was extremely skewed towards the lower values under leaf-off conditions compared to leaf-on. Furthermore, the echo height and intensity distributions obtained for the two different sensors also differed significantly. Individual tree properties were estimated fairly accurately in all acquisitions with RMSE ranging from 0.76 to 0.84 m for tree height and from 3.10 to 3.17 cm for stem diameter. It was revealed that tree species was an important model term in both and tree height and stem diameter models. A significantly higher overall accuracy of tree species classification was obtained using the leaf-off acquisition (90 vs. 98%) whereas classification accuracy did not differ much between sensors (90 vs. 93%).

1. Introduction

Over the past decade airborne laser scanning (ALS) has contributed significantly to improved efficiency of forest inventories (Eid et al., 2004; Næsset, 2007). Comparisons of ALS with other remote sensing methods like radar and optical sensors have shown that ALS is among the most promising remote sensing techniques in terms of accuracy of essential forest parameters such as height, volume, and biomass (Hyde et al., 2006; Hyde et al., 2007; Hyyppä & Hyyppä, 1999; Magnusson, 2006). Today, ALS is used operationally in stand based forest inventory where the products are biophysical characteristics like mean height and timber volume presented at the stand level (e.g. Næsset, 2007; Næsset et al., 2004). However, the first operational inventories in landscapes with a size of up to 2000 km^2 where individual trees derived from high-density ALS data are the primary units of interest, are now about to be completed. In both procedures, i.e., area-based methods and individual tree methods, biophysical parameters of interest such as canopy/tree height and volume are estimated from statistical measures derived from the laser echo distributions, in particular the laser height distribution, but also the laser intensity distribution is considered (e.g. Lim et al., 2003).

The echo distributions derived from ALS measurements are sensor dependent. Sensor and acquisition parameters like flying altitude, footprint size, pulse repetition frequency, beam divergence, and scan angle have been tested and found to influence the echo height distribution (Chasmer et al., 2006; Goodwin et al., 2006; Holmgren et al., 2003; Hopkinson, 2007; Næsset, 2004b; Næsset, 2009; Næsset et al., 2005; Yu et al., 2004). The sensor effects on echo distributions are of concern in several areas of application in forest inventory. First, the sensor effects are of interest when developing ALS methods for regional biomass-, carbon-, and forest health inventory and monitoring (Næsset & Nelson, 2007; Næsset et al., 2009; Solberg et al., 2006b). Examples of such inventories are the national forest inventory programs found in many countries. The inventory cycle in such programs is usually 5–10 years. The typical life time of commercial laser sensors is less than 4 years. Hence, the time period between repeated inventories is most likely longer than the life time of a sensor and two subsequent acquisitions will thus be conducted with different sensors. For regional and national systems for forest monitoring and carbon reporting compatibility between sensors over time is essential (Næsset et al.,

* Corresponding author. Tel.: +47 64965799; fax: +47 64965802.
E-mail address: hans-ole.orka@umb.no (H.O. Ørka).

0034-4257/$ – see front matter © 2010 Elsevier Inc. All rights reserved.
doi:10.1016/j.rse.2010.01.024

2009; Nelson et al., 2003; Nelson et al., 2004). Systematical shifts in estimated properties caused by changing sensor properties could influence on conclusions inferred from multi-temporal observations by either overestimating the true changes or making changes undetectable. Second, sensor-specific effects are important in operational forest inventory at a more local scale. An expensive part of such inventories is the field survey conducted to collect local plot data for estimation of relationships between metrics derived from the ALS data and biophysical properties of interest. If estimated models of biophysical properties could be based on already existing field plots with associated ALS metrics derived from previous acquisitions in nearby areas the costs of the inventories could be reduced. It has been demonstrated that laser data from two different areas, acquired with the same sensor, can be handled together by common regression models without loss in accuracy of the estimated stand level biophysical properties (Næsset, 2007). Hence, stability in laser echo distributions, model parameters, and predicted values across different sensors are important when considering ALS and ground data to be combined across different areas (Næsset, 2007; Næsset et al., 2005).

Another concern in forest inventory is the time of data acquisition. Appropriate acquisition periods are commonly separated into two distinct times of the year, i.e., (1) when the deciduous trees have leaves (leaf-on) and (2) the dormant period of deciduous trees (leaf-off). It is common practice to acquire ALS data for operational forest inventories under leaf-on conditions, but in some areas leaf-off conditions are preferred. One reason for avoiding the leaf-off period is the much more narrow time window of having leaf-off conditions and bare ground (without snow) at northern latitudes combined with the risk of snowfall. However, there may be several reasons why leaf-off acquisitions may be considered as an alternative season for forest inventory ALS acquisitions. First, under leaf-off conditions a larger amount of pulses will be capable of penetrating through the canopy and be reflected off the ground in deciduous forest. Higher proportions of ground echoes will give more accurate digital terrain models (DTM). ALS acquisitions for regions or even for entire nations are sometimes performed under leaf-off conditions to optimize the accuracy of the DTMs (Liang et al., 2007). Hence, forest inventories may take advantage of laser data collected for DTM generation to reduce the overall inventory costs. Second, leaf-off data may help in reducing the influence of the so-called "hardwood problem" in ALS assisted forest inventories (Nelson et al., 2007). The "hardwood problem" refers to the poorer laser based estimates of biomass sometimes found in mixed (Næsset, 2005) and deciduous (Nelson et al., 2004) forests as compared to pure coniferous forest. Næsset (2005) studied this problem in an area-based inventory of a mixed forest under leaf-on and leaf-off conditions. It was revealed that utilizing the leaf-off laser data slightly improved estimates of mean height, basal area, and timber volume compared to utilization of the leaf-on data. Furthermore, at the individual tree level, species classification have been tested and found to be promising under leaf-off conditions. In a comparative classification study of coniferous and deciduous trees using waveform data the overall accuracy was 85% under leaf-on condition and 96% under leaf-off condition (Reitberger et al., 2008). Species classification can be a strategy for reducing the impact of the "hardwood problem". Thus, there are multiple reasons why leaf-off acquisitions may be considered as an alternative to leaf-on acquisitions; (1) cost sharing of leaf-off ALS data acquired for DTM production, (2) the slightly more accurate results likely to be obtained in area-based forest inventory of certain forest types, and (3) the promising results of tree species classification obtained for individual trees. Hence, knowledge and understanding of the differences between echo distributions obtained under leaf-on and leaf-off canopy conditions are needed.

In the current study, we compared the differences in echo distributions (height and intensity) of individual trees obtained under different canopy conditions and with different sensors. Analyses of individual trees will give us better understanding of echo distributions derived from ALS data. A specific advantage of studying individual trees is that the different tree species can be analyzed independent of each other. Tree species produce different echo distributions which may provide significant differences in derived metrics (Ørka et al., 2009). Tree species is clearly an important factor in the analysis of effects of canopy conditions where only deciduous trees will be affected by the changes form leaf-off to leaf-on conditions. Likewise, the emitted pulses from different sensors may interact differently with different tree species creating a species specific sensor effect. In the current study, we addressed the species specific effects of different sensors and canopy conditions by analyzing the echo distributions of individual trees.

To the very best of our knowledge, studies of the effects of sensor and canopy conditions on echo distributions and biophysical properties have until now focused on the area-based approach and have mostly been conducted at the plot level (Hopkinson, 2007; Næsset, 2005; Næsset, 2009). As individual tree inventory now becomes operational, effects of different sensors and canopy conditions on prediction of biophysical properties of individual trees will be important as well. A proposed advantage with individual tree inventory is that a smaller amount of reference data will be needed for model calibration (Hyyppä et al., 2008). Stability of model parameters and predictions using different sensors will support the idea of using a small number of reference trees in individual tree inventory. It will also support the idea of reusing models across nearby areas flown with different sensors and contribute to lower inventory costs. Higher accuracy obtained with data acquired under leaf-off conditions would favor this time period for acquisition of ALS data for forest inventory. Therefore it is important to assess how different canopy conditions and sensors affect model parameters and predicted values of important individual tree properties likely to be a part of such inventories. In this study, we considered tree height, stem diameter, and tree species as the most important properties to be derived using the individual tree method (c.f. Holmgren & Persson, 2004; Hyyppä et al., 2001; Ørka et al., 2009; Persson et al., 2002).

The objectives of the present study were to quantify and analyze differences of (1) leaf-off vs. leaf-on conditions and (2) acquisitions with two different sensors on (a) the laser height echo distributions and (b) the laser intensity echo distributions of ALS point cloud data. The differences were analyzed for separate echo categories and tree species. Furthermore, (3) we assessed how these changes in canopy conditions and change of sensors influenced on the accuracy and model parameters for three individual tree properties derived from ALS data, i.e., (a) tree height, (b) stem diameter, and (c) tree species.

2. Material and methods

2.1. Study area

The study area is located in Østmarka forest reserve (59°50′N, 11°02′E, 14 190–370 masl) in southeastern Norway. The forest reserve is about 1800 ha in size. This forest has developed without logging and silvicultural treatments since the 1940s. Today, the forest in the reserve is size diverse and it is partly multilayered. The dominating tree species are Norway spruce (*Picea abies* (L.) Karst.) and Scots pine (*Pinus silvestris* L.). Deciduous trees are found scattered in the landscape. Birch (*Betula* ssp.) and aspen (*Poplus tremula*) are the most commonly occurring deciduous species. Data from an adjacent area outside the reserve was also used to include younger forest in the study. This particular forest area is actively managed.

2.2. Field data

Field data collection was carried out on 28 field plots of 0.1 ha size during summer 2003. The 20 plots inside the reserve were laid out subjectively to comprise spruce dominated sites (Bollandsås &

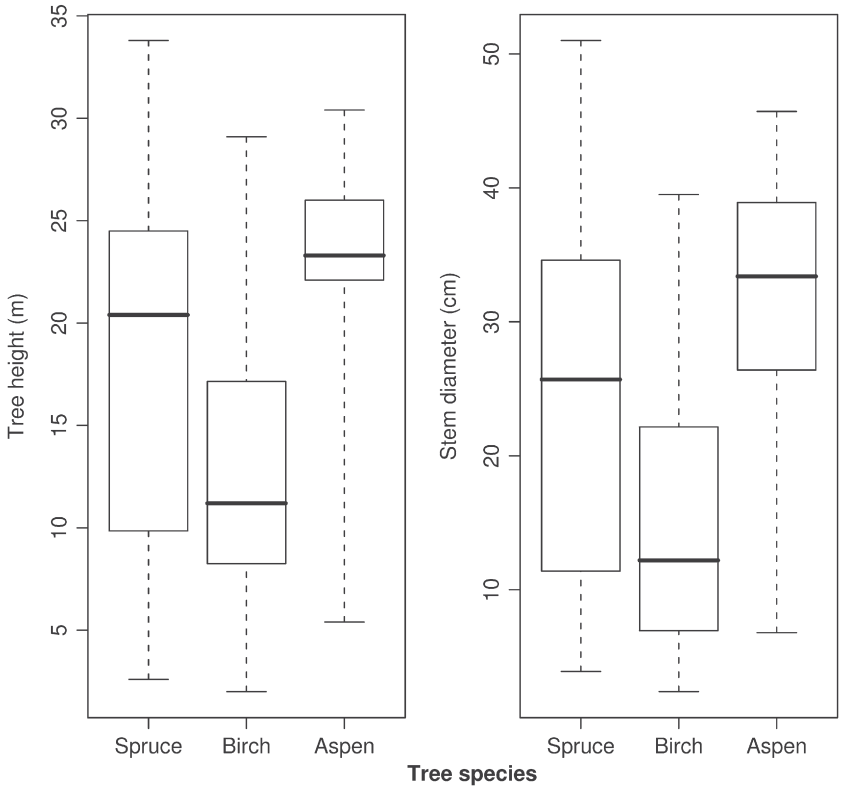

Fig. 1. Box-and-whisker plot of tree height and stem diameter for sample trees analyzed in the study. The first and third quartiles define the box, the median is showed as the horizontal line dividing the box, and the whisker defines the range of the data.

Næsset, 2007; Solberg et al., 2006a). The locations of plots outside the forest reserve were selected to cover productive forest in young and intermediate age classes. The plot center coordinates were determined with differential Global Navigation Satellite System (dGNSS) measurements (c.f. Bollandsås & Næsset, 2007; Solberg et al., 2006a). The average accuracy of the plot coordinates was 10 cm (Bollandsås & Næsset, 2007). On each sample plot the polar coordinates and diameter in breast height (dbh) were measured for all trees with dbh >3 cm. Tree species and crown radius in four cardinal directions was also recorded. Sample trees were selected in two steps. First, eight trees were selected by including the first dominant or co-dominant tree in each cardinal direction and the nearest tree to each of these. Second, all deciduous trees on the plot and a few deciduous trees just outside the plot were selected as sample trees. On all sample trees tree height was measured. The tree heights and stem diameters of the 435 sample trees are summarized in Fig. 1. The sample tree dataset contained 209 spruce trees, 203 birch trees, and 23 aspen trees.

2.3. Laser scanner data

Airborne laser scanner data were acquired during three different laser campaigns, i.e., (1) in October 2003 under leaf-on canopy conditions using the Optech ALTM 1233 instrument (Bollandsås & Næsset, 2007; Solberg et al., 2006a). This acquisition was denoted as ALTM 1233-on. The Optech ALTM 3100 instrument was used for the two last acquisitions, i.e., (2) in April 2005 under leaf-off conditions, denoted as ALTM 3100-off, and (3) in June 2005 under leaf-on conditions (Ørka et al., 2009), denoted as ALTM 3100-on. The flight specifications in the two acquisitions with the ALTM 3100 instrument used when comparing canopy conditions were identical. However, the specifications used for the ALTM 1233-on acquisition differed from those of the two ALTM 3100 acquisitions. An overview of the sensor settings and other acquisition parameters is displayed in Table 1. The acquisition parameters were decided from a goal of having a pulse density of about 5 m^{-2}. The pulse density goal was achieved with as low cost as possible, given the capacity of the instruments (i.e. both sensors were flown with the highest possible pulse repletion frequency) and the spatial distributions of the sample plots.

The initial processing of the data was accomplished by the contractor (Blom Geomatics, Norway). Planimetric coordinates (x and y) and ellipsoidal height values were computed for all echoes. For each acquisition, ground returns were found using the Terrascan software (Terrasolid Ltd, 2004) and a triangulated irregular network (TIN) was created from the echoes classified as ground returns. Heights above the

Table 1
Technical specifications of the three airborne laser data acquisitions used in the study.

	Acquisition		
	ALTM 1233-on	ALTM 3100-off	ALTM 3100-on
Date of acquisition	9 October 2003	17 April 2005	18 June 2005
Canopy conditions	Leaf-on	Leaf-off	Leaf-on
Platform	Huges 500 helicopter	Piper PA31-310	Piper PA31-310
Sensor	Optech ALTM 1233	Optech ALTM 3100	Optech ALTM 3100
Pulse width (ns)	11	16	16
Pulse energy (μJ)	84	66	66
Peak power (kW)	7.6	4.1	4.1
Wavelength (nm)	1064	1064	1064
Mean flying altitude AGL (m)	600	750	750
Pulse repetition frequency (kHz)	33	100	100
Scanner frequency (Hz)	50	70	70
Half scan angle (deg.)	11	10	10
Flying speed (ms^{-1})	35	75	75
Swath width (m)	230	264	264
Mean pulse density (m^{-2})	5.0	5.09	5.09
Beam divergence (mrad)	0.30	0.26	0.26
Footprint diameter (cm)	18	21	21

ground surface were calculated for all echoes by subtracting the respective TIN heights from the height values of all echoes recorded.

In this study, the uncalibrated intensity values recorded by the sensors were analyzed. The intensity values recorded by most laser systems are noisy for several reasons. For example, variations in recording settings such as the amplitude of the returned signal and flying altitude together with varying incident angles, variable emitted energy, and changing atmospheric conditions make the intensity values difficult to interpret. Calibration of intensity to remove noise and make intensity measurements independent of acquisition parameters is important for increased utilization of intensity measures (Höfle & Pfeifer, 2007; Kaasalainen et al., 2005). However, in the current study we did not have sufficient information to perform such corrections of the intensity values.

ALTM 1233 always records two echoes for each emitted pulse, i.e., a first and a last echo. The sensor has two separate receivers, one recording the first echo and one the last echo. When ALS data from the ALTM 1233 are used in multi-temporal studies it is necessary to calibrate recorded heights of the two receivers to avoid systematic shifts in the surface heights (Næsset, 2005; Næsset & Gobakken, 2005; Solberg et al., 2006b). In the current study, we calibrated the echoes using a parking space outside the study area as calibration surface. Five circular plots with 1 m radius where selected subjectively inside the parking area. Within each plot, we recorded the height values of all first and last echoes. The average difference in height values between the two echo categories was −5 cm. Hence, 5 cm was added to the height values of all the first echoes of the ALTM 1233-on acquisition. Both the first and last echo categories acquired by ALTM 1233 were used in this study. For convenience, we labeled them FIRST and LAST, respectively.

The Optech ALTM 3100 sensor records multiple echoes. The sensor is capable of recording up to four echoes. All echoes are recorded with the same receiver. The actual number of echoes recorded will depend on the amount of energy needed to trigger a return, the triggering algorithm, and the minimum time differences between two echoes, i.e., the minimum vertical distance required to separate the echoes. The vertical distances for the particular ALTM 3100 instrument and acquisitions used in this study are stated by the contractor (Blom Geomatics, Norway) to vary from 2.1 m for the two first returns to 3.8 m for the other returns. The number of echoes recorded by the ALTM 3100 sensor can also be one. If only one echo is recorded for an emitted pulse it is labeled as a "single echo". If more than one echo is recorded, the first echo is labeled "first echo of many". The subsequent echoes (second and third echoes) are referred to as intermediate echoes dependent of how many echoes that are recorded. The last echo recorded is always labeled as "last echo of many", even if there are only two echoes. In this study, we analyzed "first echoes of many", "single echoes", and "last echoes of many" from the ALTM 3100 sensor. For simplicity they are labeled FIRST, SINGLE, and LAST, respectively. The intermediate echoes were not provided by the contractor and thus not analyzed in the current study.

The ALTM 1233 and ALTM 3100 sensors differ conceptually in the way echoes are recorded. In particular, the FIRST and LAST echo categories of the ALTM 3100 acquisitions differ from the respective FIRST and LAST echo categories acquired by ALTM 1233. However, combining FIRST and SINGLE echoes of the ALTM 3100 is in principle equal to the FIRST echoes of the ALTM 1233 (Næsset, 2009). The combination of LAST + SINGLE echoes of ALTM 3100 may also be viewed as identical to LAST echoes of ALTM 1233, but is not. LAST + SINGLE echoes of ALTM 3100 will differ from LAST echoes of ALTM 1233 because of the vertical separation of at least 2.1 m for LAST echoes in ALTM 3100 compared to a vertical separation of zero in the ALTM 1233 (Næsset, 2009). In the subsequent analysis where we compared data collected by the two sensors, we compared aggregates of FIRST + SINGLE and LAST + SINGLE of ALTM 3100 with FIRST and LAST echoes, respectively, of ALTM 1233. The proportion of echoes of different echo categories to the total number of pulses is displayed in Table 2.

Table 2
Proportion of echoes to total number of pulses ("Total"), proportion of echoes above GTV = 1.3 m to total number of pulses ("Canopy"), and proportion of pulses below GTV = 1.3 m to total number of pulses ("Ground") for different echo categories. The total number of pulses is defined as the sum of FIRST and SINGLE echoes for the multiple echo recording sensor (ALTM 3100) and as the number of FIRST echoes for the ALTM 1233 sensor.

Acquisition and echo category	Proportions of echoes (%)		
	Total	Canopy[b]	Ground[2]
FIRST[a]			
ALTM 3100-on	36	36	0
ALTM 3100-off	57	57	0
ALTM 1233-on	100	93	7
SINGLE			
ALTM 3100-on	64	58	6
ALTM 3100-off	43	35	8
ALTM 1233-on	–	–	–
LAST			
ALTM 3100-on	37	16	21
ALTM 3100-off	53	21	32
ALTM 1233-on	102	73	29

[a] First echoes of many for ALTM 3100-on and ALTM 3100-off. First echoes for ALTM 1233-on.
[b] Canopy and ground are separated with the ground threshold value (GTV) of 1.3 m.

2.4. Extraction of individual tree segments

In this study we did not use any algorithm for automatic tree segmentation to delineate individual tree crowns. Instead field measurements were used to delineate the crown segments. For each tree, we used the field-measured tree position and a fixed crown radius to produce a circular crown segment. The crown radius was determined as the mean of the measured radii in the four cardinal directions. Echoes inside the defined crown segments were assigned to the corresponding tree. The forest in the reserve is multilayered and in many cases our method produced overlapping crown segments. This will never be the case when using canopy surface models and watershed, pouring, or other similar algorithms in automatic tree segmentation. We handled the problem of overlapping crowns in a similar way as many automatic segmentation algorithms, i.e., by assigning the echoes of the overlapping regions to the tallest tree.

The heterogeneous structure of the study area may cause echoes from higher neighboring trees to be assigned to lower trees. Such assignment errors may be due to erroneous tree positions and the assumption of circular crowns. To correct for such errors we removed echoes with higher z-values than actual field-measured tree height plus a random error component representing a 95% confidence band. This confidence band was defined as 1.96 times the standard deviation associated with random errors of (1) the DTM, (2) the laser system, and (3) field measurement of tree height. It is important to be conservative and allow such random errors to be inherent in the data. Otherwise the removal of seemingly erroneously allocated laser echoes could have led to too optimistic results. The random error of a DTM in a typically forested area was anticipated to be 30 cm (Reutebuch et al., 2003), while random errors of the laser system and the field measurements were set to 20 cm (Baltsavias, 1999) and to 5% of the tree height (h) (Daamen, 1980; Eriksson, 1970), respectively. Hence, the echoes removed were echoes higher than a threshold (T), defined as:

$$T = h + 1.96 * \sqrt{0.30^2 + 0.20^2 + (h * 0.05)^2} \quad (1)$$

In the analysis, we only included trees hit by at least one pulse in each of the three acquisitions, i.e., trees which had at least one FIRST or SINGLE echo. Thus, the dataset we analyzed comprised 412 trees, i.e., 203 spruce trees, 187 birch trees, and 22 aspen trees.

2.5. Analyzing effects of canopy conditions and different sensors on laser echo height- and intensity distributions (objectives 1 and 2)

The differences between the leaf-on and leaf-off acquisitions and the differences between the two sensors were analyzed using a visual approach to assess the differences between the echo distributions. The visual approach was to compute the probability density function for both height and intensity for different echo categories, tree species, and acquisitions. The distributions were estimated with a Gaussian kernel and bandwidth selection using "Silverman's rule of thumb" (R Development Core Team, 2008; Venables & Ripley, 2002).

In addition to the visual approach we computed the first four moments of the distributions (mean, variance, kurtosis, and skewness) and the maximum value to compare statistical differences of the echo distributions. The maximum value was included because of its importance in individual tree methods, especially for the tree height estimation. The moments and maximum values were computed for separate echo categories for both the height and intensity distributions for all echoes higher than 1.3 m above ground. In order to compare differences between ALTM 3100-on and ALTM 1233-on we also computed moments and maximum values of the combined echo categories, i.e., FIRST + SINGLE and LAST + SINGLE. Thus, to address the sensor effects and the effects of canopy conditions on the echo distributions, pair-wise differences were computed between the respective moments and maximum values of the ALTM 3100-on and ALTM 1233-on acquisitions and the ALTM 3100-on and ALTM 3100-off acquisitions. Furthermore, two-tailed *t*-tests were applied to test the significance of the differences. Finally, 95% confidence intervals of the differences were computed.

2.6. Analyzing effects of canopy conditions and different sensors on individual tree properties (objective 3)

2.6.1. Tree height

In the current study we used the maximum height of laser echoes inside individual tree crown segments to establish relationships to field-measured tree height. The maximum laser echoes were derived from the FIRST echoes of the ALTM 1233 sensor and from the combination of the echo categories FIRST + SINGLE echoes of the ALTM 3100 sensor. Regression analysis was applied to relate laser derived maximum laser heights and field-measured tree heights. Separate regressions models were established for each of the three acquisitions. Because of the hierarchical structure inherent in the data, where trees were measured within sample plots, a mixed modeling approach was applied (Eq. (2a)). We also estimated models including a term accounting for tree species to enable testing of effects of tree species (Eq. (2b)). The two tree height models (Eqs. (2a) and (2b)) were estimated according to

$$h_{ij} = \beta_0 + b_i + \beta_1\left(h_{l\max ij}\right) + \varepsilon_{ij} \quad (2a)$$

and

$$h_{ij} = \beta_0 + b_i + \beta_1\left(h_{l\max ij}\right) + \beta_2\left(s_{bij}\right) + \beta_3\left(s_{aij}\right) + \varepsilon_{ij} \quad (2b)$$

where h_{ij} is height (m) of tree j on plot i measured in field, $h_{\mathrm{lmax}ij}$ is the maximum laser height (m) of the corresponding tree, β_0 and β_1 are fixed parameters, b_i is the random intercept for plot i ($b_i \sim N(0, \sigma_b^2)$), and ε_{ij} is the error for tree j on plot i ($\varepsilon_{ij} \sim N(0, \sigma_\varepsilon^2)$). In Eq. (2b), β_2 and β_3 are fixed parameters, s_{bij} and s_{aij} are dummy variables indicating if the tree is birch or aspen, respectively. A value of 1 was assigned to s_{bij} if tree species was birch. Otherwise s_{bij} was set to 0. Correspondingly, a value of 1 was assigned to s_{aij} if tree species was aspen. Otherwise s_{aij} was set to 0.

All linear mixed models were estimated with the *R* package *nlme* (Pinheiro et al., 2008). Approximate 95% confidence intervals were computed for the model parameters to examine if estimated parameters differed between acquisitions. These confidence intervals for the β's were compared to see if parameters differ significantly between different acquisitions. We tested if there were species specific differences between estimated values (using Eq. (2a)) obtained from acquisitions with different canopy conditions (ALTM 3100-on vs. ALTM 3100-off) and different sensors (ALTM 3100-on vs. ALTM 1233-on). Two-tailed *t*-tests were applied to assess if the difference between values estimated by Eq. (2a) for separate species and acquisitions were significantly different in the statistical sense. Furthermore, we tested if models that included tree species (Eq. (2b)) were better than models without the tree species term (Eq. (2a)). The model comparisons were carried out with the likelihood ratio test for fixed-effects parameters (Pinheiro & Bates, 2000; West et al., 2007). Model comparisons were carried out with the *anova.lme* – function of the *R* package *nlme* (Pinheiro et al., 2008).

2.6.2. Stem diameter

Stem diameters of individual trees segmented from ALS data are usually estimated from tree height and crown width. Crown width is often computed as the diameter of a circle having the same area as the individual tree segment. Since we did not apply automatic tree segmentation, the crown widths used in the current study were those derived from the field measurements. In the comparison of different canopy conditions and sensors, it is therefore implicitly assumed that the size of the crown segments would be stable across acquisitions. Different model specifications of the relationship between stem diameter and the covariates, i.e., maximum laser height and crown width, have been proposed (e.g. Heurich, 2006; Hyyppä et al., 2001; Persson et al., 2002). Based on preliminary studies we chose the model proposed by Hyyppä et al. (2001). The models were estimated as mixed models including a random term for the intercept on plot level. Hence, our basic model included maximum laser height and field-measured crown width (Eq. (3a)). In addition we estimated a model also including a tree species term (Eq. (3b)). The two stem diameter models (Eqs. (3a) and (3b)) were estimated according to

$$d_{ij} = \beta_0 + b_1 + \beta_1\left(h_{l\max ij}\right) + \beta_2\left(cw_{ij}\right) + \varepsilon_{ij} \quad (3a)$$

and

$$d_{ij} = \beta_0 + b_i + \beta_1\left(h_{l\max ij}\right) + \beta_2\left(cw_{ij}\right) + \beta_3\left(s_{bij}\right) + \beta_4\left(s_{aij}\right) + \varepsilon_{ij} \quad (3b)$$

where d_{ij} is diameter (cm) of tree j on plot i measured in field, $h_{\mathrm{lmax}ij}$ is the maximum laser height (m) and cw_{ij} is crown width (m) of the same tree, β_0, β_1 and β_2 are fixed parameters, b_i is the random intercept for plot i ($b_i \sim N(0,\sigma_b^2)$), and ε_{ij} is the error for tree j on plot i ($\varepsilon_{ij} \sim N(0,\sigma_\varepsilon^2)$). In Eq. (3b), β_3 and β_4 are fixed parameters, s_{bij} and s_{aij} are dummy variables indicating if the tree is birch or aspen respectively. A value of 1 was assigned to s_{bij} if tree species was birch. Otherwise s_{bij} was set to 0. Correspondingly, a value of 1 was assigned to s_{aij} if tree species was aspen. Otherwise s_{aij} was set to 0. Model estimations and evaluations were carried out as for tree height (See Section 2.6.1).

2.6.3. Tree species

In this study, we only considered classification of trees into two species categories, i.e., spruce and deciduous trees (birch and aspen). We pooled the two deciduous species into one class because of the small number of aspen trees available in the dataset, but also because ordinary inventory practice in Norway does not discriminate between different deciduous species. The first step in individual tree species classification with ALS data is usually to perform a feature selection that aims at selecting features which differ significantly between tree species and then subsequently include these features in a classification algorithm (Brandtberg et al., 2003; Holmgren & Persson, 2004; Holmgren et al.,

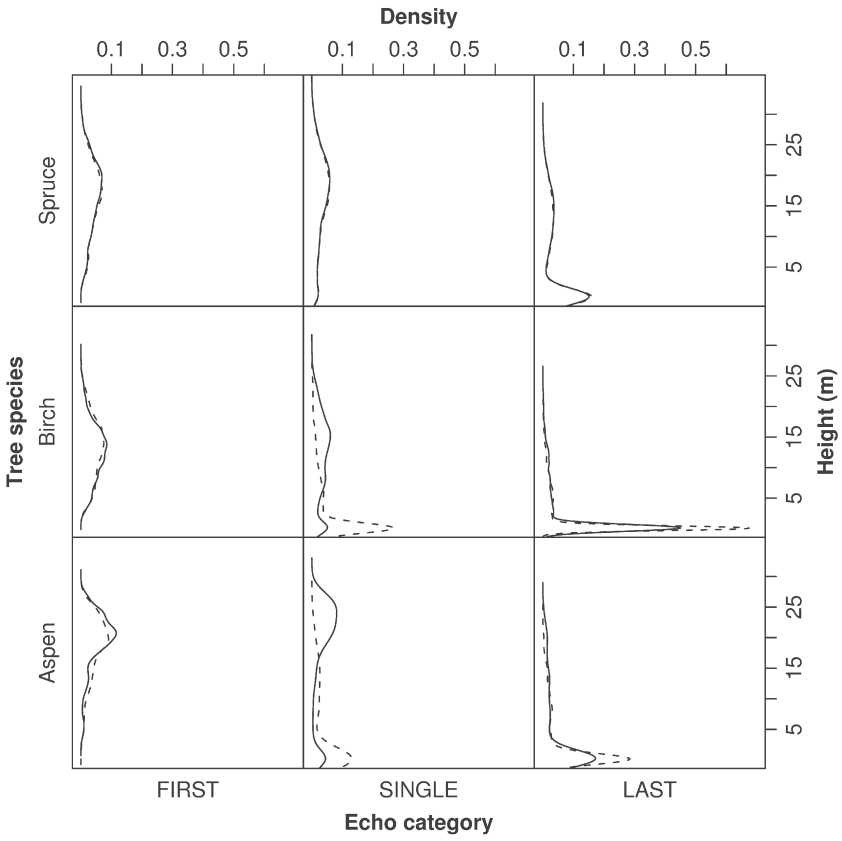

Fig. 2. Leaf-on and leaf-off echo height distributions. Distributions are computed as kernel density under leaf-on (solid line) and leaf-off (dashed line) conditions for different tree species and echo categories.

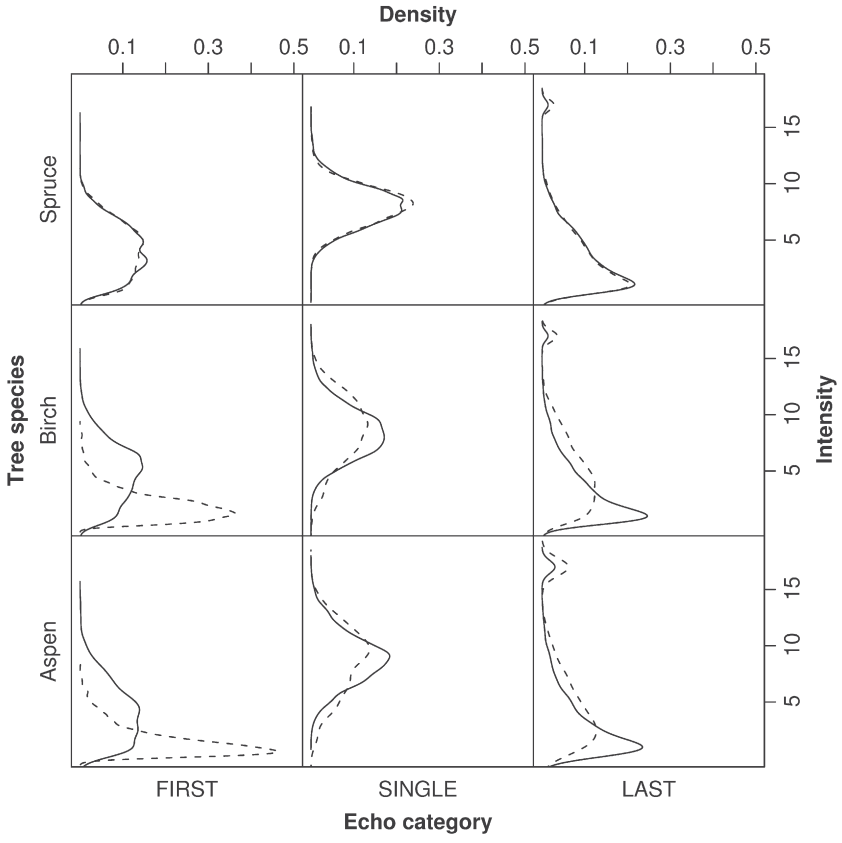

Fig. 3. Leaf-on and leaf-off echo intensity distributions. Distributions are computed as kernel density under leaf-on (solid line) and leaf-off (dashed line) conditions for different tree species and echo categories.

2008). In the current study we used a classification algorithm with a built in feature selection technique. We used the random forest algorithm proposed by Breiman (2001). The random forest algorithm has several advantages with respect to the current comparison of different ALS acquisitions in tree species classification. The random forest algorithm (1) handles large numbers of input features, (2) it computes an error matrix based on an internal validation process, and (3) it computes a measure of the importance of the features in the classification, measured as the mean decrease in the Gini-index (Breiman, 2001; Liaw & Wiener, 2002). Hence, both classification accuracies and variable selection can be derived directly and be compared for the three acquisitions. The classification was carried out with the *R* package *randomForest* (Liaw & Wiener, 2002).

The features used in the classification were ALS derived features from the height and intensity distributions. For each echo category of all acquisitions we computed height-, density-, and intensity features. Features were computed for all echoes higher than 1.3 m above ground. This height, also known as the breast height, was used as the ground threshold value (GTV). Height features computed were the maximum laser height (Hmax), the mean laser height (Hmean), coefficient of variation (Hcv), skewness (Hskew), and kurtiosis (Hkurt). In addition, we computed the 10, 20,…., 80, 90 height percentiles (H10, H20,…, H80, H90). The Hmax, Hmean, and the percentiles (H10–H90) were normalized in two ways. First, by dividing the respective height features with estimated tree height obtained using Eq. (2a), producing "normalized height features" (NHF), and second, by subtracting the value of the respective height features from estimated tree height obtained using Eq. (2a), producing "crown penetration features" (CPF). Hcv, Hkurt, and Hskew were used directly without normalization and labeled as "other height features" (OHF). The "density features" (DF) were calculated as canopy densities in accordance with Næsset (2004a). The crown was divided into vertical crown height bins by dividing field-measured tree height minus the GTV value (1.3 m) into 10 vertical bins of equal

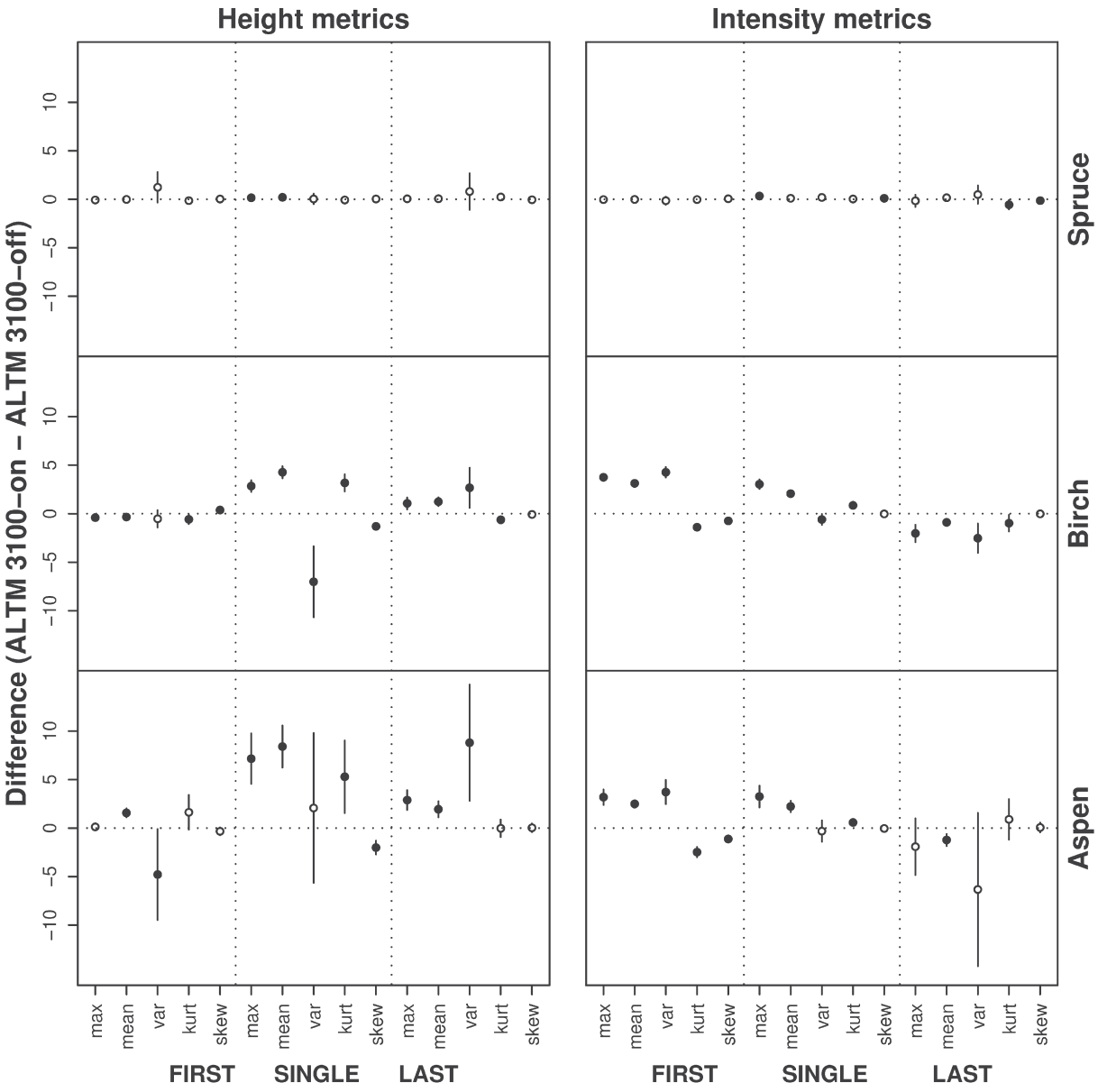

Fig. 4. Differences in height and intensity metrics between leaf-on and leaf-off canopy conditions. Mean differences (dots) and 95% confidence intervals (vertical lines) for the maximum value and the first four moments of the distributions (i.e., mean, variance (var), kurtiosis (kurt), and skewness (skew)) for different echo categories and tree species. Significant differences ($p<0.05$) according to two-tailed *t*-tests are indicated by filled dots.

height. For each echo category, tree level crown density features were calculated as the number of echoes above bin number 0 (>GTV), 1, …, 9 as proportions of total number of echoes and denoted as D0, D1, …., D9. The "intensity features" (IF) computed were maximum (Imax), mean (Imean), coefficient of variation (Icv), skewness (Iskew), and kurtiosis (Ikurt).

The classification performance was assessed using an error matrix (Congalton, 1991). From the internal random forest classification an error matrix was established and overall accuracy, producer's accuracy, and the kappa-coefficient (Cohen, 1960) were computed. The classification was performed for all 412 trees for each of the three acquisitions. However, if an insufficient number of echoes were returned from a tree, not all of the laser metrics could be calculated and with lack of information the tree could not be classified. To be able to compute all laser features we needed at least tree echoes in all echo categories. Thus, to achieve a reasonable comparison we established a subset of trees ($n=211$) which had all features computed in all echo categories. Hence, classification performance was assessed and compared on the same set of trees for all three acquisitions, in addition to the full dataset. To test if one of the datasets among the three acquisitions differed significantly we tested if the kappa-coefficients differed significantly by computing the *Z*-statistics:

$$z = \frac{\kappa_1 - \kappa_2}{\sqrt{\sigma_{\kappa_1} + \sigma_{\kappa_2}}} \quad (4)$$

where κ_1 and κ_2 are the kappa-coefficients for the two classifications to be compared, $\sigma_{\kappa 1}$ and $\sigma_{\kappa 2}$ are their respective variances and $Z \sim N(0,1)$ (c.f. Cohen, 1960).

3. Results

3.1. Effects of canopy conditions on laser echo height and intensity distributions (objective 1)

The estimated distributions for height and intensity appear in Figs. 2, 3, respectively. The mean differences and confidence intervals of the mean differences for maximum values and the four moments appear in Fig. 4.

The largest discrepancies in the height distributions between leaf-off and leaf-on canopy conditions occurred for deciduous trees in the LAST and SINGLE echo categories (Figs. 2, 4). Under leaf-off conditions, a larger portion of LAST echoes tended to come from the ground surface. In addition, the peak of the height distributions of SINGLE echoes was shifted from the upper part of the canopy under leaf-on conditions towards the ground level. There were no differences in the echo distributions computed from coniferous (evergreen) trees, i.e., the spruce trees (Figs. 2, 4). Maximum and mean laser heights were lower for aspen trees under leaf-off conditions. However, for birch trees FIRST echoes were significantly higher under leaf-off conditions (Fig. 4).

For the intensity values the largest discrepancies between data acquired under different canopy conditions occurred for deciduous trees in the FIRST echo category (Figs. 3, 4). For deciduous trees, the intensity distributions of FIRST echoes were extremely skewed to the lower values under leaf-off conditions compared to leaf-on conditions. All intensity metrics computed from FIRST echoes differed significantly between acquisitions for deciduous trees (Fig. 4). As opposed to the patterns of the FIRST echoes, the distributions of LAST echoes were less skewed under leaf-off conditions for deciduous trees. LAST echoes had higher intensity values under leaf-off conditions

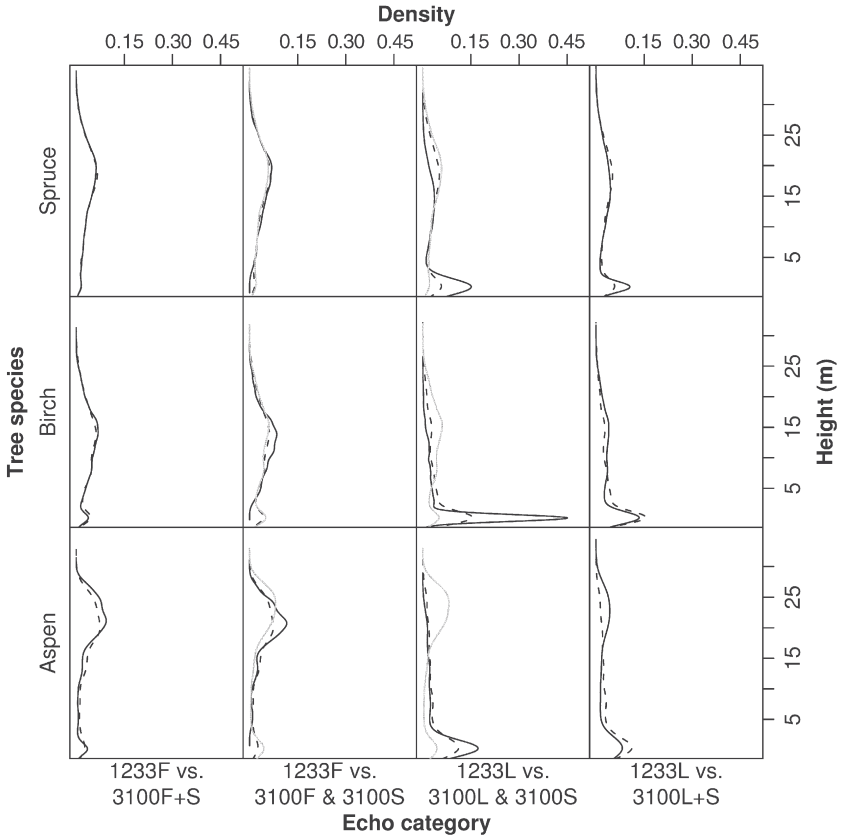

Fig. 5. Echo height distributions for different sensors. Distributions are computed as kernel density from the ALTM 3100-on (solid line) and ALTM 1233-on (dashed line) sensors for different tree species and echo categories. Echo categories presented for ALTM 1233-on are FIRST (1233F) and LAST echoes (1233L). The ALTM 3100-on echo categories FIRST (3100F), LAST (3100L), FIRST + SINGLE (3100F + S), and LAST + SINGLE (3100L + S) are displayed in black and SINGLE echoes (3100S) are displayed in gray.

compared to leaf-on conditions (Fig. 4). For SINGLE echoes, maximum intensity and mean intensity were significantly lower under leaf-off conditions. For spruce trees there were no differences between the recorded intensity distributions (Figs. 3, 4).

3.2. Effects of different sensors on laser echo height and intensity distributions (objective 2)

The estimated distributions for height and intensity for the different sensors are displayed in Figs. 5, 6, respectively. The mean differences and confidence intervals of the mean differences for maximum values and the moments appear in Fig. 7.

Only few of the compared moments which we derived from the distributions did not differ significantly between the two sensors (Fig. 7). The visual inspection indicated that FIRST echoes of ALTM 1233-on were most similar to FIRST + SINGLE echoes of ALTM 3100-on and correspondingly LAST echoes were most similar to LAST + SINGLE echoes (Fig. 5). However, moments computed indicated that echo distributions differ for all echo categories except for the combination of FIRST + SINGLE and LAST + SINGLE for spruce trees (Fig. 7).

The intensity distributions differed between the two sensors irrespective of how the echo categories of the ALTM 3100-on were combined (Fig. 7). Fig. 6 indicates that the LAST echoes produced the most similar intensity distributions of the two sensors. In Fig. 6 a species specific difference between sensors can be observed. For spruce, the shapes of the intensity distributions of FIRST echoes were almost identical for the two sensors. For deciduous trees, FIRST echoes were more skewed towards lower intensity values for the ALTM 1233-on than with ALTM 3100-on.

3.3. Effects of canopy conditions and different sensors on individual tree properties (objective 3)

3.3.1. Tree height

The estimated parameters, confidence intervals, coefficients of determination, and RMSE of estimated acquisition-specific models of tree height (Eqs. (2a) and (2b)) appear in Table 3. The smallest RMSE for tree height was obtained for the ALTM 3100-on acquisition (Table 3).

Comparison of models without a tree species term developed under leaf-on and leaf-off conditions revealed that the intercept was 58 cm higher under leaf-off conditions and that the confidence interval of the estimated slope overlapped (Table 3). The estimated height values obtained with Eq. (2a) for the acquisitions with different canopy conditions differ significantly between spruce ($p = 0.008$) and aspen ($p < 0.001$), but not for birch ($p = 0.228$). Spruce trees had on average 10 cm higher estimated height values under leaf-off conditions as compared to leaf-on conditions, whereas aspen had almost 55 cm lower estimates under leaf-off conditions. The models including a tree species term (Eq. (2b)) improved the tree height model for the ALTM 3100-on ($p < 0.001$) as well as the ALTM 3100-off ($p = 0.036$) acquisition.

The estimated intercept in models developed for the two acquisitions with different sensors were 66 cm higher with the ALTM 1233-on. The confidence interval of the intercepts and slopes did not overlap for the two models (Table 3). The estimated tree heights obtained from Eq. (2a) developed for the acquisitions with different sensors (ALTM 3100-on vs. ALTM1233-on) differed significantly for birch and spruce. Birch trees had 13 cm lower estimated values using ALTM 3100-on ($p < 0.001$) and spruce trees had 11 cm higher values using

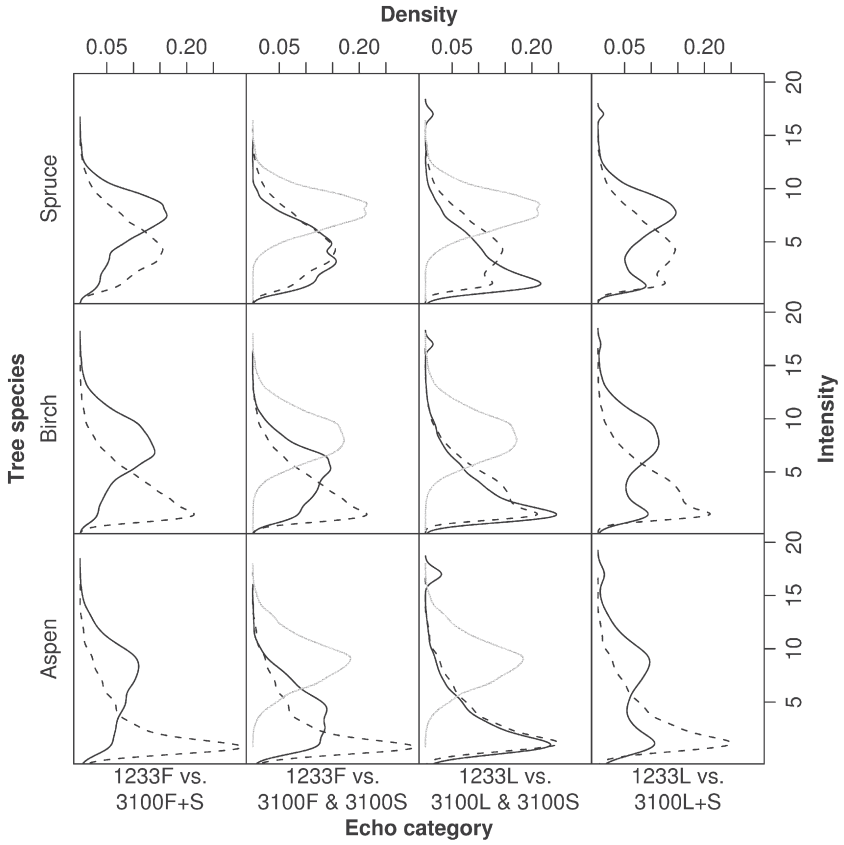

Fig. 6. Echo intensity distributions for different sensors. Distributions are computed as kernel density from the ALTM 3100-on (solid line) and ALTM 1233-on (dashed line) sensors for different tree species and echo categories. Echo categories presented for ALTM 1233-on are FIRST (1233F) and LAST echoes (1233L). The ALTM 3100-on echo categories FIRST (3100F), LAST (3100L), FIRST + SINGLE (3100F + S), and LAST + SINGLE (3100L + S) are displayed in black and SINGLE echoes (3100S) are displayed in gray.

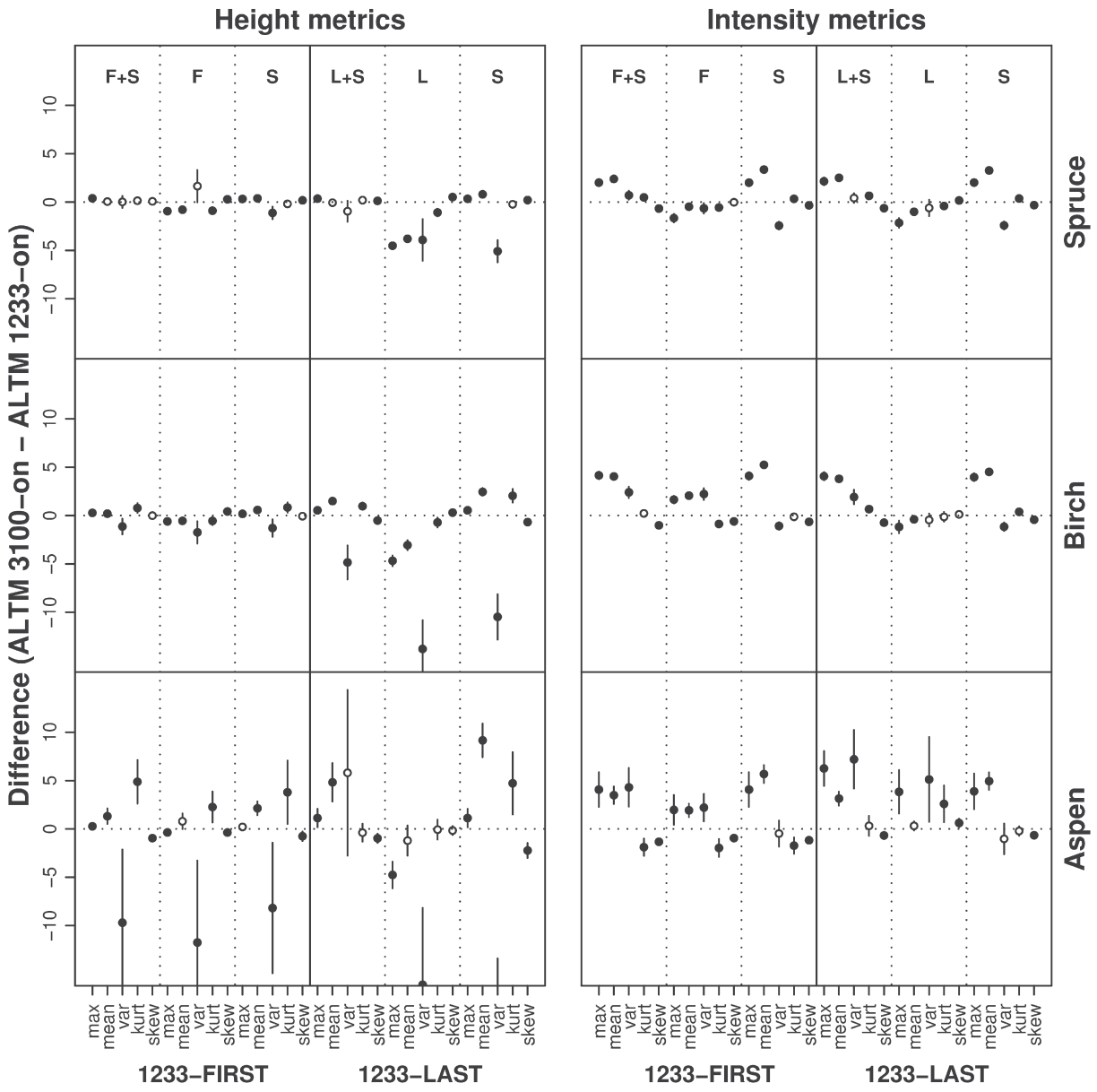

Fig. 7. Differences in height and intensity metrics between ALTM 3100-on and ALTM 1233-on. Mean differences (dots) and a 95% confidence intervals (vertical lines) for the maximum value and the first four moments of the distributions (i.e. mean, variance (var), kurtiosis (kurt), and skewness (skew)) for different species and for different comparisons of echo categories. Echo categories presented for ALTM 1233-on are FIRST (1233-FIRST) and LAST echoes (1233-LAST). For ALTM 3100-on the echo categories FIRST (F), SINGLE (S), LAST (L), FIRST + SINGLE (F + S) and LAST + SINGLE (L + S) are displayed. Significant differences ($p<0.05$) according to two-tailed *t*-tests are indicated by filled dots.

ALTM 3100-on ($p=0.027$) compared to ALTM 1233-on. There were no differences for aspen trees in estimated values using the two sensors ($p=0.510$). The variability explained by the models including the tree species term (Eq. (2b)) was significantly higher ($p<0.001$) for both acquisitions.

3.3.2. Stem diameter

The estimated parameters, confidence intervals, coefficients of determination, and RMSE of estimated acquisition-specific models for stem diameter (Eqs. (3a) and (3b)) are displayed in Table 4. The smallest overall RMSE for stem diameter was obtained with models including the tree species term (Eq. (3b)) using data from ALTM 1233-on. The smallest RMSE for models estimated according to Eq. (3a) was obtained utilizing data from the ALTM 3100-off acquisition (Table 4). For all three acquisitions the estimated model parameters had overlapping confidence intervals for both model forms (Table 4).

The estimated values obtained with models (Eq. (3a)) calibrated for different canopy conditions differed for spruce and aspen. Spruce had 0.13 cm ($p=0.014$) higher estimated values for leaf-off conditions as compared to leaf-on conditions whereas aspen had 0.66 cm ($p<0.001$) lower estimated values for leaf-off conditions. There were no differences in the estimated values of birch trees ($p=0.233$). Models which included a tree species term had significantly higher explanatory power for both canopy conditions ($p<0.001$).

The differences between the estimated values for stem diameter obtained for the two sensors (ALTM 3100-on vs. ALTM 1233-on) differed for two of the species. We found that spruce had 0.16 cm higher estimated values ($p=0.023$) whereas birch had 0.17 cm lower estimated values ($p<0.001$) with the ALTM 3100-on compared to ALTM1233-on. There were no differences in the estimated values of aspen trees ($p=0.728$) between sensors. Including a tree species term improved the stem diameter models for both sensors ($p<0.0001$).

Table 3
Estimated parameters, approximate 95% confidence intervals for parameters in parenthesis, coefficient of determination (R^2), and root mean square error (RMSE) for regression models of tree height for different laser acquisitions and model equations.[a]

	Acquisition					
	ALTM 3100-on		ALTM 3100-off		ALTM 1233-on	
Model equation[a]	2a	2b	2a	2b	2a	2b
Intercept (β_0)	0.21	0.46	0.79	0.95	0.87	1.29
	(−0.02 to 0.43)	(0.21 to 0.71)	(0.57 to 1.02)	(0.69 to 1.21)	(0.66 to 1.06)	(1.04 to 1.54)
β_1	1.00	0.99	0.98	0.97	0.97	0.97
	(0.98 to 1.00)	(0.98 to 1.00)	(0.96 to 0.99)	(0.96 to 0.98)	(0.96 to 0.98)	(0.95 to 0.98)
β_2	–	−0.35	–	−0.19	–	−0.61
		(−0.51 to −0.18)		(−0.37 to −0.01)		(−0.78 to −0.42)
β_3	–	−0.48	–	0.22	–	−0.48
		(−0.83 to −0.12)		(−0.16 to 0.60)		(−0.87 to −0.09)
σ_b	0.19	0.18	0.18	0.18	0.09	0.14
	(0.10 to 0.38)	(0.08 to 0.35)	(0.09 to 0.35)	(0.09 to 0.35)	(0.01 to 0.86)	(0.05 to 0.41)
σ_ε	0.79	0.77	0.84	0.83	0.90	0.86
	(0.73 to 0.85)	(0.71 to 0.83)	(0.78 to 0.90)	(0.78 to 0.89)	(0.84 to 0.97)	(0.80 to 0.92)
R^2	0.990	0.991	0.989	0.989	0.987	0.989
RMSE	0.78	0.76	0.83	0.82	0.90	0.84
RMSE (spruce)	0.75	0.74	0.79	0.79	0.91	0.85
RMSE (birch)	0.77	0.75	0.82	0.81	0.88	0.82
RMSE (aspen)	0.99	0.94	1.13	1.10	1.00	0.96

[a] Model equations are with or without tree species term, i.e., Eqs. (2a) and (2b), respectively.

3.3.3. Tree species

The overall classification accuracy ranged from 86.9 to 98.1% and kappa values ranged from 0.74 to 0.96 (Table 5). The class accuracy was 89.4–99.2% for spruce and 82.4–96.7% for deciduous trees (Table 5). The highest accuracy was obtained using the leaf-off dataset. The accuracy obtained using the ALTM 3100-off dataset was significantly higher than using the ALTM 3100-on ($p<0.001$) and ALTM1233-on ($p<0.001$) datasets. The accuracy of the classification obtain with the ATLM 1233-on dataset did not differ significantly from that obtain with the ALTM 3100-on dataset ($p=0.215$).

The number of trees classified is reduced when missing values occur. Trees with missing values in computed features are not classified. Of the total number of trees ($n=435$), 89% of the trees were correctly classified using data from the ALTM 1233-on acquisition, compared to 55% and 60% using the ALTM 3100-on and ALTM 3100-off, respectively. When analyzing the three different ALS datasets with exactly the same subsets of trees ($n=212$), the classification accuracies improved slightly. However, the same patterns persist in the results as when analyzing all trees (Table 5).

The feature importance, measured as the mean decrease in the Gini-index, for the classification of spruce and deciduous trees ($n=212$) using data from the three acquisitions is displayed in Fig. 8. Higher values of feature importance mean that the feature is more essential, than features with lower values, in the classification. Fig. 8 indicates that there were only minor differences in important features between the two different sensors. The normalized height features and density features from LAST echoes and intensity features from FIRST and LAST echoes were important classification features for both sensors under leaf-on conditions. Furthermore, crown penetration features (CPF) features from SINGLE echoes were important in the classification for the ALTM 3100-on acquisition. Important features in the leaf-off classification were CPF for FIRST and SINGLE echoes, density features computed from SINGLE echoes, and intensity from both FIRST and SINGLE echoes (Fig. 8).

Table 4
Estimated parameters, approximate 95% confidence intervals for parameters in parenthesis, coefficient of determination (R^2), and root mean square error (RMSE) for regression models of stem diameter for different laser acquisitions and model equations.[a]

	Acquisition					
	ALTM 3100-on		ALTM 3100-off		ALTM 1233-on	
Model equation[a]	3a	3b	3a	3b	3a	3b
Intercept (β_0)	−7.08	−4.76	−6.56	−4.34	−6.17	−4.08
	(−8.85 to −5.30)	(−6.41 to −3.11)	(−8.29 to −4.82)	(−5.97 to −2.71)	(−7.91 to −4.43)	(−5.70 to −2.45)
β_1	1.41	1.24	1.39	1.24	1.38	1.23
	(1.31 to 1.50)	(1.15 to 1.33)	(1.30 to 1.48)	(1.15 to 1.33)	(1.28 to 1.47)	(1.14 to 1.32)
β_2	1.73	2.37	1.75	2.29	1.71	2.37
	(1.43 to 2.11)	(1.98 to 2.76)	(1.37 to 2.12)	(1.90 to 2.68)	(1.33 to 2.10)	(1.98 to 2.75)
β_3	–	−3.68	–	−3.43	–	−4.03
		(−4.46 to −2.90)		(−4.21 to −2.66)		(−4.78 to −3.27)
β_4	–	−2.15	–	−1.19	–	−2.25
		(−3.84 to −0.47)		(−2.86 to −0.49)		(−3.91 to −0.59)
σ_b	2.74	2.36	2.77	2.42	2.69	2.45
	(1.89 to 4.00)	(1.60 to 3.47)	(1.91 to 4.02)	(1.65 to 3.54)	(1.83 to 3.95)	(1.67 to 3.60)
σ_ε	3.59	3.28	3.50	3.23	3.62	3.22
	(3.34 to 3.86)	(3.05 to 3.53)	(3.25 to 3.76)	(3.00 to 3.47)	(3.37 to 3.89)	(2.99 to 3.46)
R^2	0.919	0.933	0.923	0.935	0.918	0.936
RMSE	3.47	3.17	3.38	3.11	3.50	3.10
RMSE (spruce)	3.35	3.02	3.23	2.95	3.44	2.97
RMSE (birch)	3.15	2.79	3.07	2.74	3.17	2.72
RMSE (aspen)	6.13	6.15	6.17	6.13	5.96	6.01

[a] Model equations are with or without tree species term, i.e., Eqs. (3a) and (3b), respectively.

Table 5
Result of classification of spruce and deciduous trees for the three acquisitions (Table 1). Producer's accuracy for the individual tree species (spruce, birch, and aspen), overall accuracy (overall), kappa-coefficient (kappa), and the number of trees classified (*n*). Also a subset of 212 trees was analyzed separately, denoted as comparable trees.[a]

	Classification accuracy				*n*
	Spruce	Deciduous	Overall	Kappa[b]	
All trees					
ALTM 3100-on	90.1	83.2	86.9	0.74[a]	260
ALTM 3100-off	97.8	96.1	97.1	0.94[b]	241
ALTM 1233-on	89.4	90.6	90.0	0.80[a]	390
Comparable trees[1]					
ALTM 3100-on	95.9	82.4	90.1	0.79[a]	212
ALTM 3100-off	99.2	96.7	98.1	0.96[b]	212
ALTM 1233-on	95.0	91.2	93.4	0.86[a]	212

[a]Trees hit by at least three echoes of each echo category in all three acquisitions, i.e., all metrics could be computed.
[b]Different letters in superscript indicate significant differences ($p<0.05$) in kappa-coefficient between the three acquisitions.

4. Discussion and conclusions

The major findings of this study regarding the three specific research objectives indicated that:

1. Effects of canopy conditions on laser echo height and intensity distributions (objective 1):
   a. For deciduous trees, the echo height distributions derived from the LAST and SINGLE echo categories were significantly affected by changes in canopy conditions. The distributions were shifted downwards under leaf-off conditions. The height distribution of the FIRST echo category was little affected by the change in canopy conditions.
   b. For deciduous trees, the echo intensity distribution of the FIRST echoes was most affected by canopy conditions, but even the echo categories SINGLE and LAST were affected. The distribution of FIRST echoes of deciduous trees was skewed to lower intensity values under leaf-off compared to leaf-on conditions. The intensity distributions of spruce trees were not affected by canopy conditions.
2. Effects of different sensors on laser echo height and intensity distributions (objective 2):
   a. The echo height distributions differed significantly between the sensors, except for those derived for spruce trees where the combined echo categories of ALTM 3100-on (FIRST + SINGLE and LAST + SINGLE) did not differ from the corresponding echoes categories of ALTM 1233-on (FIRST and LAST).
   b. The echo intensity distributions differed significantly between sensors. A difference in the shape of the intensity distributions of FIRST echoes for deciduous trees was found. The ALTM 1233-on distributions were more skewed to lower values compared to the intensity distributions obtained with ALTM 3100-on which were more Gaussian shaped.
3. Effects of canopy conditions and different sensors on individual tree properties (objective 3):
   a. Estimates of individual tree heights had lowest RMSE when they were based on the ALTM 3100-on dataset. In most cases the parameter estimates differed between acquisitions.
   b. Individual stem diameter estimates had lowest RMSE when they were based on the ALTM 3100-off data and included a tree species term (Eq. (3b)). Among the models without a tree species term (Eq. (3a)) the ALTM 1233-on data provided the lowest RMSE. However, model parameters did not differ significantly between the acquisitions using a fixed crown width for all acquisitions.
   c. Tree species was a significant term in both the tree height and the stem diameter models. By not including tree species as a model term, the estimated values of tree height and stem diameter became significantly different for separate tree species.
   d. Leaf-off ALS data was superior to leaf-on data in discriminating between spruce and deciduous trees. There was no significant difference in classification accuracy obtained using the two different sensors.

4.1. Material and methods

A possible source of error in the analyses is related to the matching of field and laser data. Possible errors in tree coordinates, crown width, and the assumptions of circular crowns and tying echoes in the overlapping zone between crowns to the tallest tree could affect the quality of this matching. Inaccuracies in the positioning of the trees and in tree crown will introduce errors of commission (inclusion of echoes not belonging to the tree) as well as errors of omission (exclusion of echoes belonging to the tree). Birch and aspen trees are found scattered among trees of the dominating conifer species (spruce) in the forest reserve. Thus, commission and omission errors will lead to smaller differences in laser features between tree species. In addition, the assignment of echoes to the tallest tree when there is an overlap between tree crows might potentially introduce errors. If we instead had used a segmentation algorithm the number of trees would have been reduced and the proportion of dominating-/co-dominating trees had increased in the dataset (Solberg et al., 2006a). Using other assumptions, e.g. discarding the overlapping area, would also have introduced errors in the data. A visual control of the circular crown segments with the laser data provided no evidence that positional errors or errors introduced by the assumptions influenced the results of this study. Hence, we believe the current matching of echoes and trees was appropriate for the study and that the potential errors caused by the chosen method of matching field and laser data are negligible.

The current study used the raw uncalibrated intensity values. The use of intensity values calibrated with range from sensor to target is preferable. The most common calibration of intensity is range normalization (e.g. Ahokas et al., 2006; Donoghue et al., 2007; Korpela et al., 2009). Intensity calibration was not possible in the current study because of a lack of information. The use of raw intensities will introduce noise to the intensity metrics calculated for individual trees. Hence, differences between canopy conditions and sensors will be less pronounced. The two ALTM 3100 datasets were acquired at the same flying altitude and almost identical geographical location of the flight lines which minimized the impact of different ranges on intensity metrics calculated for individual trees. The utilization of raw intensities vs. calibrated intensities of the ALTM 3100 sensor has been tested for tree species classification (Korpela et al., in review). The accuracy of classification of spruce, birch, and pine improved only marginally from 73% to 75% by performing range normalization on ALTM 3100 data.

4.2. Effects of canopy conditions on laser echo height and intensity distributions (objective 1)

Studies comparing leaf-on and leaf-off echo distributions are rare. To the very best of our knowledge, the study by Næsset (2005) concerning a mixed conifer–deciduous forest is the only one addressing the influence of canopy conditions on canopy height distributions derived from ALS data. The study by Næsset (2005) was performed using a dual recording sensor (Optech ALTM 1210) and the comparison was conducted on sample plot level. Næsset (2005) found that last echoes were more affected by canopy conditions (leaf-on vs. leaf-off) than first echoes. In the current study the high influence on LAST echoes was confirmed (Figs. 2, 4). A more open canopy will

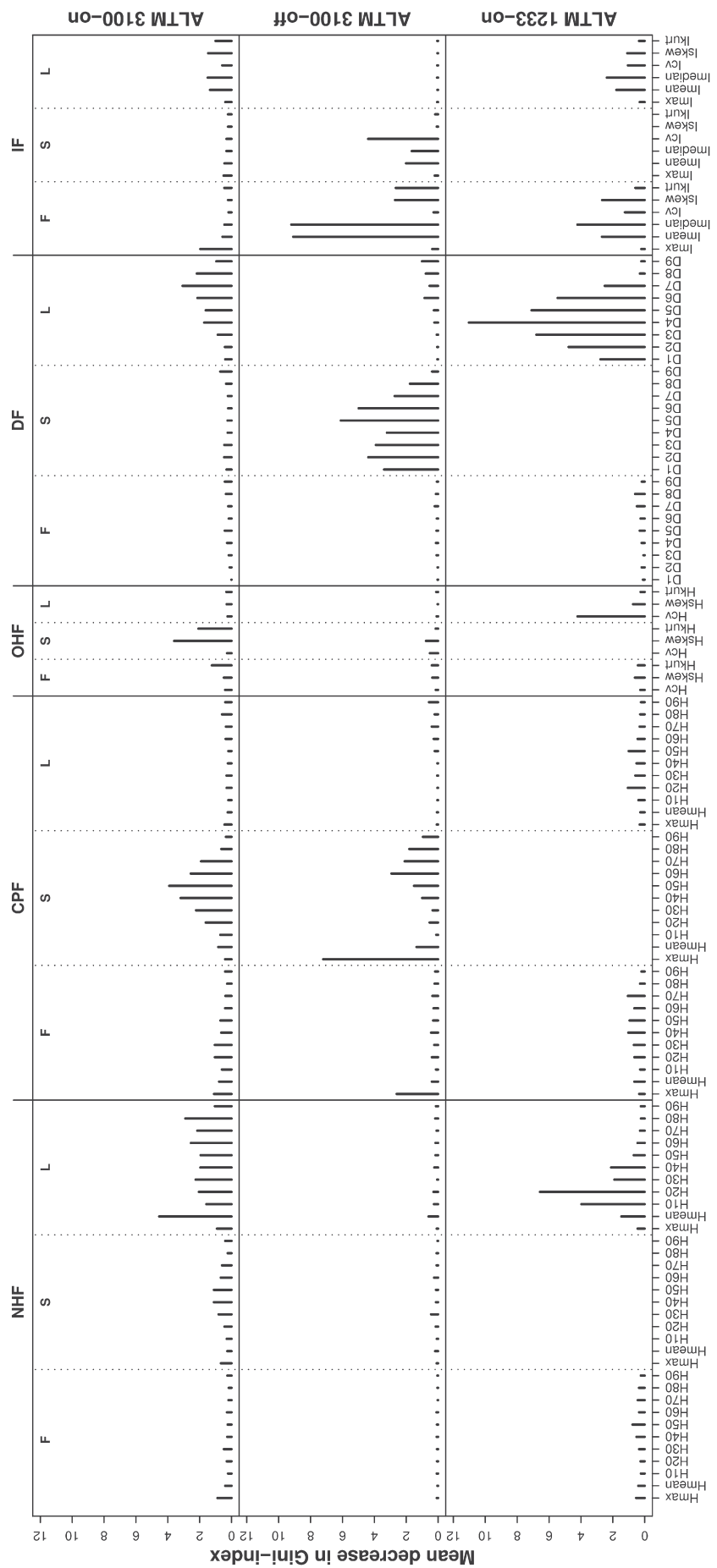

Fig. 8. Feature importance as measured by mean decrease in Gini-index values. Higher values indicate more important features for a particular acquisition (ALTM 3100-on, ALTM3100-off, and ALTM1233-on). Importance is derived for the following feature groups: normalized height feature (NHF), crown penetration feature (CPF), other height features (OHF), density features (DF), and intensity features (IF) for echo categories FIRST (F), SINGLE (S), and LAST (L). For explanation of features, see Section 2.6.3. in the text.

allow more echoes to penetrate to the ground and shift the LAST echo distribution towards the ground.

In the current study we also found that the height distribution of the SINGLE echo category was highly affected by the canopy conditions (Figs. 2, 4) whereas the influence on the FIRST echoes was only minor (Figs. 2, 4). The effect of canopy conditions on the SINGLE and FIRST echo categories are closely related. First, the proportions of echoes in the FIRST and SINGLE echo categories tend to shift between acquisitions performed under leaf-off and leaf-on canopy conditions. The number of SINGLE echoes was 20% lower under leaf-off conditions compared to leaf-on conditions (Table 2). Hence, the proportion of pulses that result in two or more echoes was greater under leaf-off conditions. The reason is the lower density of the canopy when there are no leaves on the trees. The less amount of biological matter in the higher parts of the tree crown under leaf-off result in that a larger portion of the energy of the emitted pulse will travel to lower levels of the crown making the probability of a second or even multiple echoes higher. On the other hand, under leaf-on conditions more return signals will have a short duration and the amplitude of the signals will be high which result in SINGLE echoes. This shift in the proportions of FIRST (multiple returns) and SINGLE echoes will influence on the height distributions directly. In the current study, maximum laser heights of FIRST echoes were higher in birch trees under leaf-off compared to under leaf-on conditions. It is known that SINGLE echoes tend to be higher than FIRST echoes under leaf-on conditions (Næsset, 2009; Ørka et al., 2009). Thus, targets that result in SINGLE echoes under leaf-on and FIRST echoes under leaf-off will shift the echo distribution of FIRST echoes upwards and SINGLE echoes downwards. Consequently, canopy conditions have little influence on the maximum height obtained for the individual trees. At the plot level stability of maximum height under different canopy conditions are reported by Næsset (2005) and the current study on individual trees verify this result.

The effects of the change from a permeable surface of small branches to a densely foliated crown were also observed in the intensity distributions (Fig. 3). FIRST echoes under leaf-off conditions had much lower intensity values than under leaf-on conditions for deciduous trees. The lower intensity of FIRST echoes under leaf-off conditions compared to leaf-on is a result of the longer duration and lower amplitude of the backscattered energy under leaf-off. Lower reflectivity of bark and branches compared to leaves at the wavelength used by the laser (1064 nm) will also result in decreasing intensity values under leaf-off conditions.

4.3. Effects of different sensors on laser echo height and intensity distributions (objective 2)

Potential differences between echo distributions obtained with different ALS sensors are well illustrated and known in the laser community (Chasmer et al., 2006; Hopkinson, 2007; Næsset, 2005; Næsset, 2009). While previous studies have focused on plot or stand level, the present work addressed individual trees. The two sensors that we compared represent sensors commercially available with a two year time span. Thus, differences between these two sensors illustrate effects one must be prepared to handle and account for in forest monitoring.

The ALTM 3100 sensor used in the current study had higher pulse repetition frequency (100 vs. 33 kHz), lower pulse energy (66 vs. 84 μJ), lower peak power (4.1 vs. 7.6), and larger footprint (21 vs. 18 cm) than the ALTM 1233. Because the specific algorithms used to record echoes of proprietary ALS instruments in most cases are unknown to the user and scientific communities, there are uncertainties related to the amount of energy required to trigger an echo. Different triggering algorithms are shown to produce highly different *z*-values (Wagner et al., 2004). Hence, drawing conclusions on the direction of the shifts in *z*-values base on available sensor information will be speculative since not all information is known. In the current study we observe that the combinations of FIRST + SINGLE and LAST + SINGLE, and for SINGLE echoes had higher echo distributions for the ALTM 3100-on compared to ALTM 1233-on (Fig. 7). The FIRST and LAST echoes had lower values with the ALTM 3100 sensor compared to the same echo categories recorded with ALTM 1233, while SINGLE echoes was higher than the FIRST echoes. The higher values of SINGLE echoes have also been reported previously at the plot level comparing the same sensors as used in the current study (Næsset, 2009). The likely reason for the higher SINGLE echoes is that they are returned from an area within the tree crown with high density of biological material, i.e., near or at the stem of the tree which for regularly shaped coniferous tree crowns normally will be close to the top of the tree. In areas with more biological material a larger amount of the backscatter will be reflected from the top of the canopy and only minor energy is reflected from lower canopy layers, resulting in SINGLE echoes. FIRST echoes may be returned from areas with lower density of biological material, e.g. the perimeter of the tree crown. However, using the ALTM 1233 sensor the SINGLE and FIRST echoes will always be recorded as a FIRST echo.

In the current study the echo distributions obtained from the two different sensors provided significant different moments and maximum values. There was one exception for spruce trees where FIRST and LAST echoes from ALTM 1233-on did not differ from the combinations of FIRST + SINGLE and LAST + SINGLE, respectively, of ALTM 3100-on. There was one growing season between the two ALS acquisitions which may confound with the sensor effects. Different height growth of spruce, birch, and aspen trees could affect the results. However, the intensity distributions were also highly influenced for deciduous trees (Fig. 6). Growth of trees should not necessarily influence on the intensity distributions. Hence, the difference in the backscattered signal due the more energy reaching the target with the ALTM 1233 sensor is the most likely reason for the observed differences in computed height metrics.

The raw uncalibrated intensities used in the current study indicated highly different shapes of the intensity distributions between the two sensors. Especially, the highly skewed distribution of FIRST echoes for deciduous trees obtained with the ALTM 1233-on acquisition compared to the more Gaussian distribution obtained with the ALTM 3100-on should be noticed. The distribution obtained with ALTM1233-on was very similar to the distribution of FIRST echoes of the ALTM 3100-off dataset. One explanation may be the phenology of the deciduous trees. In the autumn flight (ALTM 1233-on) the observed intensity distribution is more similar to leaf-off conditions (ALTM 3100-off) than leaf-on conditions in June (ALTM 3100-on). The foliage mass is decreasing during the summer and early autumn as chlorophyll and water are removed from the foliage, also defoliation will start already in late summer. This loss of leaf-mass will provide a signal more like the leaf-off case.

Calibration of ALS intensities is an important issue (Kaasalainen et al., 2007). Calibration of intensities obtained by ALS may increase the befit of intensity measurements in forest inventory. Simple range corrections have been applied successfully (Korpela et al., in review; Ahokas et al., 2006; Donoghue et al., 2007). However, the two conceptually different intensity distributions obtained from the two sensors for FIRST echoes indicates that calibration of intensities must incorporate sensor settings. A correction of intensities only by the range from the sensor to target will most likely be insufficient.

4.4. Effects of canopy conditions and different sensors on individual tree properties (objective 3)

4.4.1. Tree height

The most accurate estimates of individual tree height were based on data from the ALTM 3100-on acquisition. The lower RMSEs of tree height in the leaf-on case compared to the leaf-off case may be explained by the denser canopy under leaf-on conditions. A leaf-on

canopy will provide a better representation of the tree top with less noise inherent in the maximum height measured by ALS compared to leaf-off conditions. Furthermore, the lower RMSEs of tree height with the ALTM 3100-on compared to the ALTM 1233-on are explained by the sensor settings. The ALTM 3100 sensor was operated at a higher pulse repetition frequency and with lower pulse energy than the ALTM 1233 sensor. It has been shown that such sensor properties tend to decrease the penetration into tall tree canopies (Chasmer et al., 2006). Hence, less noise will be inherited in the maximum laser height with the ALTM 3100-on compared to ALTM 1233-on.

The obtained RMSEs for the different tree height models were in the range from 0.78 to 0.90 m with R^2 above 0.98 for all acquisitions, which are similar to results from other studies. Persson et al. (2002) obtained an RMSE of 0.63 m and an R^2 of 0.98 in a spruce and pine forest. In a study conducted in a similar type of forest as in the current, R^2 values of 0.92 and 0.93 were obtained for models excluding and including a tree species term, respectively (Maltamo et al., 2004). Furthermore, in the current study, the parameter estimates for maximum laser height in the tree height regression models were always less than one, indicating that the laser underestimated tree height of tall trees more than short trees. The most likely reason for the smaller underestimation of short trees is the larger influence of taller neighboring trees providing erroneous measurements. Maltamo et al. (2004) also obtained slope values below one, but in contrast to the current study their confidence interval for the slope included the value one, indicating that the slope coefficient was not significantly different from one in the statistical sense.

The results of the current study indicated that field calibrated tree height models should include tree species as an explanatory variable to provide comparative results over time. For all the three acquisitions, models that included the tree species term had significantly higher explanatory power than models not including the tree species as a variable. The estimated values differed for different tree species when the models did not include a tree species term. Thus, a systematic species specific error will be introduced if tree species is not a model term.

The idea of reusing model equations established with previously and already existing field plots and acquisitions is relevant and interesting. The current study revealed that all model parameters, i.e., intercept, slope, and species specific adjustment of the intercept differed between the models developed for the specific sensors. Therefore, this study suggests that models cannot be reused across sensors without losing accuracy. The most explicit differences are in the intercepts of the models.

4.4.2. Stem diameter

The estimated parameters for models calibrated with different acquisitions did not differ significantly. The number of models that has been proposed for estimation of stem diameter of individual trees from ALS data is large and we only tested one of these previously proposed models in the current study (Hyyppä et al., 2001). Other models may yield different results. Preliminary analysis revealed that published models estimating stem diameter from ALS data produce highly different estimates of stem diameter. We believe that more research is needed to find models performing equally well – if possible – on different sites and under different forest conditions.

Differences in RMSEs for stem diameter was only 0.06–0.09 cm for different canopy conditions and 0.03–0.07 cm for the different sensors. In addition, none of the estimated parameters differed between acquisitions. Hence, the effects of acquisitions on the stem diameter estimation seem to be minor and a common model may be established. An important constrain — and thus a limitation in the current study was the use of field-measured crown width rather than using crown width derived from the ALS data. Different acquisitions may result in different estimates of crown width when obtained from an automatic tree segmentation based on the ALS data, which in turn may alter the model parameters.

The RMSEs for stem diameter varied between 3.1 and 3.5 cm, corresponding to 15–17% of the average stem diameter. The R^2 values were 0.93 and 0.92 for models with and without tree species, respectively. Persson et al. (2002) obtained an RMSE value of 3.8 cm or 10% of the average stem diameter in a boreal conifer forest in Sweden. They reported an R^2 value of 0.83. In a pine forest in Texas, Popescu (2007) obtained an RMSE of 4.9 cm (18% of the average stem diameter), with an R^2 value of 0.87, Hence, the accuracy in this study seems to be fairly similar to results obtained in other studies.

Models with a tree species term were significantly better in all three acquisitions. When not including a tree species term in the model, significant differences in estimated values for separate species were found. We suggest that tree species should be included in models for stem diameter based on ALS data.

4.4.3. Tree species

Most of the studies dealing with the ALS data acquired under leaf-off conditions at the individual tree level have been on species classification (Brandtberg, 2007; Brandtberg et al., 2003; Liang et al., 2007; Reitberger et al., 2008). In our study the leaf-off classification performance was better in terms of classification accuracy than the leaf-on classification. Reitberger et al. (2008) also performed a comparison of conifer and deciduous tree species classification under leaf-off and leaf-on canopy conditions with a waveform laser in Germany. In that study the overall accuracy was 96% under leaf-off conditions and 85% under leaf-on conditions. In the same area Heurich (2006) got the highest accuracy under leaf-off canopy conditions, i.e., 97% overall accuracy whereas the best overall accuracy under leaf-on acquisition was 81%. In our study we obtained classification accuracies of 98 and 90% under leaf-off and leaf-on canopy conditions, respectively. Thus, it seems to be a common and consistent finding that higher classification accuracies can be obtained during the leaf-off season when using ALS for species classification.

In the current study, the *Z*-statistics of the kappa-coefficients revealed that there were no significant differences between the classifications obtained with the two sensors. The class accuracies tended to be slightly more uniform with the ALTM 1233-on compared to ALTM 3100-on. In another study sensor differences were found in the classification accuracy obtained with Optech ALTM 3100 and Leica ALS 50-II (Korpela et al., in review).

The important classification features derived from the random forest classification are quite similar in the two leaf-on acquisitions in the current study. This result indicates that there may be a set of features that may be generally applicable in tree species classification across different acquisitions. The important classification features common for the two acquisitions seemed to be normalized heights from LAST echoes, density features from LAST echoes and intensity features from FIRST and LAST echoes. However, another study conducted in the same area indicated that feature selection was influenced by species specific tree height distributions (Ørka et al., 2009). The ranking of features by the GINI-index in random forest does not account for different tree height distributions for different species in the study area (Fig. 1). Hence, the features selected by random forest are influenced by the differences in height distributions of the spruce and deciduous trees and the important classification features should be validated in other studies.

4.5. Concluding remarks

To conclude, echo distributions and derived metrics differ between sensors. However, differences in accuracy of individual tree properties are minor between sensors when the models were calibrated with field measurements. Field measurements for model calibration are important in individual tree inventories by ALS. Moreover, tree species

should be included in as a model term in tree height and stem diameter models. Differences in estimated model parameters were found for models calibrated on data from different sensors, the most affected parameter was the intercept in tree height models.

Different echo categories were affected differently by canopy conditions. Accuracy in estimates for tree height or stem diameter was minor between acquisitions with different canopy conditions. However, significantly more accurate tree species discrimination was obtained during the leaf-off conditions. The classification accuracies were in the order of 10 percentage points higher in overall accuracy. Hence, ALS based individual tree inventory could benefit from the leaf-off acquisitions without losing accuracy of tree height and stem diameter estimations, and at the same time obtain higher accuracy of tree species detection. Since tree species also are identified to be important in tree height and stem diameter models, the total accuracy of the inventory may be improved even more under leaf-off acquisition.

Acknowledgements

This research was funded by the Norwegian University of Life Sciences and the Research Council of Norway (research grant #184652) and is a contribution to the WoodWisdom-NET project entitled "New Technologies to Optimize the Wood Information Basis for Forest Industries — Developing an Integrated Resource Information System (WW-IRIS)". We also wish to thank Blom Geomatics, Norway, for providing and processing the airborne laser data.

References

Ahokas, E., Kaasalainen, S., Hyyppä, J., & Suomalainen, J. (2006). Calibration of the Optech ALTM 3100 laser scanner intensity data using brightness targets. *International Archives of Photogrammetry, Remote Sensing and Spatial Information Sciences*, *XXXVI* Part 1/A.

Baltsavias, E. P. (1999). Airborne laser scanning: Basic relations and formulas. *ISPRS Journal of Photogrammetry and Remote Sensing*, *54*, 199—214.

Bollandsås, O. M., & Næsset, E. (2007;). Estimating percentile-based diameter distributions in uneven-sized Norway spruce stands using airborne laser scanner data. *Scandinavian Journal of Forest Research*, *22*, 33—47.

Brandtberg, T. (2007). Classifying individual tree species under leaf-off and leaf-on conditions using airborne LIDAR. *ISPRS Journal of Photogrammetry and Remote Sensing*, *61*, 325—340.

Brandtberg, T., Warner, T. A., Landenberger, R. E., & McGraw, J. B. (2003). Detection and analysis of individual leaf-off tree crowns in small footprint, high sampling density LIDAR data from the eastern deciduous forest in North America. *Remote Sensing of Environment*, *85*, 290—303.

Breiman, L. (2001). Random forests. *Machine Learning*, *45*, 5—32.

Chasmer, L., Hopkinson, C., Smith, B., & Treitz, P. (2006). Examining the influence of changing laser pulse repetition frequencies on conifer forest canopy returns. *Photogrammetric Engineering and Remote Sensing*, *72*, 1359—1367.

Cohen, J. (1960). A coefficient of agreement for nominal scales. *Educational and Psychological Measurement*, *20*, 37—46.

Congalton, R. G. (1991). A review of assessing the accuracy of classifications of remotely sensed data. *Remote Sensing of Environment*, *37*, 35—46.

Daamen, W. (1980). Kontrolltaxeringen åren 1973–1977: resultat från en kontroll av datainsamlingen vid riksskogstaxeringen (Results from a check on data collection of the national forest survey in 1973–1977) Umeå.

Donoghue, D. N. M., Watt, P. J., Cox, N. J., & Wilson, J. (2007). Remote sensing of species mixtures in conifer plantations using LiDAR height and intensity data. *Remote Sensing of Environment*, *110*, 509—522.

Eid, T., Gobakken, T., & Næsset, E. (2004). Comparing stand inventories for large areas based on photo-interpretation and laser scanning by means of cost-plus-loss analyses. *Scandinavian Journal of Forest Research*, *19*, 512—523.

Eriksson, H. (1970). Om mätningsfel vid höydmätning av stående träd med olika instrument. *Inst. för skogsproduktion, skogshögskolan, Rapport och uppsatser* (pp. 1:42).

Goodwin, N. R., Coops, N. C., & Culvenor, D. S. (2006). Assessment of forest structure with airborne LIDAR and the effects of platform altitude. *Remote Sensing of Environment*, *103*, 140—152.

Heurich, M. (2006). Evaluierung und entwicklung von automatiserten erfassung von waldstructuren aus daten flugzuggetragener fernerkundungssenoren. *Forstkuche Forshungsberichte München*, *2002*, p329.

Höfle, B., & Pfeifer, N. (2007;). Correction of laser scanning intensity data: Data and model-driven approaches. *ISPRS Journal of Photogrammetry and Remote Sensing*, *62*, 415—433.

Holmgren, J., & Persson, Å. (2004;). Identifying species of individual trees using airborne laser scanner. *Remote Sensing of Environment*, *90*, 415—423.

Holmgren, J., Nilsson, M., & Olsson, H. (2003). Simulating the effects of lidar scanning angle for estimation of mean tree height and canopy closure. *Canadian Journal of Remote Sensing*, *29*, 623—632.

Holmgren, J., Persson, Å., & Söderman, U. (2008). Species identification of individual trees by combining high resolution LIDAR data with multi-spectral images. *International Journal of Remote Sensing*, *29*, 1537—1552.

Hopkinson, C. (2007). The influence of flying altitude, beam divergence, and pulse repetition frequency on laser pulse return intensity and canopy frequency distribution. *Canadian Journal of Remote Sensing*, *33*, 312—324.

Hyde, P., Dubayah, R., Walker, W., Blair, J. B., Hofton, M., & Hunsaker, C. (2006). Mapping forest structure for wildlife habitat analysis using multi-sensor (LiDAR, SAR/InSAR, ETM plus, Quickbird) synergy. *Remote Sensing of Environment*, *102*, 63—73.

Hyde, P., Nelson, R., Kimes, D., & Levine, E. (2007). Exploring LiDAR-RaDAR synergy — Predicting aboveground biomass in a southwestern ponderosa pine forest using LiDAR, SAR and InSAR. *Remote Sensing of Environment*, *106*, 28—38.

Hyyppä, H., & Hyyppä, J. (1999;). Comparing the accuracy of laser scanner with other optical remote sensing data sources for stand attributes retrieval. *Photogrammetry Journal of Finland*, *16*, 5—15.

Hyyppä, J., Kelle, O., Lehikoinen, M., & Inkinen, M. (2001). A segmentation-based method to retrieve stem volume estimates from 3-D tree height models produced by laser scanners. *IEEE Transactions on Geoscience and Remote Sensing*, *39*, 969—975.

Hyyppä, J., Hyyppä, H., Leckie, D., Gougeon, F., Yu, X., & Maltamo, M. (2008). Review of methods of small-footprint airborne laser scanning for extracting forest inventory data in boreal forests. *International Journal of Remote Sensing*, *29*, 1339—1366.

Kaasalainen, S., Ahokas, E., Hyyppa, J., & Suomalainen, J. (2005). Study of surface brightness from backscattered laser intensity: Calibration of laser data. *IEEE Geoscience and Remote Sensing Letters*, *2*, 255—259.

Kaasalainen, S., Hyyppä, J., Litkey, P., Ahokas, E., Kukko, A., & Kaartinen, H. (2007). Radiometric calibration of ALS intensity. *International Archives of Photogrammetry, Remote Sensing and Spatial Information Sciences*, *XXXVI* Part 3 / W52.

Korpela, I., Koskinen, M., Vasander, H., Holopainen, M., & Minkkinen, K. (2009). Airborne small-footprint discrete-return LiDAR data in the assessment of boreal mire surface patterns, vegetation, and habitats. *Forest Ecology and Management*, *258*, 1549—1566.

Korpela, I.S., Ørka, H.O., Maltamo, M., Tokola, T., & Hyyppä, J. (in review). Tree species classification using airborne LiDAR — Effects of stand and tree parameters, downsizing of training set, intensity normalization and sensor type.

Liang, X., Hyyppä, J., & Matikainen, L. (2007). Deciduous-coniferous tree classification using difference between first and last pulse laser signatures.*International Archives of Photogrammetry, Remote Sensing and Spatial Information Sciences*, *XXXVI*, 253—257 Part 3 / W52.

Liaw, A., & Wiener, M. (2002;). Classification and regression by randomForest. *R News*, *2*, 18—22.

Lim, K., Treitz, P., Baldwin, K., Morrison, I., & Green, J. (2003). Lidar remote sensing of biophysical properties of tolerant northern hardwood forests. *Canadian Journal of Remote Sensing*, *29*, 658—678.

Magnusson, M. (2006). Evaluation of remote sensing techniques for estimation of forest variables at stand level (doctoral thesis). In, *Acta Universitatis agriculturae Sueciae* (p. 38). Umeå: Dept. of Forest Resource Management and Geomatics, Swedish University of Agricultural Sciences.

Maltamo, M., Mustonen, K., Hyyppa, J., Pitkanen, J., & Yu, X. (2004). The accuracy of estimating individual tree variables with airborne laser scanning in a boreal nature reserve. *Canadian Journal of Forest Research-Revue Canadienne De Recherche Forestiere*, *34*, 1791—1801.

Næsset, E. (2004a). Practical large-scale forest stand inventory using a small-footprint airborne scanning laser. *Scandinavian Journal of Forest Research*, *19*, 164—179.

Næsset, E. (2004b). Effects of different flying altitudes on biophysical stand properties estimated from canopy height and density measured with a small-footprint airborne scanning laser. *Remote Sensing of Environment*, *91*, 243—255.

Næsset, E. (2005). Assessing sensor effects and effects of leaf-off and leaf-on canopy conditions on biophysical stand properties derived from small-footprint airborne laser data. *Remote Sensing of Environment*, *98*, 356—370.

Næsset, E. (2007). Airborne laser scanning as a method in operational forest inventory: Status of accuracy assessments accomplished in Scandinavia. *Scandinavian Journal of Forest Research*, *22*, 433—442.

Næsset, E. (2009). Effects of different sensors, flying altitudes, and pulse repetition frequencies on forest canopy metrics and biophysical stand properties derived from small-footprint airborne laser data. *Remote Sensing of Environment*, *113*, 148—159.

Næsset, E., & Gobakken, T. (2005;). Estimating forest growth using canopy metrics derived from airborne laser scanner data. *Remote Sensing of Environment*, *96*, 453—465.

Næsset, E., & Nelson, R. (2007;). Using airborne laser scanning to monitor tree migration in the boreal–alpine transition zone. *Remote Sensing of Environment*, *110*, 357—369.

Næsset, E., Gobakken, T., Holmgren, J., Hyyppä, H., Hyyppä, J., Maltamo, M., Nilsson, M., Olsson, H., Persson, A., & Soderman, U. (2004). Laser scanning of forest resources: The Nordic experience. *Scandinavian Journal of Forest Research*, *19*, 482—499.

Næsset, E., Bollandsas, O. M., & Gobakken, T. (2005). Comparing regression methods in estimation of biophysical properties of forest stands from two different inventories using laser scanner data. *Remote Sensing of Environment*, *94*, 541—553.

Næsset, E., Gobakken, T., & Nelson, R. (2009). Sampling and mapping forest volume and biomass using airborne LIDARs. *Proceedings of the Eight Annual Forest Inventory and Analysis Symposium, Monterey, CA, USA.* (pp. 297—301).

Nelson, R., Valenti, M. A., Short, A., & Keller, C. (2003). A multiple resource inventory of Delaware using airborne laser data. *Bioscience*, *53*, 981—992.

Nelson, R., Short, A., & Valenti, M. (2004). Measuring biomass and carbon in Delaware using an airborne profiling LIDAR. *Scandinavian Journal of Forest Research*, *19*, 500−511.

Nelson, R. F., Hyde, P., Johnson, P., Emessiene, B., Imhoff, M. L., Campbell, R., & Edwards, W. (2007). Investigating RaDAR-LiDAR synergy in a North Carolina pine forest. *Remote Sensing of Environment*, *110*, 98−108.

Ørka, H. O., Næsset, E., & Bollandsås, O. M. (2009). Classifying species of individual trees by intensity and structure features derived from airborne laser scanner data. *Remote Sensing of Environment*, *113*, 1163−1174.

Persson, Å., Holmgren, J., & Söderman, U. (2002). Detecting and measuring individual trees using an airborne laser scanner. *Photogrammetric Engineering and Remote Sensing*, *68*, 925−932.

Pinheiro, J. C., & Bates, D. M. (2000;). *Mixed-effects models in S and S-PLUS.* New York: Springer.

Pinheiro, J., Bates, D., DebRoy, S., Sarkar, D., & R Core team (2008). nlme: Linear and nonlinear mixed effects models.

Popescu, S. C. (2007). Estimating biomass of individual pine trees using airborne lidar. *Biomass & Bioenergy*, *31*, 646−655.

R Development Core Team. (2008). *R: A language and environment for statistical computing.* Vienna, Austria.: R Foundation for Statistical Computing.

Reitberger, J., Krzystek, P., & Stilla, U. (2008). Analysis of full waveform LIDAR data for the classification of deciduous and coniferous trees. *International Journal of Remote Sensing*, *29*, 1407−1431.

Reutebuch, S. E., McGaughey, R. J., Andersen, H. E., & Carson, W. W. (2003). Accuracy of a high-resolution LIDAR terrain model under a conifer forest canopy. *Canadian Journal of Remote Sensing*, *29*, 527−535.

Solberg, S., Næsset, E., & Bollandsås, O. M. (2006a). Single tree segmentation using airborne laser scanner data in a structurally heterogeneous spruce forest. *Photogrammetric Engineering and Remote Sensing*, *72*, 1369−1378.

Solberg, S., Næsset, E., Hanssen, K. H., & Christiansen, E. (2006b). Mapping defoliation during a severe insect attack on Scots pine using airborne laser scanning. *Remote Sensing of Environment*, *102*, 364−376.

Terrasolid Ltd (2004). *TerraScan user's guide.* Helsinki: Terrasolid Ltd..

Venables, W. N., & Ripley, B. D. (2002). *Modern Applied Statistics with S.* New York: Springer.

Wagner, W., Ullrich, A., melzer, T., Briese, C., & Kraus, K. (2004). From single-pulse to full-waveform airborne laser scanners: Potential and practical challenges. *International Arcives of Photogrammetry and Remote Sensing*, *XXXV*(Part B3), 201−206.

West, B., Welch, K. B., & Galecki, A. T. (2007). *Linear mixed models: A practical guide using statistical software.* Boca Raton: Chapman & Hall/CRC.

Yu, X., Hyyppä, J., Hyyppä, H., & Maltamo, M. (2004). Effects of flight altitude on tree height estimation using airborne laser scanning. *International Archives of Photogrammetry, Remote Sensing and Spatial Information Sciences*, *XXXVI*(8/W2), 96−101.

Paper III

Improving airborne laser scanning tree species identification utilizing intensity normalization and multispectral imagery

Authors:

Hans Ole Ørka*, Terje Gobakken, Erik Næsset, Liviu Ene & Vegard Lien

Address:

Norwegian University of Life Sciences, Department of Ecology and Natural Resource Management, P.O. Box 5003, NO-1432 Ås, Norway

* Corresponding author:

Hans Ole Ørka

E-mail address: hans-ole.orka@umb.no

Phone: +47 64 96 57 99

Fax: +47 64 96 58 02

Abstract

The objective of the current study was to investigate the effects of using spectral data in addition to structural three-dimensional airborne laser scanning (ALS) data for tree species identification. Spectral information from the ALS intensity and two different types of multispectral images were tested. The classification accuracy was assessed using 1520 segmented trees (52% spruce trees, 40% pine trees, and 8% deciduous trees). Both Applanix DSS images acquired simultaneously as the ALS-data and Vexcel Ultracam D images acquired on a separate flight mission were used. Intensity was normalized using the range from sensor to the target (range normalization). In addition, a source of variation in intensity known as banding is described, together with a normalization procedure for diminishing this effect. When only intensity data was used, normalization of intensities increased the overall classification accuracy for tree species with 5 - 11%. The range normalization was more beneficial than banding normalization. ALS structural information alone provided overall classification accuracies of 74 - 77%. Adding normalized intensity information to the structural information did not improve the classification. The accuracies obtained using only multispectral imagery (71 - 79%) were on the same level as using ALS structural information. However, combined use of ALS structural information and multispectral imagery from the Applanix sensor and the Vexcel Ultracam D sensor provided overall accuracies of 87 - 89% and 84 - 87%, respectively.

Keywords: Airborne laser scanning; Multispectral images; Intensity; Intensity normalization, Range normalization; Banding; Tree species identification;

1. Introduction

Airborne laser scanning (ALS) is superior compared to other remote sensing techniques, like RaDAR and optical imagery, to estimate important biophysical properties of forests such as tree height, stem volume and biomass (Hyde et al., 2006; Hyyppä & Hyyppä, 1999). However, information about tree species is also an essential parameter of forest inventories and in recent years research on tree species identification utilizing ALS data has increased (Heinzel & Koch, 2011; Korpela et al., 2010b; Ørka et al., 2009a; Suratno et al., 2009). Nevertheless, providing species information represents a challenge in the utilization of ALS in forest inventories.

There are two main approaches in ALS aided forest inventory; (1) area-based inventory and (2) individual tree inventory. Although during the last few years individual tree inventory has become commercially available, the area-based inventory (Næsset, 2002) is still dominating the operational forest inventories using ALS, mainly because of lower cost and maturity of the approach compared to individual tree approaches. Estimation of species specific volumes following an area-based approach is documented e.g. by Packalén et al. (2009). However, studies based on the individual trees approach has dominated the research on tree species identification (Hyyppä et al., 2008). An advantage of individual tree approaches over area-based approaches is that separate tree species may be considered instead of only species mixtures. Individual tree analyses result in detailed knowledge of the laser pulse - tree interactions regarding specific species (Ørka et al., 2009a). Knowledge from individual tree studies can furthermore be implemented in area-based projects or contribute to the maturation of individual tree inventories.

The procedure of individual tree species identification includes steps of object segmentation, feature computation, and object classification. First, individual tree crowns are delineated from ALS data using an object segmentation process (e.g. Persson et al., 2002; Solberg et al., 2006). Then, several classification features are computed from the ALS echoes within the tree crown segments. Features considered are statistical measures derived from the height- or intensity distribution of laser echoes (e.g. Holmgren & Persson, 2004; Korpela et al., 2010b; Ørka et al., 2009a), parameters of fitted surfaces (Holmgren & Persson, 2004) and laser estimated crown base height (Holmgren et al., 2008). Recently, three-dimensional textural features derived from alpha-shapes have also been utilized (Vauhkonen et al., 2009). Finally, species are assigned to crown segments according to a supervised or unsupervised

classifier. Linear discriminant analysis (LDA) is frequently used for individual tree species classification, but other parametric and non-parametric methods are applied (Table 1).

The average classification accuracy obtained in tree species identification studies (table 1) is approximately 83%. The errors obtained in tree species identification would further affect the accuracy of other forest estimates through species specific models, e.g. for stem diameter and stem volume (Korpela & Tokola, 2006). Many applications require higher tree species classification accuracies than those obtain using ALS. Hence, improvements of ALS tree species identification are desired. Acquisition of ALS data in the dormant period of deciduous trees seems to be one option to improve individual tree species identification. Studies comparing leaf-off and leaf-on data reported 8 - 16 percentage points increase in the overall classification accuracy (Heurich, 2006; Ørka et al., 2010; Reitberger et al., 2008). However, the leaf-off period is often limited because of short time periods where trees do not have leaves and the ground is snow-free, at least at high latitudes. Consequently, other means to improve tree species identification should be considered.

The majority of the studies have used spectral information in terms of the raw ALS intensities (Table 1). The intensity measures provided by ALS sensors are noisy and are dependent on many factors. Thus, it has been suggested that intensity normalization is necessary (Ahokas et al., 2006; Korpela et al., 2010b). Factors affecting the intensity are amongst others range from sensor to target, incidence angles, atmospheric transmittance, and transmitted power (Ahokas et al., 2006). Of the previous mentioned factors normalization based on range from the sensor to the target - range normalization - is the most important. The backscattering from different incidence angles are dependent on the target and thus it is difficult to calibrate intensity based on this factor. Atmospheric transmittance is often omitted and can be assumed to be constant during a given acquisition. This assumption also applies to the transmitted power from the sensor. Transmitted power varies between sensors and with acquisition setting such as flying altitude and pulse repetition frequency. A few studies have reported that range normalized intensity has improved tree species identification (Gatziolis, 2009; Korpela et al., 2010b). However, additional studies comparing raw and range normalized intensities are needed to confirm these results.

Different ALS sensors are known to produce different height- and intensity values over the same target due to differences in e.g. emitted energy, pulse repetition frequency, and other factors (Næsset, 2009; Ørka et al., 2010). Ørka et al (2010) found different intensity distributions between the two Optech sensors studied and suggested that intensity normalization should incorporate sensor settings. Korpela et al. (2010b) normalized intensity

Table 1. Overview of peer-reviewed studies utilizing ALS features for individual tree species classification. The table presents the reference to the study (Study), the location (Country), the sensor used (Sensor), the canopy conditions (Leaf-), the number of species classified (#SP), the overall accuracy obtained (OA), the kappa coefficient (κ), the classification method used (Classification method), and information about applying intensity normalization (Intensity normalization). The accuracy presented represents the best classification method used in the study and other methods used are in parentheses.

Study	Country	Sensor	Leaf-	#SP	OA	κ	Classification method[b]	Intensity normalization
Brandtberg et al. (2003)	US - Virginia	TopEye	Off	3	60	-	LDA	no[c]
Holmgren & Persson (2004)	Sweden	TopEye	On	2	95	0.89	LDA (QDA)	no[c]
Brandtberg (2007)	US - Virginia	TopEye	Off	3	64		LDA	no[c]
Holmgren et al. (2008)	Sweden	TopEye (MkII)	On	3	88	0.82	QDA	no[c]
Reitberger et al. (2008)	Germany	Riegl (LMS-Q560)[a]	On	2	85	0.71	KM (EM)	no
Reitberger et al. (2008)	Germany	Riegl (LMS-Q560)[a]	Off	2	96	0.92	KM (EM)	no
Holmgren et al. (2008)	Sweden	TopEye (MkII)	On	3	88	0.82	QDA	no[c]
Vauhkonen et al. (2009)	Finland	TopEye (Mark II)	On	3	95	0.90	LDA	no[c]
Ørka et al. (2009a)	Norway	Optech (ALTM3100)	On	2	89	-	LDA	no
Suratno et al. (2009)	US - Montana	Leica (ALS50)	On	4	68	0.56	LDA	yes
Kim et al. (2009)	US - Washington	Optech (ALTM 30/70)	On	2	73	-	LDA	no
Kim et al. (2009)	US - Washington	Optech (ALTM 3100)	Off	2	83	-	LDA	no
Ørka et al. (2010)	Norway	Optech (ALTM 3100)	On	2	90	0.79	RF	no
Ørka et al. (2010)	Norway	Optech (ALTM 3100)	Off	2	98	0.96	RF	no
Ørka et al. (2010)	Norway	Optech (ALTM 1233)	On	2	93	0.86	RF	no
Vauhkonen et al. (2010)	Finland	Optech (ALTM 3100) & Leica(ALS50)	On	3	78	-	RF (kMSN)	
Korpela et al. (2010b)	Finland	Optech (ALTM 3100)	On	3	84	0.72	RF (kNN, LDA, kMSN)	yes
Korpela et al. (2010b)	Finland	Leica(ALS50)	On	3	89	0.80	RF (kNN, LDA, kMSN)	yes
Heinzel & Koch (2011)	Germany	Riegl (LMS-Q560)[a]	On	6	59	-	LDA	yes
Heinzel & Koch (2011)	Germany	Riegl (LMS-Q560)[a]	On	4	84	-	LDA	yes
Heinzel & Koch (2011)	Germany	Riegl (LMS-Q560)[a]	On	2	92	-	LDA	yes

[a]Waveform recording sensor.
[b]Classification methods used are Linear Discriminant analysis (LDA), Quadratic discrimant analysis (QDA), k-means clustering (KM), Expectation-maximization algorithm (EM), randomforest (RF), k-most similar neighbor (kMSN), and k-nearest neighbor (kNN).
[c]According to Korpela et al. (2010b) the TopEye sensor has a built-in range correction of the intensity.

recordings from the Leica ALS 50 sensor by applying a sensor specific normalization equation. They normalized the intensity using both the range and the automatic gain control value (AGC) recorded by the Leica sensor. The normalized intensity provided by the Leica sensor based on range and AGC outperformed the range normalized intensity recorded by the Optech sensor in classification of tree species, with a difference in overall accuracy of 5.0 - 9.1 percentage points. Different sampling rates and footprint sizes, in addition to campaign dependent intensity recordings were suggested as explanations for these differences (Korpela et al., 2010b).

The AGC-effect on intensity is unique to Leica sensors. Another effect on intensity which is unique for Optech ALTM sensors is referred to as banding. Banding is caused by differences in intensity between scan directions of the oscillating mirror (Fig. 1). In the American Society for Photogrammetry and Remote Sensing (ASPRS) LASer (LAS) file format specification (ASPRS, 2009) the differences between scan directions of the mirror are stored in the "Scan Direction Flag" item. The Scan Direction Flag has a bit value of 1 for a positive scan direction, and a bit value of 0 for a negative scan direction. A positive scan direction is defined as a scan moving from the left to the right side of the in-track direction (negative scan direction is the opposite). Banding will result in different intensity distributions for the two scanning directions. Hence, more noise is present in the data when

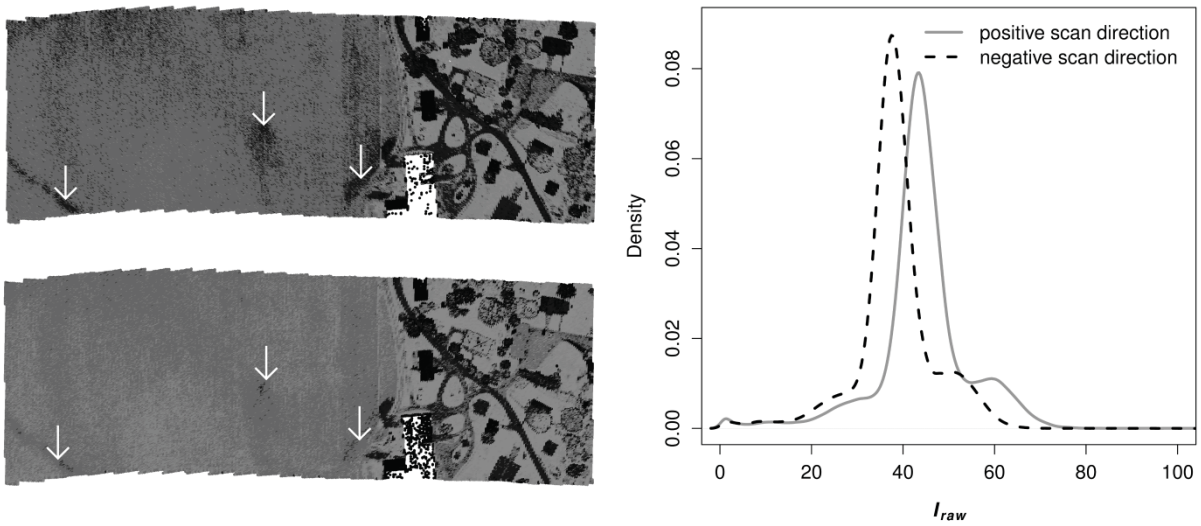

Fig. 1. A subset of an ALS flightline illustrates the banding effect, i.e., the differences in intensities between scan directions. The images to the left display the intensities of first returns with a positive scan direction (top) and negative scan direction (bottom). The images are equalized for better interpretability. The respective estimated probability density functions (*pdf*) of the raw intensities (I_{raw}) in the displayed area appear to the right. In the images the banding effect appears as brighter areas in the lower image compare to the image above (see arrows).

the effect of banding is not taken into account. Furthermore, calibration methods for the banding effect and comparisons of uncalibrated and calibrated data are needed.

Combination of ALS and multispectral images are another frequently suggested technique to improve accuracy of individual tree species identification (Heinzel et al., 2008; Korpela et al., 2010b; Persson et al., 2004). Holmgren et al. (2008) combined ALS data and multispectral images for individual tree identification. They obtained improvements in the order of 5 - 8 percentage points in overall classification accuracy compared to only utilizing ALS data. Furthermore, combining ALS and imagery data for stand delineation and species classification produced more accurate results than using each of these data sources separately (Ke et al., 2010). The main drawback by adding images to the inventory protocol is higher acquisition costs since ALS and image data usually are acquired in separate flight missions. However, acquiring ALS and image data simultaneously from the same platform is possible and an attractive option to reduce costs.

The main objective of the current research was to investigate the effects of using spectral data in addition to structural three-dimensional airborne laser scanning data for tree species identification. Spectral information from the ALS intensity and two different types of multispectral images were tested. The specific objectives were to assess effects of using

1. range normalized intensity,
2. normalization of the sensor specific banding effect,
3. inclusion of color infrared images (red, green, infrared) from the Applanix DSS sensor acquired from the same platform as the ALS data, and
4. inclusion of multispectral images (red, green, blue, infrared) from Vexcel Ultracam D sensor acquired on a separate flight.

2. Materials and methods

2.1. Study area

The study area is located in the municipality of Aurskog-Høland, southeastern Norway, 40 km east of Oslo (59°50′N, 11°40′E, 120-390 m a.s.l.) (Fig. 2). Aurskog-Høland is dominated by forests, agricultural areas and lakes. About tree quarter of the total land area, which is 890 km^2, is managed productive forest dominated by Scots pine (50%), Norway spruce (35%) and deciduous tree species (15%).

Fig. 2. Map of the study area, location of the sample plots, and ALS data cover. Inset map shows extent rectangle with black outline of the large map.

2.2. Field measurements

During the fall of 2007 and winter of 2008 field data was collected on 40 circular sample plots (Fig. 2). Half of the sample plots were located in spruce dominated stands and the other half in pine dominated stands. Furthermore, 30 of the plots were located in mature forest. The remaining 10 plots were located in young productive forest. The plots located in mature and young productive stands were equally distributed in spruce and pine dominated stands. The size of the plots was 1000 m^2. However, for four plots in young forest where the stem densities were very high and the field work exceeded one day per plot the plot size was reduced to 500 m^2.

On each sample plot, tree species, diameter at breast height (DBH) and the tree coordinates were recorded for all trees with DBH ≥ 5 cm. Totally 4299 trees were recorded on the 40 sample plots. The trees were distributed on 52% spruce, 34% pine and 14% deciduous trees. The position of the trees was determined by measuring the azimuth and distance from the plot center to the tree with a total station (Topcon Sokkia SET5F). Plot center coordinates were determined using differential Global Navigation Satellite Systems (GNSS) (Topcon Legacy E+). Random errors reported from the post-processing indicated an average error of 12 cm for the planimetric coordinates of the plot centers. The field data is further described by Breidenbach et al. (2010) and Maltamo et al. (2010).

2.3. Remote sensing data

ALS data were acquired on 12 June 2006 under leaf-on conditions using the Optech ALTM 3100 EA sensor. The ALS sensor was mounted on a Piper Navajo fixed-wing aircraft flown at approximately 800 m above ground with an average flying speed of 75 ms^{-1}. The sensor was operated with a pulse repetition frequency of 100 kHz and a scan rate of 70 Hz. The maximum scan angle was ± 5° and the beam divergence was 0.3 mrad. The sensor and acquisition settings resulted in an approximate pulse density of 7.2 m^{-2} and a footprint size of 25 cm. Five parallel flight lines spaced at approximate 8.7 km were flown across the municipality in east - west direction to cover the 40 field plots (Fig. 2).

The ALS data were delivered on the proprietary Optech comprehensive file format from the contractor (Blom Geomatics, Norway). The data contained all echoes recorded. The ALTM 3100 EA is capable of recording from one and up to four echoes for each emitted pulse. Ground echoes were identified with the proprietary algorithm of Terrascan (Terrasolid Ltd., 2004) following the principles of Axelsson (1999; 2000). From the echoes identified as ground a triangular irregular network (TIN) was created. The ground elevation underneath all echoes was computed from the TIN by linear interpolation. The relative height above ground (*dz*) was computed for every echo by subtracting the ground elevation from the recorded echo height. Additional parameters extracted from the comprehensive file format for every echo were the calibrated range from the sensor to the target and the intensity, which is a 12 bit integer indicating the amplitude of the returned signal. Furthermore, the scan direction flag as specified by the LAS file format (ASPRS, 2009) was created using the scan angle and time stamp registered for all pulses in the comprehensive file format.

The raw recorded intensities (I_{raw}) recorded by the ALTM sensor were range normalized. The range normalization was performed as:

$$I_{ran} = I_{raw} \times \left(\frac{R}{R_{ref}}\right)^{a} \quad (1)$$

where I_{ran} is the range normalized intensities, R is the range from sensor to target, and R_{ref} is the reference range. The value for parameter a was set to 2 (Ahokas et al., 2006; Korpela et al., 2010a). Furthermore, I_{raw} and I_{ran} were normalized for the sensor specific banding effect and named $I_{raw.ban}$ and $I_{ran.ban}$, respectively. Normalization was carried out using a standard histogram matching technique (Ricards & Jia, 2006). The intensities in the negative scan

direction were altered to match the histogram of intensities in the positive scan direction such that the banding effect was normalized (Fig. 3).

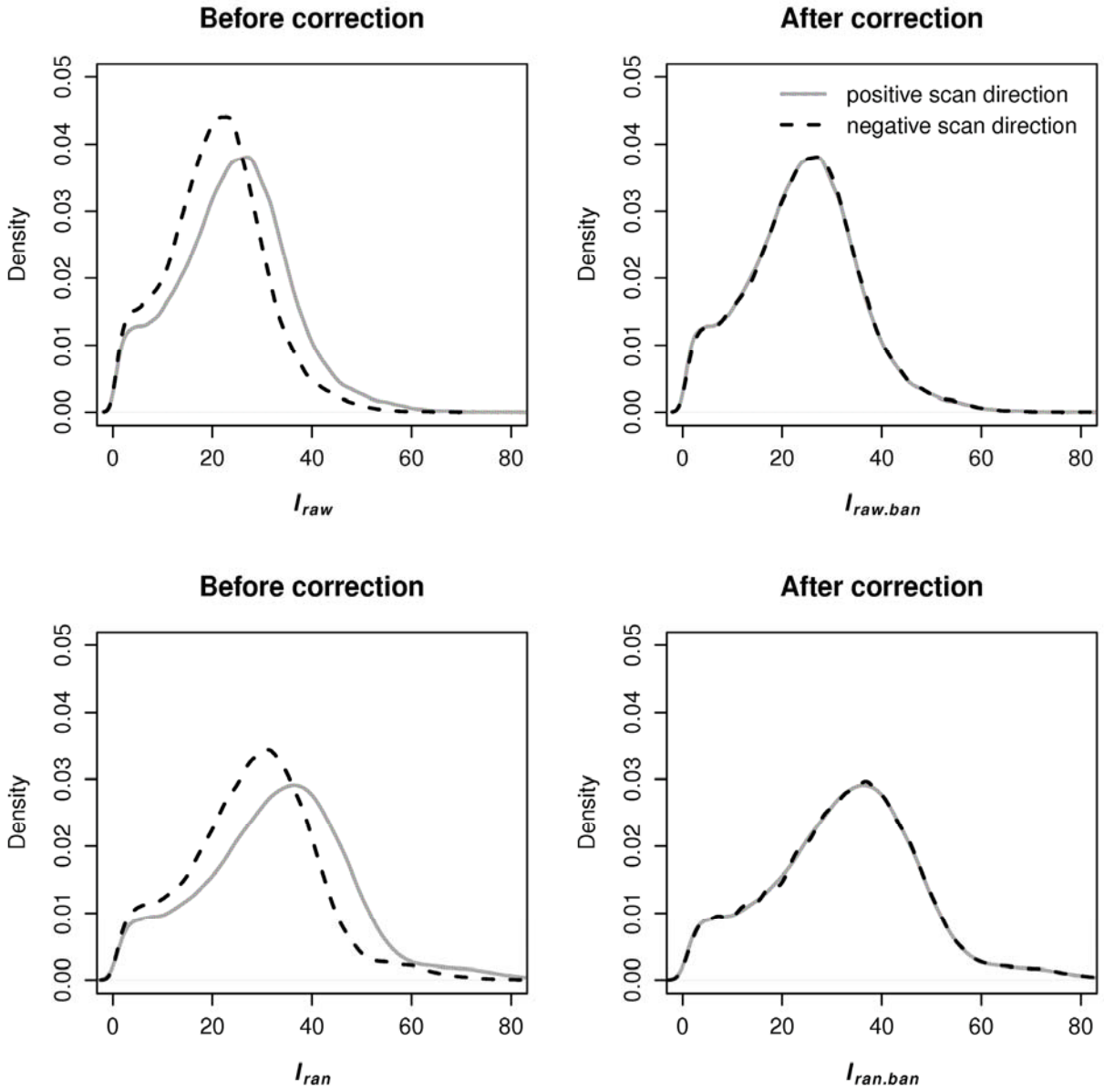

Fig. 3. Estimated probability density functions (*pdf*) for intensity values of negative and positive scan directions before and after normalization of the banding effect. The individual graphical plots show *pdf*s for raw intensities (I_{raw}), range normalized intensities (I_{ran}), and for I_{raw} and I_{ran} normalized for the banding effect ($I_{raw.ban}$, $I_{ran.ban}$).

A digital camera, Applanix Digital Sensor System 322 (referred to as Applanix), was carried on the same plane as the ALS sensor and Applanix images were acquired simultaneously with ALS data. The Applanix sensor is a medium-format digital frame camera with only one charge-coupled device. The sensor can be fully integrated with various ALS systems. The camera provides 22.2 megapixel (5436×4092) images in either color (VIS)

or color infrared (CIR). The physical pixel size was 9 μm. In the current study the camera was operated with a 60 mm lens and in CIR mode. Thus, the red, green and infrared bands with a ground sampling distance (GSD) of 12.0 cm were acquired. The overlap between the images in the along track direction was approximately 50%. Raw images together with orientation parameters were provided by the contractor.

A separate acquisition of aerial images was conducted on 28 and 29 June 2005 with a Vexcel UltraCam D (referred to as Vexcel). The Vexcel sensor is a large format digital aerial camera capable of acquiring both panchromatic and four multispectral bands (red, green, blue, and infrared). The camera provides 86.3 megapixel (7500×11500) images with a pixel size of 9 μm in the panchromatic band, while the multispectral sensor has a resolution of 8.8 megapixels (2400×3680) with a pixel size of 28.125 μm. The Vexcel images were acquired at a flight altitude of approximately 3100 m above ground with an average flying speed of 80 ms^{-1}. The focal length of both panchromatic and multispectral lenses was 101.4 mm. The GSD achieved was therefore 27.5 cm and 84.0 cm in panchromatic and multispectral bands, respectively. The delivery from the contractor included raw pansharpened images with a resolution of 7500×11500 and orientation parameters.

Pixel values from the Applanix and the Vexcel digital images were linked separately to the ALS data following the method described by Packalen et al. (2009). By using a rotation matrix, the x, y, and z coordinates of each laser echo were converted to a pixel position in the aerial images. Furthermore, the digital numbers from all multispectral bands were added to the respective laser echo in the original scale. If the laser echo position occurred on multiple images, the mean image value of all overlapping images was computed for all bands before adding the values to the respective laser echo. The average number of images per laser echo were 1.96 (SD=0.27) and 3.64 (SD=1.56) for the Applanix and Vexcel camera, respectively. The ability to locate the laser echoes in the image pixels was made possible through the GNSS and inertial navigation systems providing interior and exterior orientation parameters. Pixel values were only assigned to those laser echoes which best represent the canopy surface, i.e., first returns (first of many and single echoes). All other subsequent echoes will penetrate into the canopy and image values were not assigned to these echoes.

2.4. Individual tree crown delineation

Individual tree crown delineation was performed using an adaptive segmentation method based on a Poisson forest stand model (Ene et al., in review). The algorithm utilizes the average stem density per plot for optimizing the canopy height model smoothing. The stem

density was obtained using the area-based approach (Næsset, 2004) and trees were assumed to be randomly located within plots. Furthermore, the tree crowns were extracted using a marker-based watershed algorithm. The algorithm identified 1957 crown segments containing at least one field measured tree. In the current study 50.3% of the segments contained only one tree, 24.1% two trees, and 25.6% contained three or more trees. Of the 4299 field measured trees 4050 were covered by one of the tree crown segments identified by the algorithm. For further details about the individual tree crown delineation the reader is referred to Ene et al. (in review).

2.5. Feature computation

In classification terminology a feature is defined as a measurement on an object, so an object may have several features measured, but only one class assigned to it (Ripley, 1996). In the current study structural and intensity features were derived from the ALS data. In addition image features were derived from Vexcel data and Applanix imagery data. The structural, intensity, and image features utilized for tree species identification in the current study appear in Table 2. Features were computed for all first returns (first of many and single echoes) higher than 1.3 m above the ground surface.

Structural features were derived from the distribution of ALS echo heights (*dz*). The structural features derived were grouped into four feature groups (FGs) (Table 2). The four FGs were "relative height" (H_{rel}) (c.f. Ørka et al., 2009a), "canopy penetration depth" (H_{cpd}) (c.f. Ørka et al., 2009a), canopy density (*DF*) (c.f. Næsset, 2004), and echo proportions (*EP*) (c.f. Holmgren et al., 2008; Moffiet et al., 2005). H_{rel} and H_{cpd} consist of mean, kurtosis, skewness, coefficient of variation, and percentiles (10^{th}, 30^{th}, 50^{th}, 70^{th} and 90^{th}) derived from the echo height distribution and normalized with the 95^{th} percentile of the distribution according to Ørka et al. (2009a). Canopy density was computed by dividing the 95^{th} height percentile minus 1.3 m into 10 vertical layers of equal height. For each layer, tree level canopy densities were calculated as the number of echoes above layer number 1, 3, 5, 7, and 9 as proportions of total number of echoes, respectively. *EP* was defined as the proportion of echoes in the four different echo categories; single, first of many, intermediate, and last of many to the number of first returns (first of many and single echoes). The four FGs (H_{rel}, H_{cpd}, *DF*, and *EP*) were tested separately and in different combinations. The combination of structural FGs which achieved the highest tree species classification accuracy was used as the ALS benchmark. Furthermore, effects of including intensity and image derived features were compared to the ALS benchmark.

Four intensity FGs were created. The FGs were created from the different intensity distributions; I_{raw}, I_{ran}, $I_{raw.ban}$, and $I_{ran.ban}$. From the intensity distributions the maximum, mean, kurtosis, skewness, coefficient of variation, and percentiles (10^{th}, 30^{th}, 50^{th}, 70^{th} and 90^{th}) were derived for each segment. Furthermore, "canopy layer means" were computed as the mean intensity value of echoes in each canopy layer (Table 2). Canopy layers were defined as described for canopy density. The classification accuracy obtained with the intensity FGs were compared separately and combined with the ALS benchmark.

From the three Applanix bands and the four Vexcel bands maximum, mean, kurtosis, skewness, coefficient of variation, and percentiles (10^{th}, 30^{th}, 50^{th}, 70^{th} and 90^{th}) were derived for each segment together with "canopy layer means" from the original values, relative band values (Breidenbach et al., 2010), and band ratios (Packalén et al., 2009). The image features were combined into one Applanix FG named *DSS* and a Vexcel FG, named *VEX.* The two image FGs were combined with the ALS benchmark to test improvement in tree species classification accuracy.

Table 2. Structural, intensity, and image features computed to support tree species classification. Structural features are derived from the ALS height distribution. Intensity features are computed from the ALS raw and normalized intensity distributions. Image features are computed from each band in the imaging sensors used and for raw values, relative values, and band ratios. The features are organized into feature groups H_{rel}, H_{cpd}, I_{raw}, I_{ran}, $I_{raw.ban}$, $I_{ran.ban}$, *DSS, and VEX*

	Structural (*dz*)				**Intensity (*i*)**				**Image (*bands*)**	
Features	H_{rel}[a]	H_{cpd}[b]	***EP***	***DF***	I_{raw}	I_{ran}	$I_{raw.ban}$	$I_{ran.ban}$	***DSS***	***VEX***
Maximum value					X	X	X	X	X	X
Mean value	**X**	**X**			X	X	X	X	X	X
10^{th} percentile	**X**	**X**			X	X	X	X	X	X
30^{th} percentile	**X**	**X**			X	X	X	X	X	X
50^{th} percentile	**X**	**X**			X	X	X	X	X	X
70^{th} percentile	**X**	**X**			X	X	X	X	X	X
90^{th} percentile	**X**	**X**			X	X	X	X	X	X
Coefficient of variation	X	X			X	X	X	X	X	X
Skewness	X	X			X	X	X	X	X	X
Kurtosis	X	X			X	X	X	X	X	X
Prop. of first echoes			X							
Prop. of single echoes			X							
Prop. of last echoes			X							
Prop. of intermediate echoes			X							
Canopy density Layer 1				X						
Canopy density Layer 3				X						
Canopy density Layer 5				X						
Canopy density Layer 7				X						
Canopy density Layer 9				X						
Canopy layer mean 1					X	X	X	X	X	X
Canopy layer mean 3					X	X	X	X	X	X
Canopy layer mean 5					X	X	X	X	X	X
Canopy layer mean 7					X	X	X	X	X	X
Canopy layer mean 9					X	X	X	X	X	X

[a] Features represented with bold **X** are scaled relative to the maximum laser height H_{rel} (c.f. Ørka et al., 2009a).
[b] Features represented with bold **X** are scaled to canopy penetration depth (H_{cpd}) by subtracting the feature value from the maximum laser height (c.f. Ørka et al., 2009a).

2.6. Classification and accuracy assessment

From the 1957 available crown segments we only used a subset of 1520 where all field measured trees inside the crown segment belong to the same species. The subset of 1520 trees consisted of 783, 622, and 115 spruce, pine and deciduous trees, respectively.

Previous studies of tree species identification utilized different classification methods (Table 1). There have been some attempts to test different classification methods (Heinzel et al., 2010; Korpela et al., 2010b; Ørka et al., 2009b). In the current study we utilized linear discriminant analysis (LDA), random forest (RF) classification, and support vector machines (SVM). LDA is the most frequently used method in individual tree classification studies (Table 1). We used the LDA implementation in the R-package MASS for the classification (Venables & Ripley, 2002). RF is an extension of classification and regression trees (Breiman, 2001). RF has shown good results in comparative classification studies on individual trees (Korpela et al., 2010b; Ørka et al., 2009b). RF classification was conducted using the R-package randomForest (Liaw & Wiener, 2002). SVM has not been extensively used in individual tree species classification. However, the benchmark which RF is compared against, is often SVM (Liaw & Wiener, 2002; Pal, 2005). SVM classification was conducted using the e1071 package in R (Dimitriadou et al., 2008) using a radial kernel function.

The distribution of tree species in the study area was unbalanced. The deciduous class appeared less frequently than the conifer classes since sample plots were located in either spruce or pine dominated stands. We applied a strategy to equally well estimate the accuracy of the minority class as the two majority classes. We used equal prior probabilities in LDA, a balanced RF procedure (Chen et al., 2004), and weights in SVM. Using this strategy the producer's accuracies obtained would be more uniform and we avoided high omission errors of the minority class.

The number of features derived was high (Table 2). Feature selection was therefore applied to reduce the number of features used in the classification. In previous tree species identification studies feature selection based on the analysis of group differences, like *t*-tests (Holmgren & Persson, 2004), analysis of variance (ANOVA) (Brandtberg et al., 2003), and analysis of covariance (ANCOVA) (Ørka et al., 2009a) have been popular. We used a similar approach utilizing analysis of variance (ANOVA) and correlation analysis. First, *F*-values for the differences of features between species were computed. Features which not differed significantly at the 0.05 level were omitted. Then, the remained features were ordered from high *F*-values to low *F*-values and the feature providing the highest *F*-value was included in

the set of selected features. Furthermore, subsequent features were added to the set if they did not correlate ($r < 0.50$) with features already included.

In many studies leave-one-tree-out cross validation has been used for assessing the performance of classification algorithms (Korpela et al., 2010b; Suratno et al., 2009). Thus, spatially adjacent trees could be calibration and validation trees. To get reliable accuracy estimates, leave-one-sample-plot-out cross validation was used in the current study. According to Hastie et al. (2009) cross validation should include the feature selection step. The leave-one-sample-plot-out cross validation carried out in the current study ensured that both feature selection and accuracy assessment were spatially independent of the validation trees. The accuracy indices used were the proportion of correctly classified trees for single species (producer's accuracy), the total (overall accuracy) and the kappa coefficient (κ) (Cohen, 1960; Story & Congalton, 1986).

3. Results

3.1. Benchmark classification using structural features

The accuracies of the structural FGs and combination of these appear in Table 3. The FGs H_{rel} and H_{cpd} contained little information about tree species in the current study. The maximum kappa value obtained for H_{rel} and H_{cpd} was 0.27. A somewhat higher accuracy was achieved when utilizing canopy density features (*DF*) (κ = 0.30 - 0.34). However, echo proportions (*EP*) were the structural FG that achieved the highest accuracy (κ = 0.52 - 0.57). Combing the *DF* and *EP* further improved the accuracy (κ = 0.57 - 0.60). Adding additional structural FGs generally did not improve the classification. Hence, *EP* and *DF* were selected for the ALS benchmark. The overall accuracy obtained utilizing the ALS benchmark was 74 - 77%. The producer's accuracies obtained were 80 - 86%, 72 - 76%, and 31 - 36% for spruce, pine, and deciduous trees, respectively. The features selected in all 40 cross validation iterations were the *DF* from the highest and lowest layers, together with the proportions of last and proportion of intermediate echoes. The proportions of first and single echoes were selected in about half of the cross validation iterations and the middle *DF* was selected in one of the iterations.

3.2. Effects of intensity normalization

The accuracies of individual intensity FGs and combination of the best intensity FG with the ALS benchmark appear in Table 4. The accuracy obtained using only raw intensity was on the same level as using canopy density (κ = 0.32 - 0.34). Range normalization of the intensity (Eq. 1) resulted in an increase in the kappa value with 0.09 - 0.17. The correction of sensor

specific banding effect did not improve the classification for raw intensities and provided only a marginal increase of the kappa values for range normalized intensities using LDA and SVM. Combining the ALS benchmark and normalized (range and banding) intensity FG further improved the classification, by increasing the kappa value with 0.08 – 0.11 comparing to using only raw intensity. Compared to ALS benchmark, the increase in accuracy of the combination of the ALS benchmark and normalized intensity was minor. Including intensity resulted in improving the kappa coefficient with 0.01 when the SVM classifier was used, and lower accuracies were obtained using the two other classifiers when structural and intensity information were combined. The intensity features selected using $I_{ran.ban}$ FG were kurtosis, 90th percentile, and the coefficient of variation in all the 40 iterations of the cross validation.

Table 3. The producer's accuracy for the different species groups (Spruce, Pine and Deciduous), overall accuracies (Overall), and the kappa coefficient (κ) of different structural feature groups and combinations of these. Accuracies are presented for the different classification methods used: Linear discriminant analysis (LDA), random forest (RF), and support vector machines (SVM).

Feature groups[a]	**Spruce**	**Pine**	**Deciduous**	**Overall**	**κ**
			LDA		
H_{rel}	55.6	46.6	63.5	52.5	0.27
H_{cpd}	57.6	26.4	60.9	45.1	0.15
DF	67.4	55.3	41.7	60.5	0.34
EP	86.3	67.7	14.8	73.3	0.54
EP+DF	85.8	72.3	35.7	76.5	0.60
EP+DF+H_{rel}	86.7	66.1	35.7	74.4	0.57
EP+DF+H_{cpd}	85.2	73.5	38.3	76.8	0.61
EP+DF+Hrel+H_{cpd}	54.9	45.5	57.4	51.2	0.24
			RF		
H_{rel}	56.2	51.9	43.5	53.5	0.25
H_{cpd}	50.1	48.6	37.4	48.5	0.17
DF	61.2	57.1	30.4	57.2	0.30
EP	82.2	65.1	27.8	71.1	0.52
EP+DF	82.0	76.2	31.3	75.8	0.59
EP+DF+H_{rel}	84.8	76.7	29.6	77.3	0.61
EP+DF+H_{cpd}	84.3	73.8	31.3	76.0	0.59
EP+DF+Hrel+H_{cpd}	54.9	52.1	40.0	52.6	0.24
			SVM		
H_{rel}	51.6	48.7	63.5	51.3	0.25
H_{cpd}	45.6	47.6	56.5	47.2	0.20
DF	63.2	60.8	37.4	60.3	0.34
EP	82.1	74.4	27.0	74.8	0.57
EP+DF	80.2	73.5	33.9	73.9	0.57
EP+DF+H_{rel}	79.2	74.6	32.2	73.8	0.56
EP+DF+H_{cpd}	81.1	71.7	32.2	73.6	0.56
EP+DF+Hrel+H_{cpd}	51.0	46.8	58.3	49.8	0.23

[a]Feature groups used, see section 2.5. for detailed description. H_{rel} is relative height, H_{cpd} is canopy penetration depth, *DF* is canopy density, and *EP* is echo proportions.

Table 4. The producer's accuracy for the different species groups (Spruce, Pine and Deciduous), overall accuracies (Overall), the kappa coefficient (κ) of individual intensity feature groups, and combination of the best with the ALS benchmark. Accuracies are presented for the different classification methods used: Linear discriminant analysis (LDA), random forest (RF), and support vector machines (SVM).

Feature groups[a]	Spruce	Pine	Deciduous	Overall	κ
			LDA		
I_{raw}	50.6	74.6	13.0	57.6	0.32
I_{ran}	62.8	72.3	13.0	63.0	0.41
$I_{raw.ban}$	49.7	74.3	10.4	56.8	0.31
$I_{ran.ban}$	60.3	75.7	14.8	63.2	0.42
$EP+DF+I_{ran.ban}$	77.8	72.7	29.6	72.0	0.53
			RF		
I_{raw}	58.0	68.3	14.8	58.9	0.31
I_{ran}	72.5	77.7	19.1	70.6	0.50
$I_{raw.ban}$	56.4	65.9	17.4	57.4	0.29
$I_{ran.ban}$	72.5	76.5	20.9	70.3	0.49
$EP+DF+I_{ran.ban}$	78.5	80.7	18.3	74.9	0.57
			SVM		
I_{raw}	57.0	71.7	20.0	0.60	0.34
I_{ran}	73.2	74.1	23.5	0.70	0.48
$I_{raw.ban}$	54.8	70.7	18.3	0.59	0.31
$I_{ran.ban}$	74.3	75.2	22.6	0.71	0.49
$EP+DF+I_{ran.ban}$	78.8	81.5	24.3	0.76	0.58

[a]Feature groups used, see section 2.5. for detailed description. I_{raw} is features derived from the raw intensity, I_{ran} is features derived from the range normalized intensities $I_{raw.ban}$ and $I_{ran.ban}$ are the I_{raw} and I_{ran} normalized for the banding effect, *DF* is canopy density, and *EP* is echo proportions.

3.3. Effects of multispectral images

The accuracies obtained using only the image FGs and combination of these with ALS are presented in Table 5. Slightly higher accuracies were obtained using the Applanix data (κ = 0.55 - 0.64) compared to Vexcel data (κ = 0.52 - 0.57). However, the results were similar to the ALS benchmark. Combining image data with the ALS benchmark increased the classification accuracies and kappa values of 0.78 - 0.80 and 0.72 - 0.77 were obtained using the Applanix and Vexcel cameras, respectively. Utilizing normalized intensity in addition did not improve the classification any further. The highest accuracy was obtained using the echo proportions (*EP*), canopy density (*DF*), and Applanix data (*DSS*). The overall accuracies obtained for the classification were 87 - 89% and the producer's accuracies were 87 - 90%, 89 - 92%, and 59 - 79% for spruce, pine, and deciduous trees, respectively. Using the Vexcel camera (*VEX*) an overall accuracy of 84 - 87% was obtained. Producer's accuracies were 85 - 89% for spruce, 87 - 90% for pine, and 58 - 70% for deciduous when combining features from the ALS benchmark and Vexcel camera.

Table 5. The producer's accuracy for the different species (Spruce, Pine and Deciduous), overall accuracies (Overall), the kappa coefficient (κ) of individual image feature groups, and combined with the ALS benchmark and the best intensity feature groups. Accuracies are presented for the different classification methods used: Linear discriminant analysis (LDA), random forest (RF), and support vector machines (SVM).

Feature groups[a]	Spruce	Pine	Deciduous	Overall	κ
			LDA		
DSS	66.4	81.7	69.6	72.9	0.55
VEX	62.1	82.8	67.0	70.9	0.52
EP+DF+DSS	87.1	88.7	79.1	87.2	0.78
EP+DF+VEX	85.3	87.1	69.6	84.9	0.74
$EP+DF+I_{ran.ban}+DSS$	84.7	88.4	65.2	84.7	0.74
$EP+DF+I_{ran.ban}+VEX$	81.9	86.5	62.6	82.3	0.70
			RF		
DSS	73.7	82.8	64.3	76.7	0.60
VEX	76.0	80.7	46.1	75.7	0.57
EP+DF+DSS	87.6	90.0	69.6	87.2	0.78
EP+DF+VEX	86.2	87.1	55.7	84.3	0.72
$EP+DF+I_{ran.ban}+DSS$	86.2	90.2	63.5	86.1	0.76
$EP+DF+I_{ran.ban}+VEX$	83.3	88.1	47.0	82.5	0.69
			SVM		
DSS	75.9	86.5	61.7	79.1	0.64
VEX	69.3	84.1	55.7	74.3	0.56
EP+DF+DSS	90.0	92.1	59.1	88.6	0.80
EP+DF+VEX	88.9	89.9	58.3	87.0	0.77
$EP+DF+I_{ran.ban}+DSS$	90.0	92.3	54.8	88.3	0.79
$EP+DF+I_{ran.ban}+VEX$	87.4	88.7	56.5	85.6	0.75

[a]Feature groups used, see section 2.5. for detailed description. *DSS* is features derived from the Applanix sensor, *VEX* is features derived from the Vexcel Ultracam sensor, Iran.ban is the range and banding normalized intensity, *DF* is canopy density, and *EP* is echo proportions.

4. Discussion

4.1. Classification using structural features

Moderate classification accuracies were obtained utilizing structural information derived from ALS data. The intensity is still only an optional item in the LAS file format (ASPRS, 2009). Hence, it may not be available in operational surveys where data are delivered according to the LAS file format specification. However, applying only structural features, overall accuracies of 74 - 77% were obtained in the current study when classifying the three tree species groups commonly used in operational forest management inventories in Nordic countries (Table 3). In two other Nordic studies accuracies of 88 - 92% were obtained only using structural features (Holmgren & Persson, 2004; Vauhkonen et al., 2009). In these studies accuracies were 11 to 18 percentage points higher compared to the results obtained in the current study. The differences may be attributed to the more heterogeneous forest in the current study area or the different sensors used. Both the study by Holmgren and Persson (2004) and the study by Vauhkonen et al. (2009) used a Topeye ALS sensor. Vauhkonen et

al. (2009) used only dominant trees visible in the images where no branches overlapped with neighboring trees. The structure of the forest in the current study area is more diverse and represents practical challenges.

The normalized height features did not improve the species classification. Similar results are found in other studies in boreal forests (Korpela et al., 2010b; Ørka et al., 2009a; Ørka et al., 2010). However, in a Swedish study site the 90th percentile computed from all echoes within the crown produced the highest overall accuracy (Holmgren & Persson, 2004). Although the normalized height features carried some useful information in the current study and also in the study of Holmgren and Persson (2004), such features seem to be of minimal practical use in applications covering large areas. Moffiet et al. (2005) found a density related feature to be useful in tree species identification. Based on the study by Moffiet et al. (2005), some other studies on species identification (Ørka et al., 2009a; Ørka et al., 2010), and the results obtained in the current study, it is indicated that density features better describe the structural differences between boreal tree species than the normalized height features.

Features derived from different echo categories may be important in species identification (Ørka et al., 2009a). However, the use of separate echo categories limits the number of trees where all features can be computed and consequently, the number of trees which can be classified (Ørka et al., 2010). In the current study the information suggested to be inherent in different echo categories was incorporated using echo proportions. The echo proportions contributed significantly to the higher accuracies using structural information, which coincides well with previous findings from boreal forests (Holmgren et al., 2008). In the current study the echo proportions of last and intermediate echoes were most important. Proportions of single and last echoes was important for separating spruce, pine and deciduous trees in the study by Holmgren et al. (2008). Ørka et al. (2009a) found that the density of last echoes was important for separating spruce and birch trees because of the higher proportions of last echoes in the lower crown of spruce trees. The importance of the echo proportions in the current study was probably also due to differences in crown allometry and crown permeability for the different tree species.

4.2. Improvement using normalized ALS intensity

The current study has two main findings regarding utilization of normalized intensity. First, intensity normalization improved accuracy of species classification when only intensity features were used. Normalization based on range from sensor to target was the most important in terms of improving the classification accuracy. However, also correction of the

banding effect improved the classification slightly. Korpela et al. (2010b) found improvements of 0.03 – 0.04 in the kappa coefficient and 2 - 3 % in overall classification accuracy when conducting range normalization of intensity collected by the Optech ALTM 3100 sensor. Hence, the effect of intensity normalization was greater in the current study compared to the study by Korpela et al. (2010b). Consequently, range normalization of intensity seems to be a useful preprocessing step when intensity features are used for tree species identification and probably in other applications where intensity is utilized.

The second major finding regarding intensity was the lack of improvement in accuracy when combining intensity features with other ALS and/or image features. In another study in a boreal forest only intensity features were selected and all structural features were omitted in the feature selection carried out before classification (Korpela et al., 2010b). Furthermore, Vauhkonen et al (2009) found that combination of intensity features and other ALS features increased the accuracy when classifying spruce, pine, and deciduous trees in Finland. From Queensland, Australia Moffiet et al. (2005) reported that the intensity was not useful for tree species identification. In some studies only intensity features were selected by the selection procedures while other studies did not benefit from intensity at all, like the current one. The reasons for the highly variable results obtained with ALS intensity are most likely related to sensor properties and acquisition parameters.

In the current study, the banding effect, which is a source of intensity variation that is sensor specific and not previously described in literature, was addressed. Knowledge of variations in intensity values is important to fully understand the processes behind the recorded intensity values. However, such information is not always available from the sensor vendors. It is likely that the banding effect will be different between different sensors and even may change over time for the same instrument due to sensor maintenance and upgrades (E. Næsset, pers. comm.). Settings specific to individual data acquisitions, such as pulse repetition frequency and flying altitude may also play a role. In some acquisitions the effect may therefore be minor while in other campaigns larger effects of banding may occur. The banding normalization used in the current study is adapted from image processing (histogram matching) and is well documented and known in the remote sensing community, but is probably not optimal. Furthermore, the normalization of the banding effect was less pronounced in the current study probably due to averaging of intensity values from different scan directions inside tree crowns when computing features. The banding effect would likely be more pronounced if a raster representation of intensity with a pixel size less than the point spacing or separate echoes was utilized. Hence, further research should be carried out to

quantify effects - and to improve calibration of the banding effect. Normalization using brightness targets might provide knowledge to support better calibration of the banding effect and other intensity effects not yet documented in the literature.

Moffiet et al. (2005) reported systematic variations in the intensity values in the flight direction. They suggested that sensor and acquisition settings, like different flying altitudes and variation in the transmitted power were major factors causing variation. Furthermore, large differences in accuracy were obtained with Optech and Leica sensors in a Finnish study were sample trees and methods otherwise were equal (Korpela et al., 2010b). The observations by Moffiet et al. (2005) and Korpela et al. (2010b) together with the description of sensor specific effects in the current study and in other studies (Korpela, 2008) strongly indicate that sensor and acquisition settings are important for the utility of intensity information. Practical applications require robust and accurate classification methods which not seem to be the case in current tree species identification procedures based on intensity information. Supplementary sensor information or improving the sensors capabilities to record intensity or related information (e.g. transmitted power per pulse) may be a key for better utilization of the intensity information recorded in addition to the ALS echo coordinates.

4.3. Improvement using multispectral images

The accuracy obtained with only structural features derived from ALS might not be sufficient for many applications and improvements can be obtained by applying spectral information. The obtained classification accuracies using the Vexcel images were only slightly lower than applying the ALS structural information alone (benchmark). Using only the Applanix images the accuracy was slightly better than the ALS benchmark. Thus, ALS data and multispectral imagery equally well separate tree species in the current study. Consequently, ALS data will be the first choice in forest inventory because of the better accuracy for e.g. timber volume and tree height (e.g. Hyyppä & Hyyppä, 1999) without any reduction of species identification accuracy compared to multispectral imagery.

Inclusion of multispectral image features in addition to ALS data improved the tree species classification accuracies. Combining ALS and Applanix data acquired simultaneously during the same flight mission provided the highest accuracies. The Vexcel data were acquired the year before the field inventory, furthermore the data have a higher GSD and the data were pansharpened before delivery. The pansharpening process altered the image values and might be one of the reasons for the lower accuracy of the classification based on Vexcel

imagery. The high GSD in multispectral bands of the Vexcel sensor compared to the Applanix sensor, i.e., 84 vs. 12 cm, was likely another reason for the lower accuracies obtained using the Vexcel sensor. A higher GSD of the Vexcel imagery results in averaging of image values over a larger area making the variation between trees less apparent. However, high flying altitudes are necessary to keep data acquisition costs low, which requires higher GSDs as one of the consequences. Simultaneous acquisitions of ALS and image data will add restrictions on the acquisition parameters and the costs will increase compared to acquiring ALS data only. For instance, an acquisition of imagery will require specific weather conditions and sun angles and thus the possible acquisition time will be narrowed compare to only flying with an ALS sensor which even might be flown at night time.

Combining aerial spectral information and ALS data has improved tree species classification in other studies (Hill & Thomson, 2005; Holmgren et al., 2008; Jones et al., 2010). The current study together with the study of Holmgren et al. (2008) are the only two studies combing ALS and multispectral images to identify species of individual trees and report combined and separate accuracies for the two remote sensing sources. Holmgren et al. (2008) reported increase in accuracies of 0.11 in the kappa values and 8 percentage points in overall accuracy. The improvements in overall accuracy are similar to the current study. However, the improvement in kappa was higher in the current study, mainly because of the better identification of deciduous trees when utilizing the spectral information in addition to ALS information.

4.4. Other aspects of the study

The major problem in the current study was to distinguish the deciduous trees from conifer trees. A similar challenge was also reported from a boreal forest site in Finland (Korpela et al., 2010b). In the current study, all FGs, and in particular the intensity features, resulted in low accuracies for deciduous trees. However, spruce and birch trees have been separated quite successfully in previous studies using intensity features (Ørka et al., 2009a). Both in the current study and in the study by Ørka et al. (2009a) the deciduous trees appear in conifer dominated stands. The sample plots in the current study are more spatially distributed and the sample of deciduous trees is smaller. Although we tried to account for the smaller sample of deciduous trees in the classification the unbalanced species distribution was likely the cause for the low accuracies of the minority class. However, separating the dominating species (spruce and pine) was successfully conducted and producer accuracies near 90% were

obtained. The producer's accuracies of deciduous were higher and better balanced for LDA than for the two other classification methods tested.

Different classification methods were used in the current study. The conclusions for all methods were similar. The highest classification accuracy was obtained with SVM. Both SVM and RF perform better than LDA in most cases. However, LDA was better for the different ALS structural FGs (Table 3). Furthermore, SVM and RF are attractive because they have the possibility to perform accurately without feature selection (Ørka et al., 2009b).

5. Conclusions

The current study presents promising result for combining ALS and multispectral images for individual tree species identification. In addition, normalization of ALS intensity improved the classification accuracy, and we suggest that the normalization of intensity should be carried out when utilizing such information. However, intensity did not improve the accuracy beyond the levels obtained using only ALS structural information or ALS combined with aerial images.

Acknowledgement

This research is part of the Flexwood ("Flexible Wood Supply Chain") project founded by the 7th framework programme of the European Commission, THEME 2 Food, Agriculture and Fisheries, and Biotechnology (Grant agreement no.: 245136). Additional financial support is provided by the Norwegian University of Life Sciences. We wish to thank Blom Geomatics, Norway for providing and processing the remote sensing data.

References

Ahokas, E., Kaasalainen, S., Hyyppä, J., & Suomalainen, J. (2006). Calibration of the Optech ALTM 3100 laser scanner intensity data using brightness targets. *International Archives of Photogrammetry, Remote Sensing and Spatial Information Sciences, XXXVI, Part 1/A*

ASPRS (2009). Las Specification: Version 1.3 – R10. *Photogrammetric Engineering and Remote Sensing, 75*, 1035-1042.

Axelsson, P. (1999). Processing of laser scanner data - algorithms and applications. *ISPRS Journal of Photogrammetry and Remote Sensing, 54*, 138-147.

Axelsson, P. (2000). DEM generation from laser scanner data using adaptive TIN models. *International Archives of Photogrammetry and Remote Sensing, 33*, 111-118.

Brandtberg, T., Warner, T.A., Landenberger, R.E., & McGraw, J.B. (2003). Detection and analysis of individual leaf-off tree crowns in small footprint, high sampling density LIDAR data from the eastern deciduous forest in North America. *Remote Sensing of Environment, 85*, 290-303.

Brandtberg, T. (2007). Classifying individual tree species under leaf-off and leaf-on conditions using airborne LIDAR. *ISPRS Journal of Photogrammetry and Remote Sensing, 61*, 325-340.

Breidenbach, J., Næsset, E., Lien, V., Gobakken, T., & Solberg, S. (2010). Prediction of species specific forest inventory attributes using a nonparametric semi-individual tree crown approach based on fused airborne laser scanning and multispectral data. *Remote Sensing of Environment, 114*, 911-924.

Breiman, L. (2001). Random forests. *Machine Learning, 45*, 5-32.

Chen, C., Liaw, A., & Breiman, L. (2004). Using random forest to learn imbalanced data. In, *Tech. Rep*: Dept. Statistics, Univ. California Berkeley.

Cohen, J. (1960). A coefficient of agreement for nominal scales. *Educational and Psychological Measurement, 20*, 37-46.

Dimitriadou, E., Hornik, K., Leisch, F., Meyer, D., & Weingessel, A. (2008). *e1071: Misc Functions of the Department of Statistics (e1071)*: TU Wien.

Ene, L., Næsset, E., & Gobakken, T. (in review). Single tree detection in heterogeneous boreal forests using airborne laser scanning and area based stem number estimates

Gatziolis, D. (2009). LiDAR intensity normalization in rugged forested terrain. In S.C. Popescu, R. Nelson, K. Zhao & A. Neuenschwander (Eds.), *Proceedings of Silvilaser 2009 - The 9th international conference on lidar applications for assessing forest ecosystems*. Texas A&M University, College Station, Texas, USA

Hastie, T., Tibshirani, R., & Friedman, J. (2009). *The elements of statistical learning: data mining, inference, and prediction (Second Edition)*. New York: Springer.

Heinzel, J., Weinacker, H., & Kock, B. (2008). Full automatic detection of tree species based on delineated single tree crowns - a data fusion approach for airborne laser scanning data and aerial photographs. *Silvilaser 2008, Edinburgh, UK*

Heinzel, J., Ronneberger, O., & Koch, B. (2010). A comparison of support vector and linear classification of tree species. In, *Proceedings of SilviLaser 2010, 14.-17. September 2010*. Freiburg, Germany.

Heinzel, J., & Koch, B. (2011). Exploring full-waveform LiDAR parameters for tree species classification. *International Journal of Applied Earth Observation and Geoinformation, 13*, 152-160.

Heurich, M. (2006). Evaluierung und entwicklung von automatiserten erfassung von waldstructuren aus daten flugzuggetragener fernerkundungssenoren. *Forstkuche Forshungsberichte München, 2002*, p329.

Hill, R.A., & Thomson, A.G. (2005). Mapping woodland species composition and structure using airborne spectral and LiDAR data. *International Journal of Remote Sensing, 26*, 3763-3779.

Holmgren, J., & Persson, Å. (2004). Identifying species of individual trees using airborne laser scanner. *Remote Sensing of Environment, 90*, 415-423.

Holmgren, J., Persson, Å., & Söderman, U. (2008). Species identification of individual trees by combining high resolution LIDAR data with multi-spectral images. *International Journal of Remote Sensing, 29*, 1537-1552.

Hyde, P., Dubayah, R., Walker, W., Blair, J.B., Hofton, M., & Hunsaker, C. (2006). Mapping forest structure for wildlife habitat analysis using multi-sensor (LiDAR, SAR/InSAR, ETM plus , Quickbird) synergy. *Remote Sensing of Environment, 102*, 63-73.

Hyyppä, H., & Hyyppä, J. (1999). Comparing the accuracy of laser scanner with other optical remote sensing data sources for stand attributes retrieval. *The Photogrammetric Journal of Finland, 16*, 5 -15.

Hyyppä, J., Hyyppä, H., Leckie, D., Gougeon, F., Yu, X., & Maltamo, M. (2008). Review of methods of small-footprint airborne laser scanning for extracting forest inventory data in boreal forests. *International Journal of Remote Sensing, 29*, 1339-1366.

Jones, T.G., Coops, N.C., & Sharma, T. (2010). Assessing the utility of airborne hyperspectral and LiDAR data for species distribution mapping in the coastal Pacific Northwest, Canada. *Remote Sensing of Environment, 114*, 2841-2852.

Ke, Y.H., Quackenbush, L.J., & Im, J. (2010). Synergistic use of QuickBird multispectral imagery and LIDAR data for object-based forest species classification. *Remote Sensing of Environment, 114*, 1141-1154.

Kim, S., McGaughey, R.J., Andersen, H.E., & Schreuder, G. (2009). Tree species differentiation using intensity data derived from leaf-on and leaf-off airborne laser scanner data. *Remote Sensing of Environment, 113*, 1575-1586.

Korpela, I., Ørka, H.O., Hyyppä, J., Heikkinen, V., & Tokola, T. (2010a). Range and AGC normalization in airborne discrete-return LiDAR intensity data for forest canopies. *ISPRS Journal of Photogrammetry and Remote Sensing, 65*, 369-379.

Korpela, I., Ørka, H.O., Maltamo, M., Tokola, T., & Hyyppä, J. (2010b). Tree species classification using airborne LiDAR - Effects of stand and tree parameters, downsizing of training set, intensity normalization, and sensor type. *Silva Fennica, 44*, 319-339.

Korpela, I.S., & Tokola, T.E. (2006). Potential of aerial image-based monoscopic and multiview single-tree forest Inventory: A simulation approach. *Forest Science, 52*, 136-147.

Korpela, I.S. (2008). Mapping of understory lichens with airborne discrete-return LiDAR data. *Remote Sensing of Environment, 112*, 3891-3897.

Liaw, A., & Wiener, M. (2002). Classification and regression by randomForest. *R News, 2*, 18-22.

Maltamo, M., Bollandsås, O.M., Vauhkonen, J., Breidenbach, J., Gobakken, T., & Næsset, E. (2010). Comparing different methods for prediction of mean crown height in Norway spruce stands using airborne laser scanner data. *Forestry, 83*, 257-268.

Moffiet, T., Mengersen, K., Witte, C., King, R., & Denham, R. (2005). Airborne laser scanning: Exploratory data analysis indicates potential variables for classification of individual trees or forest stands according to species. *ISPRS Journal of Photogrammetry and Remote Sensing, 59*, 289-309.

Næsset, E. (2002). Predicting forest stand characteristics with airborne scanning laser using a practical two-stage procedure and field data. *Remote Sensing of Environment, 80*, 88-99.

Næsset, E. (2004). Practical large-scale forest stand inventory using a small-footprint airborne scanning laser. *Scandinavian Journal of Forest Research, 19*, 164-179.

Næsset, E. (2009). Effects of different sensors, flying altitudes, and pulse repetition frequencies on forest canopy metrics and biophysical stand properties derived from small-footprint airborne laser data. *Remote Sensing of Environment, 113*, 148-159.

Ørka, H.O., Næsset, E., & Bollandsås, O.M. (2009a). Classifying species of individual trees by intensity and structure features derived from airborne laser scanner data. *Remote Sensing of Environment, 113*, 1163-1174.

Ørka, H.O., Næsset, E., & Bollandsås, O.M. (2009b). Comparing classification strategies for ALS tree species recognition. In S.C. Popescu, R. Nelson, K. Zhao & A. Neuenschwander (Eds.), *Proceedings of Silvilaser 2009 - The 9th international conference on lidar applications for assessing forest ecosystems* (pp. 46 - 53). Texas A&M University, College Station, Texas, USA

Ørka, H.O., Næsset, E., & Bollandsås, O.M. (2010). Effects of different sensors and leaf-on and leaf-off canopy conditions on echo distributions and individual tree properties derived from airborne laser scanning. *Remote Sensing of Environment, 114*, 1445-1461.

Packalén, P., Suvanto, A., & Maltamo, M. (2009). A two stage method to estimate species-specific growing stock. *Photogrammetric Engineering and Remote Sensing, 75*, 1451-1460.

Pal, M. (2005). Random forest classifier for remote sensing classification. *International Journal of Remote Sensing, 26*, 217-222.

Persson, Å., Holmgren, J., & Söderman, U. (2002). Detecting and measuring individual trees using an airborne laser scanner. *Photogrammetric Engineering and Remote Sensing, 68*, 925-932.

Persson, Å., Holmgren, J., Söderman, U., & Olsson, H. (2004). Tree species classification of individual trees in Sweden by combining high resolution laser data with high resolution near-infrared digitalt images. *International Archives of Photogrammetry, Remote Sensing and Spatial Information Sciences, Vol. XXXVI, Part 8/W2*, 204-207.

Reitberger, J., Krzystek, P., & Stilla, U. (2008). Analysis of full waveform LIDAR data for the classification of deciduous and coniferous trees. *International Journal of Remote Sensing, 29*, 1407-1431.

Ricards, J.A., & Jia, X. (2006). *Remote sensing digital image analysis, An Introduction (Fourth edition)*. Berlin, Germany: Springer.

Ripley, B.D. (1996). *Pattern recognition and neural networks*. Cambridge: Cambridge University Press.

Solberg, S., Næsset, E., & Bollandsås, O.M. (2006). Single tree segmentation using airborne laser scanner data in a structurally heterogeneous spruce forest. *Photogrammetric Engineering and Remote Sensing, 72*, 1369-1378.

Story, M., & Congalton, R.G. (1986). Accuracy assessment - a users perspective. *Photogrammetric Engineering and Remote Sensing, 52*, 397-399.

Suratno, A., Seielstad, C., & Queen, L. (2009). Tree species identification in mixed coniferous forest using airborne laser scanning. *ISPRS Journal of Photogrammetry and Remote Sensing, 64*, 683-693.

Terrasolid Ltd. (2004). *TerraScan user's guide*. Helsinki: Terrasolid Ltd.

Vauhkonen, J., Tokola, T., Packalén, P., & Maltamo, M. (2009). Identification of Scandinavian Commercial Species of Individual Trees from Airborne Laser Scanning Data Using Alpha Shape Metrics. *Forest Science, 55*, 37-47.

Vauhkonen, J., Korpela, I., Maltamo, M., & Tokola, T. (2010). Imputation of single-tree attributes using airborne laser scanning-based height, intensity, and alpha shape metrics. *Remote Sensing of Environment, 114*, 1263-1276.

Venables, W.N., & Ripley, B.D. (2002). *Modern Applied Statistics with S*. New York: Springer.

Paper IV

Subalpine zone delineation using LiDAR and Landsat imagery

Authors:

Hans Ole Ørka[a,*], Michael A. Wulder[b], Terje Gobakken[a] & Erik Næsset[a]

Address:

[a] Norwegian University of Life Sciences, Department of Ecology and Natural Resource Management, P.O. Box 5003, NO-1432 Ås, Norway

[b] Canadian Forest Service (Pacific Forestry Centre), Natural Resources Canada, 506 West Burnside Road, Victoria, Canada BC V8Z 1M5

* Corresponding author:

Hans Ole Ørka

E-mail address: hans-ole.orka@umb.no

Phone: +47 64965799;

Fax: +47 64965802

Abstract

The subalpine zone or ecotone is the transition between the forest and alpine vegetation communities. Substantial changes in position and extent of the subalpine zone are expected as a result of a warmer climate. In Norway, as in many other nations, low productivity or non-merchantable forests, like the subalpine zone, are not routinely subject to inventory programs. The awareness of the expected changes and the interest in full carbon accounting at the national level has dictated a need for data capture in these mountainous areas. Specifically, quantifying the area covered by the subalpine zone, including a capacity to characterize changes in ecotone location over time, are required to obtain reliable inventory estimates of biomass and carbon stocks. The capacity to characterize the ecotone is also desired to enable monitoring of the changes in the zone boundaries over time providing information on change rates and change processes. We propose an approach for integrating strip samples of Light Detection and Ranging (LiDAR) data with Landsat imagery to delineate the subalpine zone. In the current study the subalpine zone was defined according to international definitions based on tree heights and canopy cover to provide the basis for reporting according to established international standards. The three-dimensional measurements of forest structure obtained from LiDAR enable a heuristic delineation of the subalpine zone. The method was implemented using 53 laser sample strips in Hedmark County, Norway, and validated with field measurements at 26 locations. The subalpine zone boundaries were found to be accurately derived when validating using an image gradient technique. Furthermore, binomial logistic regression and alpha-cuts were used to upscale the LiDAR classes to the entire county area (27 400 km^2) using satellite images supported with information derived from a digital terrain model. The products included a hard classification needed for inventory stratification and a probability surface suitable for monitoring changes in the extent and location of the subalpine zone.

Keywords: Subalpine zone; Forest-tundra ecotone; LiDAR; Airborne laser scanning; Satellite data; Landsat; Canopy coverage; Logistic regression; Regional forest inventory.

1. Introduction

Forest- and tree lines are expected to advance as a result of a warmer climate (Dalen & Hofgaard, 2005; Harsch et al., 2009), with changes in human use and activities in mountain areas also expected to affect the alpine forest- and tree lines. For instance, the presence of grazing animals been shown to force the tree line below its climatic constraints indicating that diminished grazing would result in advancing forest- and tree-lines (Cairns & Moen, 2004; Hofgaard, 1997). We are also mindful that the effect of land use change on forest- and tree lines may override the responses of climate change on the vegetation in the subalpine zone (Hofgaard, 1997).

The subalpine zone is defined as the transition between the forest and alpine vegetation communities (Kimmins, 1997). Transitions between two different vegetation communities are referred to as ecotones (Clements, 1905). The forest-tundra ecotone is also often understood as analogous to the subalpine zone, with various definitions and terms for this ecotone in usage (c.f. Callaghan et al., 2002; Löve, 1970). However, there is a common understanding that the subalpine zone is limited downwards by the forest line and upwards by the tree line (Kimmins, 1997). Forest- and tree lines are often defined according to tree height (h), tree density (N) and/or canopy coverage (C). The definitions applied in the current study were selected to provide results consistent with the needs in international reporting. The definitions of "forest" and "other wooded land" by the United Nations Food and Agricultural Organization (FAO) was applied for the forest line (C > 10 % of trees with h > 5 m) and the tree line (C > 10 % of trees and shrubs with h > 0.5 m or C > 5 % of trees with h > 5 m), respectively (FAO, 2006).

In a recent meta-analysis it was shown that half of the tree lines included in a global study had advanced during the last century, while only 1% of the studies indicated recession (Harsch et al., 2009). Although advance in tree lines is expected at many sites worldwide, tree line dynamics might follow different patterns at a regional level, e.g. along a mountain range (Dalen & Hofgaard, 2005). Different regional tree line dynamics are linked to differences in environmental and anthropogenic factors at specific locations, including historic land use, soil, temperature, and variability in precipitation – even over short distances. Small study sites provide important knowledge in the dynamics of the subalpine zone (e.g. Dalen & Hofgaard, 2005). However, a complete mapping of the subalpine zone is needed to fully understand these local and regional differences. Such maps can be combined with information on grazing pressure to analyze which of the confounding effects, reduced grazing or climate change, impact the subalpine most.

The expected changes in the subalpine zone have increased the demand for information and monitoring. Changes in the subalpine zone will have an influence on the forest as well as the related alpine areas, biodiversity, landscape characteristics, biomass, and carbon pools. Countries that have ratified the Kyoto protocol are also committed to report land use change attributable to deforestation, aforestation and reforestation (UNFCCC, 2008). Consequently, there is an urgent need for an updated complete national mapping of the subalpine zone and monitoring of the future development. Specially, the interest in full carbon accounting required inventories and monitoring of low biomass areas as the subalpine zone.

National inventories and monitoring systems have typically not included the subalpine zone, as the focus has traditionally been on productive forests with resource management aims. Furthermore, it is also expensive to establish and measure field plots in remote mountainous areas. The lack of information on the area and the extent of the subalpine zone results in an inability to monitor the any changes in this ecotone. National forest inventories are under pressure to develop protocols to incorporate the need for inventory and monitoring of the subalpine zone.

Remote sensing offers possibilities for mapping and monitoring of large areas. Especially, medium resolution optical satellite images (ground sample distance of 10 – 30 meters) have been important through the provision of data with sufficient spatial detail over large areas at low costs to meet a range of information needs (Cohen & Goward, 2004; Falkowski et al., 2009). The opening of the United States Geological Survey (USGS) Landsat archive to provide data for free (Woodcock et al., 2008) has further accentuated the utility of this data. Combining medium resolution satellite images and other spatial data (e.g. elevation, solar radiation, climate, soil) improve the accuracy of the remote sensing analysis (Franklin, 1995; Rogan & Miller, 2007). A drawback of medium resolution satellite images is that the spatial resolution (30 m) often results in a mixture of within pixel vegetation conditions, reducing the capacity to classify beyond broad vegetation types over heterogeneous areas (Wulder, 1998). High spatial resolution remote sensing techniques, including imagery from satellite and airborne platforms and Light Detection and Ranging (LiDAR), provide detailed information about forests and individual trees. However, high acquisition costs make such data unsuitable for large area wall-to-wall monitoring. To overcome this, high-resolution remote sensing techniques may be applied to sample remote areas with either images (Falkowski et al., 2009) or LiDAR (Næsset et al., 2009) rather than seeking a full areal coverage. Comparisons of high spatial resolution image and LiDAR remote sensing have

shown that LiDAR is among the most promising remote sensing techniques in terms of accuracy of height, volume, and biomass of forested areas (e.g. Hyde et al., 2006; Hyyppä & Hyyppä, 1999; Lefsky et al., 2001). By combining data from medium resolution satellite images and samples of high spatial resolution LiDAR data the strengths of both sources can be integrated. LiDAR data acquired in sampling mode provide detailed information on specific locations suitable for extrapolation or model calibration. Furthermore, satellite and other spatial data supported can be deployed to provide full coverage of the region of interest, to provide modeling and extrapolation options, and to support stratification.

The basis for the current study is a framework were a large area inventory is conducted using airborne scanning LiDAR operated in a strip sampling mode (Næsset et al., 2009). The main objective of the current research was to develop a method combining samples of LiDAR with full coverage optical satellite data to identify the subalpine zone over a large region. The result should increase the information about the area and location of the subalpine zone without increasing inventory cost. The specific objectives were to:

1) Identify the subalpine zone using a heuristic classification based on the direct measurements provided LiDAR.
2) Model and map the subalpine zone through integration of LiDAR, satellite and elevation data to represent the entire study area of interest.

2. Background

2.1. LiDAR remote sensing

LiDAR provides three dimensional point measurements (x,y,z – coordinates) of the landscape. In the subalpine zone, LiDAR has shown potential for detecting small trees (Næsset & Nelson, 2007; Næsset, 2009a) and the forest line has also been detected (Rees, 2007). Næsset & Nelson (2007) found that 91 % of trees taller than 1 m had positive height measurements by LiDAR, which could aid the detection of small trees in the subalpine zone. Rees (2007) identified the forest area by extracting LiDAR echoes representing 2 m tall trees with a spacing lower than 10 m between trees. Parameters used to define the forest- and tree lines like tree height, tree density, and canopy cover are accurately estimated from LiDAR data (See table 1). LiDAR is an attractive data source for identifying forest- and tree lines as direct measures, rather than solely empirical, relationships may be formed.

Table 1. Overview of parameters used in definitions of forest- and tree lines and how they can be derived from LiDAR data at the individual tree- and plot levels.

Parameter	Level	Summary	References
Tree height	Individual tree	Derived as the maximum laser height inside a crown segment. This height will always be underestimated, usually with less than 1m. The level of underestimation depends on factors such as sensor-/acquisition settings, size (shrub, tree) and species.	Andersen et al. (2006) Gaveau & Hill (2003) Ørka et al. (2010)
	Plot	Both mean- and dominant height are derived with an accuracy of 2.5-13.6% and 3.6-8.4%, respectively. Estimation of mean height is not influenced by the sensor used, when models are properly calibrated with field data.	Næsset et al. (2004) Næsset (2009b)
Tree density	Individual tree	Individual tree detection with LiDAR data will find on the order of 41-71% of the trees. Number of stems cannot be derived directly without considerable bias.	Persson et al. (2002) Solberg et al. (2006)
	Plot	Number of stems can be derived with an accuracy of 17–50%.	Maltamo et al. (2004) Næsset (2002)
Canopy cover	Individual	Canopy cover cannot be computed for individual trees, but density measures like LAI may be derived. However, the projection from segmented trees may support estimation of canopy coverage at plot and stand level.	
	Plot	Various cover metrics are derived from LiDAR data. The cover metrics used are linked to canopy cover, but exact definitions are often not provided. Validation of LiDAR derived cover metrics are often done with hemispherical photography and high correlations are obtained ($r^2 = 0.70 – 0.78$). Different sensor-/acquisition settings may influence the estimates of canopy cover.	Hopkinson & Chasmer (2009) Morsdorf et al. (2006) Riano et al. (2004)

2.2. Satellite remote sensing

To identify the subalpine zone we propose to create a two class mask that separates the area of interest. Spectral information from satellite images is an important source to produce such class based masks for large areas. For example, a single Landsat scene may provide a basis for separation of forested and non-forested areas (McRoberts, 2006). Studies have shown that Landsat data are sensitive to the changes in surface and vegetation structure in the forest-tundra ecotone in Central Siberia (Ranson et al., 2004). Furthermore, Hill et al. (2007) used images from another multispectral satellite sensor (SPOT 5 HRG) to represent the alpine ecotone in Central Europe. However, limitations in accuracy obtain with satellite images alone have motivated the combination of spectral data from satellites and other spatial data layers (Franklin, 1995; Rogan & Miller, 2007; Wulder et al., 2006). Using spatial data layers alone to create masks are an option used in national forest inventories to create forest- and mire masks (Tomppo et al., 2008). However, spatial data layers have often limitations in coverage and are often not up to date in remote mountainous areas. Hence, for mapping the subalpine zone spatial data layers alone will often be insufficient. One source of information frequently available in remote areas is digital terrain models (DTMs). There are a number of variables than can be derived from DTMs, including slope, aspect, solar radiation, curvature, and different indices which may relate to the presence of the subalpine zone. For example, in a recent study in a forest-tundra ecotone in tropical Andes different topographic variables were used to predict the probability of forest (Bader & Ruijten, 2008). Table 2 summarizes the use of spatial and spectral data and the different methods for combining such data layers to create class based masks.

There are many statistical approaches for creating masks from spatial data layers supported by sample plot data. Table 3 summarize assumptions for different parametric and non-parametric methods and gives references to use in remote sensing to create masks. In the case of separating a transition from forest to alpine both parametric logistic regression and non-parametric regression trees have potential to include variables derived for example from DTMs without any assumptions related to the distribution of the variables. Ecotones, like the subalpine zone, are best represented by soft classifiers which provide a probability surface (Foody, 1996). Probability surfaces are possible to obtain from regression trees. However, binomial logistic regression directly provides a probability measure. Binomial logistic regression is widely used in the remote sensing community to create class-based masks (e.g. Wulder et al., 2006).

Table 2. Overview of approaches used to develop class-based masks

Approach	Description	Summary	References
Spatial:			
	Using available spatial data to create masks	Assume that the spatial data are updated at the time of inventory.	Tomppo et al. (2008)
Spectral:			
	Using the spectral signature from images as an input for masking	Using the spectral signature of targets to develop the mask either thru supervised methods (with calibration data) or unsupervised methods.	Haapanen et al. (2004) Rack (2001)
Combine spatial and spectral:			
• Classification of spectral and spatial data	Include spatial data in the classification of the mask (supervised or unsupervised)	Spatial layers such as elevation, slope, aspect, soil, climatic maps, fire history, are used, dependent on the mask problem. Increase accuracy compared to pure spectral is reported. Specific consideration regarding classification methods must be taken because spatial data often do not follow a Gaussian distribution.	Ricchetti (2000) [a] Rogan et al. (2003) Wulder et al. (2006)
• Pre-stratified with spatial data	Use spatial data to mask out areas of little interest for the target, but which are spectrally similar	Pre-stratification is much used and increase accuracy of classification. Selection of strata is dependent on the task. Two examples are (1) selected forest stands susceptible to mountain pine beetle as a stratum to use in classification of mountain pine beetle red attack, and (2) stratify the US into ecologically similar mapping zones for use with strata specific non-forest/forest models.	Blackard et al. (2008) Franklin et al. (2003)
• Post-classification sorting with spatial data	Using ancillary data to split mixed classes	Involve knowledge about class dispersal in the spatial layers used e.g. over slope to separate spectral similar classes occurring on flat and steep terrain, respectively. Increased accuracy compared to only using spectral data.	Hutchinson (1982) [a]

[a] Creation of more than two classes.

Table 3. Statistical approaches for creating masks from spatial data layers supported by sample plot data

Approach	Summary	Methods	References
Parametric methods:			
Distance based (Statistical classifiers)	Assign class label to new objects, often based on Euclidian distance. Easily available in RS software. Assume Gaussian distribution of input features, not valid for e.g. DTMs	Maximum likelihood Minimum distance	Franklin et al. (2003) Hill et al. (2007) Nelson et al. (2005)
Logistic regression	Assign probability of class to new objects. Do not assume Gaussian distribution of input features	Logistic regression	Koutsias & Karteris (1998) McRoberts (2006) Nelson et al. (2005) Wulder et al. (2006)
Regression	Assign a continuous response variable via regression and the split into two classes based on a threshold, e.g. estimate tree cover with GLM	Any suitable linear or non-linear regression model	Heiskanen & Kivien (2008)
Non-parametric methods:			
Neighbourhood-methods	Much used in forest inventory. Require many training plots, preserve same variance in predictions as in training data.	k-NN k-MSN	McRoberts et al. (2002) Nelson et al. (2005) Tomppo et al. (2008)
Classification and regression trees	Methods handle different data types such as DTMs and soil data well because they do not assume any distribution. Easy to interpret results from classification.	CART	Blackard et al. (2008) Rogan et al. (2003)
Machine learning algorithms	Often regarded as black-boxes. Have shown potential in remote sensing applications. May not need large training datasets.	Support vector machines Neural networks	Cao et al. (2009) Olofson et al. (2004)

4. Materials and methods

4.1. Study area

The study area, Hedmark County, is located in southeast Norway (Fig. 1). The total land area of Hedmark is approximately 27 400 km^2. The county is covered by boreal and alpine vegetation zones with a slightly continental climate (Moen, 1999). Elevations range from 120 to 2180 m asl.

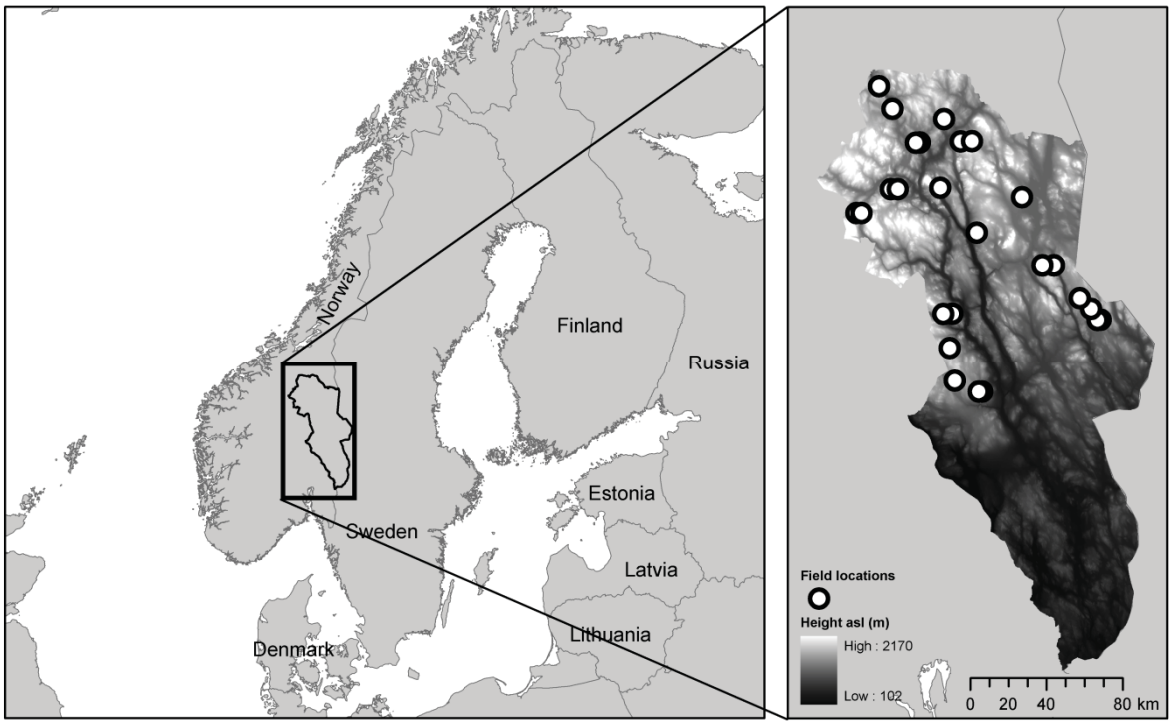

Fig. 1. Study area and field locations.

4.2. Field data

During summer 2008 the forest- and tree lines were mapped in field at 26 locations (Fig. 1) in Hedmark County. Locations were selected subjectively based on the following criteria: placed in the LiDAR sample transects, availability of ortophotos, accessible for field work, and spatially well distributed over the county. The subalpine zone was manually digitized by applying common practices following the forest- and tree lines in the field. Digitizing was conducted with a simple Bluetooth GPS receiver (Holux M-1000) connected to a Personal Data Assistant with a Geographical Information System. As shown in Fig. 2, the forest structure and type of forest varies between the field locations. The total length of forest lines digitized in field was 38.6 km and the length of the tree lines was 42.3 km.

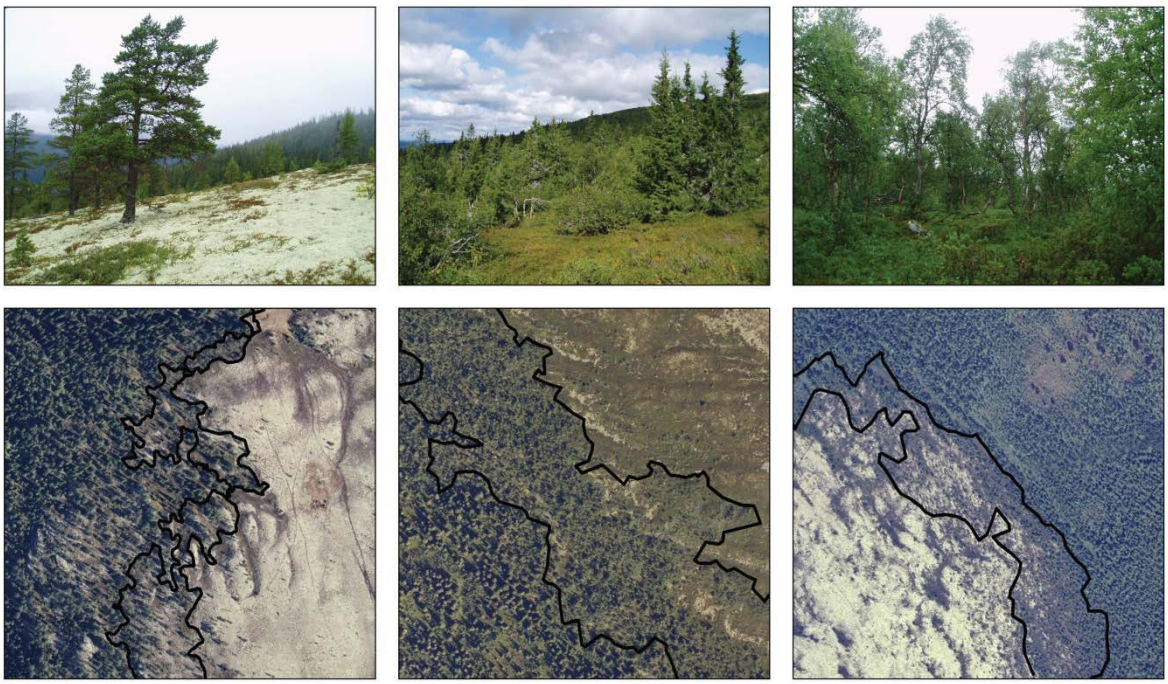

Fig.2. Three different sites with ground photo and orthophotos with tree line and forest line (black lines). Sites from left; Heimrabben – Lichen-pine forest, Danseren – Vaccinium-spruce forest (birch at tree line), and Bjørnsjøklettan – Lichen-birch forest.

4.3. LiDAR data

LiDAR data were acquired during summer 2006 with the Optech ALTM 3100 laser scanner. Detailed parameters and settings for the acquisitions and sensors appear in Table 4. Parallel flight lines were flown in east-west direction with a distance between adjacent flight lines of 6 km. The total length of all flight lines was more than 4500 km and the LiDAR dataset consist of a sample of 8.4 % of the study area. The initial processing of the data was accomplished by the contractor (Blom Geomatics, Norway). Planimetric coordinates (x and y) and ellipsoidal height values were computed for all echoes. For each acquisition, ground returns were determined using the Terrascan software (Terrasolid Ltd., 2004) and a triangulated irregular network (TIN) was created from the echoes classified as ground returns. Heights above the ground surface were calculated for all echoes by subtracting the respective TIN heights from the height values of all echoes recorded.

Table 4. Sensors and acquisition settings

Parameters	
Platform	PA31 Piper Navajo
Sensor	ALTM 3100
Mean flying altitude AGL (m)	800
Pulse repetition frequency (kHz)	100
Scan frequency (Hz)	55
Half scan angle (deg.)	17
Mean flying speed (ms^{-1})	ca. 75
Mean pulse density (m^{-2})	2.7 [a]
Beam divergence (mrad)	0.26
Footprint diameter (cm)	21 [a]

[a]Computed after Baltsavias (1999) based on mean acquisition settings.

4.4. Landsat data

Four different Landsat 5 TM images were obtained from USGS to covering the study area. The scenes used were path 197 row 18 and 16 acquired on 3 June 2007 and path 198 row 18 and 17 acquired on 10 June 2007. The images were georeferenced using 1:5000 maps and orthorectified using a DTM with 25 m spatial resolution. The images were resampled to the size of the DTM during orthorectification. Furthermore, the orthorectified images were converted to top of atmospheric reflectance (TOA) by the procedure developed by Han et al. (2007). The TOA corrections account for differences in viewing geometry and sensor. However, variations in absolute atmospheric conditions between images were not corrected. The TOA corrected images were mosaiced together. The RMS of all four images was less than 1/3 pixel. From the TOA corrected Landsat mosaic the normalized difference vegetation index (NDVI) and the brightness, greenness and wetness from the tassel cap transformation were derived and used (Crist & Kauth, 1986; Huang et al., 2002; Kauth & Thomas, 1976).

4.5. Digital elevation data

Digital elevation data were supplied by the Norwegian Mapping Authority as a DTM with 25m spatial resolution. From the DTM, elevation, slope, solar radiation and curvature were derived and utilized. Slope was computed for each raster cell in the DTM using the average maximum technique on a fitted plane to a 3 × 3 cell neighborhood (Burrough & McDonell, 1998). Global solar radiation in watt hours per square meter (WH m^{-2}) was computed using the DTM in accordance with Fu and Rich (1999). Curvature describe the shape of the terrain and was computed in a 3 × 3 cell neighborhood (Moore et al., 1991; Zeverbergen & Thorne, 1987). In addition, the location (latitude and longitude) of the pixels was used in the modeling.

4.6. Procedure for delineate the subalpine zone

Fig. 3 outlines the proposed procedure for obtaining the full coverage map of the subalpine zone. The flow chart introduces the input data described above. During Step 1, the procedure identifies cover types- forest, alpine and subalpine areas in the LiDAR data, using a heuristic classification. Step 2 describes the use of LiDAR-, satellite- and spatial data layers to produce a map showing the probability of forest. Furthermore, alpha-cuts were identified to produce a map with hard classes i.e. the cover types- forest, alpine and subalpine. At last, the accuracy of both the LiDAR derived classes and the full coverage class map produced was assessed. The two steps of the procedure and the accuracy assessment are described in further detail below.

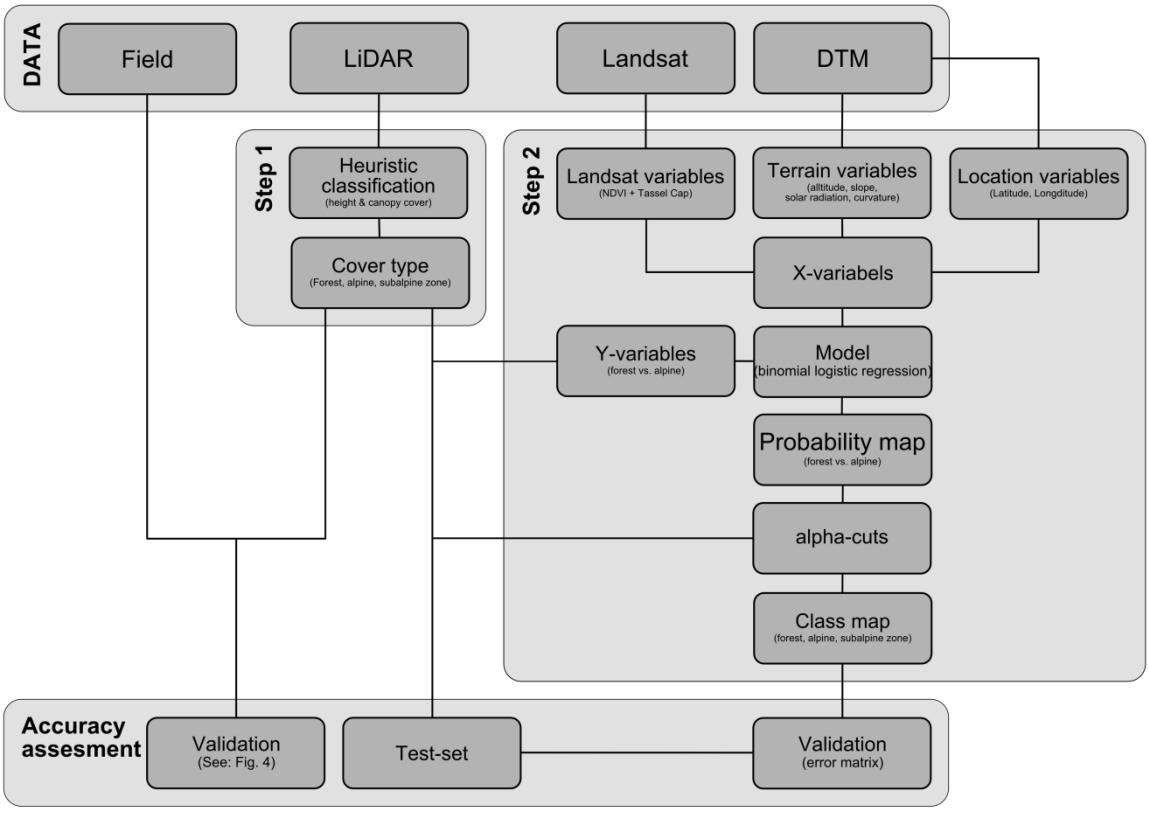

Fig. 3. Flow chart describing input data, analysis and accuracy assessment.

4.6.1. Identify the subalpine zone using LiDAR data (Step 1)

A heuristic classification procedure for automatically assigning an area to a cover type was developed. The point cloud obtained from LiDAR sensors can be viewed as a sample of the forest canopy where each echo (x, y, z – point) is a sample point. Classifying the point according to presence or absence of canopy makes the point cloud a sample of a binomial

distribution (canopy vs. not canopy). Hence, the canopy cover can be computed as the number of echoes in the canopy over the total number of echoes:

$$C = \frac{N_c}{N_t} \quad (1)$$

where C is canopy cover, N_c is number of first returns in canopy, and N_t is total number of first returns. Similar approaches have frequently been used (c.f. Hopkinson & Chasmer, 2009). Canopy hits were defined based on a height threshold. One height threshold was used for defining tree canopy (HT_{trees}) and one threshold was used for defining shrubs and trees ($HT_{shrub+trees}$). The height thresholds were used to separate canopy returns (N_c) in Eq. 1. The canopy thresholds were set in accordance with the heights in the FAO definitions (HT_{trees} = 5 m and $HT_{shrub+trees}$ = 0.5 m). Hence, canopy cover for trees (C_{trees}) was computed as the number of first returns above 5 m divided by the total number of first returns. Canopy cover for trees and shrubs ($C_{shrub+trees}$) was computed as the number of first returns above 0.5 m divided by the total number of first returns. Then the classes, i.e., forest, alpine or subalpine zone, were assigned according to this pseudo code:

if($C_{trees} > CT_1$)
    class = forest
else
    if($C_{trees} > CT_2$ or $C_{shrub+trees} > CT_1$)
        class = subalpine zone
    else
        class = alpine

where CT_1 and CT_2 represent the two different canopy cover thresholds. The canopy cover thresholds used to assign classes were CT_1 = 0.10 and CT_2= 0.05 which correspond to the canopy coverage values in the FAO definitions of forest and other wooded land.

4.6.2. Model and map the subalpine zone using full coverage data (Step 2)

To predict the cover type based on the Landsat and other data with full areal coverage, a binomial logistic regression was estimated (Eq. 2). The spectral indices (NDVI, brightness, wetness, and greenness), elevation, slope, solar radiation, curvature, and location variables

(latitude and longitude) were candidate variables in the estimation. The initial model including all candidate variables was of the form:

$$\log\left(\frac{\pi(\text{FOREST})}{1-\pi(\text{FOREST})}\right) = \beta_0 + \beta_1 x_1 + \ldots + \beta_k x_k \quad (2)$$

where $\pi_{(FOREST)}$ is the probability of a pixels being forest, β_0, β_1 - β_k are fixed parameters and x_1 - x_k are the variables used. Variable selection was conducted using a manual backward elimination process. In addition, highly correlated variables were removed to avoid co-linearity. The reference data included plots of size 625m^2, equal to pixel size, laid out every 3rd km along the LiDAR transects. Reference data were pre-stratified according to the potential subalpine zone area using the DTM. Only areas between 675 and 1150 m asl were included in the analysis. A total of 534 reference plots, where the LiDAR derived cover type was forest or alpine, were used in the binomial logistic regression. The fit of the final model was evaluated with Naglekerkes R^2 (Nagelkerke, 1991), the deviance test and the Hosmer-Lemeshows goodness-of-fit test (Hosmer et al., 1997).

The final binomial logistic regression model was used to predict a probability surface in the potential subalpine area in Hedmark. The probability surface represents the probability of an area, a pixel, being forest. Even though ecotones are best represented by a probability surfaces a hard classification is often needed when presenting thematic maps of the subalpine zone or when information will be used in international reporting (Hill et al., 2007). Hill et al. (2007) tested two approaches to present the probability surface as a thematic map using alpha-cuts. In the current study we used the probability of forest for the reference plots, estimated by the binomial logistic regression model and probability density functions to identify alpha-cuts. Separate density functions were estimated for the three cover types (forest, alpine and subalpine) using a Gaussian kernel and bandwidth of 0.05 (R Development Core Team, 2009). Then the alpha-cuts were set for the upper and lower boundaries where the subalpine zone according to the density functions had a higher density than forest and alpine areas.

4.6.3. Accuracy assessment

The accuracy of the LiDAR derived cover type classes was validated with the field measured forest- and tree lines. At the 26 field locations three cover type classes (forest, alpine, subalpine zone) were determined (Fig. 4a). The cover type map (Fig. 4A) was validated

against the field measured tree- and forest lines separately. In the accuracy assessment an image gradient based method was utilized (Pitas, 2000; Wulder et al., 2007). In the LiDAR cover type map either forest or alpine was subset. Hence, the two classes were treated separately (Fig. 4B). Furthermore, the rate of change in a local neighborhood was computed for both cover types separately as the gradient:

$$|\nabla f(x,y)| = \sqrt{[f(x+1,y) - f(x,y)]^2 + [f(x,y+1) - f(x,y)]^2} \quad (3)$$

where $|\nabla f(x,y)|$ is the gradient and x and y are row and column in the raster file created at each location. The computed image gradient (Eq. 3, Fig. 4C) was combined with information about the distance to the field measured line (Fig 4D). Furthermore, image gradient values for different pixel distances from the field measured lines were averaged over all field locations. The largest values indicate the strongest gradient or highest rate of change in classes between pixels.

In order to evaluate the use of canopy coverage thresholds and height thresholds in the heuristic classification of LiDAR data a sensitivity analysis of these thresholds was conducted. Hence, different height thresholds (HT_{trees} = 2 – 10 m and $HT_{shrub+trees}$ = 0.25 – 1 m) and canopy coverage thresholds (CT_1 = 0.055 – 0.20 and CT_2 = 0.005 – 0.15) were tested. The mean gradient value at the forest- and tree line, respectively were recorded for every combination of height and canopy cover thresholds. In addition the number of pixels from the peak of the image gradient to the field measured line was evaluated for both the forest- and tree line.

The logistic regression model and the alpha-cut were validated using a test dataset which covered the plots located ± 1 km in the east – west direction of the calibration plots. The test dataset plots were classified according to Step 1 (Section 4.6.1). The classification accuracy of the binomial logistic regression model and alpha-cuts was validated both for the calibration and the test datasets.

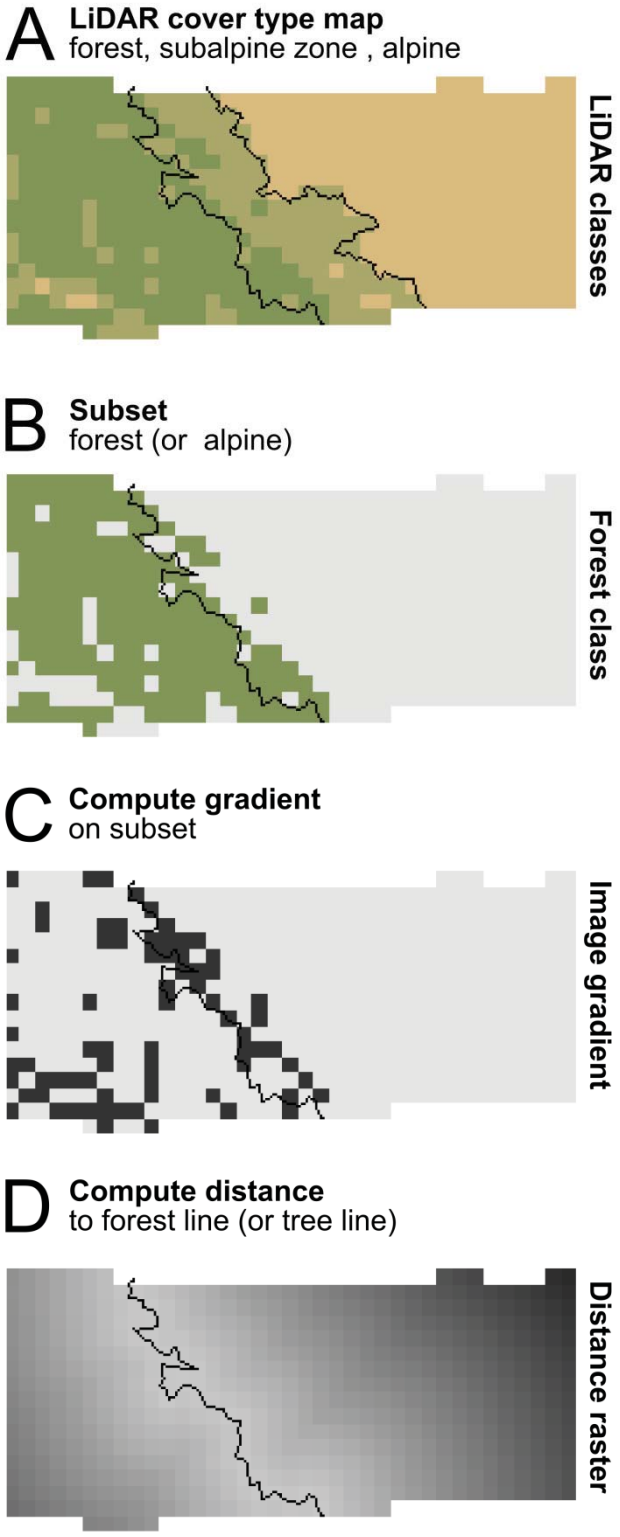

Fig. 4. Illustration of the accuracy assessment of the heuristic cover type classification from LiDAR (See section 4.9). A is the cover type classification. The forest and alpine cover types are treated separately through the subsequent steps (B) and the image gradient (Eq. 3) are computed (C). The gradient values (C) are combined with the distance to the field measured line (D) to produce average gradient values at different distances from field measured lines.

5. Results

5.1. Accuracy of heuristic LiDAR cover type classification

The predicted forest- and tree lines showed a good correspondence with the field measured lines (Fig 5). The average image gradient values peak at the location of field measured lines. Consequently, the heuristic classification of the LiDAR data shifts most frequently between pixels near the field measured lines. The high gradient values below the field measured forest line reflect the patchiness of the forest near the forest line (Fig. 5). In the subalpine zone and in the alpine area the gradient values are low. Hence, the vegetation above the forest line appears more homogeneous as classified by LiDAR data. A visual inspection of all the field locations indicated that four forest lines (15.4 %) and two tree lines (7.7 %) did not have a satisfactory accuracy. Examples from three of the 26 field locations illustrating accuracy and errors of the heuristic LiDAR cover type classification appear in Fig. 6.

The sensitivity analysis presented in Fig. 7 demonstrates that the accuracy in pixels obtained was indifferent to the selection of height and canopy cover thresholds. The offset was within plus or minus one pixel (50 m) for many combinations of height- and canopy cover thresholds. However, the selected height and canopy thresholds corresponding to the FAO definitions were close to having the highest average image gradient values as illustrated in the contour plots in Fig. 7. Higher values could be obtained by reducing the height threshold by 0.5 m. Minor changes in the canopy coverage thresholds, e.g. by 0.01 units, did not affect the accuracy at all.

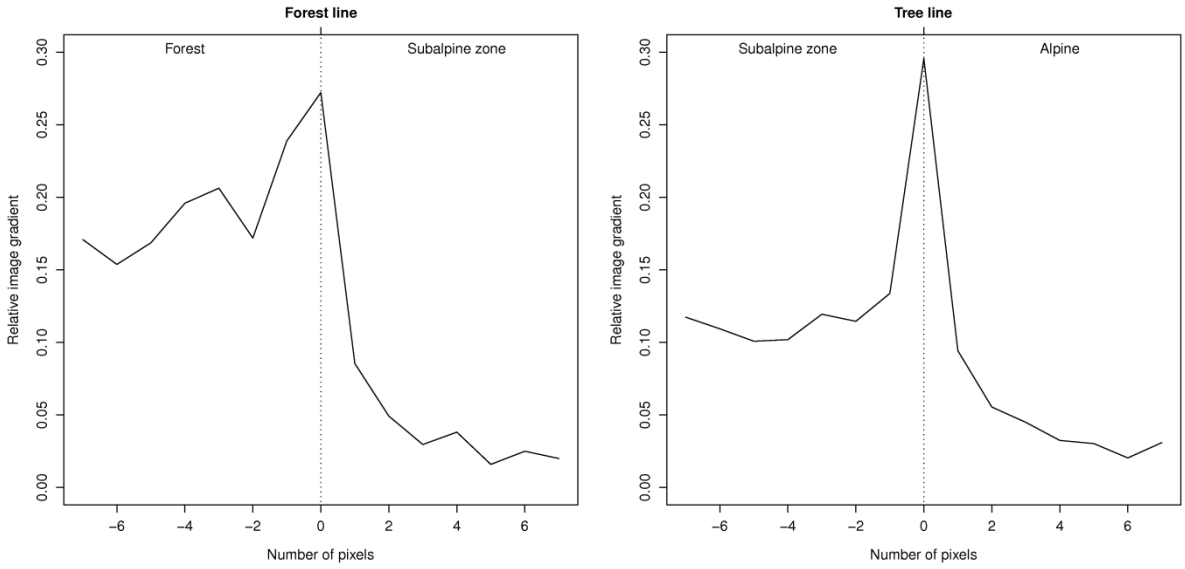

Fig. 5. Results of the accuracy assessment of the heuristic cover type classification from LiDAR. The average image gradient values (Eq. 3) for different distances from the field measured forest- (left) and tree lines (right). The field measured forest- and tree lines appear as vertical dotted lines.

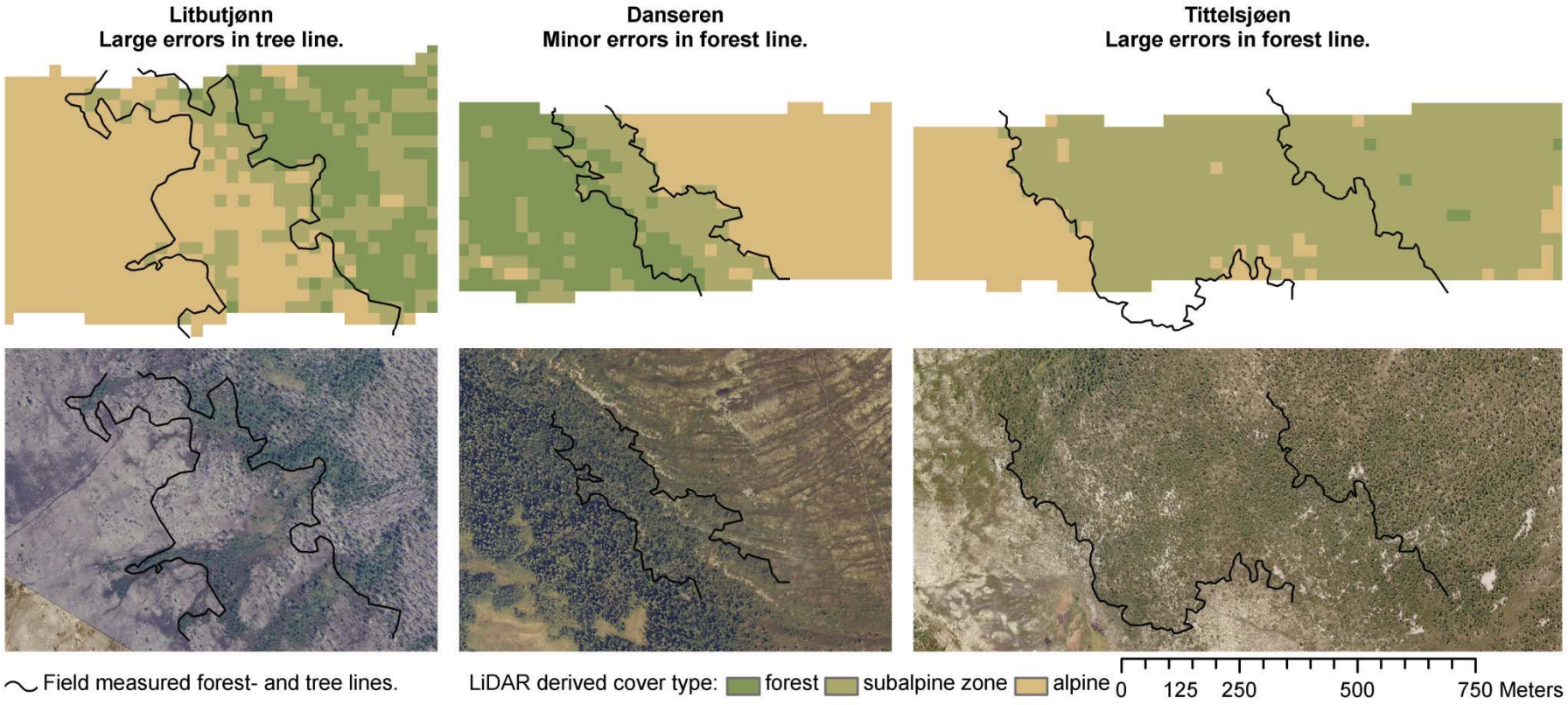

Fig. 6. Examples of the heuristic cover type classification from LiDAR (above). For comparison orthophotos are display below. Forest- and tree lines appear on both cover type classification and on orthophotos as black lines.

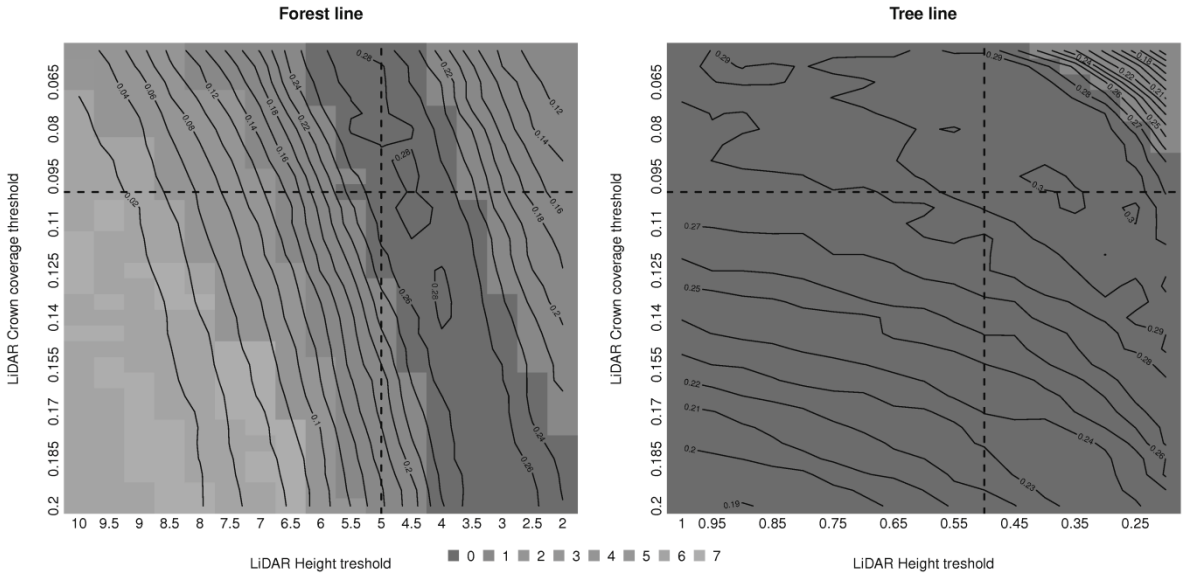

Fig. 7. Results of the sensitivity analysis were different height (x axis) and canopy thresholds (y axis) are used in the heuristic LiDAR classification of cover types (forest, subalpine zone and alpine). The contours represent average image gradient values (Eq. 3) at the field measured forest (left) and tree lines (right). The distance from the highest image gradient value (Eq. 3) to field measured forest- and tree lines are represented by the number of pixels offset in gray scale from 1 to 7. The dashed lines represent the values initially used in the current study.

5.2. Accuracy of subalpine mask

The selected variables and fit statistics for the estimated binomial logistic regression model are presented in Table 5. The two Landsat variables greenness and NDVI were highly correlated (r = 0.85). During the modeling NDVI was selected because of better models obtained compared to using greenness. We included both NDVI and brightness because of the significant contribution of both indices to the model. The elevation and slope variables derived from the digital terrain model were strong explanatory variables. However, neither the solar radiation nor the curvature provided additional information. Wetness and longitude were significant variables in the model following a backward elimination procedure ($0.05>p>0.01$). However, the variables were removed to get a simpler model without an essential reduction in Akaike information criterion (AIC). The Hosmer and Lemeshow statistics (Hosmer et al., 1997) indicated that the final model fitted the data sufficient well ($p = 0.40$). The proportion of variation explained by the model expressed by Nagelkerke's R^2 was 0.73.

Alpha-cuts were selected according to the probability density functions estimated for the three cover type classes (Fig. 8). The crossing of the subalpine and alpine density functions in Fig. 8 resulted in a lower alpha-cut of 0.16 and the crossing of forest and subalpine resulted in an upper alpha-cut of 0.79. Hence, pixels having a probability of forest between 0.16 and 0.79 were classified as subalpine zone. The selected alpha-cuts resulted in

an overall classification accuracy of 68.8 % and a kappa value of 0.52. The error matrix for the calibration and the test data sets appear in Table 6.

Predicting the probabilities for every pixel in the county and assign classes to the pixels based on the estimated alpha-cut values resulted in a map of the subalpine zone in Hedmark with a total area of 3660 km^2, representing 14% of the land area in Hedmark.

Table 5. Parameters and fit statistics for the logistic regression model.

Coefficient	**Estimate**	**Z**	**p-value**
Intercept	4.088e+00	2.56	0.010
NDVI	1.783e+01	8.60	0.000
Brightness	-1.997e+01	-6.38	0.000
Elevation	-1.038e-02	-5.93	0.000
Slope	1.040e-01	3.33	0.001
Latitude	1.305e-05	3.54	0.000
Model fit:			
Hosmer-Lemeshow goodness of fit[a]		-0.85	0.397
Deviance test			1

[a]Hosmer-Lemeshow goodness of fit (Hosmer et al., 1997)

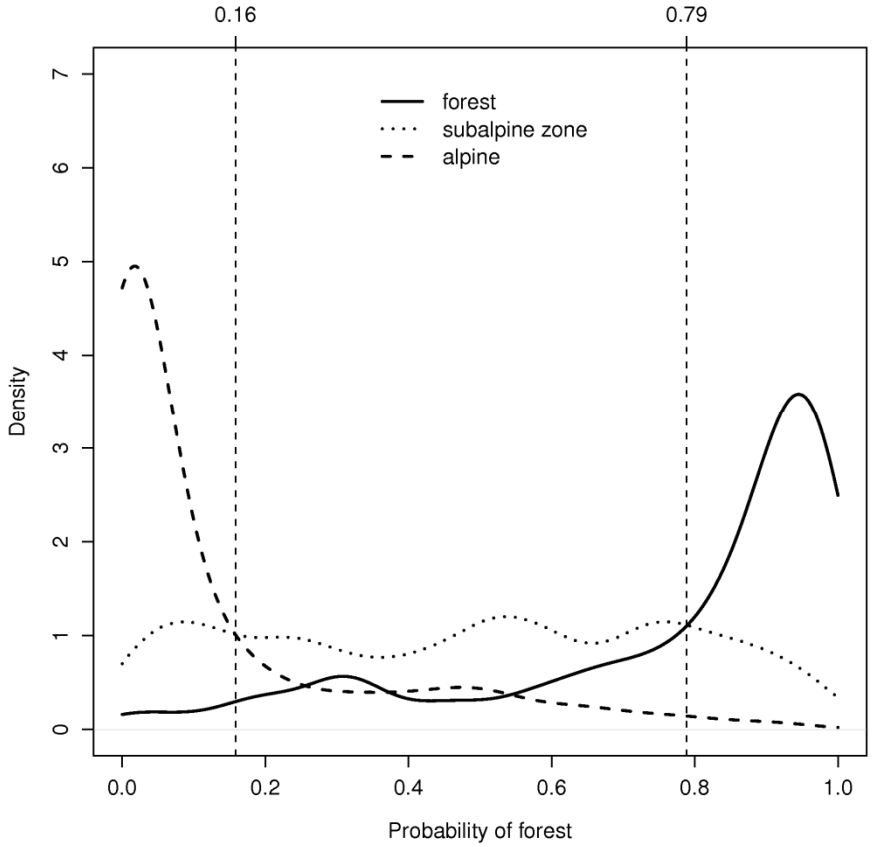

Fig. 8.The probability density functions for forest, alpine and subalpine zones used to set alpha-cuts. The resulting alpha-cuts are displayed as vertical lines.

Table 6. Error matrix and accuracy measures of the class map created using logistic regression and alpha-cuts.

	References				
	Forest	Subalpine zone	Alpine	Sum	User accuracy
Calibration dataset:					
Forest	126	19	5	150	84.0
Subalpine zone	61	68	81	210	32.4
Alpine	7	22	254	283	89.8
Sum	194	109	340	643	
Producer accuracy	64.9	62.4	74.7		
Overall accuracy					69.7
Kappa					0.53
Test dataset:					
Forest	274	115	7	396	69.2
Subalpine zone	55	133	47	235	56.6
Alpine	25	161	495	681	72.7
Sum	354	409	549	1312	
Producer accuracy	77.4	32.5	90.2	0	
Overall accuracy					68.8
Kappa					0.52

6. Discussion

In this study, the subalpine zone in Hedmark County, Norway was successfully mapped. The method presented benefited from utilizing high spatial resolution LiDAR data sampled for parts of the county. A heuristic classification of the LiDAR data enabled an accurate depiction of the subalpine zone over a large geographical area without calibration based on field measurements. The information derived from LiDAR data was combined with Landsat and elevation data to produce full coverage maps of the subalpine zone. Collecting expensive field data from remote mountainous areas is not needed using this method. The current study demonstrate that a national forest inventory utilizing scanning LiDAR operated as a strip sampling tool (Næsset et al., 2009) may exploit the LiDAR data and additional remote sensing data to derive the area of the subalpine zone without increasing field inventory costs.

An improved capacity for the national forest inventory to capture the entire forested area, rather than limited to managed forest areas at lower altitudes, is increasingly desired and may be aided by the approach presented here. The ability to portray transitional areas enhances our ability to monitor and report on carbon stocks and change and to ensure that all relevant forested areas are included. Studies of climate change may also be aided by the ability to map the subalpine zone over large areas. Hence, changes in the subalpine zone can be monitored over vast areas and not only at specific sites. Changes found over time will be important for describing the change processes and the rates of transition among cover types.

LiDAR measures both tree height and canopy cover precisely (Table 1). The current study utilized tree heights and canopy cover derived directly from LiDAR data. However, these variables are only proxies for the real values. A LiDAR pulse will always penetrate into the canopy before an echo is trigged (Gaveau & Hill, 2003; Ørka et al., 2010). In previous studies, canopy cover has often been derived for measurements above a certain height threshold often equal to the height where reference data were collected with e.g. hemispheric camera (e.g. Riano et al., 2004). The current study used height thresholds of 0.5 and 5 m, which is in accordance with international forest definitions. The sensitivity analysis preformed in the current study confirmed the penetration of LiDAR echoes into the canopy. The accuracy of both forest- and tree lines would have been slightly improved in the heuristic LiDAR cover type classification with height threshold values approximate 0.5 meter lower than those used. Changing the canopy coverage thresholds in the sensitivity analysis did not increase the accuracy of the heuristic classification.

Different LiDAR sensors and acquisition settings are known to affect the measurements of forest canopies (Næsset, 2005; Ørka et al., 2010). Hence, flying with a different sensor, a different pulse repetition frequency or flying at higher altitudes will affect the penetration into the canopy (Chasmer et al., 2006; Næsset, 2009b; Ørka et al., 2010). The distance an emitted LiDAR pulse has to penetrate into the canopy before an echo is recorded will affect the LiDAR proxies used for tree height and canopy cover directly. Tree height underestimation compared to true tree height was in the range of 0.35 – 1.47 m in another subalpine area in Norway (Næsset, 2009a). The underestimation in the study by Næsset (2009a) was affected by sensor and acquisition settings together with tree species and the terrain model. Differences in measurements obtained with different sensors and acquisitions usually necessitate field data for properly calibration of models. In the current study focus was on large area inventory and on areas with low economical value where no alternative methods are currently available. Thus, the need for an accurate calibration was judged to be less relevant. Hence, using information directly derived from the LiDAR data will add value to the current inventory without increasing costs. However, proper calibration with information from field plots would undoubtedly increased the accuracy, but also costs.

When mapping the forest- and tree lines in the field the uppermost line was followed. Hence, there could be areas with lower density of trees or lower tree heights below the mapped areas. In Fig. 6, the site at Litbutjønn illustrates such a case. In the south there are areas matching the criteria of the subalpine zone about 100 meters after an open/alpine area. When following the tree line to the north the tree density slightly decreased and thus an error

was made when mapping the tree line in field. At the Danseren site, only minor errors were introduced by following the forest line. The third location in Fig. 6, Tittelsjøen, the LiDAR derived forest line was affected by the species composition at the location. The tree species will influence the LiDAR measurements (Næsset, 2009a; Ørka et al., 2009). At Tittelsjøn, the tree line is abrupt and formed by birch and was well delineated with the classification of LiDAR data. The forest line is diffuse and comprised of spruce trees. The spruce trees have a conical form and hence the canopy cover at base is much greater than the canopy coverage at 5 m. LiDAR will therefore underestimate canopy coverage significantly at that spruce dominated site.

The binomial logistic regression model developed included five variables important for characterizing the subalpine zone in Hedmark. Two Landsat derived variables were used in the model, NDVI and brightness. The two variables describe different vegetation (NDVI) and non-vegetation (brightness) properties. The probability of forest increase when NDVI increase and brightness decrease. For the DTM derived attributes, altitude and slope were important. Higher altitudes reduce the probability of forest and steeper slopes increase the probability for forest. Even though solar radiation and topographic position illustrated by curvature ought to be important for tree growth, these variables were not statistically significant. In tropical Andes, altitude, aspect and a compound topographic index was significant when estimating the probability of forest (Bader & Ruijten, 2008). The only common variable with the current study and the study by Bader and Ruijten (2008) was altitude, which indicates the importance of altitude as an overall driving factor for forest- and tree lines.

The accuracy obtained for classification with the binomial logistic regression model and alpha-cuts was within the range of expected accuracies in satellite image classification (Wilkinson, 2005). The current study tried to mask out a transition that has a high degree of mixing with the two classes forming the transition (Table 6). In light of the high mixing that occurred, the obtained accuracy was considered acceptable for area estimation and monitoring transitions over large areas.

In the current study, only the alpine transition zones were registered. However, the heuristic classification of LiDAR data did not distinguish between forest-alpine transitions and other forest – non-forest transitions inside the potential area for the subalpine zone. Hence, the areas below the forest zone will include other transitions zones and also non-forested areas (Fig. 5). Transitions occurring in the forest may consist of mountain peat lands or transitions related to change in nutrient level, e.g. from deep soils to bare rock. Hence,

enhancement which including land cover classification could be implemented to improve the separation of these transitions.

The remote sensing products produced in the current study are important in monitoring areas in the subalpine zone. Maps of changes in the subalpine zone over time can be combined with information about human activity and grazing by animals etc. to separate the response of climate change on the tree lines from effects of land use change. As pointed out by Hill et al. (2007), hard classifications of ecotones are often needed for map products. Hill et al. (2007) used two different approaches to produce alpha-cuts used to divide the subalpine zone into classes. In the current study a new method for dividing the probability surface into hard classes was presented. As opposed to the methods presented by Hill et al. (2007), our method uses information about ecotone derived using LiDAR to produce these alpha-cuts. The proposed method produces a hard classification from which an estimate of the area of the subalpine zone can be derived. The method described also has a probability surface as one of its products. Probability surfaces or results from soft classifiers are more robust in monitoring and change detection in transition zones (Foody, 2001). In the alpine environment, it has been reported that diffuse tree lines are more likely to have advanced than krumholz and abrupt tree lines (Harsch et al., 2009). Therefore, monitoring of the subalpine zone is best done by using the probability map, but the classified map provide area estimates and a tool for estimating the biomass using LiDAR-assisted inventory procedure such as those proposed by e.g. Næsset et al. (2009).

7. Conclusions

The procedure proposed in the current study will be suitable for mapping current state and monitoring future changes in the subalpine zone at a regional scale. The method for delineating subalpine using samples of LiDAR data is simple, heuristic and straightforward. The use of logistic regression and alpha-cut provide both a hard classification usable for map products and area estimation and a probability surface suitable for monitoring purposes. The method can also be extended to other types of transition between forest and non-forest. If detailed monitoring is requested, for example monitoring of regeneration, growth, and mortality of single trees, then methods utilizing field calibration based on a statistically sound sample of ground data are indeed required.

Acknowledgements

This research was funded by the Norwegian University of Life Sciences and the Research

Council of Norway (research grant #192792/I99) and is a contribution to the NORKLIMA project entitled “Effects of changing climate on the alpine tree line and mountain forest carbon pools along 1500 km n-s and elevation gradients” (research grant #184636/S30). We also wish to thank Blom Geomatics, Norway, for providing and processing the LiDAR data.

References

Andersen, H.E., Reutebuch, S.E., & McGaughey, R.J. (2006). A rigorous assessment of tree height measurements obtained using airborne lidar and conventional field methods. *Canadian Journal of Remote Sensing, 32*, 355-366.

Bader, M.Y., & Ruijten, J.J.A. (2008). A topography-based model of forest cover at the alpine tree line in the tropical Andes. *Journal of Biogeography, 35*, 711-723.

Baltsavias, E.P. (1999). Airborne laser scanning: basic relations and formulas. *ISPRS Journal of Photogrammetry and Remote Sensing, 54*, 199-214.

Blackard, J.A., Finco, M.V., Helmer, E.H., Holden, G.R., Hoppus, M.L., Jacobs, D.M., Lister, A.J., Moisen, G.G., Nelson, M.D., Riemann, R., Ruefenacht, B., Salajanu, D., Weyermann, D.L., Winterberger, K.C., Brandeis, T.J., Czaplewski, R.L., McRoberts, R.E., Patterson, P.L., & Tymcio, R.P. (2008). Mapping US forest biomass using nationwide forest inventory data and moderate resolution information. *Remote Sensing of Environment, 112*, 1658-1677.

Burrough, P.A., & McDonell, R.A. (1998). *Principles of Geographical Information Systems*. New York: Oxford University Press.

Cairns, D.M., & Moen, J. (2004). Herbivory Influences Tree Lines. *Journal of Ecology, 92*, 1019-1024.

Callaghan, T.V., Werkman, B.R., & Crawford, R.M.M. (2002). The tundra-taiga interface and its dynamics: Concepts and applications. *Ambio*, 6-14.

Cao, X., Chen, J., Matsushita, B., Imura, H., & Wang, L. (2009). An automatic method for burn scar mapping using support vector machines. *International Journal of Remote Sensing, 30*, 577-594.

Chasmer, L., Hopkinson, C., Smith, B., & Treitz, P. (2006). Examining the influence of changing laser pulse repetition frequencies on conifer forest canopy returns. *Photogrammetric Engineering and Remote Sensing, 72*, 1359-1367.

Clements, F.E. (1905). *Research methods in ecology*. Lincoln, Neb.: University Publishing Company.

Cohen, W.B., & Goward, S.N. (2004). Landsat's role in ecological applications of remote sensing. *Bioscience, 54*, 535-545.

Crist, E.P., & Kauth, R.J. (1986). The Tasseled Cap de-mystified((transformations of MSS and TM data)). *Photogrammetric Engineering and Remote Sensing, 52*, 81-86.

Dalen, L., & Hofgaard, A. (2005). Differential regional treeline dynamics in the Scandes Mountains. *Arctic Antarctic and Alpine Research, 37*, 284-296.

Falkowski, M.J., Wulder, M.A., White, J.C., & Gillis, M.D. (2009). Supporting large-area, sample-based forest inventories with very high spatial resolution satellite imagery. *Progress in Physical Geography, 33*, 403-423.

FAO (2006). Global Forest Resources Assessment 2005 - Progress towards sustainable forest management. In, *FAO Forestry Paper 147*. Rome: Food and Agriculture Organization of the United Nations.

Foody, G.M. (1996). Fuzzy modelling of vegetation from remotely sensed imagery. *Ecological Modelling, 85*, 3-12.

Foody, G.M. (2001). Monitoring the magnitude of land-cover change around the southern limits of the Sahara. *Photogrammetric Engineering and Remote Sensing, 67*, 841-848.

Franklin, J. (1995). Predictive vegetation mapping: geographic modelling of biospatial patterns in relation to environmental gradients. *Progress in Physical Geography, 19*, 474.

Franklin, S., Wulder, M., Skakun, R., & Carroll, A. (2003). Mountain Pine Beetle red-attack damage classification using stratified Landsat TM data in British Columbia, British Columbia, Canada. *Photogrammetric Engineering & Remote Sensing, 69*, 283-288.

Fu, P., & Rich, P.M. (1999). Design and implementation of the Solar Analyst: an ArcView extension for modeling solar radiation at landscape scales. In, *Proceedings of the 19th Annual ESRI User Conference*. San Diego, USA: ESRI.

Gaveau, D.L.A., & Hill, R.A. (2003). Quantifying canopy height underestimation by laser pulse penetration in small-footprint airborne laser scanning data. *Canadian Journal of Remote Sensing, 29*, 650-657.

Haapanen, R., Ek, A.R., Bauer, M.E., & Finley, A.O. (2004). Delineation of forest/nonforest land use classes using nearest neighbor methods. *Remote Sensing of Environment, 89*, 265-271.

Han, T., Wulder, M.A., White, J.C., Coops, N.C., Alvarez, M.F., & Butson, C. (2007). An Efficient Protocol to Process Landsat Images for Change Detection With Tasselled Cap Transformation. *Geoscience and Remote Sensing Letters, 4*, 147-151.

Harsch, M., A., Hulme, P., E., McGlone, M., S., & Duncan, R., P. (2009). Are treelines advancing? A global meta-analysis of treeline response to climate warming. *Ecology Letters, 12*, 1040-1049.

Heiskanen, J., & Kivinen, S. (2008). Assessment of multispectral, -temporal and -angular MODIS data for tree cover mapping in the tundra-taiga transition zone. *Remote Sensing of Environment, 112*, 2367-2380.

Hill, R.A., Granica, K., Smith, G.M., & Schardt, M. (2007). Representation of an alpine treeline ecotone in SPOT 5 HRG data. *Remote Sensing of Environment, 110*, 458-467.

Hofgaard, A. (1997). Inter-Relationships between Treeline Position, Species Diversity, Land Use and Climate Change in the Central Scandes Mountains of Norway. *Global Ecology and Biogeography Letters, 6*, 419-429.

Hopkinson, C., & Chasmer, L. (2009). Testing LiDAR models of fractional cover across multiple forest ecozones. *Remote Sensing of Environment, 113*, 275-288.

Hosmer, D.W., Hosmer, T., leCessie, S., & Lemeshow, S. (1997). A comparison of goodness-of-fit tests for the logistic regression model. *Statistics in Medicine, 16*, 965-980.

Huang, C., Wylie, B., Yang, L., Homer, C., & Zylstra, G. (2002). Derivation of a tasselled cap transformation based on Landsat 7 at-satellite reflectance. *International Journal of Remote Sensing, 23*, 1741-1748.

Hutchinson, C. (1982). Techniques for combining Landsat and ancillary data for digital classification improvement. *Photogrammetric Engineering & Remote Sensing, 48*, 123-130.

Hyde, P., Dubayah, R., Walker, W., Blair, J.B., Hofton, M., & Hunsaker, C. (2006). Mapping forest structure for wildlife habitat analysis using multi-sensor (LiDAR, SAR/InSAR, ETM plus , Quickbird) synergy. *Remote Sensing of Environment, 102*, 63-73.

Hyyppä, H., & Hyyppä, J. (1999). Comparing the accuracy of laser scanner with other optical remote sensing data sources for stand attributes retrieval. *Photogramm. J. Finland, 16*, 5 -15.

Kauth, R.J., & Thomas, G.S. (1976). The tasseled cap—a graphic description of the spectral-temporal development of agricultural crops as seen by Landsat. In, *Final proceedings: 2nd international symposium on machine processing of remotely sensed data*. West Lafayette, India: Purdue University.

Kimmins, J.P. (1997). *Forest Ecology, A foundation for sustainable management, 2nd ed.* Upper Saddle River, New Jersey: Prentice-Hall Inc.

Koutsias, N., & Karteris, M. (1998). Logistic regression modelling of multitemporal Thematic Mapper data for burned area mapping. *International Journal of Remote Sensing, 19*, 3499-3514.

Lefsky, M.A., Cohen, W.B., & Spies, T.A. (2001). An evaluation of alternate remote sensing products for forest inventory, monitoring, and mapping of Douglas-fir forests in western Oregon. *Canadian Journal of Forest Research-Revue Canadienne De Recherche Forestiere, 31*, 78-87.

Löve, D. (1970). Subarctic and Subalpine: Where and What? *Arctic and Alpine Research, 2*, 63-73.

Maltamo, M., Eerikäinen, K., Pitkänen, J., Hyyppä, J., & Vehmas, M. (2004). Estimation of timber volume and stem density based on scanning laser altimetry and expected tree size distribution functions. *Remote Sensing of Environment, 90*, 319-330.

McRoberts, R.E., Nelson, M.D., & Wendt, D.G. (2002). Stratified estimation of forest area using satellite imagery, inventory data, and the k-Nearest Neighbors technique. *Remote Sensing of Environment, 82*, 457-468.

McRoberts, R.E. (2006). A model-based approach to estimating forest area. *Remote Sensing of Environment, 103*, 56-66.

Moen, A. (1999). *National atlas of Norway: Vegetation*. Hønefoss: Norwegian Mapping Authority, Hønefoss.

Moore, I.D., Grayson, R.B., & Landson, A.R. (1991). Digital Terrain Modelling: A Review of Hydrological, Geomorphological, and Biological Applications. *Hydrological Processes, 5*, 3–30.

Morsdorf, F., Kotz, B., Meier, E., Itten, K.I., & Allgower, B. (2006). Estimation of LAI and fractional cover from small footprint airborne laser scanning data based on gap fraction. *Remote Sensing of Environment, 104*, 50-61.

Næsset, E. (2002). Predicting forest stand characteristics with airborne scanning laser using a practical two-stage procedure and field data. *Remote Sensing of Environment, 80*, 88-99.

Næsset, E., Gobakken, T., Holmgren, J., Hyyppä, H., Hyyppä, J., Maltamo, M., Nilsson, M., Olsson, H., Persson, A., & Söderman, U. (2004). Laser scanning of forest resources: The Nordic experience. *Scandinavian Journal of Forest Research, 19*, 482-499.

Næsset, E. (2005). Assessing sensor effects and effects of leaf-off and leaf-on canopy conditions on biophysical stand properties derived from small-footprint airborne laser data. *Remote Sensing of Environment, 98*, 356-370.

Næsset, E., & Nelson, R. (2007). Using airborne laser scanning to monitor tree migration in the boreal-alpine transition zone. *Remote Sensing of Environment, 110*, 357-369.

Næsset, E. (2009a). Influence of terrain model smoothing and flight and sensor configurations on detection of small pioneer trees in the boreal-alpine transition zone utilizing height metrics derived from airborne scanning lasers. *Remote Sensing of Environment, 113*, 2210-2223.

Næsset, E. (2009b). Effects of different sensors, flying altitudes, and pulse repetition frequencies on forest canopy metrics and biophysical stand properties derived from small-footprint airborne laser data. *Remote Sensing of Environment, 113*, 148-159.

Næsset, E., Gobakken, T., & Nelson, R. (2009). Sampling and mapping forest volume and biomass using airborne LIDARs. *Proceedings of the Eight Annual Forest Inventory and Analysis Symposium, Monterey, CA, USA*, 297-301.

Nagelkerke, N.J.D. (1991). A note on a general definition of the coefficient of determination. *Biometrika, 78*, 691-692.

Nelson, M.D., McRoberts, R.E., Liknes, G.C., & Holden, G.R. (2005). Comparing forest/nonforest classifications of Landsat TM imagery for stratifying FIA estimates of forest land area. In R.E. McRoberts, G.A. Reams, P.C. Van Deusen, W.H. McWilliams & C.J. Cieszewski (Eds.), *Proceedings of the fourth annual Forest Inventory and Analysis symposium* (pp. 121-128). New Orleans, Louisiana

Olthof, I., King, D.J., & Lautenschlager, R.A. (2004). Mapping deciduous forest ice storm damage using Landsat and environmental data. *Remote Sensing of Environment, 89*, 484-496.

Ørka, H.O., Næsset, E., & Bollandsås, O.M. (2009). Classifying species of individual trees by intensity and structure features derived from airborne laser scanner data. *Remote Sensing of Environment, 113*, 1163-1174.

Ørka, H.O., Næsset, E., & Bollandsås, O.M. (2010). Effects of different sensors and leaf-on and leaf-off canopy conditions on echo distributions and individual tree properties derived from airborne laser scanning. *Remote Sensing of Environment, 114*, 1445-1461.

Persson, Å., Holmgren, J., & Söderman, U. (2002). Detecting and measuring individual trees using an airborne laser scanner. *Photogrammetric Engineering and Remote Sensing, 68*, 925-932.

Pitas, I. (2000). *Digital image processing algorithms and applications*. New York: Wiley.

R Development Core Team (2009). *R: A Language and Environment for Statistical Computing*. Vienna, Austria.: R Foundation for Statistical Computing.

Rack, J. (2001). Forest / nonforest classification of landsat TM data for annual inventory phase one stratification. In G.A. Reams, R.E. McRoberts & P.C. Van Deusen (Eds.), *Proceedings of the Second Annual Forest and Inventory Symposium* (pp. 8-10). Salt Lake City, Utah

Ranson, K.J., Sun, G., Kharuk, V.I., & Kovacs, K. (2004). Assessing tundra-taiga boundary with multi-sensor satellite data. *Remote Sensing of Environment, 93*, 283-295.

Rees, W.G. (2007). Characterisation of Arctic treelines by LiDAR and multispectral imagery. *Polar Record, 43*, 345-352.

Riano, D., Valladares, F., Condes, S., & Chuvieco, E. (2004). Estimation of leaf area index and covered ground from airborne laser scanner (Lidar) in two contrasting forests. *Agricultural and Forest Meteorology, 124*, 269-275.

Ricchetti, E. (2000). Multispectral satellite image and ancillary data integration for geological classification. *Photogrammetric Engineering and Remote Sensing, 66*, 429–436.

Rogan, J., Miller, J., Stow, D., Franklin, J., Levien, L., & and Fischer, C. (2003). Land coverchange mapping in California using classification trees with Landsat TM and ancillary data. *Photogrammetric Engineering and Remote Sensing, 69*, 793–804.

Rogan, J., & Miller, J. (2007). Integrating GIS and remotely sensed data for mapping forest disturbance and change. In M.A. Wulder & S.E. Franklin (Eds.), *Understanding forest disturbance and spatial pattern* (pp. 133-171). Boca Raton, FL, USA: CRC Taylor & Francis.

Solberg, S., Næsset, E., & Bollandsås, O.M. (2006). Single tree segmentation using airborne laser scanner data in a structurally heterogeneous spruce forest. *Photogrammetric Engineering and Remote Sensing, 72*, 1369-1378.

Tomppo, E., Olsson, H., Stahl, G., Nilsson, M., Hagner, O., & Katila, M. (2008). Combining national forest inventory field plots and remote sensing data for forest databases. *Remote Sensing of Environment, 112*, 1982-1999.

UNFCCC (2008). *Kyoto protocol reference manual on accounting of emissions and assigned amount*

Wilkinson, G.G. (2005). Results and implications of a study of fifteen years of satellite image classification experiments. *IEEE Transactions on Geoscience and Remote Sensing, 43*, 433-440.

Woodcock, C., Allen, R., Anderson, M., Belward, A., Bindschadler, R., Cohen, W., Gao, F., Goward, S., Helder, D., & Helmer, E. (2008). Free access to Landsat imagery. *Science, 320*, 1011.

Wulder, M. (1998). Optical remote-sensing techniques for the assessment of forest inventory and biophysical parameters. *Progress in Physical Geography, 22*, 449-476.

Wulder, M.A., White, J.C., Bentz, B., Alvarez, M.F., & Coops, N.C. (2006). Estimating the probability of mountain pine beetle red-attack damage. *Remote Sensing of Environment, 101*, 150-166.

Wulder, M.A., Han, T., White, J.C., Butson, C.R., & Hall, R.J. (2007). An approach for edge matching large-area satellite image classifications. *Canadian Journal of Remote Sensing, 33*, 266-277.

Zeverbergen, L.W., & Thorne, C.R. (1987). Quantitative Analysis of Land Surface Topography. *Earth Surface Processes and Landforms, 12*, 47–56.

ISBN 978-82-575-0986-6
ISSN 1503-1667

Norwegian University of Life Sciences
NO–1432 Ås, Norway
Phone +47 64 96 50 00
www.umb.no, e-mail: postmottak@umb.no